

A proposed forecast methodology for natural-origin Willapa Bay Coho (*O. kisutch*)

Dan Auerbach, Thomas Buehrens, Neala Kendall
Fish Program
Washington Department of Fish and Wildlife
Olympia, Washington

Introduction

Preseason forecasts of expected salmon returns provide a basis for planning and adaptively managing harvest. Natural-origin Willapa Bay (WB) coho salmon (*Oncorhynchus kisutch*) are subject to the annual catch limit (ACL) requirements of the Magnuson Stevens Act (MSA), as administered within the Pacific Fishery Management Council (PFMC) planning processes¹. The Scientific and Statistical Committee (SSC) of PFMC is charged with reviewing the forecast methodology that is used to develop estimates of returning WB natural-origin coho salmon, as these estimates inform annual fisheries.

In support of the SSC review, this document describes a forecast framework proposed for use by the Washington Department of Fish and Wildlife (WDFW). The approach offers several advantages:

- A rigorous characterization of uncertainty in observations and represented biological processes through implementation of multiple hierarchical state-space forecast models, including a state-of-the-science multi-stock spatio-temporal Integrated Population Model (IPM) and basic (AR1) time-series model based on DeFilippo et. al (2021) *Improving short-term recruitment forecasts for coho salmon using a spatiotemporal integrated population model*
- A framework to compare multiple candidate models by evaluating model performance measures calculated from one-step-ahead forecasts, with scope to add additional candidate models and develop model-averaged ensemble forecasts as appropriate in the future
- A structure that includes direct observations of Willapa coho salmon while drawing inference from multiple stocks and leveraging existing processes of dataset compilation: Escapement and harvest estimates of natural-origin fish; marine survival estimates of Willapa hatchery-origin fish; return, survival, and smolt data from neighboring Bingham Creek and other WA Coast coho salmon stocks
- A transparent, readily reproducible implementation suited to ongoing refinement via a public GitHub repository of the proposed approach (<https://github.com/daauerbach/ST-IPM>), developed from archived the public GitHub repository of code and data used in DeFilippo et. al (2021)

¹See for example: <https://www.pcouncil.org/documents/2021/02/e-3-situation-summary-review-of-2020-fisheries-and-summary-of-2021-stock-forecasts.pdf/>

Proposed Method

Current Method

The current approach to developing preseason forecasts of returning natural-origin WB coho salmon combines estimates of smolt outmigration with estimates of marine survival. Smolt estimates are generated by scaling presumed Willapa basin smolt production to the observed smolt production in the Chehalis River based on relative habitat quantity, with the Chehalis basin abundance derived by regressing past abundances against flow characteristics (abundances in previous years are directly estimated by expanding a count of tagged smolts by the proportion of tagged fish in terminal catch). Marine survival estimates are generated by relating the coded wire tagged (CWT) natural-origin Bingham Creek smolt to adult survival estimates to environmental covariates in multiple linear regressions.

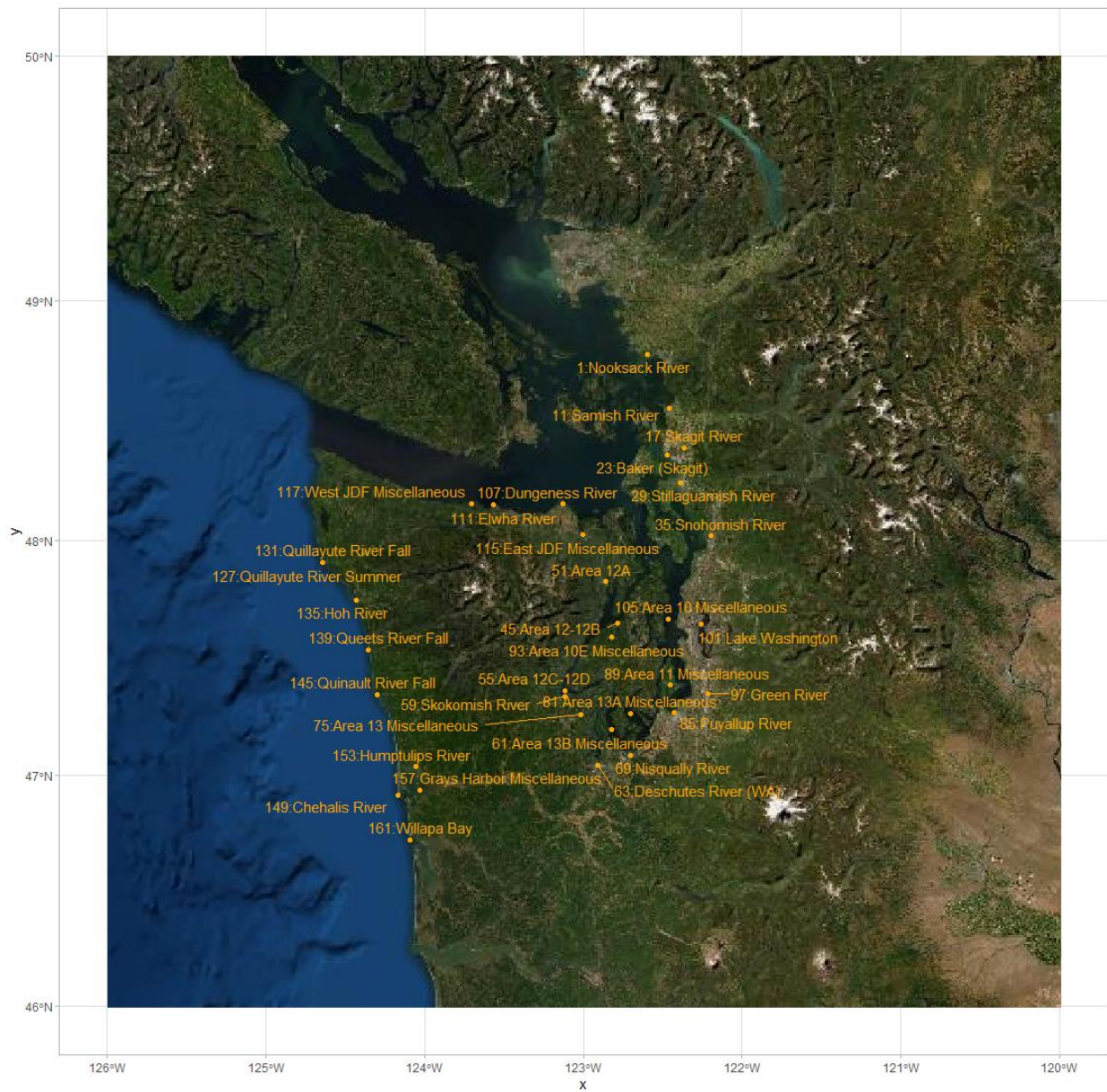
Proposed new method: overview and data sources

The proposed new approach applies the forecast models and the model evaluation approach developed by DeFilippo et. al (2021) (attached). The models include both a multi-population spatio-temporal integrated population model (STIPM) and naïve timeseries models, which are then compared in their performance, thereby facilitating model selection or model averaging to attain a final forecast. To operationalize this research, we updated source datasets, reviewed and translated the original analysis script into a streamlined workflow, and re-evaluated model fit and performance.

In the current implementation, predictions are calculated for natural-origin Willapa Bay coho salmon alongside 33 other natural-origin Washington coho salmon stocks tracked within the coho version of the Fishery Regulation Assessment Model (FRAM²). The annually-updated FRAM database provides estimated spawning escapement and harvest-related mortality, including both terminal and pre-terminal catches, the sum of which constitute pre-fishery run size, which is the target for forecasts. While the naïve time-series models only utilize pre-terminal run size, the STIPM also make use of estimates of released and recovered coded wire tagged natural- and hatchery-origin coho smolts, which are indexed to the FRAM stock units and extracted from the Regional Mark Information System (RMIS) database to inform marine survival parameters. Finally, WDFW and Tribal Co-manager staff provide estimates of smolt outmigration from several long-term monitoring stations that are also indexed to FRAM stock units.

The latest available versions of these data form a full dataset, from which progressive subsets of years are used in a “one-ahead” evaluation of forecast skill. In contrast to leave-one-out or other cross validation on the full span of years, this more closely mimics the data that would be available to generate future predictions in a given year. The resulting performance measures then assess the relative accuracy and precision of candidate models and quantitatively characterize their behavior (e.g., the absolute magnitude of forecast error as well as the tendency to under- or over-forecast). As a result of implementation in a Bayesian framework, full posterior distributions are produced for each forecast, enabling robust quantification of uncertainty and facilitating risk-based management.

²Coho FRAM is used by the PFMC Salmon Technical Team (STT) to plan annual fisheries and by the Pacific Salmon Commission Coho Technical Committee to perform post-season review. It includes a coast-wide set of unmarked and marked units of natural and hatchery stocks, accounting for landed and non-landed mortality to age 3 fish through 5 calendar year time steps. See https://framverse.github.io/fram_doc/ for additional information.



86

87 *Figure 1: Washington natural-origin coho populations included in the full dataset, showing Coho FRAM StockID*

88

89 *Model description*

90

91 The proposed approach involves fitting candidate models to a training dataset and comparing
 92 their one-year-ahead forecast performance over the most recent 11 years relative to
 93 observations. This approach then allows selection of a best model according to one-ahead
 94 performance measures or facilitates model-averaging of forecasts weighted by prior
 95 performance.

96

97 While future work may add ensemble members (see Discussion), the current implementation
98 includes the STIPM (Figure 2-3) along with a multi-population naïve time-series model (state-space
99 lag-1 auto-regressive AR1; Figure 3). For the state-space AR1, parameters are estimated
100 independently for each population based on the run-size in past years (through the most recent
101 year of available data, which is typically 2-3 years prior to the year of interest).

102
103 The STIPM is fundamentally a population dynamics model. For each population, adult escapement
104 in one generation is used to estimate smolt recruitment via a Beverton-Holt function, pre-fishery
105 run size is estimated by multiplying smolt abundance and year- and population-specific estimates
106 of marine survival, and escapement is estimated by subtracting estimated harvest from run size.
107 The model parameters are informed jointly by multiple likelihood contributions, within a Bayesian
108 model fitting framework, that compares state estimates with observations at multiple points in the
109 coho life cycle:

- 110
111 1) Adult escapement estimates (states) from the model are fitted to FRAM escapement
112 estimates that are treated as observations,
113 2) Smolt abundance estimates (states) from the model are fitted to smolt abundance
114 estimates that are treated as observations (when available for a particular population
115 and year),
116 3) Marine survival estimates (states) from the model are fitted to CWT releases and
117 expanded recoveries (when CWT data for wild coho are available for a particular
118 population and year). For other populations, estimates of marine survival are fitted to
119 CWT releases and expanded recoveries from a spatially paired hatchery population
120 after adjustment for a hatchery-specific deviation from estimated natural-origin survival
121 (with this deviation itself estimated), and
122 4) Harvest estimates (states) from the model are fitted to FRAM harvest estimates that are
123 treated as observations.

124
125 Population-specific parameters are estimated hierarchically, allowing populations to share
126 information and for data-poor populations to benefit from more data-rich populations.
127 Marine survival estimates are estimated using a spatio-temporal Gaussian process, in which
128 spatial correlation in the temporal evolution of marine survival is estimated and facilitates
129 sharing of information across space and time to inform marine survival estimates for all
130 populations and years, regardless of whether smolt data or CWT data are available. Priors
131 for most parameters (and hyperparameters) were vague, uninformative, and/or designed to
132 avoid biologically improbable or impossible parameter space. Notable exceptions included
133 the productivity and capacity among-population hyper-means and hyper-variances, which
134 were given priors based on the results reported in Barrowman et al. (2003) but were
135 widened to account for the possibility that populations in our dataset differed in their central
136 tendencies from those in Barrowman. Regardless, all prior-posterior pairs were compared to
137 ensure that priors were not driving posteriors at the expense of information contained in
138 likelihoods.

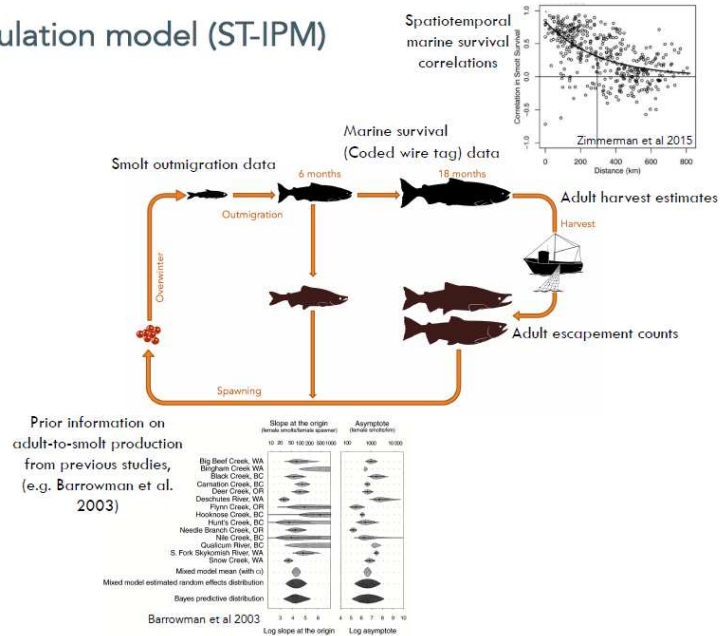
139
140 Full descriptions of the models above, their equations, priors, and extensive model
141 convergence and model fit diagnostics are described in DeFillipo et al. (2021) and its
142 supplementary materials.

143
144 A final model developed for this SSC review, which was not included in the DeFillipo et al.
145 (2021) paper, is the use of a simple tailing mean of abundance, which involved taking the 3-

146 year arithmetic mean of available FRAM run-size observations at various year lags prior to
 147 the forecast year. No estimates of uncertainty are available for this method, and it is not a
 148 formal statistical model, but is provided for comparison since it has been a common method
 149 used by state fishery managers to develop salmon forecasts. It also illustrates the scope to
 150 add alternative models that may be of interest.

Spatiotemporal integrated population model (ST-IPM)

- 1) Integrated model structure
 - Propagates uncertainty
 - Uses all available data
- 2) Bayesian Hierarchical design
 - Share information between stocks
 - Introduce prior information from previous studies
- 3) Spatiotemporal marine survival modelling
 - Predict marine survival using spatial and temporal autocorrelation



151
 152 *Figure 2 Conceptual overview of STIPM model*

Performance evaluation

Theoretical considerations

155 There are numerous methods available to evaluate model performance, and these differing
 156 options may produce different results when applied to a particular set of models. Consequently, it
 157 is important to consider a model's desired application in order to select the appropriate model
 158 evaluation method. Many model evaluation methods involve calculating the fit of the model to an
 159 entire dataset. However, these methods can over-estimate model skill for out-of-sample prediction
 160 tasks because model skill evaluations using the whole dataset involve comparing model
 161 predictions with observations that were used in fitting the model; a situation that is unrealistic for
 162 out of sample prediction tasks.

163 To avoid overestimates of model performance for out-of-sample prediction tasks, performance
 164 evaluation in these cases should involve dividing a dataset into two random subsets, fitting a
 165 model to the first random "training" dataset and evaluating its predictive performance on second
 166 random "validation" dataset that has been held out of the original model fitting routine.
 167 Alternatively, a model may be iteratively fitted to different random subsets of an entire dataset
 168 and performance calculated on based on predictions of the left-out subset of observations during
 169 each iteration (e.g., k-fold or leave-one-out cross validation). While such methods provide robust
 170 estimates of out-of-sample prediction skill for applications where the data points we hope to

174 predict are randomly distributed with respect to the training set (e.g., results from a randomized
175 field experiment), these methods are ill-suited to future predictions using time-series models where
176 the data points to be predicted are inherently non-random (i.e., they occur later in time than the
177 observations). As a result, k-fold and leave-one-out cross validation methods will also tend to
178 over-estimate model skill for future prediction tasks (Burkner et al. 2020).

179

180 To determine a model's skill at predicting the future, performance evaluation methods should
181 directly measure model performance in predicting future data points. To accomplish this, an
182 evaluation of future prediction skill can be made by iteratively refitting models to progressively
183 larger subsets of a full timeseries in which future datapoints have been left out, and then
184 evaluating model performance in predicting the future datapoint(s) of interest. Since the desired
185 application for all models discussed herein is prediction of future run-sizes, all evaluations of
186 model performance are based on iterative leave-future-out model fits to a progressively
187 expanded training set (adding years to a shared initial portion of the series). See Figure 3 for a
188 schematic of this process.

189

190 *Performance evaluation approach*

191

192 DeFilipo et al. (2021) compared one-step-ahead performance of the STIPM and three naïve
193 time-series models (random walk, AR1, MA1) against a compilation of the historical preseason
194 forecasts of record supplied by managers for the selected stocks. They calculated model
195 performance scores, including Mean Absolute Scaled Error (MASE), Root Mean Squared Error
196 (RMSE), and Median Symmetric Accuracy (MSA) and found that the STIPM and naïve timeseries
197 models generally provided modest but consistent improvements in forecast skill relative to
198 historical forecasts of record. In addition, the STIPM generally performed the best of the models
199 developed by DeFilippo et al. (2021); however, the best model varied among populations and
200 differences between the models were often minor.

201

202 Theoretically, the ability to incorporate more recent data into forecast model fitting should
203 substantially improve forecast skill. Therefore, in addition to comparing among candidate models,
204 we were interested in determining how both absolute and relative (among model) performance
205 were affected by the number of years between the forecast year of interest and the data used in
206 forecasting that year. To evaluate the influence of data lag on forecast skill we assessed model
207 performance against observed returns subject to alternative temporal lags in the available data
208 used in model fitting. One-ahead forecasts were developed for the years 2009 to 2019, based
209 on data subsets spanning 1998 to one, two or three years prior to the predicted year. For
210 example, a 2009 prediction was generated from spawning escapement and harvest estimates
211 from 2008, 2007, and 2006 for the lag-1, lag-2 and lag-3 alternatives. For the purposes of
212 forecasting a given year, preliminary escapement and harvest estimates from the prior year (i.e.,
213 lag-1) may be available for some stocks, but the lag-1 represents more of a "hypothetical best
214 case" than a practically likely alternative. The lag-2 (e.g., with 2007 data available to forecast
215 2009) constitutes a plausible best case under current data management timelines (i.e., these data
216 are typically being compiled for reporting and evaluation concurrently with the timing of
217 preseason forecasts), while the lag-3 serves as a realistic worst case of which data are available,
218 with the PSC CoTC having completed post-season FRAM runs for this year.

219

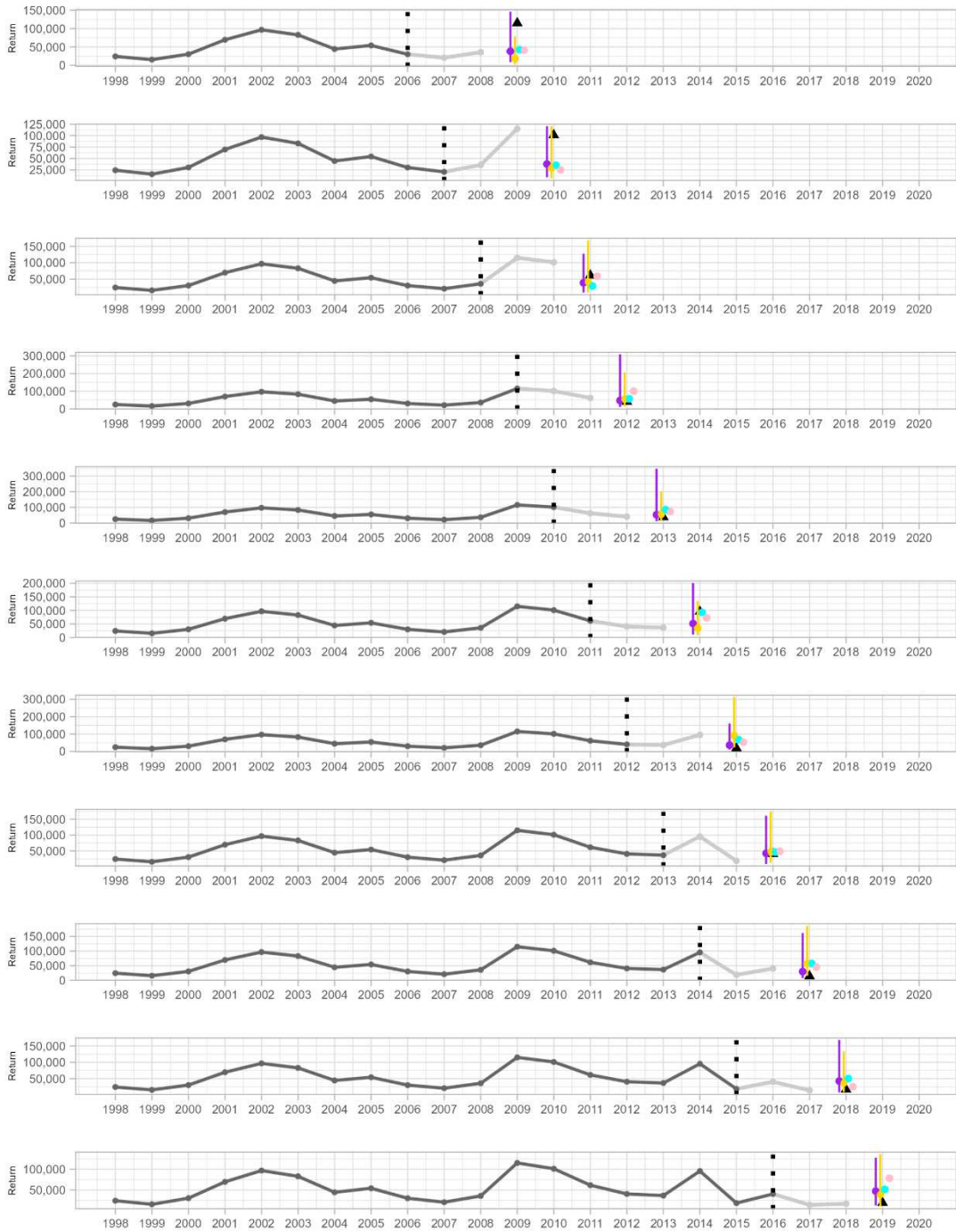
220 Before conducting the one-ahead exercise, we modified the original dataset by removing two
221 FRAM units known to lack a biological basis (Port Gamble Bay Wild and Area 7/7A Independent
222 Wild); we limited the years evaluated to those from 1998 onward that are known to be reliable

223 in the FRAM post-season database; and we added observations made after 2015. We also
224 made minor revisions to the AR1 Stan code (reparameterization) to facilitate improved
225 convergence. Data manipulation revisions followed a line-by-line cross-check process against the
226 original to ensure the fidelity and appropriateness of assigned objects. Finally, we followed
227 DeFilippo et al. (2021) in assessing convergence for the one-ahead model fitting.
228

229 *Performance evaluation results*

230
231 Under the lag-3 scenario of data availability (which we consider the most conservative/worst
232 case scenario), the AR1 and STIPM models exhibited similar performance, which was better than
233 the performance of the trailing mean or historical forecasts. Median symmetric accuracy was
234 used to assess model performance (MSA—a model skill measure that is based on the log
235 accuracy ratio, is interpretable as a percentage, is robust to outliers, and equally penalizes over-
236 and under-forecasts; Morley et al. 2018). The lag-3 AR1 and STIPM posterior medians had MSA
237 values of 94% and 117% respectively, which was an improvement over the lagged trailing mean
238 and previously submitted forecasts (166% and 147%, respectively; Table 1). The two models
239 produced a mixture of under- and over-forecasts related to large year-to-year reversals in the
240 time series, as well as longer-term variation in population abundance (Figures 3 and 4). For
241 example, both models underpredicted the large 2014 run while overpredicting the low 2015
242 return, and the smaller returns of 2006-2008 influenced the accuracy of predicting the relatively
243 large returns at the beginning of the one-ahead series (2009 and 2010). The observed returns in
244 2018 and 2019 fell within the 95% credible interval of both models but were below the 25th
245 percentiles of the posterior distributions (Figure 4). More broadly, all four models (AR1, STIPM,
246 trailing 3-year mean, and actual historical forecast) under-forecasted early in the time-period,
247 oscillated between under- and over-forecasts in the middle of the time period, and over-
248 forecasted in the most recent years (Figures 4 and 5), which were some of the lowest run-sizes in
249 the record for Willapa coho.

250
251 In addition to evaluating the performance of the new models under the worst-case scenario for
252 data availability, we were interested in determining what the utility of more recent data would
253 be for improving coho forecasts. Comparing among models and among all data lags, the lag-1
254 ST-IPM showed the best overall median symmetric accuracy (65%), and all models generally
255 performed better than at progressively larger time lags (Figure 6, Table 1). Interestingly, model
256 error for the lag-2 forecasts was generally greater than lag-3, which is an unexpected result and
257 likely an artifact of the short set of one-step-ahead years evaluated rather than a result that can
258 be expected to persist in the future. Although the lag-1 alternative is not currently realistic, these
259 results suggest that a faster data management cycle might yield appreciable gains in preseason
260 forecast accuracy.
261

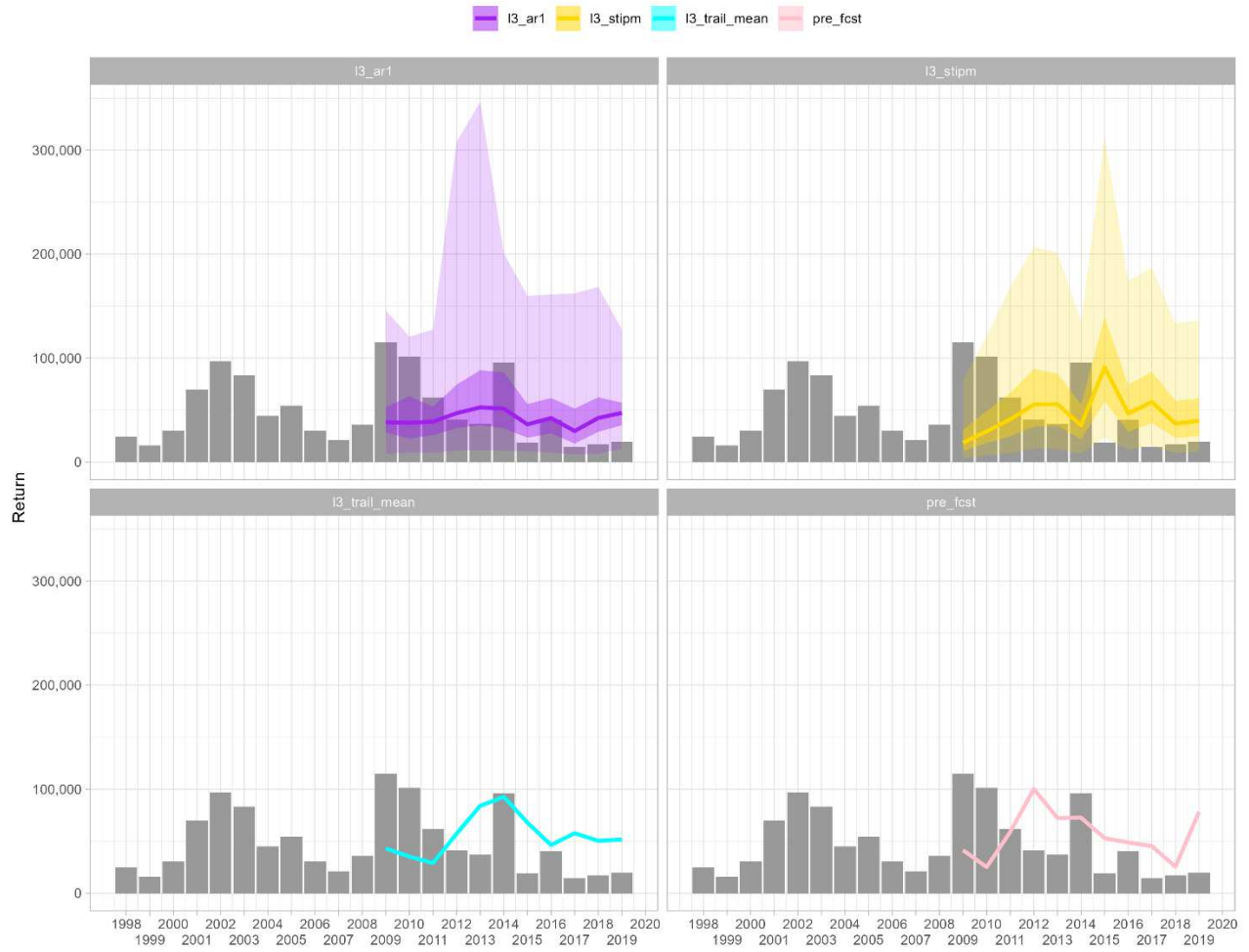


262
 263
 264
 265
 266
 267
 268
 269

Figure 3 Schematic of one-ahead forecasts used in model performance assessment. One-ahead lag-3 posterior median forecasts (filled circles, with 95% credible intervals) for AR1 (purple) and STIPM (gold) are shown alongside the observed return in the forecast year (black triangles), the previously submitted preseason FRAM forecast (pink), and the lagged 3-year trailing mean (cyan). In each panel, the darker shaded line shows the years of observations used in model fitting to generate the single year forecast, and the lighter shading (separated by the vertical dashed line) indicates the years of observations that were not used in model-fitting (under the lag-3 scenario, they would not have been available at the time of forecast preparation. Note varied Y-axis scale across panels to accommodate 95% CI.

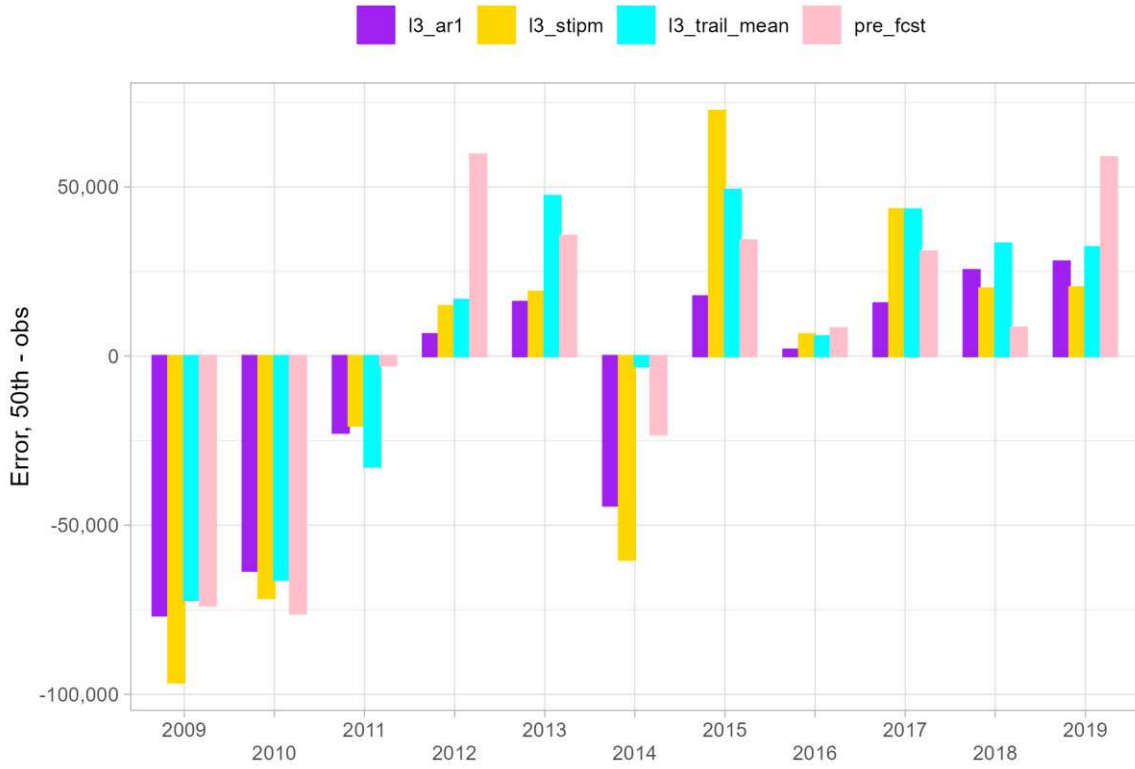
270

Willapa Bay Natural



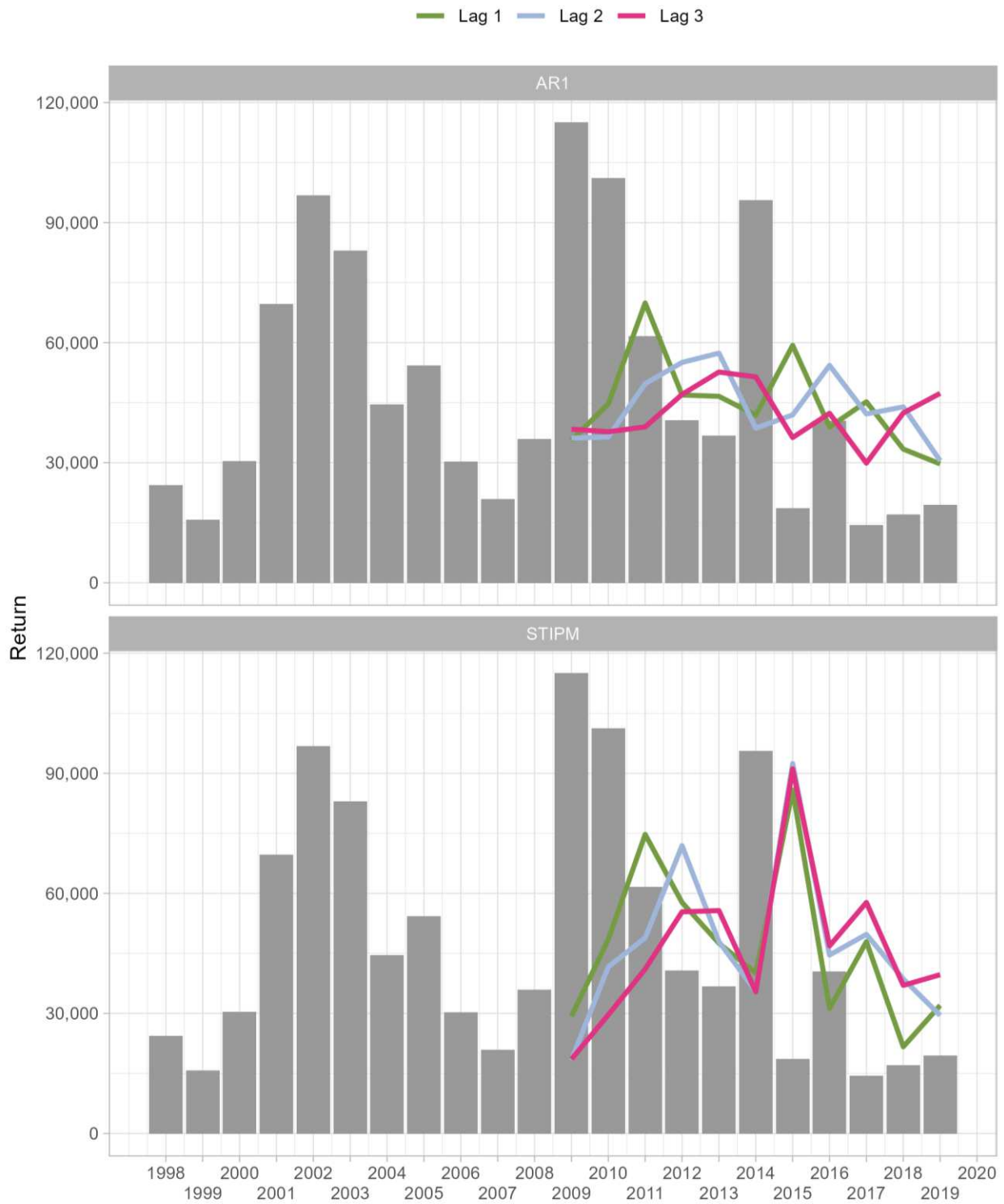
271
272
273
274

Figure 4 Observed Willapa Bay run-size (bars) and one-ahead lag-3 posterior median forecasts (heavy line) with 50% and 95% credible intervals (darker and lighter shaded ribbons, respectively) for AR1 (purple) and STIPM (gold) models. Also shown are the previously submitted preseason FRAM forecast (pink), and the lagged 3-year trailing mean (cyan).



275
276
277

Figure 5 One-ahead Willapa Bay coho run size forecast error of posterior median (AR1, purple, and STIPM, gold), the point estimate of the lagged 3-year trailing mean (cyan), and the previously submitted preseason FRAM forecast (pink).



278

279
280
281

Figure 6 Posterior medians of one-ahead forecasts generated with the AR1 model (top panel) and STIPM model (bottom panel) with observed run-sizes (bars) for comparison. Line colors show different lags between the forecast year, and the most recent year of data used in fitting the model.

One-ahead Performance Measures				
AR1 and STIPM calculated from posterior median				
	msa	me	mpe	rmse
Lag 1				
AR1	96.0%	-6,209	15.5%	37,632
STIPM	65.2%	-3,995	27.1%	42,317
TRAIL_MEAN	84.8%	2,203	36.4%	41,583
Lag 2				
AR1	125.1%	-6,739	35.6%	39,065
STIPM	126.6%	-3,758	30.7%	47,728
TRAIL_MEAN	148.4%	3,216	42.4%	43,666
Lag 3				
AR1	94.7%	-8,723	15.9%	36,478
STIPM	117.1%	-4,755	36.4%	49,570
TRAIL_MEAN	166.0%	4,900	40.9%	42,217
Previous FRAM forecast	146.7%	5,463	49.2%	45,002
Median Symmetric Accuracy (MSA), Mean Error (ME)				
Median Percent Error (MPE), Root Mean Square Error (RMSE)				

283
284
285

Table 1 Summary forecast accuracy measures of 2009-2019 one-ahead predictions. Shown are median symmetric accuracy (MSA), mean error (ME), median percent error (MPE), and root mean square error (RMSE).

286

287

Discussion

288

289 We propose to implement a systematic forecasting approach that leverages available data while
 290 rigorously presenting uncertainty. Within that framework, we propose to use multiple peer-
 291 reviewed models including both a biologically driven IPM and a naïve timeseries model, both of
 292 which are aligned with existing management units and well-integrated with real-world workflows
 293 and timelines for data compilation.

294

295 In its current form the proposed forecast method addresses several concerns that have been
296 raised with respect to past approaches. Perhaps most significant is the explicit incorporation of
297 escapement and harvest observations specific to the WB natural-origin population. In addition,
298 marine survival estimates based on CWTs from the WB hatchery coho stock are included
299 alongside the previously considered Bingham Creek natural-origin CWT and smolt migrant
300 records (as well as those for other WA coastal stocks, e.g., Humptulips, Hoh, Quillayute, etc.).
301

302 Beyond the direct inclusion of WB data, a core advantage of the proposed framework is the
303 ability to examine and compare forecast options readily and reproducibly. The scripted one-
304 ahead performance evaluation provides a nuanced view of how and when alternative forecast
305 methods produce inaccurate predictions and facilitates a robust means of either selecting a best
306 model or performing weighted model-averaging to develop a best model.
307

308 In addition to incorporating WB data and facilitating robust model evaluation, the hierarchical
309 state-space models quantify forecast uncertainty and thereby facilitate a more rigorous discussion
310 of risk and tradeoffs in policy processes. By generating full posterior distributions for forecasts,
311 managers can identify the probability that the observed run size will be smaller (or greater) than
312 any value of interest, thereby facilitating season setting that contains risks within levels deemed
313 acceptable.
314

315 *Future work and additional STIPM applications*

316

317 Beyond short term forecasting, the development of the biologically-based STIPM creates a host of
318 other opportunities to better understand the status of natural origin Washington Coho stocks. For
319 example, the spatio-temporal model of marine survival could be used to generate marine survival
320 spatially continuous “heat maps” over past decades, which could be used to examine factors
321 influencing marine survival and its evolution over time. The estimates of productivity and capacity
322 (i.e., posterior distributions of BH parameters) provide valuable empirically generated
323 information to relate to or update existing population reference points. Finally, the ability to
324 forecast forward with the model readily enables population viability analyses and even future
325 management strategy evaluation (i.e., the model can provide alternative realizations of the stock
326 in 10, 50 or 100 years, in which alternative harvest scenarios may be simulated).

327 Outside of these non-forecast benefits, and despite the forecast improvements of the current
328 proposed approach, several opportunities exist for subsequent refinement to address remaining
329 limitations. These can be divided into changes that apply more generally and those strictly
330 related to the STIPM.

331 332 Improvements for all models & approach

- 333 • *Use of covariates*
334 Neither the naïve timeseries models nor the STIPM include covariates to predict interannual
335 changes in survival or abundance. Candidate models of each type could be developed
336 that include environmental or other covariates thought to influence coho productivity, such
337 as ocean indicators, and these models could be competed against the current set of
338 models
- 339 • *Ensembles*

340 Currently our proposed approach involves fitting multiple models and calculating model
341 performance, which facilitates either selecting a best model or using performance statistics
342 to construct model-averaged forecasts. However, we have not yet performed a one-
343 ahead evaluation using different weighting methods to determine what weights provide
344 optimal model-averaged ensemble forecasts.

- 345 • *Columbia River and other FRAM stocks*

346 The current forecast approach covers all populations in Washington State except the
347 Columbia River. The current approach could easily be extended to include the two
348 Washington State Columbia River stocks, or even stocks outside Washington.

349 Additional STIPM Improvements

- 351 • *Include additional smolt trapping data*

352 Time series of smolt trap observations that could not be readily reconciled with Coho
353 FRAM stocks were not included. However, future work could examine how best to
354 integrate these valuable data.

- 355 • *Hatcheries*

356 A current limitation of the STIPM identified by DeFillipo et al. is its inability to quantify the
357 contributions of hatchery spawners to natural origin recruitment. As a result, productivity
358 parameters are likely artificially inflated due to the presence of recruits produced by
359 hatchery spawners in some populations. Incorporating hatchery spawner contributions,
360 including the potential to estimate any differences in their per-capita productivity, is
361 simple enough to accomplish within the STIPM given data that quantify the number of
362 hatchery fish escaping to spawn naturally in each of the FRAM units. Unfortunately, we are
363 unaware of a comprehensive, consistently compiled dataset of this type, despite various
364 population monitoring programs that estimate the proportions of hatchery and natural
365 origin spawners annually. Future efforts to translate monitoring program results into
366 comparable FRAM unit estimates could facilitate better accounting for the contributions of
367 hatchery spawners, likely both improving forecasts and aiding estimation of more accurate
368 biological reference points.

- 369 • *Spatial Kernel*

370 Currently, a squared exponential kernel utilizing Euclidean distance is used to model the
371 spatio-temporal evolution of marine survival. However, Euclidean distance is likely a less
372 relevant measure of spatial relatedness than distance by water. Distance by water was
373 not used because a squared exponential covariance matrix constructed with non-Euclidean
374 distances is not guaranteed to be positive definite. However, alternative spatial
375 covariance constructions such as Gaussian Markov Random Fields or Conditional
376 Autoregressive Models facilitate development of non-Euclidean covariance matrices in a
377 manner that ensures they are positive definite. Therefore, efforts should be made in the
378 future to explore non-Euclidean covariance structures that better reflect the biology of
379 spatially correlated changes in survival.

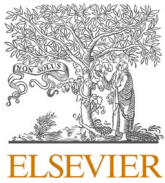
- 380 • *Habitat Quantity*

381 Currently, a static measure (not year-specific) of the length of linear stream habitat used
382 by coho salmon in each stock is used as an offset in the capacity parameter estimation.
383 However, available habitat is not static, and capacity is likely to change, particularly
384 after restoration (e.g., dam removal) or altered watershed management (e.g., forest
385 conversion or altered timber harvest) that result in large changes to available habitat.
386 These changes could be better accommodated by incorporating non-static estimates of
387 available habitat.

- 388
- *Observation error in CWT datasets*
- 389 Currently, CWT data used to estimate marine survival are assumed to be beta-binomially
390 distributed, where the (rounded) expanded number of CWT recovered are assumed to be
391 “successes” resulting from a series of binomial “trials” (CWT-tagged smolt releases), where
392 the probability of success is the estimated marine survival. As opposed to a standard
393 binomial, the observed probability of survival for each population and year can differ
394 from the underlying “true” survival probability due to an additional latent variance
395 generating process (such as the sampling-based expansion of raw coded wire tags to
396 expanded). While the beta-binomial is one approach to account for this latent variance in
397 CWT-based marine survival estimates, several methods have been developed by others
398 and could be compared (e.g., Satterthwaite et al. 2013, Allen et al. 2017, Shelton et al.
399 2018, Shelton et al. 2020).
- 400

References

- 401
402
- 403 Allen, S. D., W. H. Satterthwaite, D. G. Hankin, D. J. Cole, M. S. Mohr. 2017. Temporally varying
404 natural mortality: Sensitivity of a virtual population analysis and an exploration of
405 alternatives. *Fisheries Research*, 185: 185-197.
406 <https://doi.org/10.1016/j.fishres.2016.09.002>.
407
- 408 Barrowman, N.J., Myers, R.A., Hilborn, R., Kehler, D.G., Field, C.A., 2003. The variability
409 among populations of coho salmon in the maximum reproductive rate and
410 depensation. *Ecol. Appl.* 13, 784–793. [https://doi.org/10.1890/1051-0761\(2003\)](https://doi.org/10.1890/1051-0761(2003)013[0784:TVAPOC]2.0.CO;2)
411 [013\[0784:TVAPOC\]2.0.CO;2](https://doi.org/10.1890/1051-0761(2003)013[0784:TVAPOC]2.0.CO;2).
412
- 413 Bürkner, P., J. Gabry, and A. Vehtari. 2020. Approximate leave-future-out cross-validation for
414 Bayesian time series models. *Journal of Statistical Computation and Simulation*, 90(14):
415 2499-2523. DOI: 10.1080/00949655.2020.1783262.
416
- 417 DeFilippo L. B., T. W. Buehrens, M. Scheuerell, N. W. Kendall, D. E. Schindler. 2021. Improving
418 short-term recruitment forecasts for coho salmon using a spatiotemporal integrated
419 population model. *Fisheries Research*, 242: 106014.
420 <https://doi.org/10.1016/j.fishres.2021.106014>.
421
- 422 Morley, S.K., Brito, T.V., Welling, D.T., 2018. Measures of model performance based on the log
423 accuracy ratio. *Sp. Weather*. <https://doi.org/10.1002/2017SW001669>.
424
- 425 Satterthwaite, W.H., M. S. Mohr, M. R. O'Farrell, and B. K. Wells. 2013. A comparison of
426 temporal patterns in the ocean spatial distribution of California's Central Valley Chinook
427 salmon runs. *Canadian Journal of Fisheries and Aquatic Sciences* 70(4): 574 – 584.
428 <https://doi.org/10.1139/cjfas-2012-0395>.
429
- 430 Shelton, A. O., W. H. Satterthwaite, E. J. Ward, B. E. Feist, and B. Burke. 2018. Using hierarchical
431 models to estimate stock-specific and seasonal variation in ocean distribution, survivorship,
432 and aggregate abundance of fall run Chinook salmon. *Canadian Journal of Fisheries and*
433 *Aquatic Sciences* 67(1): 95-108. <https://doi.org/10.1139/cjfas-2017-0204>.
434
- 435 Shelton, A. O., G. H. Sullaway, E. J. Ward, B. E. Feist, K. A. Somers, V. J. Tuttle, J. T. Watson, W.
436 H. Satterthwaite. 2020. Redistribution of salmon populations in the northeast Pacific ocean
437 in response to climate. *Fish and Fisheries* 22(3): 503-517.
438 <https://doi.org/10.1111/faf.12530>.



Improving short-term recruitment forecasts for coho salmon using a spatiotemporal integrated population model

Lukas B. DeFilippo^{a,*,1}, Thomas W. Buehrens^{a,b}, Mark Scheuerell^c, Neala W. Kendall^b, Daniel E. Schindler^a

^a University of Washington, School of Aquatic and Fishery Sciences, 1122 NE Boat Street, Seattle, WA, 98105, United States

^b Washington Department of Fish and Wildlife, Olympia, WA, United States

^c U.S. Geological Survey Washington Cooperative Fish and Wildlife Research Unit, School of Aquatic and Fishery Sciences, University of Washington, 1122 NE Boat Street, Seattle, WA, 98105, United States

ARTICLE INFO

Handled by Steven X. Cadrin

Keywords:

Spatiotemporal
Integrated population model (IPM)
Forecast
Coho salmon
Marine survival
Gaussian process

ABSTRACT

Fishery managers often rely on forecasts of future population abundance to set allowable harvest quotas or exploitation rates. While there has been substantial research devoted to identifying environmental factors that can predict recruitment for individual populations, such correlations often degrade over time, thereby limiting their utility for management. Conversely, examining multiple populations at once to detect shared, spatially structured patterns can offer insights into their recruitment dynamics that are advantageous for forecasting. Here, we develop a population dynamics model for natural origin coho salmon (*Oncorhynchus kisutch*) stocks in Washington State that leverages spatial and temporal autocorrelation in marine survival to improve one-year-ahead forecasts of adult returns. Executed in a Bayesian hierarchical integrated modelling framework, our spatiotemporal approach incorporates multiple data types and shares information among stocks to estimate key biological parameters that are informative for forecasting. Retrospective evaluation of one-year-ahead forecast skill indicated that the spatiotemporal integrated population model (ST-IPM) outperformed existing forecasts of Washington State coho salmon returns by 25–38 % on average. Moreover, the ST-IPM estimates parameters that were previously non-identifiable for many stocks, and propagates uncertainty from multiple contributing data sources into model forecasts. Our results add to a growing body of work demonstrating the utility of spatiotemporal and integrated approaches for modelling population dynamics, and the framework developed here has broad applications to the assessment and management of coho salmon in Washington State and elsewhere throughout their range.

1. Introduction

A central challenge to forecasting fish population dynamics lies in anticipating environmentally-driven variation in recruitment (Cushing, 1982; Walters and Martell, 2004). While retrospective analyses can often detect relationships between environmental conditions and fish production for individual populations, such correlations are often weak and diminish over time, thereby limiting their utility for tactical management (Drinkwater and Myers, 1987; Myers, 1998; Walters and Collie, 1988, but see Hare et al., 2010; Scheuerell and Williams, 2005; Tommasi et al., 2017). Among the main reasons why such relationships may be unreliable are spurious correlations among autocorrelated time-series,

non-stationarity, and the confounding effect of multiple latent processes acting on fish stocks simultaneously (Kilduff et al., 2014; Litzow et al., 2019; Mueter et al., 2002b; Wells et al., 2017). Alternatively, recruitment may be better understood by examining multiple stocks at once to detect shared, spatially structured patterns (Myers and Mertz, 1998; Peterman et al., 1998; Pyper et al., 2001). Not only does a multi-population approach reduce the risk of spurious correlations, but spatial coherence in stock dynamics integrates across the many ecosystem processes that may be jointly influencing recruitment (Walters and Martell, 2004).

While recruitment patterns can be detected from spawner-recruit residuals or survival estimates, such data are often noisy and of

* Corresponding author.

E-mail address: ldefilip@uw.edu (L.B. DeFilippo).

¹ Present address: Resource Assessment and Conservation Engineering Division, NOAA Alaska Fisheries Science Center, Seattle, WA 98115, USA.

<https://doi.org/10.1016/j.fishres.2021.106014>

Received 18 February 2021; Received in revised form 4 May 2021; Accepted 10 May 2021

Available online 27 May 2021

0165-7836/© 2021 The Author(s). Published by Elsevier B.V. This is an open access article under the CC BY license (<http://creativecommons.org/licenses/by/4.0/>).

limited availability and scope (Myers et al., 1995). Inferences from short time-series with large measurement errors can be misleading (Clark and Bjørnstad, 2004; De Valpine and Hastings, 2002; Walters and Ludwig, 1981), and reliance on a single data type can exclude complementary information available from other sources. This is particularly disadvantageous in a multi-population context where biological quantities of interest may be informed by different types of data across stocks. Conversely, ‘integrated’ approaches to population modelling can use all available information to estimate parameters through a joint likelihood that captures and propagates the uncertainties in each contributing data source (Deriso et al., 1985; Fournier and Archibald, 1982; Maunder and Punt, 2013). Similar to state-space models (Valpine and Hilborn, 2005), integrated population models (IPMs) describe the data as noisy realizations of underlying biological processes which are represented as latent, unobserved states (Scheuerell et al., 2020). When structured hierarchically, IPMs can facilitate sharing information among data rich and data poor populations (Jiao et al., 2011; Punt et al., 2011) and are increasingly being used to estimate spatially structured biological dynamics (Cao et al., 2019; Grüss et al., 2019; Kristensen et al., 2014; Punt, 2019) and forecast population trajectories (Buhle et al., 2018).

In anadromous Pacific salmon (*Oncorhynchus* spp.), recruitment is typically defined as the number of mature adults that return from a given year-class (Ricker, 1954), which depends heavily on cohort survival during marine residency. Considered a critical period in the life cycle, conditions experienced during early marine residency are particularly influential in determining year-class strength (Beamish and Mahnken, 2001; Beamish et al., 2004; but see Ruggerone and Connors, 2015). Consequently, identifying drivers of salmonid early marine survival is a subject of substantial research interest (reviewed in Beamish, 2018; Chittenden et al., 2009; Percy, 1992). Such investigations have identified relationships between marine survival and environmental conditions expressed at basin (e.g. Pacific Decadal Oscillation (PDO), North Pacific Gyre Oscillation (NPGO); Di Lorenzo et al., 2008; Kilduff et al., 2015; Mantua et al., 1997), regional (e.g. coastal upwelling, sea surface temperature; Kilduff et al., 2014; Koslow et al., 2002), and local (e.g. estuaries; Mahnken et al., 1998; Teo et al., 2009) scales. As a result, recruitment can be correlated among populations at spatial scales that match those of the dominant oceanic features affecting survival (Mueter et al., 2002b, 2002a).

Here, we develop an integrated population model that leverages spatial correlations in marine survival to improve state-wide forecasts for Washington natural origin coho salmon (*O. kisutch*) returns. Pre-season forecasts for these stocks are used to determine allowable harvest rates each year such that under-forecasting can lead to foregone harvest opportunities, while over-forecasting may risk overfishing (Pacific Fishery Management Council, 2016). Most Washington coho salmon spend their first eighteen months in freshwater, after which they migrate to the ocean where the majority will spend another eighteen months before returning to spawn at age three. Historically, preseason forecasts for many of these stocks were based on sibling regressions (Peterman, 1982) which used observed returns of jacks — precocious males that mature after only six months at sea — to predict returns of ‘adult’ (age three) males and females originating from the same cohort. The rationale behind this approach is that if early marine survival is a key determinant of year-class strength, then returns of jacks that matured early but still experienced this critical period can inform the survivorship of the entire cohort. However, lack of reliable jack abundance data and weakening of the jack-to-adult relationship now limits the performance of sibling regressions for natural origin coho salmon in Washington. Consequently, many forecast methods currently in use rely instead on environmental indicators to predict marine survival (e.g. Rupp et al., 2012b; Zimmerman, 2018). Unfortunately, environmentally based forecasts have failed to predict large fluctuations in abundance in some years (e.g. Wainwright, 2021). In this study, we explore an alternative forecasting approach that relies on spatial and temporal auto-correlation in marine survival rather than sibling or environmental

relationships. Executed in a Bayesian hierarchical integrated modelling framework, our approach incorporates multiple data types as well as prior information, and facilitates sharing information among populations. Retrospective evaluation of one-year-ahead forecast accuracy from 2002 to 2017 indicated that the spatiotemporal IPM (ST-IPM) outperformed existing adult return forecasts by 25–38 % on average. Our results emphasize the utility of integrated and spatiotemporal approaches for modelling population dynamics, and the framework developed here has broad applications to the assessment and management of coho salmon in Washington State and elsewhere throughout their range.

2. Methods

2.1. Coho salmon life history

Mature coho salmon in Washington typically migrate upriver in late summer and fall to spawn between October and December in small streams and mainstem channels of larger rivers (Ohlberger et al., 2019). The year that a cohort is spawned is referred to as its ‘brood year’. Embryos produced in brood year y overwinter in the gravel and emerge as fry in the spring of year $y + 1$. Most juveniles then spend ~ 1 year rearing in freshwater before outmigrating to the ocean as smolts in spring of the following year ($y + 2$) from early April to early June. Most coho salmon spend roughly eighteen months at sea before returning to spawn in their natal habitats in the fall of year $y + 3$ (Bradford et al., 2000). However, some males mature and return to spawn as ‘jacks’ after only six months at sea. Because jack abundance data are generally of lower quality for many natural origin coho salmon stocks in Washington State and jacks comprise only a small portion of total cohort recruitment (Quinn, 2005), only age three individuals are considered in the present study.

2.2. Populations and data

Our analysis includes data from thirty-six coho salmon management units (henceforth ‘stocks’) throughout the Salish Sea (Puget Sound, southern Strait of Georgia, and Strait of Juan de Fuca) and Washington coast (Fig. 1, Table S1) which are currently forecasted for management purposes. These management units are defined in the Coho Fisheries Regulation Assessment Model (FRAM; Pacific Fishery Management Council Model Evaluation Workgroup, 2008), and may represent single spawning populations, or aggregations of multiple spawning populations. While all of these stocks are of natural origin (henceforth ‘wild’), unknown numbers of hatchery origin fish may also be present on the spawning grounds and counted towards the escapement.

The data types included in our integrated model are (1) quantity of habitat occupied by each population (stream length), (2) adult escapement counts, (3) harvest abundance, (4) smolt outmigration counts, and (5) coded wire tag (CWT) marine survival estimates (Table S1). The quantity of occupied habitat was obtained from SalmonScape, a Washington Department of Fish and Wildlife interactive web map of species distributions (<https://apps.wdfw.wa.gov/salmonscape/>) and included all habitat known or presumed to be used by coho salmon for spawning and/or rearing. Adult escapement and harvest numbers were generated by FRAM (Pacific Fishery Management Council Model Evaluation Workgroup, 2008), which obtains its escapement data from the Washington Department of Fish and Wildlife (WDFW) Salmon Conservation and Reporting Engine (SCoRE; (<https://fortress.wa.gov/dfw/score/score/species/coho.jsp?species=Coho>)) before aggregating it at the management unit spatial scale at which FRAM operates. These escapement data were generally derived from redd counts or area-under-the-curve estimates of live spawners expanded to account for un-surveyed areas and times. Smolt outmigration estimates were based on smolt trapping from WDFW and tribal comanagers (e.g., Anderson et al., 2019). Finally, CWT marine survival estimates were collated as part of the Salish Sea

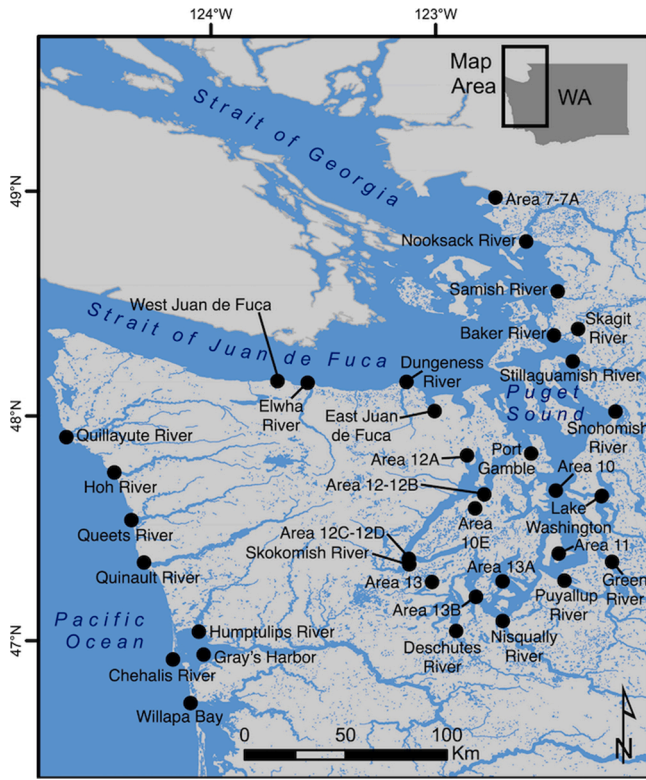


Fig. 1. Map of the Salish Sea and Washington coast with the marine entry points of all coho salmon stocks included in this study indicated by black circles.

Marine Survival Project (<https://marinesurvivalproject.com/>) as described in Zimmerman et al. (2015). The abundances of the stocks included in this study were highly variable, with arithmetic mean (\pm standard deviation) annual returns ranging from 264 ± 227 fish for Port Gamble Bay, up to $166,630 \pm 87,520$ fish for the Snohomish River, and a median average return of 9705 fish across all stocks (Table S2).

2.3. Model design

The ST-IPM specifies returns of adult (age three) coho salmon as the product of smolt production and marine survival. For stocks and years where smolt outmigration data are collected, these observations are available to inform predictions of adult returns. When these data are absent, smolt outmigration is predicted as a density-dependent function of spawner abundance (escapement) (Barrowman et al., 2003). While spawner-recruit relationships have limited utility for short-term forecasting (Walters, 1989) and watersheds become fully saturated at relatively low coho salmon spawner abundance (Bradford et al., 2000), escapement-based estimates of smolt production may provide a useful baseline for predicting variation in adult returns that is not explained by ocean mortality. Moreover, propagating uncertainty from the adult-to-smolt production relationships and data into model forecasts could be advantageous for managers wishing to consider forecast uncertainty in harvest control decisions.

Marine survival can be estimated using CWT data when available or inferred from the difference between smolt outmigration counts and adult returns for a given cohort. However, such information does not become available until after the fishing season, and thus cannot be directly used in forecasting. While CWT and smolt outmigration data can be used to estimate properties of marine survival time-series such as historical averages, autocorrelation, and recent trends that may be useful for forecasting (Winship et al., 2015), these data are only

available for a handful of stocks. For stocks that lack both CWT and smolt abundance data, the influences of juvenile production versus marine survival on adult returns cannot be distinguished.

The rationale behind the modelling approach presented here is to leverage the spatially correlated marine survival patterns of coho salmon (Coronado and Hilborn, 1998; Zimmerman et al., 2015) to share information among stocks. By assuming that nearby populations experience similar patterns of ocean mortality, retrospective estimates of marine survival time-series can be reconstructed even for stocks that lack informative data. Furthermore, by introducing prior information from previous studies (Barrowman et al., 2003; Thorson et al., 2015a) and adopting a hierarchical model design (Jiao et al., 2011; Punt et al., 2011), we can further refine estimates of marine survival and smolt production, allowing improved inference on statistical properties of these time-series that may be useful for forecasting.

2.3.1. Smolt production

For each coho salmon stock (i), the number of smolts ($R_{i,y}$) migrating to the ocean in a given calendar year (y) was assumed to depend on the number of spawners (escapement) two calendar years earlier ($S_{i,y-2}$) according to a Beverton-Holt function (Beverton and Holt, 1957):

$$R_{i,y} = \frac{S_{i,y-2}}{1 + \frac{a_i}{R_{max,i} d_i}} e^{\epsilon_{i,y}}, \epsilon_{i,y} \sim \text{Normal}(0, \sigma_{R_i}) \quad (1)$$

where $S_{i,y-2}$ and $R_{i,y}$ represent state estimates (*i.e.* model predictions) of the true spawner and smolt abundance respectively, a_i is a stock-specific productivity term describing the slope (in smolts produced per spawner) of the function at the origin, $R_{max,i}$ is the maximum asymptotic smolt production, expressed as the number of smolts produced per kilometer of habitat, and d_i is the kilometers of stream habitat for each stock (Barrowman et al., 2003). While the Ricker function is also commonly used for some Pacific salmon species, overcompensation is unlikely to occur in coho salmon (Barrowman et al., 2003; Bradford et al., 2000). Deviations from the Beverton-Holt adult-to-smolt relationship ($\epsilon_{i,y}$) were assumed to follow a lognormal distribution (Peterman, 1981) with a mean of zero and a variance of $\sigma_{R_i}^2$. To facilitate sharing information and allow for correlation between a and R_{max} , these parameters were modelled hierarchically as random variables arising from a common bivariate lognormal distribution that was shared among stocks (Buhle et al., 2018):

$$\theta_i = \begin{pmatrix} \log(a_i) \\ \log(R_{max,i}) \end{pmatrix} \sim \text{MVN}(\log(\mu_\theta), \Sigma_\theta) \quad (2)$$

where $\log(\mu_\theta)$ is the vector of lognormal hypermeans for the Beverton-Holt parameters ($\log(\mu_\theta) = \log(\mu_a), \log(\mu_{R_{max}})$) and Σ_θ is the variance-covariance matrix. To improve posterior sampling efficiency and mitigate the bias that can result from estimating hierarchical models using Monte Carlo methods (Betancourt, 2016; Monnahan et al., 2017), we implemented a multivariate extension of the non-centered parameterization, with the variance-covariance matrix Σ_θ decomposed into the Cholesky factor (L_{Ω_θ}) of the correlation matrix Ω_θ and a vector of error terms σ_θ (where $\sigma_a = \sqrt{\Sigma_{a,a}}$, $\sigma_{R_{max}} = \sqrt{\Sigma_{R_{max},R_{max}}}$):

$$\theta_i = \log(\mu_\theta) + \text{diag}(\sigma_\theta) L_{\Omega_\theta} z_{\theta_i} \quad (3)$$

where:

$$\Omega_\theta = L_{\Omega_\theta} L_{\Omega_\theta}^\top \quad (4)$$

and:

$$\Sigma_\theta = \text{diag}(\sigma_\theta) \Omega_\theta \text{diag}(\sigma_\theta) \quad (5)$$

In a non-centered parameterization, z_{θ_i} is a vector of standard scaling factors for each parameter and stock ($z_{a_i}, z_{R_{max,i}}$) that follows a normal distribution with a mean of zero and a standard deviation of one

(Betancourt, 2016; Monnahan et al., 2017). Of the thirty-six management units included in this study, smolt outmigration data of any kind were available for only nine, and among these, the data were typically available for only a subset of years (Table S1). Consequently, we chose to use informative priors based on the posterior distributions reported by a previous hierarchical analysis of coho salmon adult-to-smolt production (Barrowman et al., 2003). Note that that Barrowman et al. (2003) assume a 1:1 sex ratio and report the posterior mean of R_{max} in units of female smolts/km, which is doubled here to represent R_{max} in total smolts/km:

$$\text{Log}(\mu_a) \sim \text{Normal}(4.27, 0.75) \quad (6)$$

$$\text{Log}(\mu_{R_{max}}) \sim \text{Normal}(7.27, 2) \quad (7)$$

$$\sigma_a \sim \text{Normal}(0.43, 0.25) \quad (8)$$

$$\sigma_{R_{max}} \sim \text{Normal}(0.64, 0.25) \quad (9)$$

To explore prior sensitivity, we compared the resulting posteriors to those from model fits that used vague prior distributions (Fig. S1).

The Cholesky factor of the correlation matrix was drawn from an LKJ prior distribution (Lewandowski et al., 2009):

$$\mathbf{L}_{\Omega_0} \sim \text{LKJCorr}(\eta) \quad (10)$$

where η is a shape parameter that specifies the expected degree of correlation between α and R_{max} , which we fixed at 2, representing a weakly informative prior expectation of weaker correlation between parameters (Stan Development Team, 2020). Stock-specific standard deviations of Beverton-Holt adult-to-smolt errors (σ_{R_i}) were also modelled hierarchically among management units using a non-centered approach:

$$\log(\sigma_{R_i}) = \log(\mu_{\sigma_R}) + \sigma_{\sigma_R} z_{\sigma_{R_i}} \quad (11)$$

2.3.2. Marine survival

Marine survival was assumed to be density-independent (but see Emlen et al., 1990) and unrelated to variation in freshwater production (but see Chasco et al., 2021; Haeseker et al., 2012; McCormick et al., 2009). While there is evidence of density-dependence in the marine phase (e.g. Ruggerone and Connors, 2015), this is generally observed in more abundant species such as sockeye (*O. nerka*) and pink (*O. gorbuscha*) salmon, and operates based on the aggregate density of salmon in ocean foraging areas rather than the abundance of any one stock (Ohlberger et al., 2019; Pyper and Peterman, 1999; Ruggerone and Nielsen, 2004).

Information on a population's marine survival can come from CWT data or be inferred from the difference between smolt outmigration and adult returns. Of the thirty-six stocks included in our analysis, CWT data were available for only fifteen, and smolt outmigration data were available for an additional two (excluding the seven stocks for which both data exist) (Table S1). Because marine survival of southern coho salmon populations can be spatially correlated at relatively fine spatial scales (Zimmerman et al., 2015), we specified marine survival anomalies as a spatial Gaussian field (a Gaussian process in two or more dimensions, e.g. Ward et al., 2015; Webster et al., 2020) to facilitate sharing information among stocks. For each stock i , marine survival over time was expressed as a mean-reverting lag-1 autoregressive (AR-1) process of the form:

$$\text{Logit}(\lambda_{i,y}) = \begin{cases} \psi_i = \mu_\psi + \sigma_\psi z_\psi, & y = 1 \\ \mu_{\lambda_i} + \phi_i (\text{Logit}(\lambda_{i,y-1}) - \mu_{\lambda_i}) + \xi_{i,y}, & y > 1 \end{cases} \quad (12)$$

$$\xi_i \sim \text{MVN}(\mathbf{0}, \Sigma_\xi)$$

where $\lambda_{i,y}$ is the marine survival in year y for stock i and μ_{λ_i} is the mean of the logit marine survival time series for stock i , which followed a hierarchical normal distribution among stocks with hyperparameters μ_ψ and

σ_ψ . In model year-one, there is no previous state estimate to inform that year's marine survival so the time-series for each stock was initialized at ψ_i , which was hierarchically normally distributed among stocks with a mean of μ_ψ and a variance of σ_ψ^2 . The autocorrelation terms for each stock (ϕ_i) were drawn from uniform prior distributions bounded between -1 and 1. The marine survival deviations for each stock ($\xi_{i,y}$) were multivariate normally distributed with a mean of zero and variance-covariance matrix of Σ_ξ . The covariance between stocks i and j was expressed as a function of Euclidean distance between their marine entry locations according to a squared exponential kernel of the form:

$$\Sigma_{\xi_{i,j}} = \gamma^2 \exp\left(-\frac{(x_i - x_j)^2}{2\rho^2}\right) + \delta_{ij}\sigma_d, \delta_{i,j} = \begin{cases} 1, & i - j = 0 \\ 0, & i - j \neq 0 \end{cases} \quad (13)$$

where, x_i and x_j are the coordinates of the marine entry point for stocks i and j in eastings and northings, γ^2 is the marginal variance of the function, ρ is the length scale, and σ_d is the error standard deviation, which is applied only when $i = j$ according to the Kronecker delta function δ_{ij} .

2.3.3. Harvest and escapement

Of the individuals that survive natural marine mortality ($R_{i,y}\lambda_{i,y}$), a portion are harvested in fisheries:

$$C_{i,y} = R_{i,y-1}\lambda_{i,y-1}u_{i,y} \quad (14)$$

where $C_{i,y}$ is the number of individuals from stock i harvested in year y according to the exploitation rate $u_{i,y}$, which was specified as a multivariate random walk:

$$\text{Logit}(u_{i,y}) = \begin{cases} \vartheta_i = \mu_\vartheta + \sigma_\vartheta z_\vartheta, & y = 1 \\ \text{Logit}(u_{i,y-1}) + \epsilon_{i,y}, & y > 1 \end{cases} \quad (15)$$

$$\epsilon_i \sim \text{MVN}(\mathbf{0}, \Sigma_\epsilon)$$

The logit harvest rates for model year-one (ϑ_i) were initialized hierarchically as in eq. 12 with hyper-parameters μ_ϑ and σ_ϑ . Harvest process errors ($\epsilon_{i,y}$) were multivariate normally distributed with a mean of 0 and variance-covariance matrix Σ_ϵ , which was parameterized with a single variance term (σ_ϵ^2) on the diagonal, and covariance ($\rho_\epsilon\sigma_\epsilon^2$) on the off-diagonal elements (e.g. Holmes et al., 2012). The number of individuals returning to spawn in a given year ($S_{i,y}$) was then calculated as the difference between the total number of smolts that survived natural ocean mortality in the previous year ($R_{i,y-1}\lambda_{i,y-1}$) minus those that were harvested ($C_{i,y}$).

$$S_{i,y} = R_{i,y-1}\lambda_{i,y-1} - C_{i,y} \quad (16)$$

State estimates of spawning abundance were then used recursively in the subsequent estimation of smolt production (eq. 1).

2.3.4. Likelihoods

The observed smolt ($J_{i,y}$), escapement ($E_{i,y}$), and harvest ($H_{i,y}$) abundance data were assumed to follow lognormal likelihoods:

$$J_{i,y} \sim \text{Lognormal}(\text{Log}(R_{i,y}), \sigma_J) \quad (17)$$

$$E_{i,y} \sim \text{Lognormal}(\text{Log}(S_{i,y}), \sigma_E) \quad (18)$$

$$H_{i,y} \sim \text{Lognormal}(\text{Log}(C_{i,y}), \sigma_H) \quad (19)$$

where σ_J , σ_E and σ_H represent the observation error terms for the smolt, escapement and harvest data respectively, and $R_{i,y}$, $S_{i,y}$, and $C_{i,y}$ are the model-generated state estimates of smolt, escapement, and harvest abundance. The escapement observation error term (σ_E) could not be reliably estimated, and so was fixed at 0.2 and subject to testing with alternative values (e.g. Fleischman et al., 2013).

For the CWT data, the estimated number of tagged fish that were

recovered ($n_{i,y}$) was assumed to follow a beta-binomial likelihood with a number of trials ($N_{i,y}$) equal to the total number of tagged fish that were released, and a probability of recovery ($p_{i,y}$).

$$n_{i,y} \sim \text{Binomial}(p_{i,y}, N_{i,y}) \quad (20)$$

To allow for extra-binomial variance in tag recoveries (for instance, due to incomplete sampling of the harvest and escapement), the probability of recovery was assumed to follow a beta distribution, implemented as a conjugate prior to the binomial:

$$p_{i,y} \sim \text{Beta}(\alpha_{i,y}, \beta_{i,y}) \quad (21)$$

The shape parameters of the beta distribution ($\alpha_{i,y}, \beta_{i,y}$) were specified in terms of mode

(λ') and concentration (κ):

$$\alpha_{i,y} = \left(\lambda'_{i,y}\right)(\kappa - 2) + 1 \quad (22)$$

$$\beta_{i,y} = \left(1 - \lambda'_{i,y}\right)(\kappa - 2) + 1 \quad (23)$$

where $\lambda'_{i,y}$ corresponds to the adjusted state estimate of marine survival. For ten of the stocks in our study, available CWT data were collected from an adjacent hatchery rather than the wild stock itself. Hatchery and wild coho salmon populations have been shown to exhibit similar trends and interannual patterns in marine survival, but average mortality is typically lower for wild stocks (Coronado and Hilborn, 1998). As such, a hierarchically distributed offset term (e.g. Ohlberger et al., 2019) was applied to the likelihood to account for hatchery-specific deviations in survival from associated wild populations:

$$\text{Logit}(\lambda'_{i,y}) = \begin{cases} \text{Logit}(\lambda_{i,y}), & h_i = 0 \\ \text{Logit}(\lambda_{i,y} + \tau_i), & h_i = 1 \end{cases} \quad (24)$$

Here, τ_i is the marine survival offset term for stock i which is applied if the marine survival data for that stock is based on a hatchery ($h_i = 1$). For stocks with marine survival data based on CWT recoveries of wild fish ($h_i = 0$) no adjustment is required. The hatchery offset terms themselves were hierarchically distributed:

$$\tau_i = \mu_\tau + \sigma_\tau z_{\tau_i} \quad (25)$$

where μ_τ is the average offset term among stocks and σ_τ is the standard deviation.

2.4. Model estimation and validation

Posterior sampling was performed via Hamiltonian Monte Carlo (HMC) No-U-turn sampling (NUTS) through the Stan model building software (Stan Development Team, 2020), implemented in R (R Core team, 2015) via the Rstan package (Gelman, 2014). Sampling occurred using five HMC chains with lengths of 2000 iterations (for simulated forecast trials) to 20,000 iterations (for fits to the complete data set). The first half of samples was discarded as a "warmup" and each subsequent sample was saved to build the posterior distribution. Convergence was assessed using the Gelman-Rubin diagnostic (Gelman & Rubin, 1992) and effective number of samples, as well as trace-plots and autocorrelation plots of HMC chains. Posterior sampling was monitored for divergent transitions and low Bayesian Fraction of Missing Information (BFMI), neither of which were present in fits to the complete data set. Model goodness of fit was assessed by examining model fits to the observed data (Fig. S2) and comparing the model's predictive distributions to observed data (posterior predictive check, Fig. S3). Model performance was assessed by simulating data with known parameter values and evaluating the model's ability to recover them (Fig. S4-S6). Prior influence was examined by comparing prior and posterior distributions for model parameters (Fig. S7). A complete glossary of all model terms and prior distributions can be found in Table S3.

2.5. Forecast evaluation

The ST-IPM generates one-year-ahead adult return forecasts for a given calendar year y by multiplying the preceding year's marine survival ($\lambda_{i,y-1}$) and smolt outmigration estimates ($R_{i,y-1}$) for each stock. In simulated forecast trials, we assume that model fits are informed only by data that would realistically be available to biologists and managers at the time of forecast development. According to the current management cycle, preseason forecasts of adult returns for the fall of year y are prepared in January of year y , when the most recent smolt outmigration data available are from year $y-1$. However, while harvest data from fall of year $y-1$ will have been collected by January of year y , these data are seldom formalized and entered into widely accessible databases at this point in time. As such, we assume that only harvest data up to year $y-2$ are available for conditioning model forecasts of year y . Similarly, only CWT recoveries from outmigrating smolts tagged in year $y-3$ are assumed to be available for forecasts of year y due to the constraints of collecting and processing these data. The time at which the escapement data become available is variable among management units, but we assume that at least preliminary escapement estimates for year $y-1$ would be available in January of year y to inform forecast development.

To provide both sufficient training data to condition the model and enough simulated forecasts to reliably calculate performance metrics, we produced one-year-ahead forecasts of adult returns for 2002–2017. Forecast accuracy was calculated using the arithmetic mean absolute scaled error (MASE):

$$\text{MASE}_{i,y} = \frac{|P_{i,y} - A_{i,y}|}{\frac{1}{n-1} \sum_1^n |A_{i,t} - A_{i,t-1}|} \quad (26)$$

Where $P_{i,y}$ is the forecasted adult return (sum of model-estimated harvest ($C_{i,y}$) and escapement ($E_{i,y}$)) for stock i in year y , $A_{i,y}$ is the observed return (the sum of the observed harvest and escapement), and $\frac{1}{n-1} \sum_1^n |A_{i,t} - A_{i,t-1}|$ measures the degree of interannual variability between training years (t) in the observed adult returns during the training period of length n years. MASE has a number of advantages over alternative accuracy metrics (e.g. Mean absolute predictive error (MAPE), Root mean square error (RMSE)), including scale independence, symmetry, insensitivity to outliers, and interpretability (Hyndman and Koehler, 2006; Ward et al., 2014). We also compared forecast accuracy using RMSE, and Median Symmetric Accuracy (MSA) of the Log Accuracy Ratio (LAR) (Morley et al., 2018), which did not qualitatively alter our findings (Table S4). For all metrics, forecast skill was evaluated with respect to both the observed adult abundance data, as well as state estimates produced by the ST-IPM conditioned on all years' data (Table S4, Fig. S9-S10). We compared the forecast skill of the ST-IPM to published records of past forecasts for these stocks that were agreed upon by the state and tribal co-managers. The methods used to generate these forecasts vary among management units and over time, and the specific details of each approach are not necessarily publicly documented. In addition to the published forecasts, we also compared the performance of the ST-IPM to state-space implementations of several common univariate time-series models fitted to the adult return data, including a random walk and lag -1 autoregressive (AR-1) and moving average (MA-1) models.

3. Results

3.1. Smolt production

There was substantial variability among coho salmon stocks in both smolt productivity (α) and capacity (R_{max}) (Figs. 2 and 3). Median smolt capacity among stocks ($\mu_{R_{max}}$) was estimated to have a median value of 687 smolts/km (95% credible interval = 487 to 960 smolts/km), with a

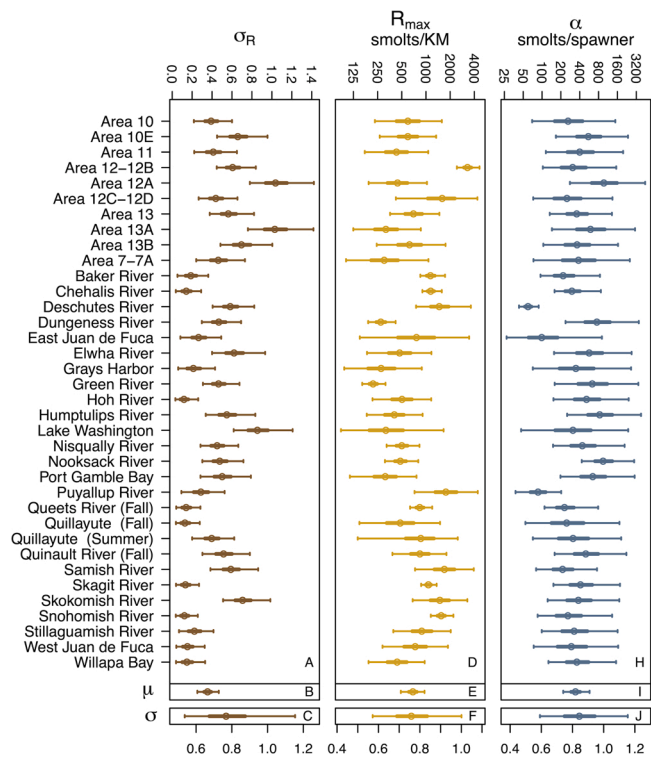


Fig. 2. Posterior distributions of Beverton-Holt adult-to-smolt parameters. Circles represent the posterior medians, and thick and thin lines represent 50 % and 95 % credible intervals respectively. Left-hand panels (A, B, C) depict posterior distributions for the error terms (σ_R) of the adult-to-smolt relationship, middle panels (D, E, F) show posteriors for asymptotic smolt production (R_{max}), and right-hand panels (H, I, J) show posteriors for productivity parameters (α). Parameters for individual stocks are shown in panels A, D, and H, and exponentiated lognormal means and lognormal standard deviations are indicated by μ and σ symbols respectively (panels B, C, E, F, I, J).

lognormal standard deviation ($\sigma_{R_{max}}$) of 0.76 (95% credible interval = 0.57 to 1.0). Note that we do not apply a bias correction factor to lognormal hypermean parameters (*i.e.* $\log(\mu_{R_{max}})$, $\log(\mu_\alpha)$, $\log(\mu_{\sigma_R})$) such that their exponentiated values ($\mu_{R_{max}}$, μ_α and μ_{σ_R}) are interpretable as medians of the among-stock distributions. Our $\mu_{R_{max}}$ values differ from those reported by Barrowman et al. (2003) ($\mu_{R_{max}} = 1437$ smolts/km, $\sigma_{R_{max}} = 0.64$), indicating lower median asymptotic smolt capacity per km, and greater variability among the stocks in our study. Area 12–12B, the Puyallup and Samish Rivers, Area 12C–12D, and the Snohomish River exhibited the largest R_{max} estimates, while Port Gamble Bay, Area 7–7A, Grays Harbor, and the Dungeness and Green Rivers had the lowest (Figs. 2,3). Median smolt productivity among stocks (μ_α) was estimated to be 342 smolts/spawner (95% credible interval = 246 to 764 smolts/spawner) with an among-stock standard deviation (σ_α) of 0.84 (95% credible interval = 0.6 to 1.15). Despite the use of informative priors, these values differ substantially from those reported by Barrowman et al. (2003) ($\mu_\alpha = 71.52$ smolts/spawner, $\sigma_\alpha = 0.43$), indicating greater median smolt productivity, and greater variability among the stocks in our study. Area 12A, the Nooksack, Humptulips, and Dungeness Rivers, and Port Gamble Bay exhibited some of the largest estimates of smolt productivity, while the Baker and Samish Rivers, East Juan de Fuca, Puyallup and Deschutes stocks had the lowest (Figs. 2,3). The among-population median of the Beverton-Holt adult-to-smolt error terms (μ_{σ_R}) was 0.36 (95% credible interval = 0.25 to 0.47), with a lognormal standard deviation (σ_{σ_R}) of 0.78 (95 % credible interval = 0.54 to 1.15). Areas 12A and 13A, Lake Washington, the Skokomish River, and Area 13B were estimated to have the greatest variation about the adult-to-smolt relationship, while the Queets, Skagit,

Quillayute, Snohomish, and Hoh Rivers showed the least (Figs. 2,3) (Fig. 4).

3.2. Marine survival

Average marine survival across all stocks and years ($\text{Logit}^{-1}(\mu_{\phi_i})$) was estimated to be 0.051 (95% credible interval = 0.033 to 0.076), with an among-stock standard deviation of 0.55 (95% credible interval = 0.3 to 0.84). Most stocks exhibited strong lag-1 temporal autocorrelation in marine survival (ϕ_i) with only 3 stocks exhibiting a median estimate of ϕ_i below 0.25, and 27 stocks with estimates greater than 0.5. Estimation of the Gaussian field indicated spatial autocorrelation in marine survival anomalies with a length scale (ρ) of 78.5 km (95 % credible interval = 63.4 to 98.1 km) (Fig. 4). This value of ρ implies a median correlation of 0.5 at a Euclidean distance of ~ 93 km, and a correlation of less than 0.1 between stocks whose marine entry points were ~ 168 km or more apart (Fig. 4). Clusters of stocks with highly correlated marine survival corresponded geographically to the Strait of Juan de Fuca, northern Puget Sound and the Strait of Georgia, central and southern Puget Sound, and the Washington coast (Figs. 1,5).

3.3. Forecast performance

Evaluation of one-year-ahead forecast skill from 2002 to 2017 averaged across the thirty-six stocks considered in this study indicated that the MASE for the existing published forecasts was 0.93 while that of the ST-IPM was 0.70, a difference of 25 % (Figs. 6,7). The random walk, AR-1, and MA-1 models exhibited MASE values of 0.74, 0.72, 0.76, and respectively (Table S4, Fig. S8). Importantly, the ST-IPM did not always outperform the published forecasts, exhibiting slightly greater MASE values for the Stillaguamish, Skokomish, Hoh, Elwha River, East Juan de Fuca, Area 12C–12D, Area 11, Area 10E, and Area 10 stocks. The ST-IPM and published forecasts also differed somewhat in their tendency to produce large ($>|50\%$) biases. The existing forecast methods over-forecasted by 50% or more in 187 instances (stock-year combinations) and under-forecasted by 50% or more in 139. Conversely, the ST-IPM over-forecasted by 50% or more in 205 instances and under-forecasted by 50 % in 86 instances. The published forecasts have been developed using different approaches over time, and it is possible that aggregating over sixteen years could mask recent improvements in methodology. However, restricting our comparison of forecast skill to only the last five years in our study (2013–2017) did not qualitatively alter the relative performance of each method, resulting in a MASE of 0.83 for the published forecasts versus 0.61 for ST-IPM. Using alternative metrics of forecast skill had little qualitative effect on the overall assessment of forecast performance (Table S4). Similarly, evaluation of forecast accuracy with respect to the state estimates of adult returns instead of observed data did not qualitatively alter our findings (Table S4, Fig. S9–S10). MASE for the published forecasts with respect to state estimates of adult returns was 1.1, compared to 0.79 for the ST-IPM, and 0.83, 0.81, and 0.86 for the random walk, AR-1, and MA-1 models respectively (Table S4, Fig. S9–S10).

4. Discussion

We developed a spatiotemporal integrated population model (ST-IPM) to forecast adult returns of wild Washington State coho salmon. In retrospective evaluations of one-year-ahead forecast skill with respect to both state estimates and observed data, the ST-IPM outperformed the existing published forecasts for these stocks by $\sim 25\text{--}38\%$ on average, depending on the specific metrics used. There are several features of the ST-IPM that likely contribute to its forecast skill. A hierarchical and integrated design allows the ST-IPM to incorporate multiple data types and share information among stocks (Buhle et al., 2018; Jiao et al., 2011) while stage-specific modelling of the life cycle disentangles the effects of juvenile production from ocean mortality (Rose, 2000;

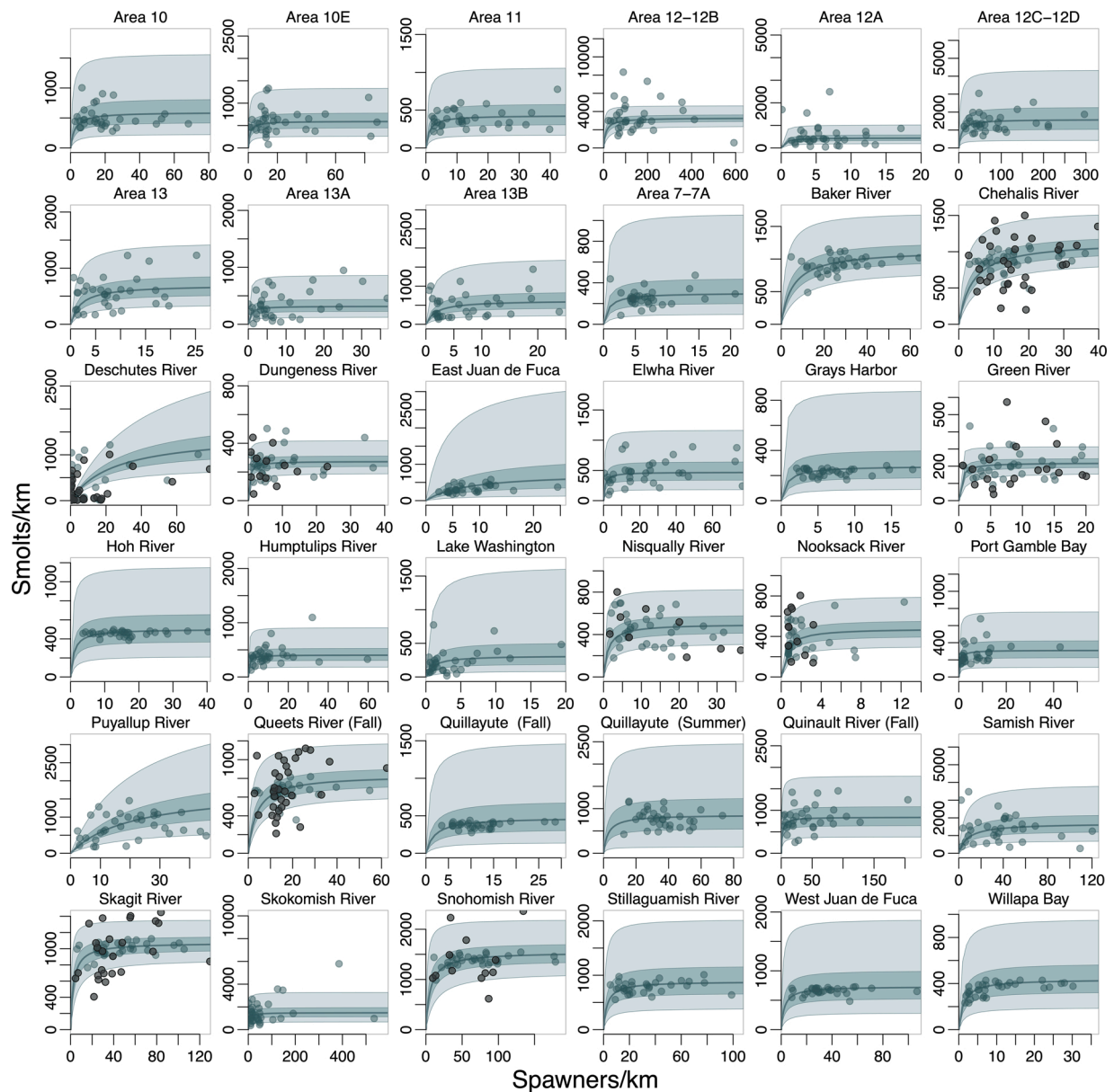


Fig. 3. Estimated adult-to-smolt production relationships for coho salmon stocks. In each panel, the median deterministic portion of the Beverton-Holt adult-to-smolt function is shown as a solid blue line, with the 50% and 95% credible intervals shown as dark and light shaded blue boundaries respectively. Where available, observed adult-to-smolt data are plotted as dark grey circles. Individual adult-to-smolt state estimates are shown in all panels as blue circles.

Scheuerell et al., 2020). Additionally, leveraging spatial correlations among populations can improve estimation of shared, environmentally-driven processes, particularly for those that lack informative data (Thorson et al., 2013). Collectively, these characteristics of the ST-IPM facilitate estimation of key biological quantities such as marine survival and temporal autocorrelation therein, which we found to be substantial (>0.5) for most stocks in our analysis.

Temporal autocorrelation can be a particularly useful property for predicting future states (Johnson et al., 2016; Punt, 2011; Winship et al., 2015). By assuming that conditions in the near future will be similar to recent observations, forecasting via autocorrelation represents an implicit treatment of environmental effects on population dynamics (Haltuch et al., 2018). Implicit approaches to environment-recruitment modelling avoid the challenges of identifying explicit functional relationships between environmental variables and stock dynamics, and are generally less prone to prediction error (Johnson et al., 2016; Punt, 2011; Winship et al., 2015). For Pacific salmon in particular, ecosystem impacts on ocean survival can be the result of many interacting factors

that have indirect, nonlinear, or cascading effects on cohorts during early marine residency (Emmett et al., 2006; Schroeder et al., 2014; Tucker et al., 2016; Wells et al., 2017, 2016). Such complex environmental dynamics will be difficult to predict using explicit mechanistic models, but may manifest as spatiotemporal autocorrelation in affected biological processes such as growth and survival (Mueter et al., 2002a; Mueter et al., 2002b; Peterman and Dörner, 2012; Pyper et al., 2005).

While our analysis indicates that the ST-IPM outperforms the existing published forecasts on average, there are some stocks for which other forecast approaches appear better suited. The degree to which any alternative method outperformed the ST-IPM for a given stock was generally minor, but nonetheless it may be beneficial for managers to compare among models for each stock, or consider an ensemble approach (Jardim et al., 2020; Stewart and Hicks, 2018). Although we found that the ST-IPM generally outperformed the random walk, moving average (MA-1), and autoregressive (AR-1) models (Fig. S8, S10), the improvements were often minor and simpler models offer advantages in ease of implementation and transparency to stakeholders that may offset

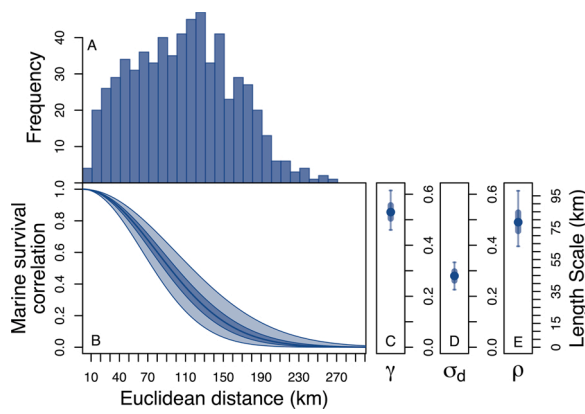


Fig. 4. Marine survival correlation as a function of Euclidean distance between stocks' marine entry locations. Panel A shows the frequency distribution of pairwise Euclidean distances between the thirty-six coho salmon stocks included in this study. Panel B shows the specified correlation in marine survival anomalies as a function of distance according to the squared exponential kernel (eq. 13). The median estimate (based on the length scale parameter ρ) is shown as a solid blue line, and 50 % and 95 % credible intervals are shown as dark and light shaded boundaries respectively. Panels C-E show the posterior distributions for the parameters of the squared exponential kernel: the marginal standard deviation (γ , panel C), error standard deviation (σ_d , panel D) and the length scale (ρ , panel E). Medians are shown as circles and 50 % and 95 % credible intervals are shown as thick and thin lines respectively.

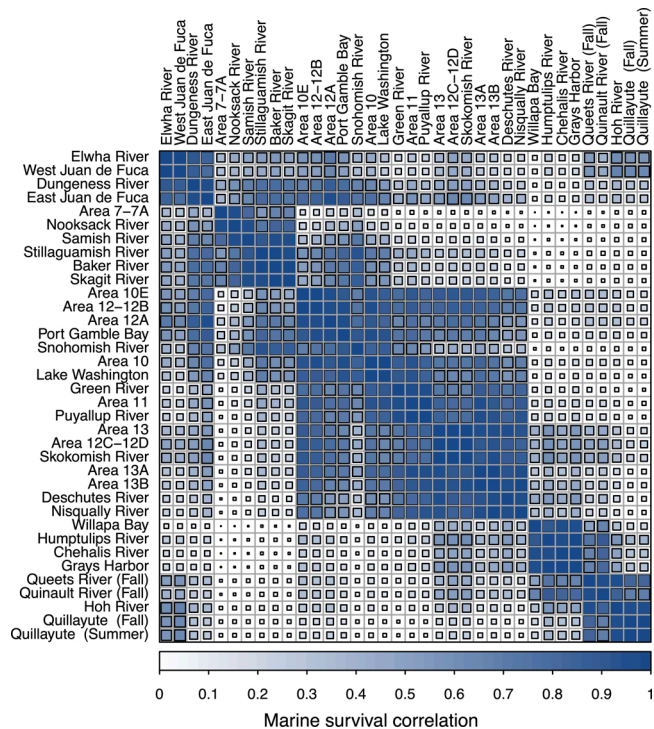


Fig. 5. Estimated pairwise marine survival correlations between stocks. The size and color intensity of squares in each cell represents the strength of marine survival correlations between any two stocks as a function of Euclidean distance as determined by the squared exponential kernel. Stocks are ordered on each axis by hierarchical clustering of their marine survival correlations.

a small loss of forecast skill. Previous research has shown that simple autoregressive forecasts outperform more complex models (Ward et al., 2014), so it is not necessarily surprising that the AR-1 exhibited comparable forecast skill to the ST-IPM despite the greater complexity of the latter. Given the large uncertainty in the adult-to-smolt relationships for

many stocks, this component of the ST-IPM may contribute little to, or possibly detract from forecast accuracy. However, for managers interested in considering uncertainty in harvest control decisions (e.g. Privitera-Johnson and Punt, 2020), propagating uncertainty from the adult-to-smolt production relationships into estimates of forecast uncertainty may nonetheless be desirable. Furthermore, the integrated life cycle design of the ST-IPM offers additional functionality (described below) that may be valuable to managers beyond its use as a forecast model.

It is important to note that even in cases where the ST-IPM does improve forecast skill, it may not necessarily lead to better management outcomes. Closed loop simulation analysis of sockeye salmon (*O. nerka*) stocks has demonstrated that implementation error can negate the potential benefits of improved preseason forecasts (Dorner et al., 2009). However, Walters (1989) found that the value of preseason forecasts for Pacific salmon populations can be substantial when opportunities for in-season fisheries management are limited, as is the case for Washington coho stocks. Understanding the relative importance of preseason forecast accuracy versus other factors (e.g. harvest control rules, environmental conditions) to achieving management objectives should be an important consideration in identifying research and management priorities (Rupp et al., 2012a). It is worth noting that forecast error for several stocks remained substantial under every modelling approach considered here, and management outcomes for these stocks may be more tractably improved by developing in-season management capacity, or adopting harvest control rules that explicitly account for uncertainty (Privitera-Johnson and Punt, 2020). We recommend that future studies evaluate management outcomes across a suite of harvest control rules, forecast methods, and environmental scenarios using closed-loop simulation analysis.

There are several next steps that could be taken to continue development of the ST-IPM. The design of the spatial Gaussian field could be improved by specifying covariance as a function of marine 'over-water' rather than Euclidean distance (e.g. Hocking et al., 2018) and allowing for anisotropic covariance, such that decorrelation distance varies depending on direction (Thorson et al., 2015b). The ST-IPM's current treatment of observation error is also incomplete, as there are errors in the stock assignments of harvested fish that we did not explicitly consider. Greater transparency in the data inputs and assumptions used to generate FRAM harvest estimates will be necessary to appropriately propagate these uncertainties. Furthermore, the stocks included in our analysis likely differ substantially in the precision and bias of their smolt outmigration and adult escapement counts, which the ST-IPM does not account for. The ST-IPM's estimates of adult-to-smolt production may also be biased by unknown levels of hatchery-origin spawners present in the wild escapement (Falcu and Suring, 2018). Future model developments could be made to estimate the prevalence of hatchery-origin fish within the spawning population (e.g. Buhle et al., 2018), although the data available to do so may be limited for many of the stocks included in this study.

The presence of hatchery-origin spawners, errors in FRAM stock assignments, and variable data quality may have contributed to our estimates of smolt productivity and capacity differing substantially from those of Barrowman et al. (2003). Given that Barrowman et al. (2003) focused on populations with little or no hatchery-origin spawners and high quality smolt and adult enumeration data, we recommend that our estimates (i.e. μ_{Rmax} , μ_a) be interpreted more cautiously against theirs from a biological standpoint. The presence of hatchery-origin spawners misattributed as recruits would tend to positively bias estimates of productivity by inflating recruitment resulting from low parental spawner abundances. Systematic misattribution of harvest among populations due to errors in FRAM fishery stock assignments could have similar effects. Furthermore, our estimates of Beverton-Holt parameters and hyperparameters were often highly uncertain (Fig. 2) and sensitive to the priors that were assumed (compare Fig. 2 to Fig. S1). Future efforts to address data quality issues and differentiate hatchery and wild

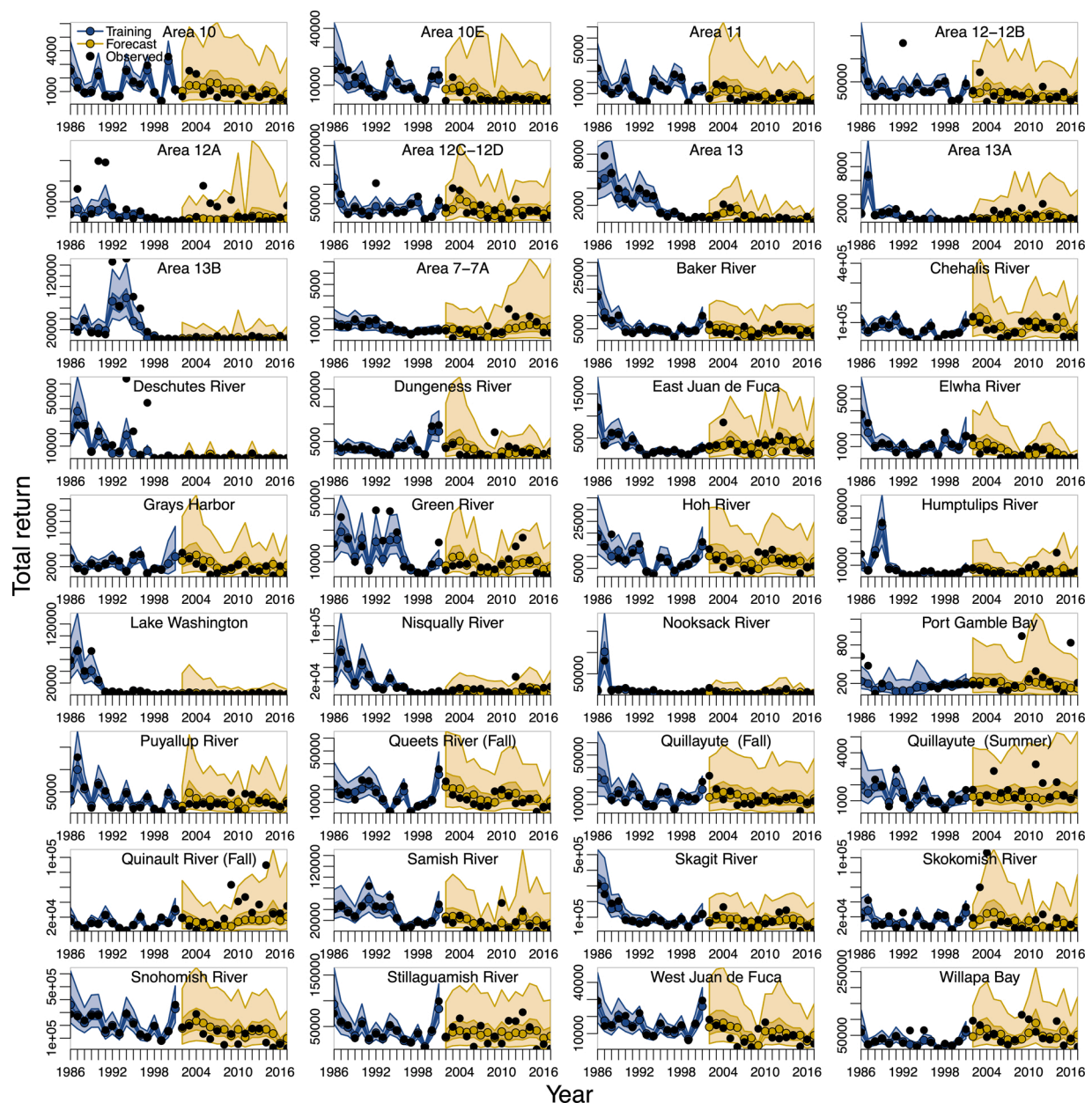


Fig. 6. One-year-ahead forecasts of total adult returns from the spatiotemporal integrated population model (ST-IPM). In each panel, model fits to the minimum extent of historical adult return data available for conditioning the model prior to forecasting are shown in blue, and one-year ahead forecasts are shown in gold. Median estimates are shown as colored circles connected by solid lines, while 50 % and 95 % credible intervals are shown as dark and light shaded boundaries respectively. Observed adult return data are shown as black dots.

spawners could potentially resolve some of the differences between our estimates of productivity and capacity and those reported by Barrowman et al. (2003). However, there are also plausible biological reasons for the discrepancies, such as the fact that Barrowman et al. (2003) generally included smaller streams with high quality rearing habitat, potentially explaining the generally lower values of smolt capacity estimated in our study.

While the ST-IPM does not currently incorporate environmental information (other than freshwater habitat size) the model structure can readily accommodate covariates in both the adult-to-smolt and marine survival components (Maunder and Thorson, 2019; Maunder and Waters, 2003; Miller et al., 2016; Schirripa et al., 2009; Subbey et al., 2014). Freshwater covariates such as river discharge (Lawson et al., 2004; Mathews and Olson, 1980; Ohlberger et al., 2018) and habitat quality (Sharma and Hilborn, 2001) may explain some variation in

adult-to-smolt production and offer predictive power for stocks that lack smolt outmigration observations. Similarly, ocean indicators could be evaluated for their ability to 'soak up' autocorrelation in marine mortality or explain independent residual variation. Failing to account for temporal and spatial autocorrelation can impede detection of robust correlations between environmental conditions and biological processes (Dormann, 2007; Walters and Martell, 2004) such that the ST-IPM may serve as a useful framework for identifying and evaluating such relationships. While beyond the scope of the present study, future work could use the ST-IPM to evaluate plausible environmental variables and functional forms (e.g. linear, nonlinear, non-stationary etc.). Inclusion of marine covariates could improve forecast performance (Logerwell et al., 2003), or may simply be informative towards process-level understanding of salmonid marine survival (Beamish et al., 2000; Quinn et al., 2005; Sharma et al., 2013; Zimmerman et al., 2015).

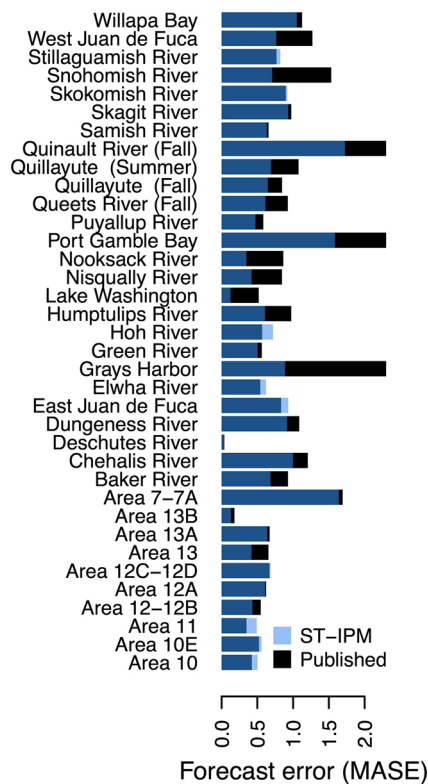


Fig. 7. Comparison of one-year ahead forecast skill of the spatiotemporal integrated population model (ST-IPM) to existing published forecasts from 2002-2017. Blue bars for each stock represent the forecast error based on mean absolute scaled error (MASE) for one-year-ahead forecasts from the ST-IPM, while black bars show the MASE of the published forecasts.

While the ST-IPM was used for short-term forecasting here, there are several other applications in which it may also be well-suited. As a life cycle model, the ST-IPM generates estimates of stage-specific productivity and capacity, as well as the spawner abundance that produces maximum sustained yield (S_{MSY}) (Moussalli and Hilborn, 1986; Ohlberger et al., 2019). As such, the ST-IPM – particularly if coupled with FRAM – could lead to an improved stock assessment framework for coho salmon that uses all available data, shares information among stocks, and propagates uncertainties into estimates of stock status and management reference points. The ST-IPM also produces state estimates of marine survival (adjusted for hatchery and sampling biases) for many wild coho salmon stocks throughout Washington State that lack coded wire tag data. Such estimates are not only useful for understanding and projecting the dynamics of these stocks (Buhle et al., 2018), but may also be instructive in continuing investigations of Salish Sea marine survival. Finally, by providing a cohesive structural model of coho salmon population dynamics with parameter estimates and associated uncertainties, the ST-IPM can readily serve as an operating model for management strategy evaluation (MSE, Punt et al., 2016). Such analyses could investigate the performance of alternative harvest control policies under a range of environmental scenarios, consider the impacts of data quality and availability on management performance, or explore effects of habitat alterations and interventions at various stages of the life cycle. It would be useful for future studies to pursue these applications of the ST-IPM while continuing its development and operationalization as a forecasting tool.

CRedit authorship contribution statement

Lukas B. DeFilippo: Conceptualization, Methodology, Software, Validation, Formal analysis, Writing - original draft, Writing - review &

editing, Visualization, Funding acquisition. **Thomas W. Buehrens:** Conceptualization, Methodology, Resources, Writing - review & editing. **Mark Scheuerell:** Methodology, Writing - review & editing. **Neala W. Kendall:** Project administration, Resources, Writing - review & editing. **Daniel E. Schindler:** Funding acquisition, Resources, Project administration, Conceptualization, Writing - review & editing.

Declaration of Competing Interest

The authors declare that they have no known competing financial interests or personal relationships that could have appeared to influence the work reported in this paper.

Acknowledgements

This research was funded by the Pacific Salmon Commission Southern Endowment Fund, grant number SF-2019-SP-11. We acknowledge Washington Department of Fish and Wildlife staff Benjamin Warren for providing database support, Dale Gombert for providing stream length estimates, and Angelika Hagen-Breaux for providing FRAM output. We would also like to thank Marlene Bellman (Northwest Indian Fisheries Commission) for providing the published preseason forecasts for each management unit, David French for creating the map for Fig. 1, and Mara Zimmerman for useful conversations. Additionally, we are grateful to Will Satterthwaite, Jan Ohlberger, Marisa Litz, and Laurie Peterson for helpful comments on earlier drafts which greatly improved the quality of this manuscript. Finally, we thank the many state and tribal biologists who have contributed to the collection of data used in this study. Any use of trade, firm, or product names is for descriptive purposes only and does not imply endorsement by the U.S. Government.

Appendix A. Supplementary data

Supplementary material related to this article can be found, in the online version, at doi:<https://doi.org/10.1016/j.fishres.2021.106014>.

References

- Anderson, J.H., Krueger, K.L., Kinsel, C., Quinn, T., Ehinger, W.J., Bilby, R., 2019. Coho salmon and habitat response to restoration in a small stream. *Trans. Am. Fish. Soc.* 148, 1024–1038.
- Barrowman, N.J., Myers, R.A., Hilborn, R., Kehler, D.G., Field, C.A., 2003. The variability among populations of coho salmon in the maximum reproductive rate and depensation. *Ecol. Appl.* 13, 784–793. [https://doi.org/10.1890/1051-0761\(2003\)013\[0784:TVAPOC\]2.0.CO;2](https://doi.org/10.1890/1051-0761(2003)013[0784:TVAPOC]2.0.CO;2).
- Beamish, R.J., 2018. *The Ocean Ecology of Pacific Salmon and Trout*. American Fisheries Society.
- Beamish, R.J., Mahnken, C., 2001. A critical size and period hypothesis to explain natural regulation of salmon abundance and the linkage to climate and climate change. *Prog. Oceanogr.* 49, 423–437. [https://doi.org/10.1016/S0079-6611\(01\)00034-9](https://doi.org/10.1016/S0079-6611(01)00034-9).
- Beamish, R.J., Noakes, D.J., McFarlane, G.A., Pinnix, W., Sweeting, R., King, J., 2000. Trends in coho marine survival in relation to the regime concept. *Fish. Oceanogr.* 9, 114–119. <https://doi.org/10.1046/j.1365-2419.2000.00126.x>.
- Beamish, R.J., Mahnken, C., Neville, C.M., 2004. Evidence that reduced early marine growth is associated with lower marine survival of Coho salmon. *Trans. Am. Fish. Soc.* 133, 26–33. <https://doi.org/10.1577/T03-028>.
- Betancourt, M., 2016. *Diagnosing Suboptimal Cotangent Disintegrations in Hamiltonian Monte Carlo*.
- Beverton, R.J.H., Holt, S.J., 1957. *On the Dynamics of Exploited Fish Populations, On the Dynamics of Exploited Fish Populations*. Springer Science & Business Media, Dordrecht. <https://doi.org/10.1007/978-94-011-2106-4>.
- Bradford, M.J., Myers, R.A., Irvine, J.R., 2000. Reference points for coho salmon (*Oncorhynchus kisutch*) harvest rates and escapement goals based on freshwater production. *Can. J. Fish. Aquat. Sci.* <https://doi.org/10.1139/f99-281>.
- Buhle, E.R., Scheuerell, M.D., Cooney, T.D., Ford, M.J., Zabel, R.W., Thorson, J.T., 2018. Using Integrated Population Models to Evaluate Fishery and Environmental Impacts on Pacific Salmon Viability. NOAA Tech. Memo. <https://doi.org/10.7289/V5/TM-NWFSC-140>. NMFS-NWFSC-140 44.
- Cao, J., Thorson, J.T., Punt, A.E., Szuwalski, C., 2019. A novel spatiotemporal stock assessment framework to better address fine-scale species distributions: development and simulation testing. *Fish. Fish.* 1–18. <https://doi.org/10.1111/faf.12433>.

- Chasco, B., Burke, B., Crozier, L., Zabel, R., 2021. Differential impacts of freshwater and marine covariates on wild and hatchery Chinook salmon marine survival. *PLoS One*. <https://doi.org/10.1371/journal.pone.0246659>.
- Chittenden, C.M., Beamish, R.J., McKinley, R.S., 2009. A critical review of Pacific salmon marine research relating to climate. *ICES J. Mar. Sci.* 66, 2195–2204. <https://doi.org/10.1093/icesjms/fsp174>.
- Clark, J.S., Bjornstad, O.N., 2004. Population time series: process variability, observation errors, missing values, lags, and hidden states. *Ecology*. <https://doi.org/10.1890/03-0520>.
- Coronado, C., Hilborn, R., 1998. Spatial and temporal factors affecting survival in coho salmon (*Oncorhynchus kisutch*) in the Pacific Northwest. *Can. J. Fish. Aquat. Sci.* 55, 2067–2077. <https://doi.org/10.1139/cjfas-55-9-2067>.
- Cushing, D.H., 1982. Climate and fisheries. *Clim. Fish.* [https://doi.org/10.1016/0272-7714\(87\)90048-5](https://doi.org/10.1016/0272-7714(87)90048-5).
- De Valpine, P., Hastings, A., 2002. Fitting population models incorporating process noise and observation error. *Ecol. Monogr.* [https://doi.org/10.1890/0012-9615\(2002\)072\[0057:FPMIPN\]2.0.CO;2](https://doi.org/10.1890/0012-9615(2002)072[0057:FPMIPN]2.0.CO;2).
- Deriso, R.B., Quinn II, T.J., Neal, P.R., 1985. Catch-age analysis with auxiliary information. *Can. J. Fish. Aquat. Sci.* 42, 815–824. <https://doi.org/10.1139/f85-104>.
- Di Lorenzo, E., Schneider, N., Cobb, K.M., Franks, P.J.S., Chhak, K., Miller, A.J., McWilliams, J.C., Bograd, S.J., Arango, H., Courchiter, E., Powell, T.M., Riviere, P., 2008. North Pacific Gyre Oscillation links ocean climate and ecosystem change. *Geophys. Res. Lett.* 35 <https://doi.org/10.1029/2007GL032838>.
- Dormann, C.F., 2007. Effects of incorporating spatial autocorrelation into the analysis of species distribution data. *Glob. Ecol. Biogeogr.* <https://doi.org/10.1111/j.1466-8238.2006.00279.x>.
- Dorner, B., Peterman, R.M., Su, Z., 2009. Evaluation of performance of alternative management models of Pacific salmon (*Oncorhynchus* spp.) in the presence of climatic change and outcome uncertainty using Monte Carlo simulations. *Can. J. Fish. Aquat. Sci.* <https://doi.org/10.1139/f09-144>.
- Drinkwater, K.F., Myers, R.A., 1987. Testing predictions of marine fish and shellfish landings from environmental variables. *Can. J. Fish. Aquat. Sci.* <https://doi.org/10.1139/f87-189>.
- Emlen, J.M., Reisenbichler, R.R., McGie, A.M., Nickelson, T.E., 1990. Density-dependence at sea for coho salmon (*Oncorhynchus kisutch*). *Can. J. Fish. Aquat. Sci.* <https://doi.org/10.1139/f90-200>.
- Emmett, R.L., Krutzikowsky, G.K., Bentley, P., 2006. Abundance and distribution of pelagic piscivorous fishes in the Columbia River plume during spring/early summer 1998–2003: relationship to oceanographic conditions, forage fishes, and juvenile salmonids. *Prog. Oceanogr.* 68, 1–26. <https://doi.org/10.1016/j.pocean.2005.08.001>.
- Falcy, M.R., Suring, E., 2018. Detecting the effects of management regime shifts in dynamic environments using multi-population state-space models. *Biol. Conserv.* <https://doi.org/10.1016/j.biocon.2018.02.026>.
- Fleischman, S.J., Catalano, M.J., Clark, R.A., Bernard, D.R., Chen, Y., 2013. An age-structured state-space stock-recruit model for Pacific salmon (*Oncorhynchus* spp.). *Can. J. Fish. Aquat. Sci.* 70, 401–414. <https://doi.org/10.1139/cjfas-2012-0112>.
- Fournier, D., Archibald, C.P., 1982. A general theory for analyzing catch at age data. *Can. J. Fish. Aquat. Sci.* 39, 1195–1207. <https://doi.org/10.1139/f82-157>.
- Gelman, A., 2014. RStan: the R interface to Stan. R Packag 1–22 version 2.
- Grüss, A., Gao, J., Thorson, J., Rooper, C., Thompson, G., Boldt, J., Lauth, R., 2019. Estimating synchronous changes in condition and density in eastern Bering Sea fishes. *Mar. Ecol. Prog. Ser.* 635, 169–185. <https://doi.org/10.3354/meps13213>.
- Haeseker, S.L., McCann, J.A., Tuomikoski, J., Chockley, B., 2012. Assessing freshwater and marine environmental influences on life-stage-specific survival rates of Snake River spring-summer Chinook salmon and steelhead. *Trans. Am. Fish. Soc.* <https://doi.org/10.1080/00028487.2011.652009>.
- Haltuch, M.A., Brooks, E.N., Brodzia, J., Devine, J.A., Johnson, K.F., Klibansky, N., Nash, R.D.M., Payne, M.R., Shertzer, K.W., Subbey, S., Wells, B.K., 2018. Unraveling the recruitment problem: a review of environmentally-informed forecasting and management strategy evaluation. *Fish. Res.* 1–19. <https://doi.org/10.1016/j.fishres.2018.12.016>.
- Hare, J.A., Alexander, M.A., Fooarty, M.J., Williams, E.H., Scott, J.D., 2010. Forecasting the dynamics of a coastal fishery species using a coupled climate - population model. *Ecol. Appl.* <https://doi.org/10.1890/08-1863.1>.
- Hocking, D.J., Thorson, J.T., O'Neil, K., Letcher, B.H., 2018. A geostatistical state-space model of animal densities for stream networks. *Ecol. Appl.* 28, 1782–1796.
- Holmes, E.E., Ward, E.J., Wills, K., 2012. MARSS: multivariate autoregressive state-space models for analyzing time-series data. *R J.* <https://doi.org/10.32614/rj-2012-002>.
- Hyndman, R.J., Koehler, A.B., 2006. Another look at measures of forecast accuracy. *Int. J. Forecast.* <https://doi.org/10.1016/j.ijforecast.2006.03.001>.
- Jardim, E., Azevedo, M., Brodzia, J., Brooks, E.N., Johnson, K.F., Klibansky, N., Millar, C.P., Minto, C., Mosqueira, I., Nash, R.D.M., 2020. Operationalizing Ensemble Models for Scientific Advice to Fisheries Management.
- Jiao, Y., Cortés, E., Andrews, K., Guo, F., 2011. Poor-data and data-poor species stock assessment using a Bayesian hierarchical approach. *Ecol. Appl.* <https://doi.org/10.1890/10-0526.1>.
- Johnson, K.F., Councill, E., Thorson, J.T., Brooks, E., Methot, R.D., Punt, A.E., 2016. Can autocorrelated recruitment be estimated using integrated assessment models and how does it affect population forecasts? *Fish. Res.* <https://doi.org/10.1016/j.fishres.2016.06.004>.
- Kilduff, D.P., Botsford, L.W., Teo, S.L.H., 2014. Spatial and temporal covariability in early ocean survival of Chinook salmon (*Oncorhynchus tshawytscha*) along the west coast of North America. *ICES J. Mar. Sci.* <https://doi.org/10.1093/icesjms/fsu031>.
- Kilduff, D.P., Di Lorenzo, E., Botsford, L.W., Teo, S.L.H., 2015. Changing central Pacific El Niños reduce stability of North American salmon survival rates. *Proc. Natl. Acad. Sci.* 112, 10962–10966. <https://doi.org/10.1073/pnas.1503190112>.
- Koslow, J.A., Hobday, J., Boehlert, G.W., 2002. Climate Variability and Marine Survival of Coho Salmon (*Oncorhynchus kisutch*) in the Oregon Production Area, pp. 65–77.
- Kristensen, K., Thygesen, U.H., Andersen, K.H., Beyer, J.E., 2014. Estimating Spatio-Temporal Dynamics of Size-Structured Populations, 336, pp. 326–336.
- Lawson, P.W., Logerwell, E.A., Mantua, N.J., Francis, R.C., Agostini, V.N., 2004. Environmental factors influencing freshwater survival and smolt production in Pacific Northwest coho salmon (*Oncorhynchus kisutch*). *Can. J. Fish. Aquat. Sci.* 61, 360–373. <https://doi.org/10.1139/f04-003>.
- Lewandowski, D., Kurowicka, D., Joe, H., 2009. Generating random correlation matrices based on vines and extended onion method. *J. Multivar. Anal.* <https://doi.org/10.1016/j.jmva.2009.04.008>.
- Litzow, M.A., Ciannelli, L., Puerta, P., Wettstein, J.J., Rykaczewski, R.R., Opiekun, M., 2019. Nonstationary environmental and community relationships in the North Pacific Ocean. *Ecology*. <https://doi.org/10.1002/ecy.2760>.
- Logerwell, E.A., Mantua, N., Lawson, P.W., Francis, R.C., Agostini, V.N., 2003. Tracking environmental processes in the coastal zone for understanding and predicting Oregon coho (*Oncorhynchus kisutch*) marine survival. *Fish. Oceanogr.* 12, 554–568. <https://doi.org/10.1046/j.1365-2419.2003.00238.x>.
- Mahnken, C., Ruggerone, G., Waknitz, W., Flagg, T., 1998. A historical perspective on salmonid production from Pacific Rim hatcheries. *North Pacific Anadromous Fish Comm. Bull.*
- Mantua, N.J., Hare, S.R., Zhang, Y., Wallace, J.M., Francis, R.C., 1997. Pacific interdecadal climate oscillation with impacts on salmon production. *Am. Meteorol. Soc.* 78, 1069–1079. [https://doi.org/10.1175/1520-0477\(1997\)078<1069:apicow>2.0.co;2](https://doi.org/10.1175/1520-0477(1997)078<1069:apicow>2.0.co;2).
- Mathews, S.B., Olson, F.W., 1980. Factors affecting Puget sound Coho Salmon (*Oncorhynchus kisutch*) runs. *Can. J. Fish. Aquat. Sci.* <https://doi.org/10.1139/f80-176>.
- Maunder, M.N., Punt, A.E., 2013. A review of integrated analysis in fisheries stock assessment. *Fish. Res.* 142, 61–74. <https://doi.org/10.1016/j.fishres.2012.07.025>.
- Maunder, M.N., Thorson, J.T., 2019. Modeling temporal variation in recruitment in fisheries stock assessment: a review of theory and practice. *Fish. Res.* 217, 71–86. <https://doi.org/10.1016/j.fishres.2018.12.014>.
- Maunder, M.N., Watters, G.M., 2003. A general framework for integrating environmental time series into stock assessment models: model description, simulation testing, and example. *Fish. Bull.* 101, 89–99.
- McCormick, S.D., Lerner, D.T., Monette, M.Y., Nieves-Puigdollé, K., Kelly, J.T., Björnsson, B.T., 2009. Taking it with you when you go: how perturbations to the freshwater environment, including temperature, dams, and contaminants, affect marine survival of salmon. *Am. Fish. Soc. Symp.*
- Miller, T.J., Hare, J.A., Alade, L.A., 2016. A state-space approach to incorporating environmental effects on recruitment in an age-structured assessment model with an application to southern New England yellowtail flounder. *Can. J. Fish. Aquat. Sci.* <https://doi.org/10.1139/cjfas-2015-0339>.
- Monnahan, C.C., Thorson, J.T., Branch, T.A., 2017. Faster estimation of Bayesian models in ecology using Hamiltonian Monte Carlo. *Methods Ecol. Evol.* <https://doi.org/10.1111/2041-210X.12681>.
- Morley, S.K., Brito, T.V., Welling, D.T., 2018. Measures of model performance based on the log accuracy ratio. *Sp. Weather.* <https://doi.org/10.1002/2017SW001669>.
- Moussalli, E., Hilborn, R., 1986. Optimal Stock Size and Harvest Rate in Multistage Life History Models, pp. 135–142.
- Mueter, F.J., Peterman, R.M., Pyper, B.J., 2002a. Opposite effects of ocean temperature on survival rates of 120 stocks of Pacific salmon (*Oncorhynchus* spp.) in northern and southern areas. *Can. J. Fish. Aquat. Sci.* 59, 456–463. <https://doi.org/10.1139/f02-020>.
- Mueter, F.J., Ware, D.M., Peterman, R.M., 2002b. Spatial correlation patterns in coastal environmental variables and survival rates of salmon in the north-east Pacific Ocean. *Fish. Oceanogr.* 11, 205–218. <https://doi.org/10.1046/j.1365-2419.2002.00192.x>.
- Myers, R.A., 1998. When do environment-recruitment correlations work? *Rev. Fish. Biol. Fish.* 8, 285–305. <https://doi.org/10.1023/A:1008828730759>.
- Myers, R.A., Mertz, G., 1998. Reducing uncertainty in the biological basis of fisheries management by meta-analysis of data from many populations: a synthesis. *Fish. Res.* [https://doi.org/10.1016/S0165-7836\(98\)00126-X](https://doi.org/10.1016/S0165-7836(98)00126-X).
- Myers, R.A., Bridson, J., Barrowman, N.J., 1995. Summary of worldwide spawner and recruitment data. *Can. Tech. Rep. Fish. Aquat. Sci.* No. 2024.
- Ohlberger, J., Buehrens, T.W., Brenkman, S.J., Crain, P., Quinn, T.P., Hilborn, R., 2018. Effects of past and projected river discharge variability on freshwater production in an anadromous fish. *Freshw. Biol.* <https://doi.org/10.1111/fwb.13070>.
- Ohlberger, J., Brenkman, S.J., Crain, P., Pess, G.R., Duda, J.J., Buehrens, T.W., Quinn, T.P., Hilborn, R., 2019. A Bayesian life-cycle model to estimate escapement at maximum sustained yield in salmon based on limited information. *Can. J. Fish. Aquat. Sci.* <https://doi.org/10.1139/cjfas-2017-0382>.
- Pacific Fishery Management Council, 2016. Pacific Coast Salmon Fishery Management Plan for Commercial and Recreational Salmon Fisheries Off the Coasts of Washington, Oregon, and California.
- Pacific Fishery Management Council Model Evaluation Workgroup, 2008. Fishery Regulation and Assessment Model (FRAM), Technical Documentation for Coho and Chinook – v.3.0. Portland, OR.
- Pearcy, W.G., 1992. Ocean ecology of North Pacific salmonids. *Books Recruit. Fish. Oceanogr.*
- Peterman, R.M., 1981. Form of random variation in smolt-to-adult relations and its influence on production estimates. *Can. J. Fish. Aquat. Sci.* 38, 113–119. <https://doi.org/10.1139/f81-151>.

- Peterman, R., 1982. Model of salmon age structure and its use in preseason forecasting and studies of marine survival. *Can. J. Fish. Aquat. Sci.* 39, 1444–1452. <https://doi.org/10.1139/f82-195>.
- Peterman, R.M., Dörner, B., 2012. A widespread decrease in productivity of sockeye salmon (*Oncorhynchus nerka*) populations in western North America. *Can. J. Fish. Aquat. Sci.* 69, 1255–1260. <https://doi.org/10.1139/F2012-063>.
- Peterman, R.M., Pyper, B.J., Lapointe, M.F., Adkison, M.D., Walters, C.J., 1998. Patterns of covariation in survival rates of British Columbian and Alaskan sockeye salmon (*Oncorhynchus nerka*) stocks. *Can. J. Fish. Aquat. Sci.* 55, 2503–2517. <https://doi.org/10.1139/cjfas-55-11-2503>.
- Privitera-Johnson, K.M., Punt, A.E., 2020. Leveraging scientific uncertainty in fisheries management for estimating among-assessment variation in overfishing limits. *ICES J. Mar. Sci.* <https://doi.org/10.1093/icesjms/fsz237>.
- Punt, A.E., 2011. The impact of climate change on the performance of rebuilding strategies for overfished groundfish species of the U.S. west coast. *Fish. Res.* <https://doi.org/10.1016/j.fishres.2011.02.019>.
- Punt, A.E., 2019. Spatial stock assessment methods: a viewpoint on current issues and assumptions. *Fish. Res.* 213, 132–143. <https://doi.org/10.1016/j.fishres.2019.01.014>.
- Punt, A.E., Smith, D.C., Smith, A.D.M., 2011. Among-stock comparisons for improving stock assessments of data-poor stocks: the “robin Hood” approach. *ICES J. Mar. Sci.* 68, 972–981. <https://doi.org/10.1093/icesjms/fsr039>.
- Punt, A.E., Butterworth, D.S., de Moor, C.L., De Oliveira, J.A.A., Haddon, M., 2016. Management strategy evaluation: best practices. *Fish. Fish.* 17, 303–334. <https://doi.org/10.1111/faf.12104>.
- Pyper, B., Peterman, R., 1999. Relationship among adult body length, abundance, and ocean temperature for British Columbia and Alaska sockeye salmon (*Oncorhynchus nerka*), 1967–1997. *Can. J. Fish. Aquat. Sci.* 56, 1716–1720. <https://doi.org/10.1139/f99-167>.
- Pyper, B.J., Mueter, F.J., Peterman, R.M., Blackburn, D.J., Wood, C.C., 2001. Spatial covariation in survival rates of Northeast Pacific pink salmon (*Oncorhynchus gorbuscha*). *Can. J. Fish. Aquat. Sci.* 58, 1501–1515. <https://doi.org/10.1139/f01-096>.
- Pyper, B.J., Mueter, F.J., Peterman, R.M., 2005. Across-species comparisons of spatial scales of environmental effects on survival rates of Northeast Pacific Salmon. *Trans. Am. Fish. Soc.* 134, 86–104. <https://doi.org/10.1577/t04-034.1>.
- Quinn, T.P., 2005. *The Behavior and Ecology of Pacific Salmon and Trout*. UBC press.
- Quinn, T.P., Dickerson, B.R., Vøllestad, L.A., 2005. Marine survival and distribution patterns of two Puget Sound hatchery populations of coho (*Oncorhynchus kisutch*) and chinook (*Oncorhynchus tshawytscha*) salmon. *Fish. Res.* 76, 209–220. <https://doi.org/10.1016/j.fishres.2005.06.008>.
- R Core Team, 2015. R: A language and environment for statistical computing. R Foundation for Statistical Computing, Vienna, Austria. URL <http://www.R-project.org/>.
- Ricker, W.E., 1954. Stock and recruitment. *J. Fish. Res. Board Canada* 11, 559–623. <https://doi.org/10.1139/f54-039>.
- Rose, K.A., 2000. Why are quantitative relationships between environmental quality and fish populations so elusive? *Ecol. Appl.* [https://doi.org/10.1890/1051-0761\(2000\)010\[0367:WAQRBE\]2.0.CO;2](https://doi.org/10.1890/1051-0761(2000)010[0367:WAQRBE]2.0.CO;2).
- Ruggerone, G.T., Connors, B.M., 2015. Productivity and life history of sockeye salmon in relation to competition with pink and sockeye salmon in the North Pacific Ocean. *Can. J. Fish. Aquat. Sci.* 72, 818–833. <https://doi.org/10.1139/cjfas-2014-0134>.
- Ruggerone, G.T., Nielsen, J.L., 2004. Evidence for competitive dominance of Pink salmon (*Oncorhynchus gorbuscha*) over other Salmonids in the North Pacific Ocean. *Rev. Fish Biol. Fish.* <https://doi.org/10.1007/s11160-004-6927-0>.
- Rupp, D.E., Wainwright, T.C., Lawson, P.W., 2012a. Effect of forecast skill on management of the Oregon coast coho salmon (*Oncorhynchus kisutch*) fishery. *Can. J. Fish. Aquat. Sci.* <https://doi.org/10.1139/F2012-040>.
- Rupp, D.E., Wainwright, T.C., Lawson, P.W., Peterson, W.T., 2012b. Marine environment-based forecasting of coho salmon (*Oncorhynchus kisutch*) adult recruitment. *Fish. Oceanogr.* 21, 1–19. <https://doi.org/10.1111/j.1365-2419.2011.00605.x>.
- Scheuerell, M.D., Williams, J.G., 2005. Forecasting climate-induced changes in the survival of Snake River spring/summer chinook salmon (*Oncorhynchus tshawytscha*). *Fish. Oceanogr.* 14, 448–457. <https://doi.org/10.1111/j.1365-2419.2005.00346.x>.
- Scheuerell, M.D., Ruff, C.P., Anderson, J.H., Beamer, E.M., 2020. An integrated population model for estimating the relative effects of natural and anthropogenic factors on a threatened population of steelhead trout. *J. Appl. Ecol.*
- Schirripa, M.J., Goodyear, C.P., Methot, R.M., 2009. Testing different methods of incorporating climate data into the assessment of US west Coast sablefish. *ICES J. Mar. Sci.* 66, 1605–1613. <https://doi.org/10.1093/icesjms/fsp043>.
- Schroeder, I.D., Santora, J.A., Moore, A.M., Edwards, C.A., Fiechter, J., Hazen, E.L., Bograd, S.J., Field, J.C., Wells, B.K., 2014. Application of a data-assimilative regional ocean modeling system for assessing California Current System ocean conditions, krill, and juvenile rockfish interannual variability. *Geophys. Res. Lett.* <https://doi.org/10.1002/2014GL061045>.
- Sharma, R., Hilborn, R., 2001. Empirical relationships between watershed characteristics and coho salmon (*Oncorhynchus kisutch*) smolt abundance in 14 western Washington streams. *Can. J. Fish. Aquat. Sci.* <https://doi.org/10.1139/cjfas-58-7-1453>.
- Sharma, R., Vélez-Espino, L.A., Wertheimer, A.C., Mantua, N., Francis, R.C., 2013. Relating spatial and temporal scales of climate and ocean variability to survival of Pacific Northwest Chinook salmon (*Oncorhynchus tshawytscha*). *Fish. Oceanogr.* 22, 14–31. <https://doi.org/10.1111/fog.12001>.
- Stan Development Team, 2020. Stan Modeling Language Users Guide and Reference Manual, Version 2.26. <https://mc-stan.org>.
- Stewart, L.J., Hicks, A.C., 2018. Interannual stability from ensemble modelling. *Can. J. Fish. Aquat. Sci.* <https://doi.org/10.1139/cjfas-2018-0238>.
- Subbey, S., Devine, J.A., Schaarschmidt, U., Nash, R.D.M., 2014. Modelling and forecasting stock-recruitment: current and future perspectives. *ICES J. Mar. Sci.* <https://doi.org/10.1093/icesjms/fsu148>.
- Teo, S.L.H., Botsford, L.W., Hastings, A., 2009. Spatio-temporal covariability in coho salmon (*Oncorhynchus kisutch*) survival, from California to southeast Alaska. *Deep. Res. Part II Top. Stud. Oceanogr.* 56, 2570–2578. <https://doi.org/10.1016/j.dsr2.2009.03.007>.
- Thorson, J.T., Stewart, L.J., Taylor, I.G., Punt, A.E., 2013. Using a recruitment-linked multispecies stock assessment model to estimate common trends in recruitment for US West Coast groundfishes. *Mar. Ecol. Prog. Ser.* 483, 245–256. <https://doi.org/10.3354/meps10295>.
- Thorson, James T., Cope, J.M., Kleisner, K.M., Samhoury, J.F., Shelton, A.O., Ward, E.J., 2015a. Giants’ Shoulders 15 Years Later: Lessons, Challenges and Guidelines in Fisheries Meta-analysis, pp. 342–361. <https://doi.org/10.1111/faf.12061>.
- Thorson, James T., Shelton, A.O., Ward, E.J., Skaug, H.J., 2015b. Geostatistical delta-generalized linear mixed models improve precision for estimated abundance indices for West Coast groundfishes. *ICES J. Mar. Sci.* <https://doi.org/10.1093/icesjms/fsu243>.
- Tommasi, D., Stock, C.A., Pegion, K., Vecchi, G.A., Methot, R.D., Alexander, M.A., Checkley, D.M., 2017. Improved management of small pelagic fisheries through seasonal climate prediction. *Ecol. Appl.* 27, 378–388. <https://doi.org/10.1002/eap.1458>.
- Tucker, S., Hipfner, J.M., Trudel, M., 2016. Size- and condition-dependent predation: a seabird disproportionately targets standard individual juvenile salmon. *Ecology.* <https://doi.org/10.1890/15-0564.1>.
- Valpine, Pde, Hilborn, R., 2005. State-space likelihoods for nonlinear fisheries time-series. *Can. J. Fish. Aquat. Sci.* 62, 1937–1952. <https://doi.org/10.1139/f05-116>.
- Wainwright, T.C., 2021. Ephemeral relationships in salmon forecasting: a cautionary tale. *Prog. Oceanogr.* <https://doi.org/10.1016/j.pcean.2021.102522>.
- Walters, C.J., 1989. Value of short term forecasts of recruitment variation for harvest management. *Can. J. Fish. Aquat. Sci.* <https://doi.org/10.1139/f89-247>.
- Walters, C., Collie, J.S., 1988. Is Research on Environmental Factors Useful to Fisheries Management? *Can. J. Fish. Aquat. Sci.* 45, 1848–1854.
- Walters, C.J., Ludwig, D., 1981. Effects of measurement errors on the assessment of stock–Recruitment relationships. *Can. J. Fish. Aquat. Sci.* <https://doi.org/10.1139/f81-093>.
- Walters, C.J., Martell, S.J.D., 2004. Fisheries ecology and management. *Fish. Manag. Ecol.* <https://doi.org/10.1046/j.1365-2400.1999.00126.x>.
- Ward, E.J., Holmes, E.E., Thorson, J.T., Collen, B., 2014. Complexity is costly: a meta-analysis of parametric and non-parametric methods for short-term population forecasting. *Oikos.* <https://doi.org/10.1111/j.1600-0706.2014.00916.x>.
- Ward, E.J., Jannot, J.E., Lee, Y.W., Ono, K., Shelton, A.O., Thorson, J.T., 2015. Using spatiotemporal species distribution models to identify temporally evolving hotspots of species co-occurrence. *Ecol. Appl.* <https://doi.org/10.1890/15-0051.1>.
- Webster, R.A., Soderlund, E., Dykstra, C.L., Stewart, L.J., 2020. Monitoring change in a dynamic environment: spatio-temporal modelling of calibrated data from different types of fisheries surveys of Pacific halibut. *Can. J. Fish. Aquat. Sci.*
- Wells, B.K., Santora, J.A., Schroeder, I.D., Mantua, N., Sydeman, W.J., Huff, D.D., Field, J.C., 2016. Marine ecosystem perspectives on Chinook salmon recruitment: a synthesis of empirical and modeling studies from a California upwelling system. *Mar. Ecol. Prog. Ser.* 552, 271–284. <https://doi.org/10.3354/meps11757>.
- Wells, B.K., Santora, J.A., Henderson, M.J., Warzybok, P., Jahncke, J., Bradley, R.W., Huff, D.D., Schroeder, I.D., Nelson, P., Field, J.C., Ainley, D.G., 2017. Environmental conditions and prey-switching by a seabird predator impact juvenile salmon survival. *J. Mar. Syst.* <https://doi.org/10.1016/j.jmarsys.2017.05.008>.
- Winship, A.J., O’Farrell, M.R., Satterthwaite, W.H., Wells, B.K., Mohr, M.S., 2015. Expected future performance of salmon abundance forecast models with varying complexity. *Can. J. Fish. Aquat. Sci.* 72, 557–569.
- Zimmerman, M., 2018. 2018 Wild Coho Forecasts for Puget Sound, Washington Coast, and Lower Columbia.
- Zimmerman, M.S., Irvine, J.R., Neill, M.O., Anderson, J.H., Greene, C.M., Weinheimer, J., Trudel, M., Rawson, K., Zimmerman, M.S., Irvine, J.R., Neill, M.O., Anderson, J.H., Greene, C.M., Weinheimer, J., Trudel, M., Spatial, K.R., Zimmerman, S., Irvine, J.R., Neill, O., Anderson, J.H., Correigh, M., Trudel, M., Zimmerman, M.S., Neill, M.O., Anderson, J.H., Rawson, K., 2015. Spatial and Temporal Patterns in Smolt Survival of Wild and Hatchery Coho Salmon in the Salish Sea. <https://doi.org/10.1080/19425120.2015.1012246>.

Table S1. Data availability and habitat area by management unit.

Stock name	Smolt abundance	Escapement data	Harvest data	Coded wire tag	Habitat area (km)
Area 10		32 years	32 years		39.9
Area 10E		32 years	32 years		130.8
Area 11		32 years	32 years		44.8
Area 12-12B		32 years	32 years	30 years (wild)	95.4
Area 12A		32 years	32 years	25 years (hatchery)	76.3
Area 12C-12D		32 years	32 years		202.7
Area 13		32 years	32 years	5 years (wild)	64.8
Area 13A		31 years	31 years		46.7
Area 13B		32 years	32 years		360.9
Area 7-7A		31 years	31 years		115.1
Baker River		32 years	32 years	22 years (wild)	102.1
Chehalis River	32 years	32 years	32 years	30 years (wild)	2514.2
Deschutes River	33 years	32 years	32 years	18 years (wild)	132.3
Dungeness River	13 years	32 years	32 years	10 years (hatchery)	129.7
East Juan de Fuca		32 years	32 years		301.3
Elwha River		32 years	32 years		13.7
Grays Harbor		30 years	30 years		211.0
Green River	19 years	32 years	32 years	28 years (hatchery)	339.3
Hoh River		32 years	32 years		263.1
Humptulips River		32 years	32 years		268.6
Lake Washington		32 years	32 years		513.3
Nisqually River	10 years	32 years	32 years	23 years (hatchery)	317.6
Nooksack River	14 years	32 years	32 years	29 years (hatchery)	692.5
Port Gamble River		25 years	25 years		12.8
Puyallup River		32 years	32 years	30 years (hatchery)	580.1
Queets River (Fall)	33 years	32 years	32 years		381.2
Quillayute River (Fall)		32 years	30 years		761.6
Quillayute River (Summer)		32 years	30 years		19.3
Quinault River (Fall)		32 years	32 years	29 years (hatchery)	234.3
Samish River		32 years	32 years		188.2
Skagit River	29 years	32 years	32 years	21 years (hatchery)	1050.6
Skokomish River		32 years	32 years	29 years (hatchery)	106.1
Snohomish River	15 years	32 years	32 years		1358.8
Stillaguamish River		32 years	32 years		694.2
West Juan de Fuca		32 years	32 years		242.2
Willapa Bay		32 years	32 years	23 years (hatchery)	2028.2

Table S2. Arithmetic mean return size and standard deviation by management unit

Stock name	Average return	Standard deviation
Area 10	1199	877
Area 10E	7114	6518
Area 11	1079	841
Area 12-12B	31152	26064
Area 12A	5730	7615
Area 12C-12D	40211	25809
Area 13	1591	1893
Area 13A	1041	1259
Area 13B	21920	38695
Area 7-7A	1165	606
Baker River	5078	3140
Chehalis River	69046	34464
Deschutes River	8607	14776
Dungeness River	2919	2351
East Juan de Fuca	3446	2274
Elwha River	884	868
Grays Harbor	2016	1135
Green River	13564	11962
Hoh River	8901	4591
Humptulips River	7030	8732
Lake Washington	10509	21002
Nisqually River	14221	15145
Nooksack River	8729	13996
Port Gamble River	264	227
Puyallup River	31843	24207
Queets River (Fall)	13989	8090
Quillayute River (Fall)	15513	6381
Quillayute River (Summer)	1510	693
Quinault River (Fall)	20674	19071
Samish River	25119	20863
Skagit River	92845	67527
Skokomish River	17810	20629
Snohomish River	166630	87520
Stillaguamish River	39573	22825
West Juan de Fuca	12341	6998
Willapa Bay	45428	28341

Table S3. Glossary of model terms and prior distributions.

Parameter	Description	Prior
a_i	Smolt productivity (smolts/spawner)	Hierarchical (eq.2)
R_{max_i}	Smolt capacity (smolts/km)	Hierarchical (eq.2)
σ_{R_i}	Standard deviation of Beverton-Holt errors	Hierarchical (eq.11)
μ_a	Mean smolt productivity	$\mu_a \sim \text{Lognormal}(4.27, 0.75)$
$\mu_{R_{max}}$	Mean smolt capacity	$\mu_{R_{max}} \sim \text{Lognormal}(7.27, 2)$
σ_a	Smolt productivity standard deviation	$\zeta_a \sim \text{Normal}(0.43, 0.25)$
$\sigma_{R_{max}}$	Smolt capacity standard deviation	$\zeta_{R_{max}} \sim \text{Normal}(0.64, 0.25)$
$\mathbf{L}_{\Omega_\theta}$	Cholesky factor of a, R_{max} correlation matrix	$\mathbf{L}_{\Omega_\theta} \sim \text{LKJCorr}(\eta)$
μ_{σ_R}	Mean standard deviation of Beverton-Holt errors	$\mu_{\sigma_R} \sim \text{Normal}(0, 5)$
σ_{σ_R}	standard deviation of Beverton-Holt error standard deviations	$\sigma_{\sigma_R} \sim \text{Normal}(0, 5)$
$S_{i,y=1,2}$	Unobserved spawning events	$S_{i,y=1,2} \sim \text{Lognormal}(0, 10)$
ψ_i	Initial marine survival	Hierarchical (eq. 12)
μ_ψ	Mean initial logit marine survival	$\mu_\psi \sim \text{Normal}(0, 10)$
σ_ψ	Standard deviation of initial logit marine survival	$\sigma_\psi \sim \text{Normal}(0, 5)$
μ_{λ_i}	Population-specific average logit marine survival	Hierarchical $\mu_{\lambda_i} \sim \text{Normal}(\mu_{\mu_{\lambda_i}}, \sigma_{\mu_{\lambda_i}})$
$\mu_{\mu_{\lambda_i}}$	Average logit marine survival hyper-mean	$\mu_{\mu_{\lambda_i}} \sim \text{Normal}(0, 10)$
$\sigma_{\mu_{\lambda_i}}$	Average logit marine survival standard deviation	$\sigma_{\mu_{\lambda_i}} \sim \text{Normal}(0, 5)$
ϕ_i	Marine survival lag-1 temporal autocorrelation	$\phi_i \sim \text{Uniform}(-1, 1)$
γ	Marginal standard deviation of Gaussian field	$\gamma \sim \text{Normal}(0, 5)$
ρ	Length scale of Gaussian field	$\rho \sim \text{Gamma}(1, 0.1)$
σ_d	Error standard deviation of Gaussian field	$\sigma_d \sim \text{Normal}(0, 5)$
ϑ_i	Initial logit harvest rate	Hierarchical $\vartheta_i \sim \text{Normal}(\mu_\vartheta, \sigma_\vartheta)$

μ_{ϑ}	Mean initial logit harvest rate	$\mu_{\vartheta} \sim Normal(0,10)$
σ_{ϑ}	Initial logit harvest rate standard deviation	$\sigma_{\vartheta} \sim Normal(0,5)$
ρ_{ϵ}	Harvest rate correlation	$\rho_{\epsilon} \sim Uniform(-1,1)$
σ_{ϵ}	Harvest rate marginal standard deviation	$\sigma_{\epsilon} \sim Normal(0,5)$
σ_J	Smolt observation error	$\sigma_J \sim Normal(0,5)$
σ_E	Escapement observation error	Fixed (0.2)
σ_H	Harvest observation error	$\sigma_H \sim Normal(0,5)$
κ	Coded wire tag effective sample size	$\kappa \sim Uniform(2, 500)$
τ_i	Hatchery offsets	Hierarchical (eq.25)
μ_{τ}	Mean hatchery offset	$\mu_{\tau} \sim Normal(0,5)$
σ_{τ}	Standard deviation of hatchery offsets	$\sigma_{\tau} \sim Normal(0,5)$

Table S4. Forecast performance of the spatiotemporal integrated population model (ST-IPM), existing published forecasts, random walk, lag-1 autoregressive (AR-1) and lag-1 moving average (MA-1) models by a suite of metrics: Mean absolute scaled error (MASE), root mean squared error (RMSE), and median symmetric accuracy (MSA) with respect to both the observed data (obs) and state estimates (state) from the ST-IPM conditioned all data presently available.

Method	MASE (obs)	RMSE (obs)	MSA (obs)	MASE (state)	RMSE (state)	MSA (state)
ST-IPM	0.70	19004	0.68	0.79	18087	0.61
Published	0.93	29064	1.0	1.1	28520	0.98
Random Walk	0.74	20540	0.78	0.83	19571	0.71
AR-1	0.72	19788	0.73	0.81	18681	0.66
MA-1	0.76	21218	0.74	0.86	20188	0.71

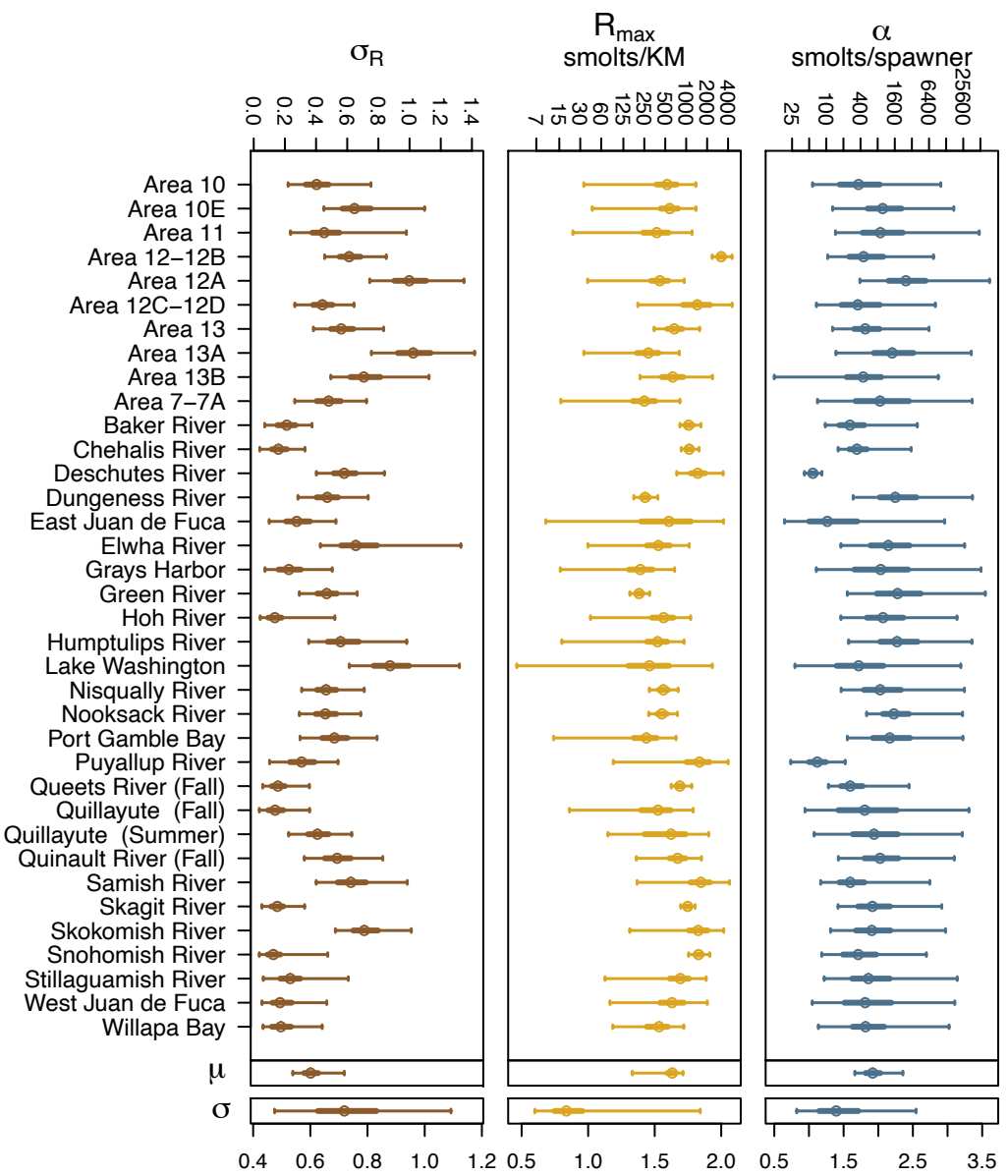
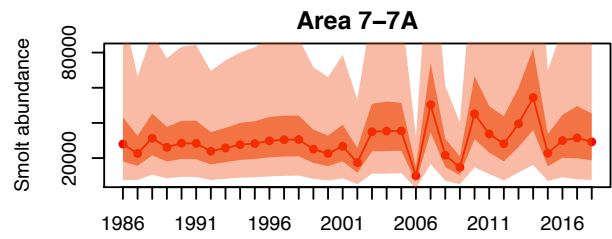
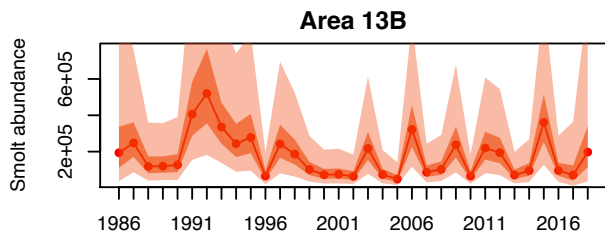
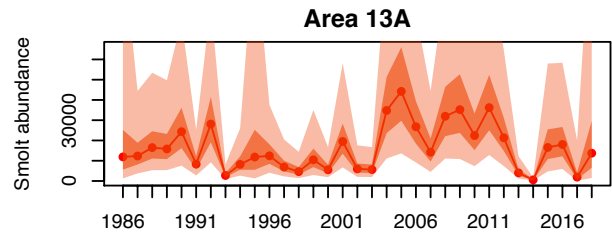
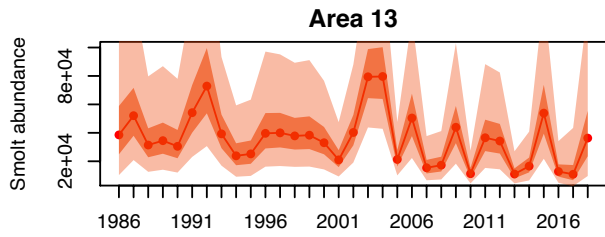
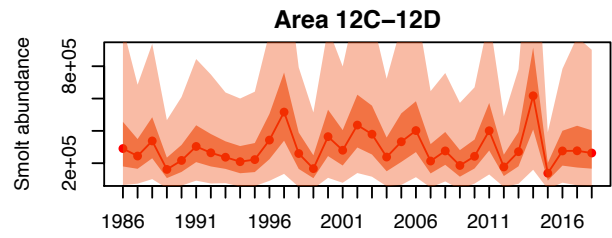
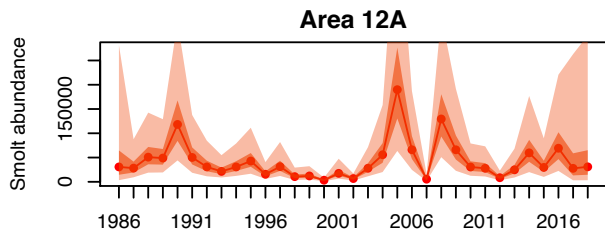
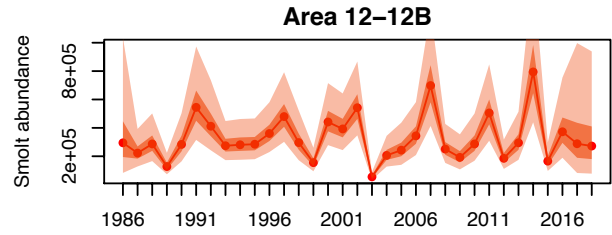
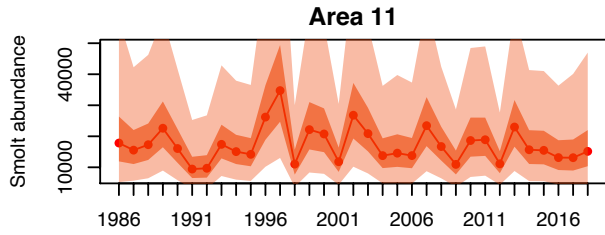
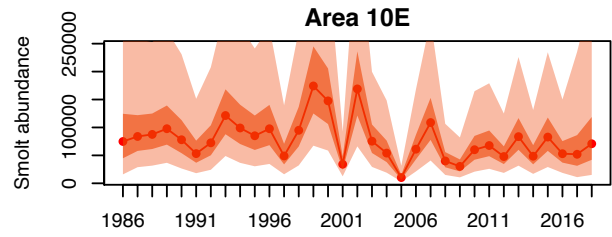
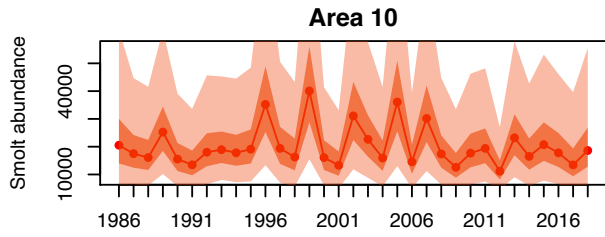
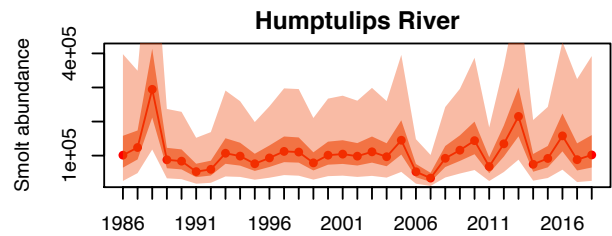
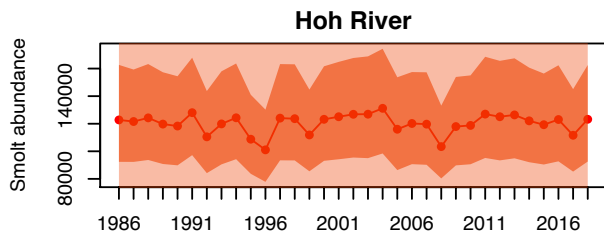
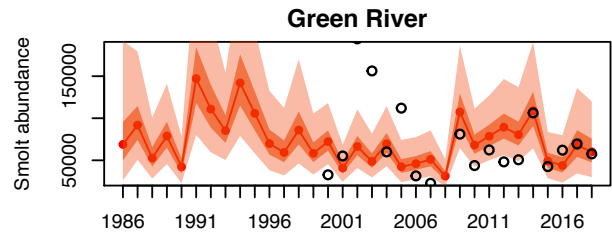
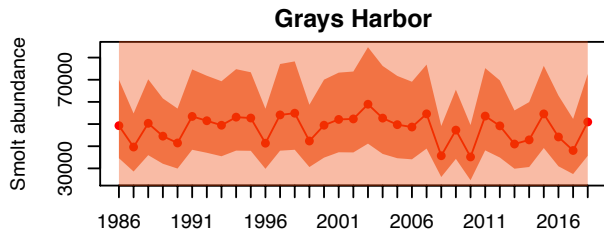
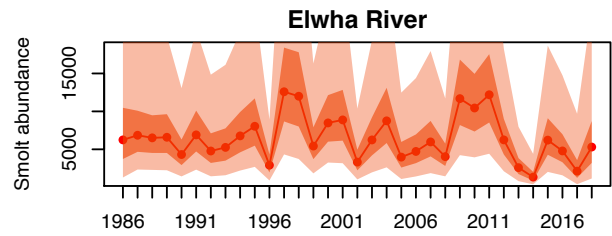
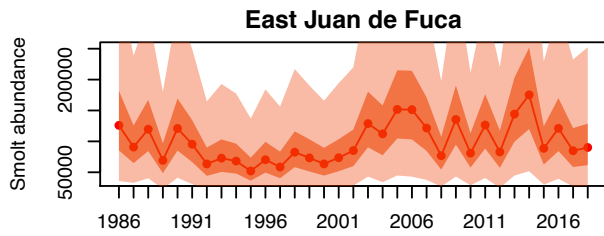
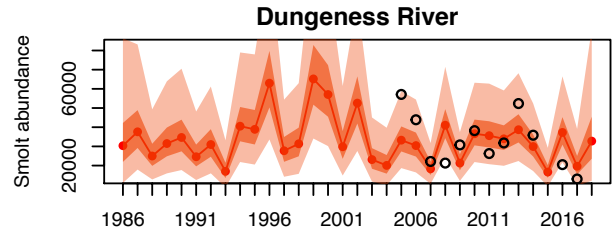
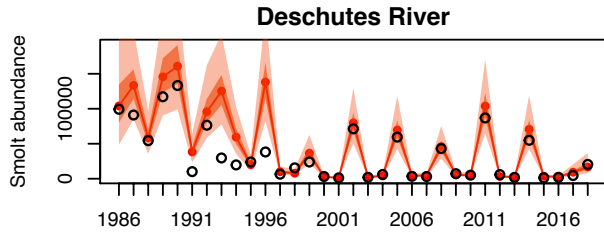
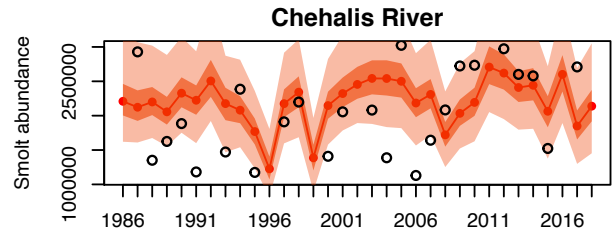
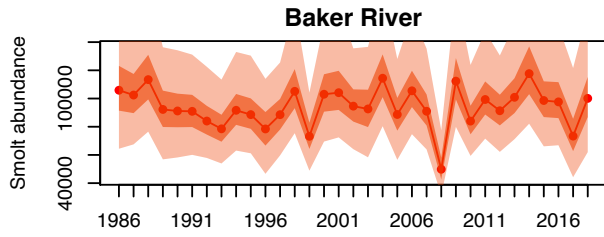
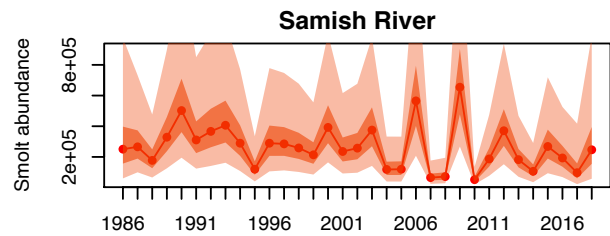
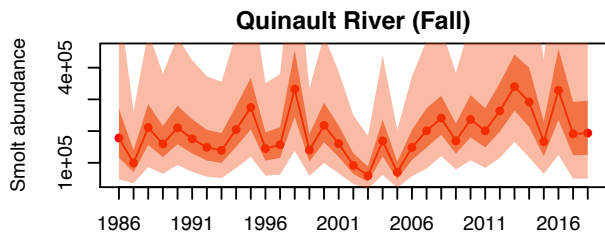
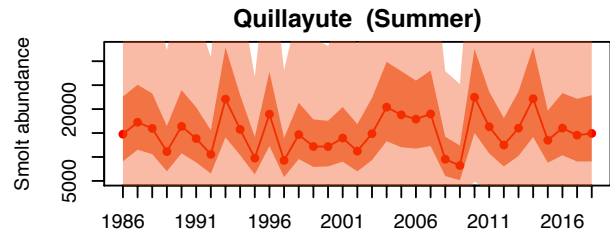
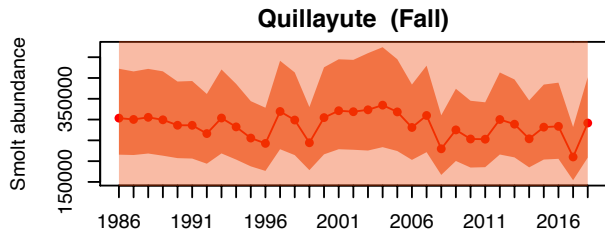
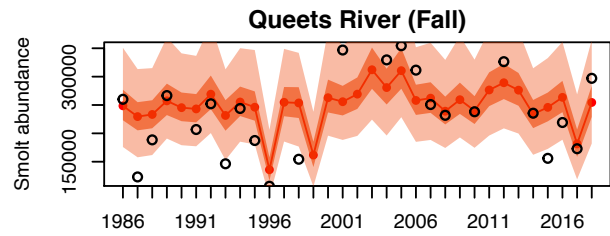
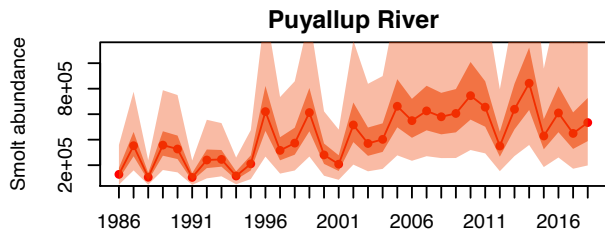
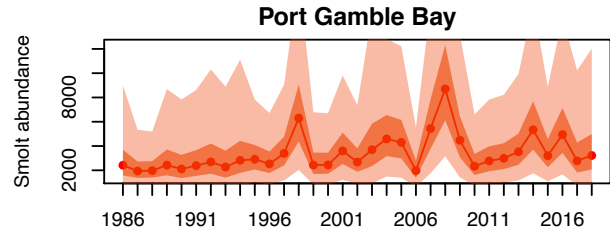
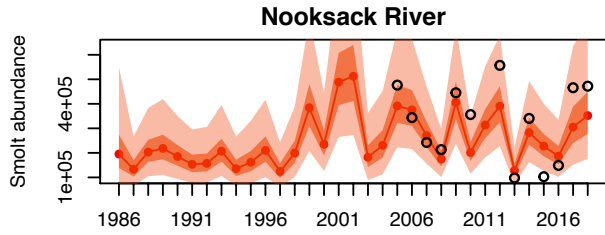
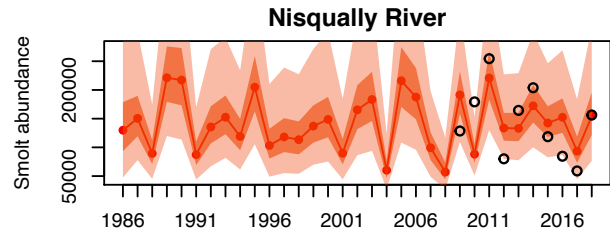
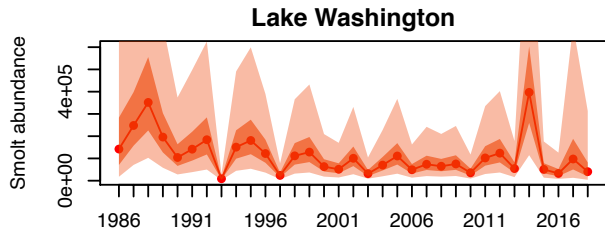
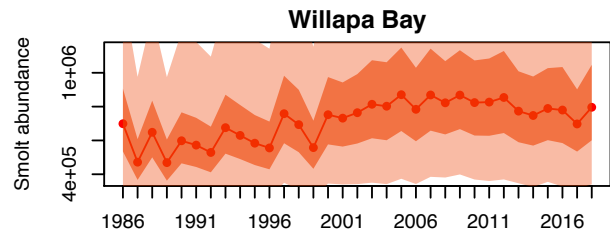
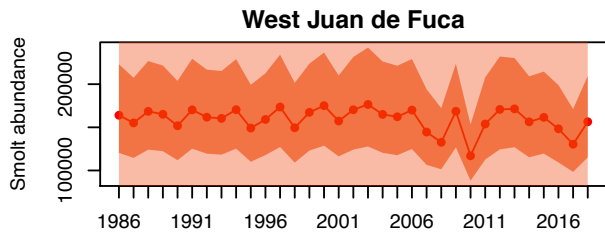
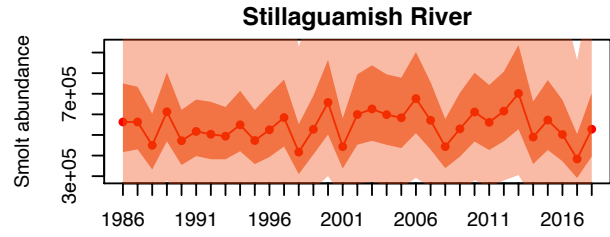
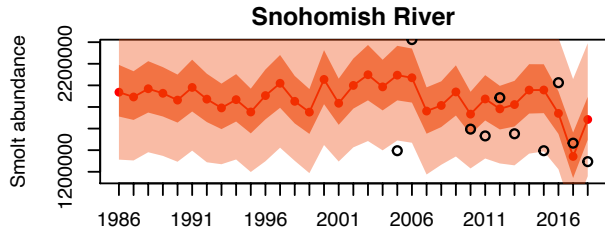
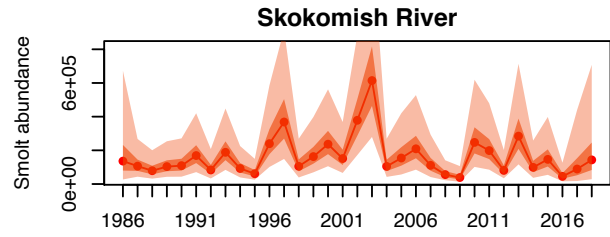
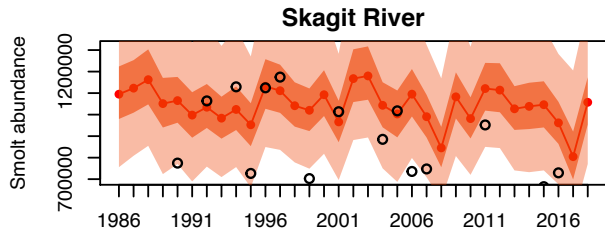


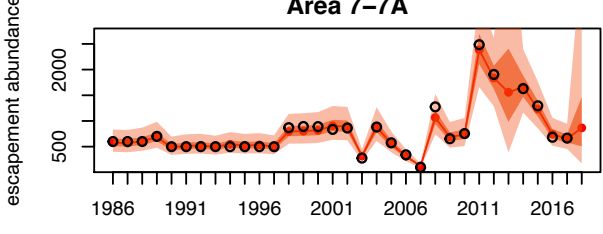
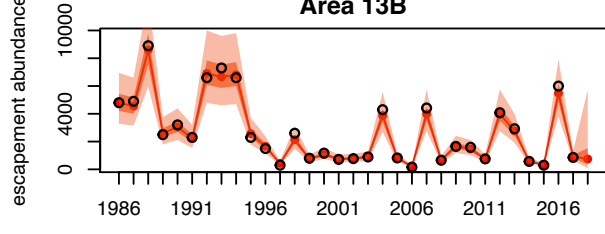
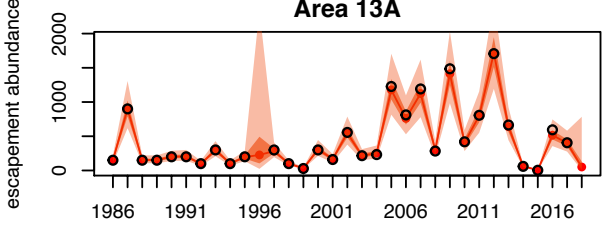
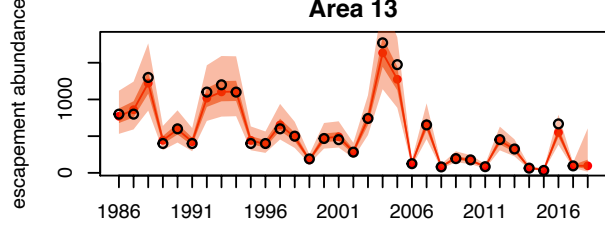
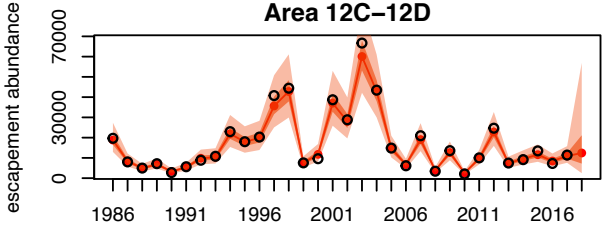
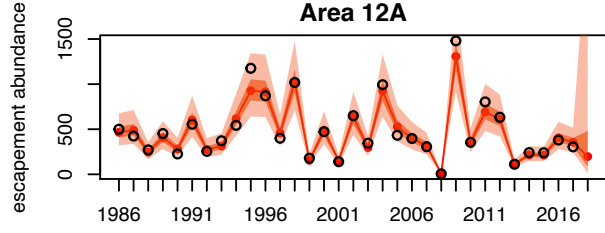
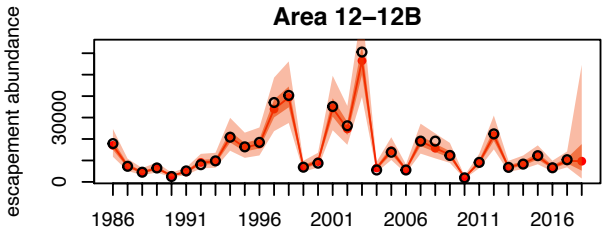
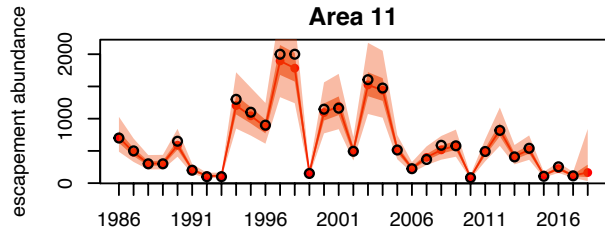
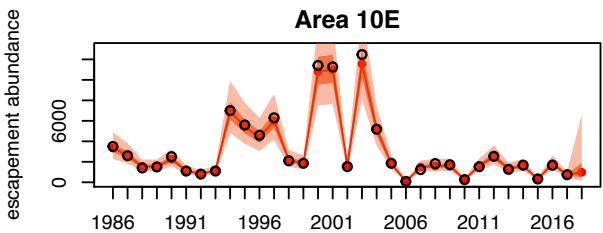
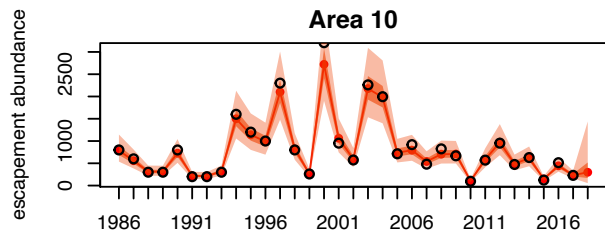
Figure S1. Estimation of Beverton-Holt adult-to-smolt parameters estimated using vague priors. The details of this figure are identical to those of figure 2 in the main text except the posteriors shown here are from model fits which used vague priors for the hyperparameters of the Beverton-Holt adult-to-smolt parameters ($\mu_a, \mu_{R_{max}}, \sigma_a, \sigma_{R_{max}}$). Specifically, the priors used here were: $\mu_a \sim Normal(4.27, 5)$, $\mu_{R_{max}} \sim Normal(7.27, 5)$, $\sigma_a \sim Normal(0.43, 5)$, and $\sigma_{R_{max}} \sim Normal(0.64, 5)$.

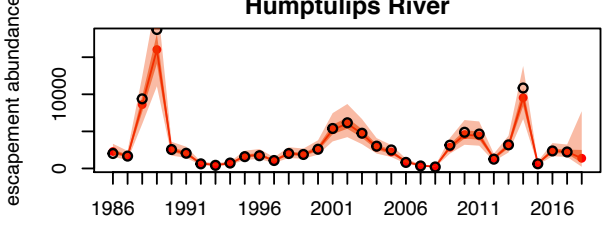
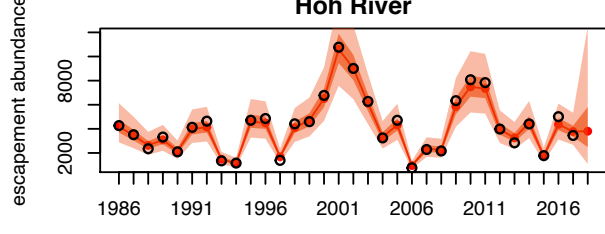
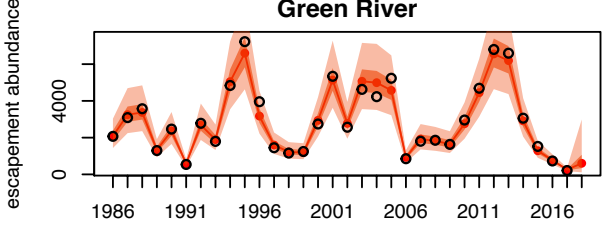
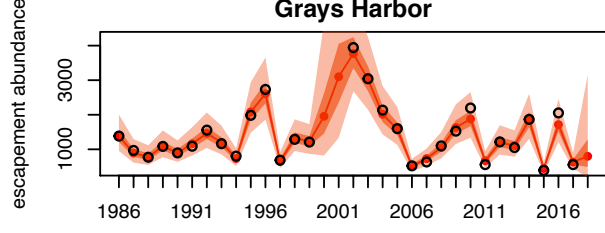
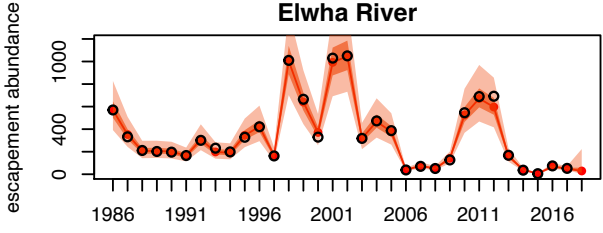
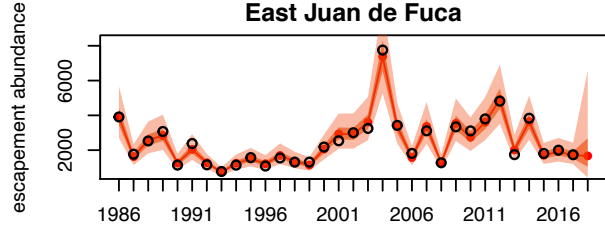
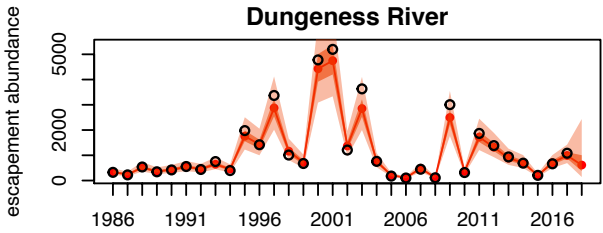
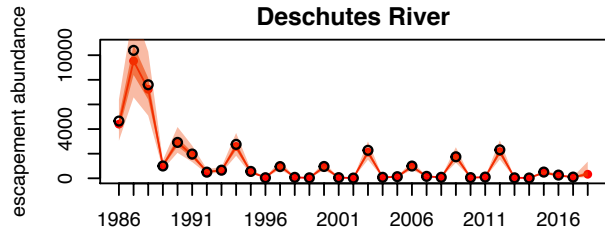
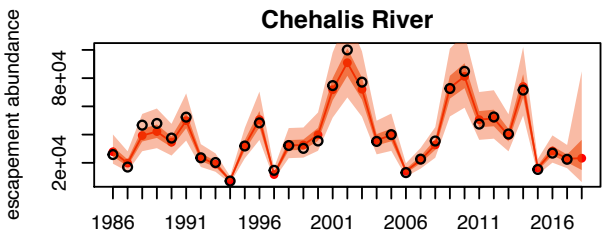
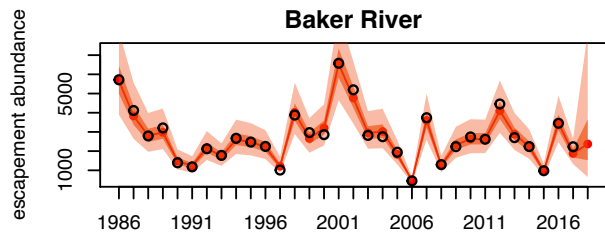


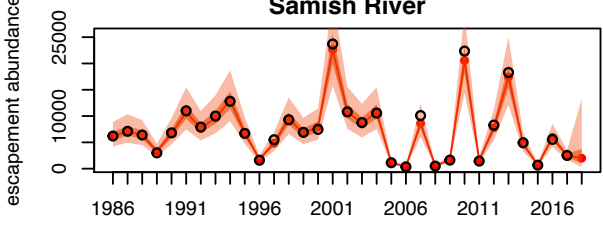
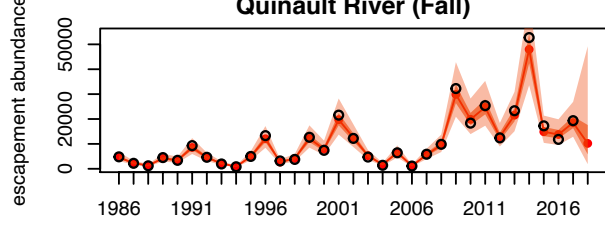
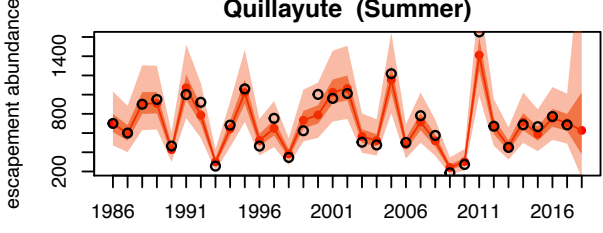
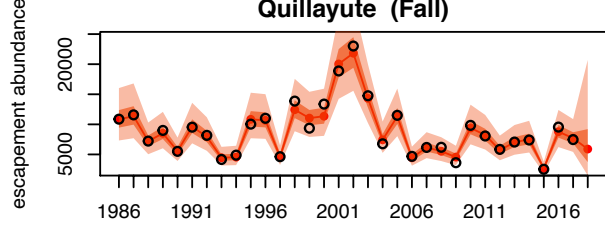
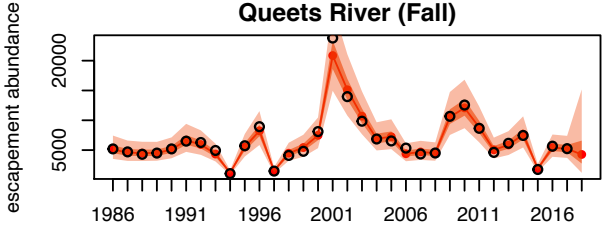
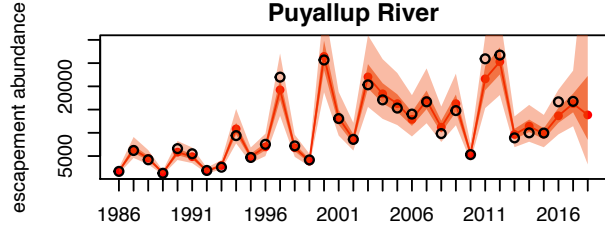
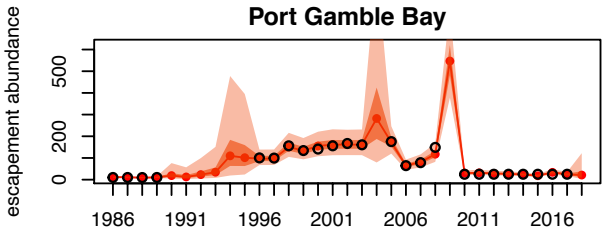
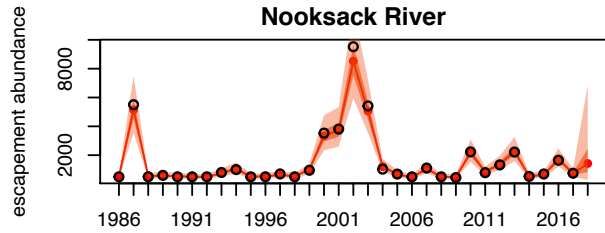
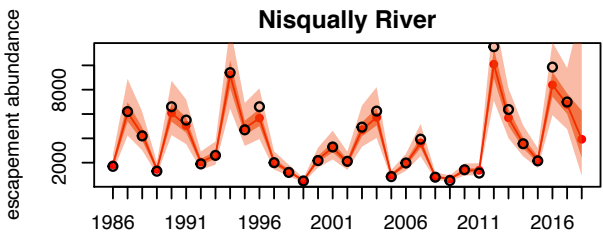
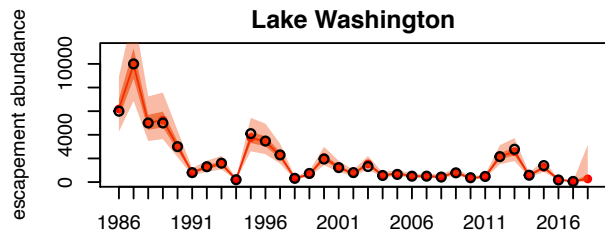


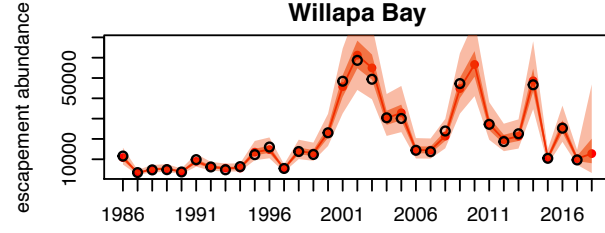
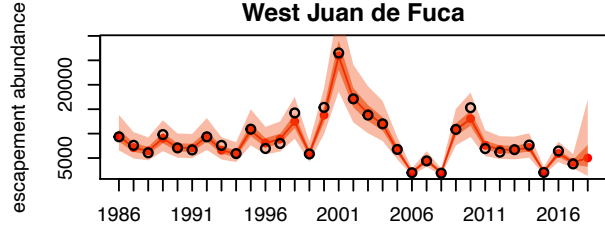
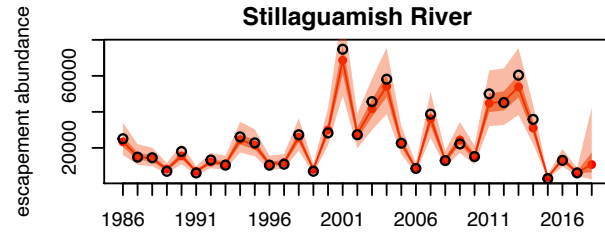
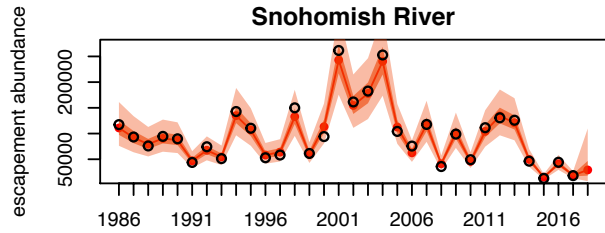
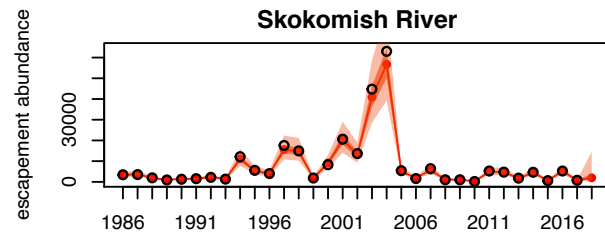
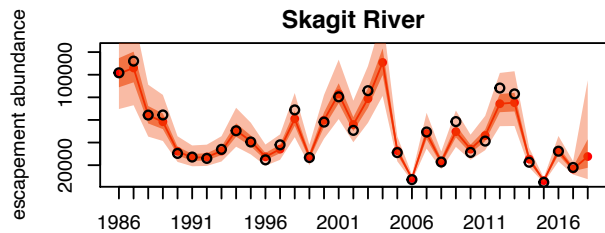


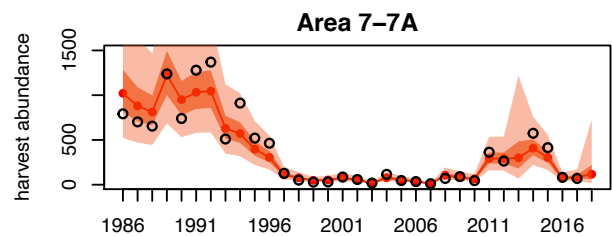
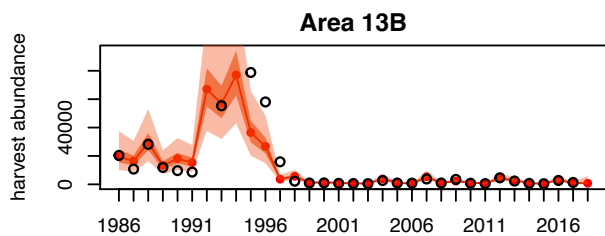
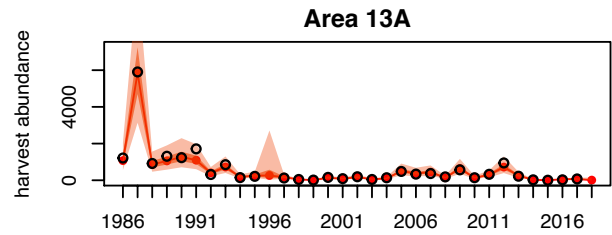
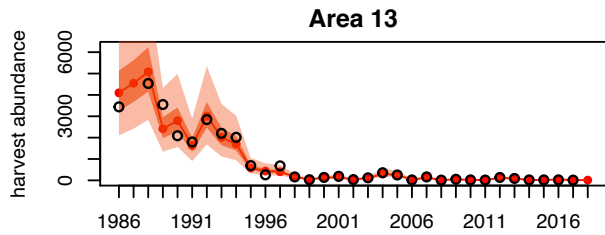
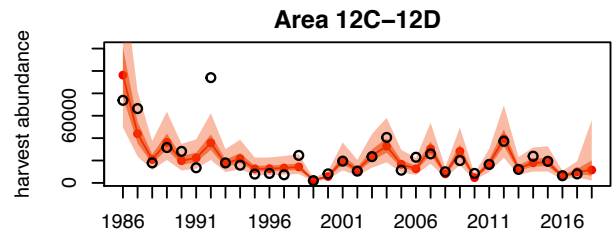
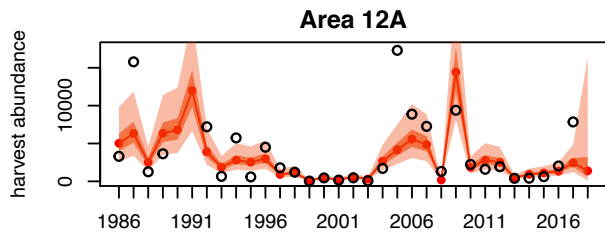
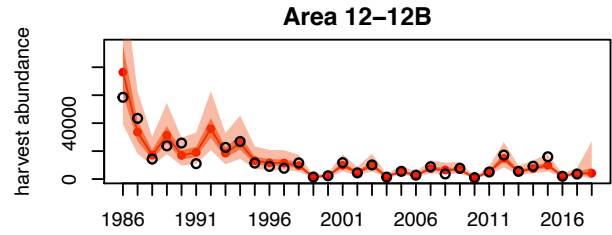
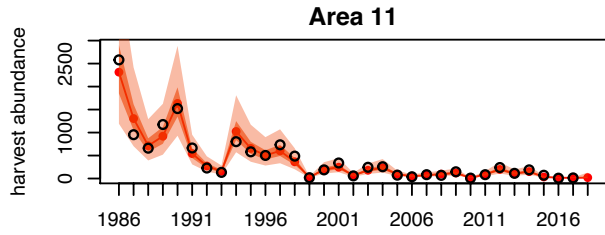
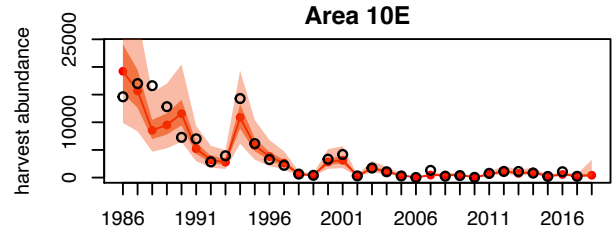
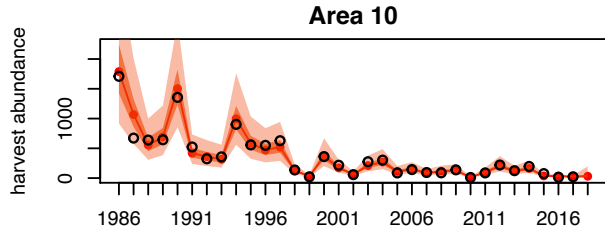


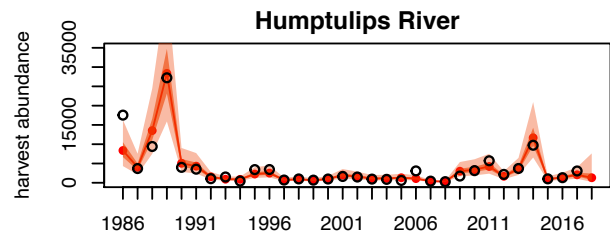
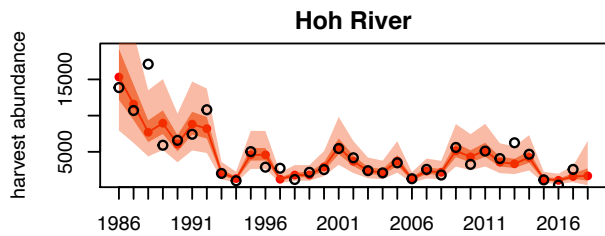
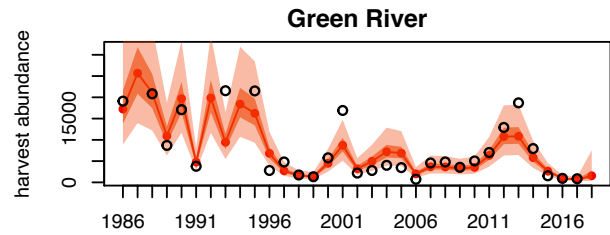
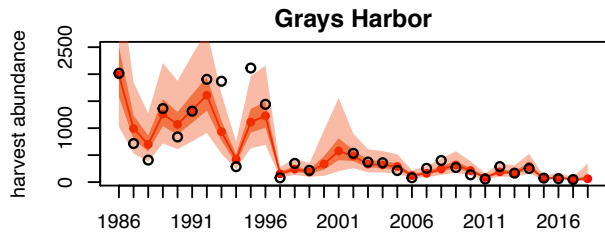
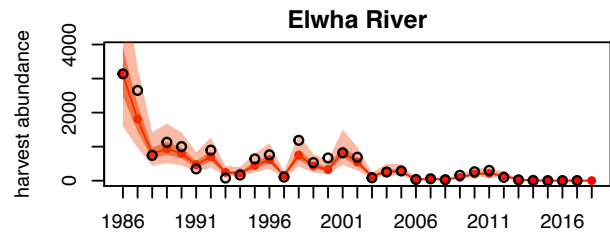
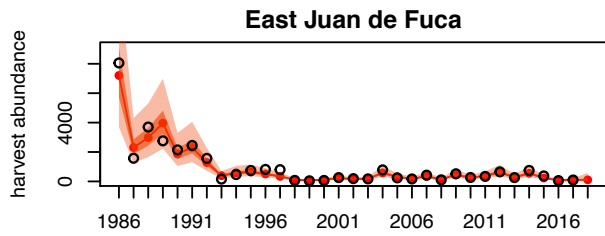
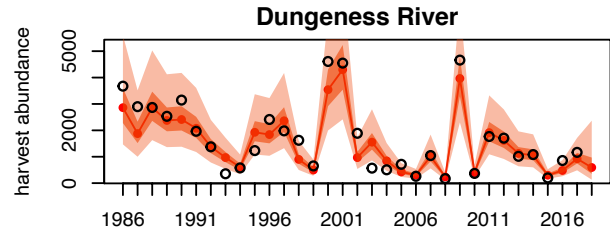
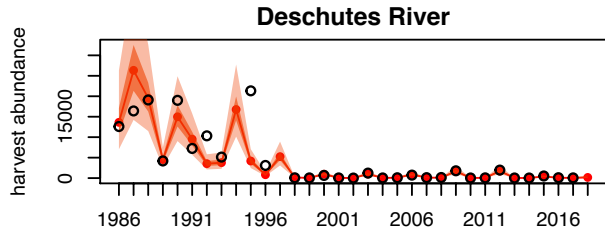
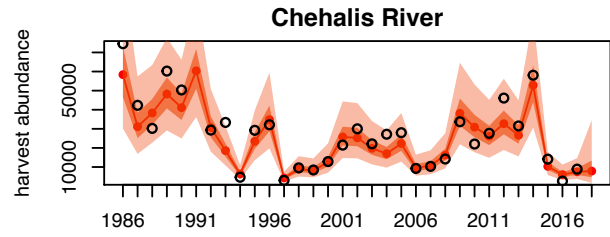
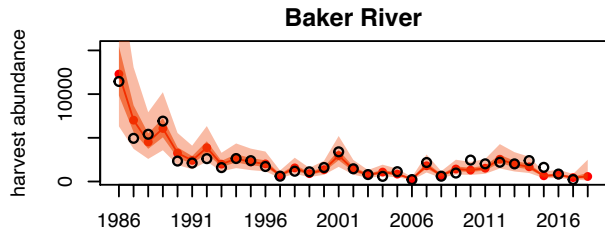


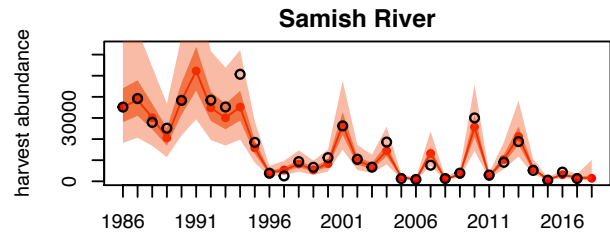
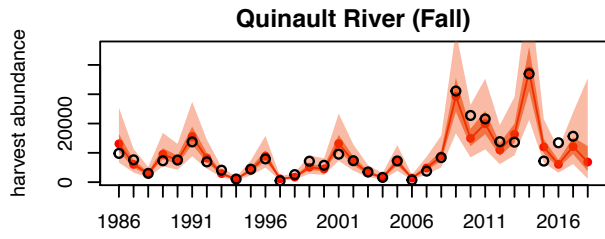
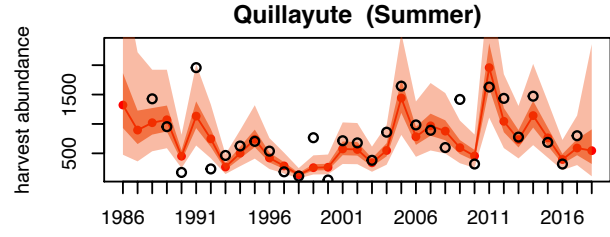
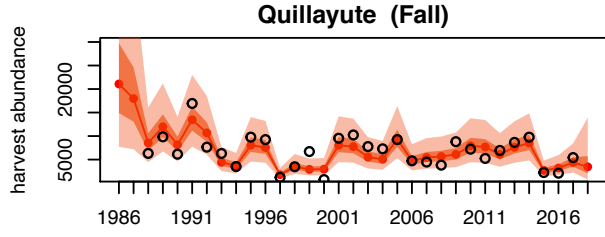
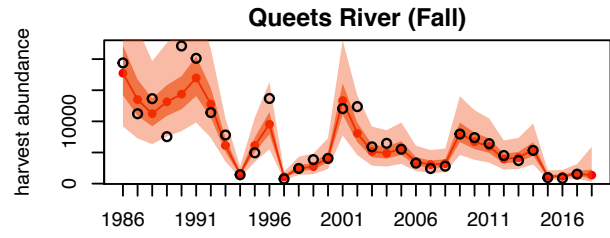
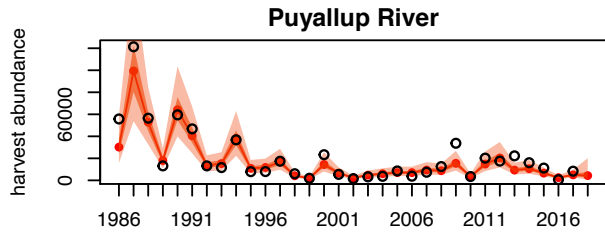
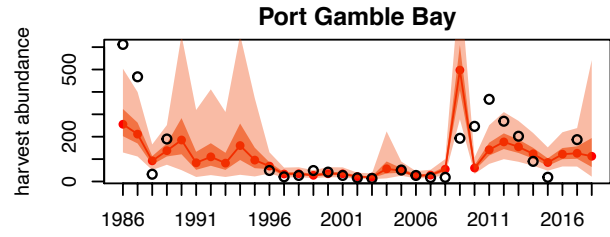
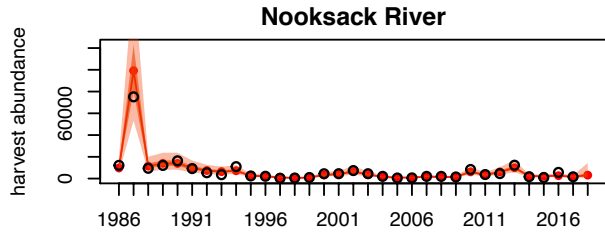
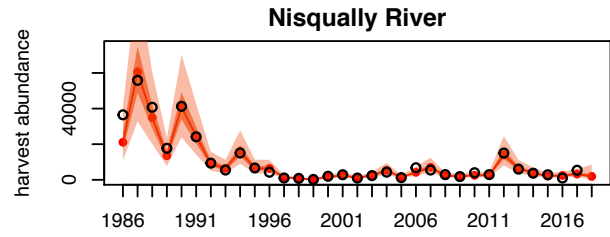
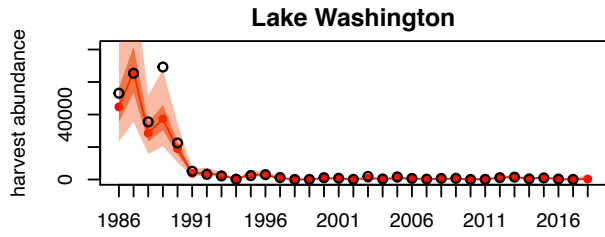


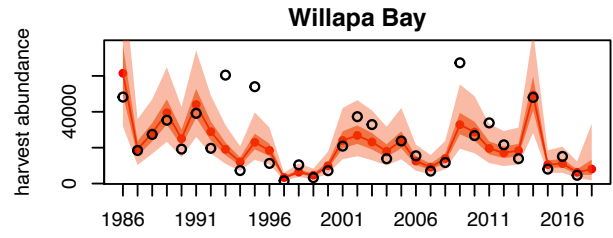
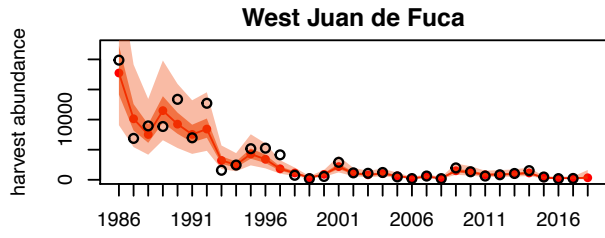
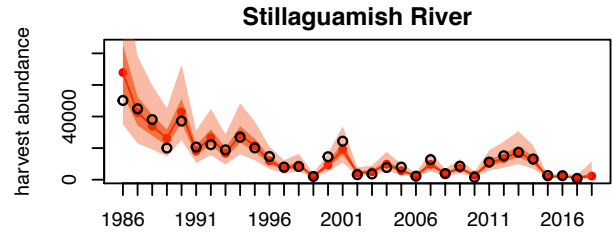
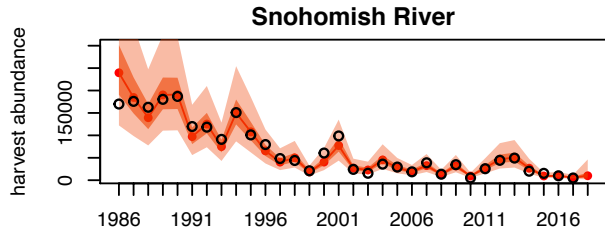
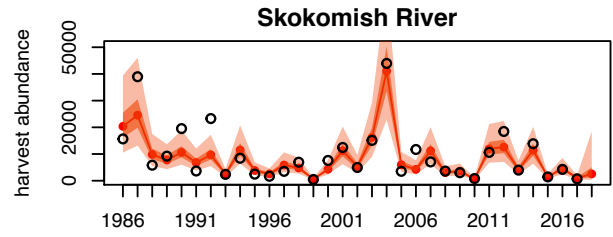
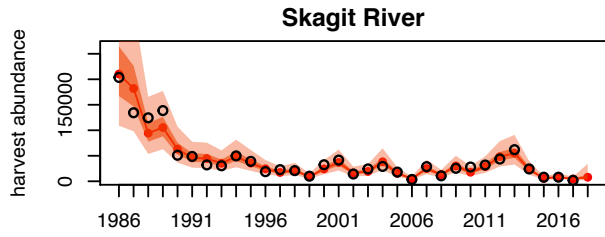


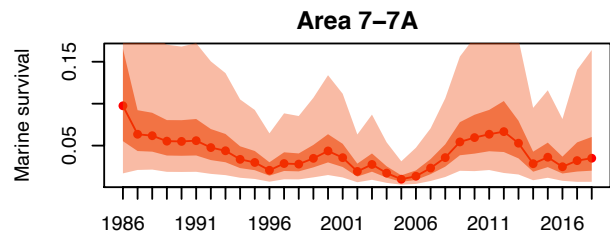
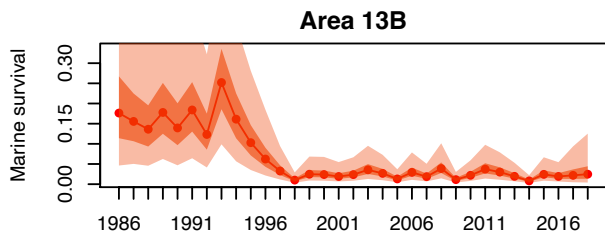
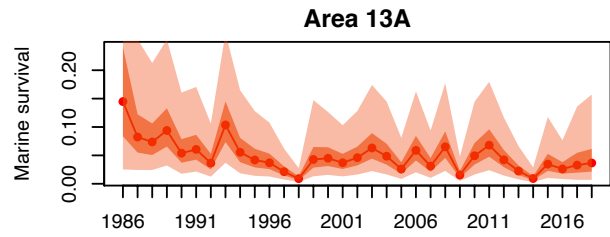
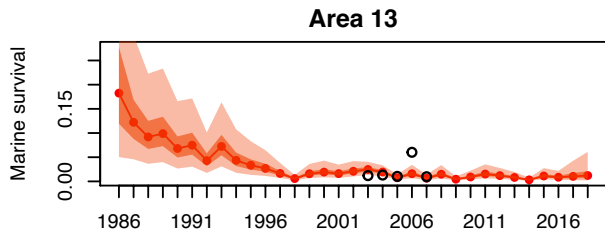
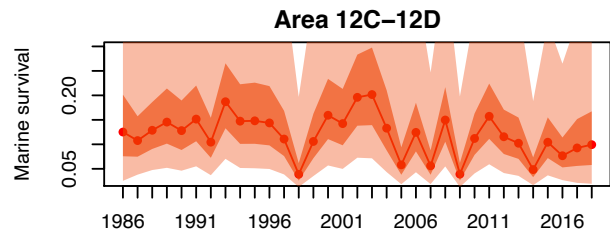
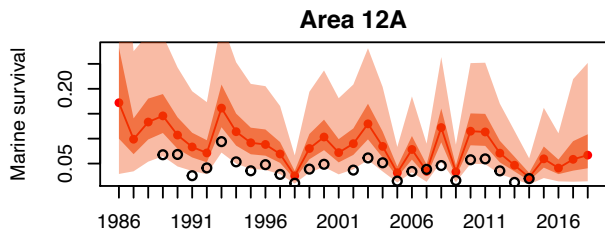
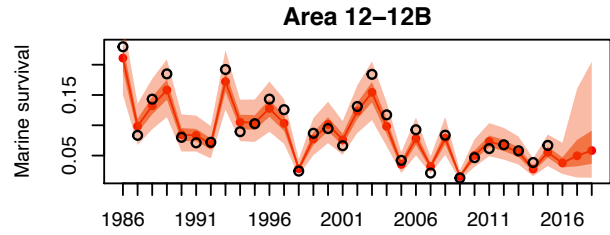
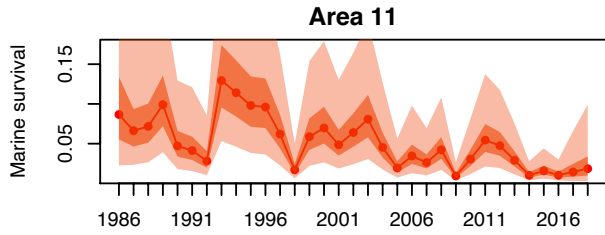
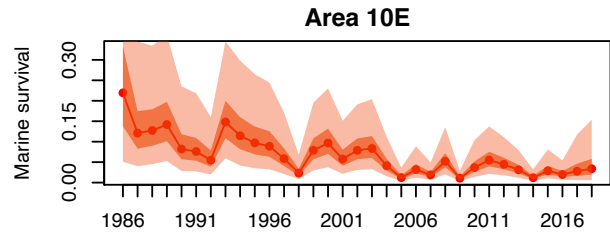
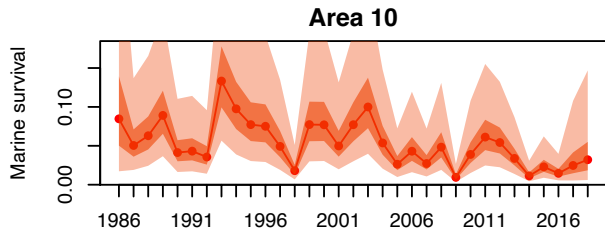


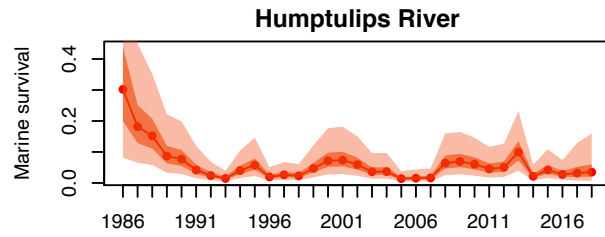
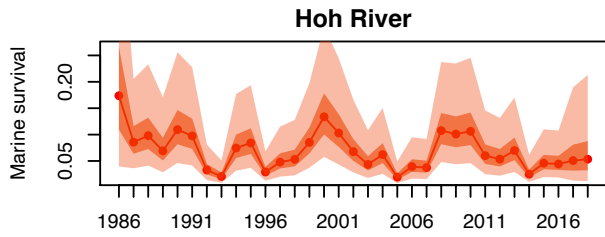
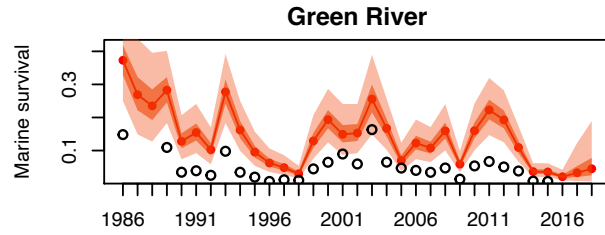
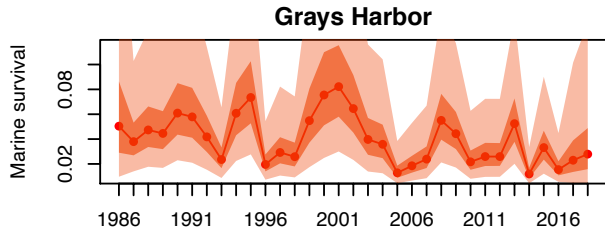
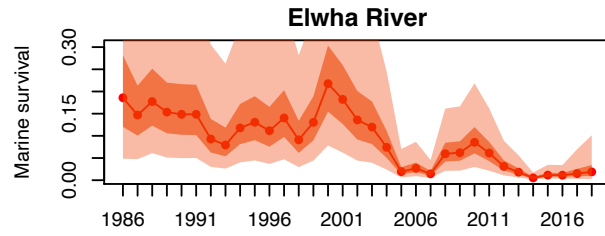
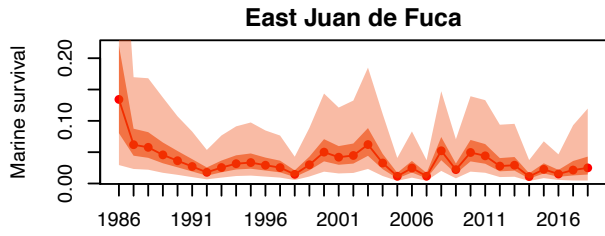
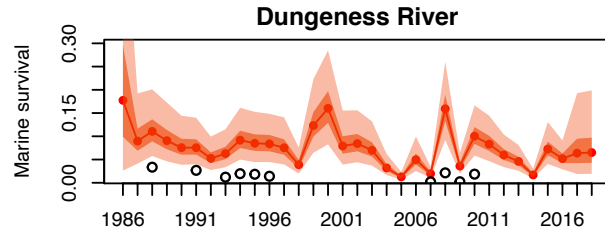
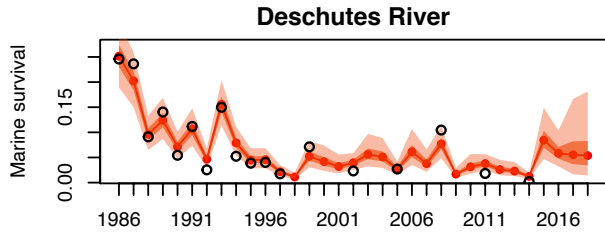
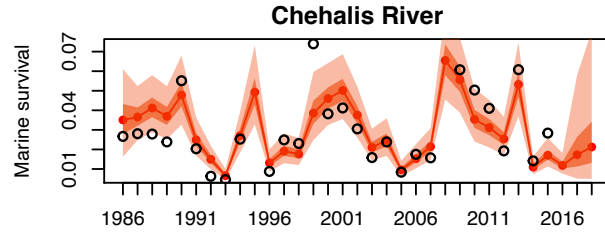
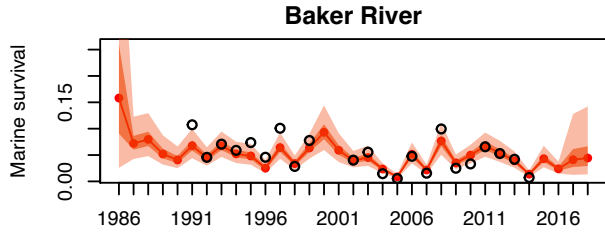


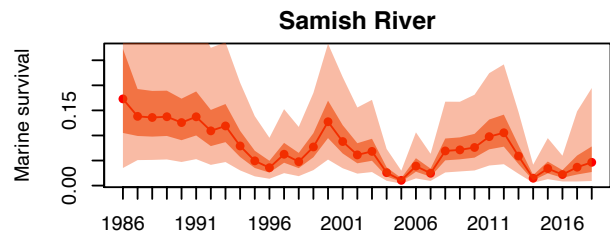
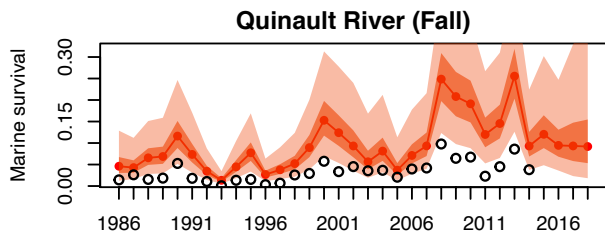
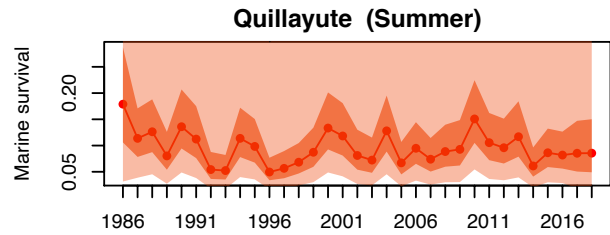
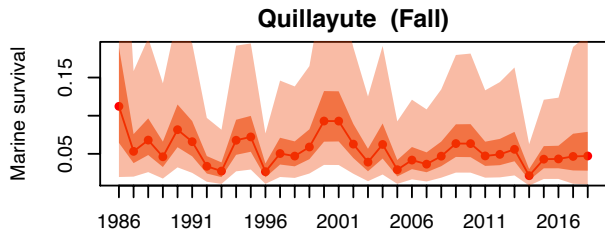
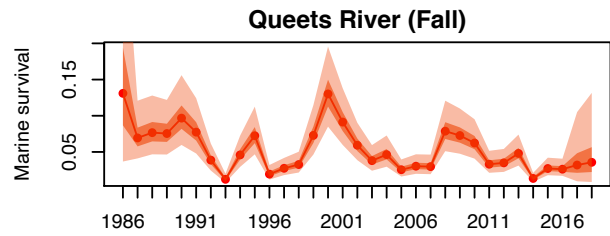
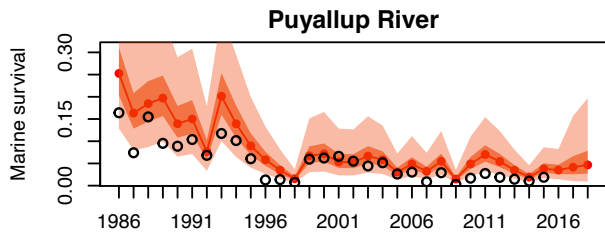
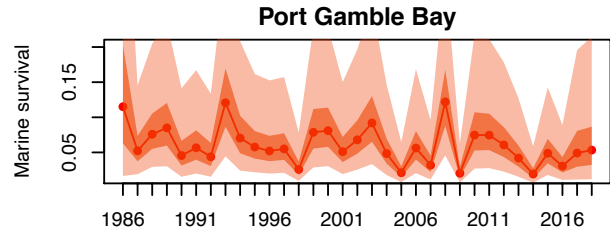
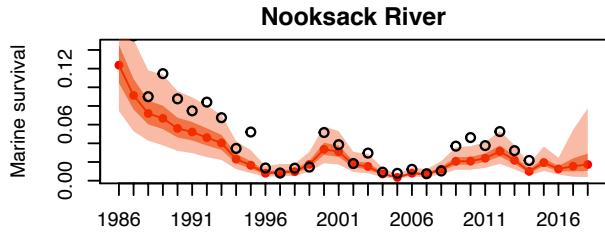
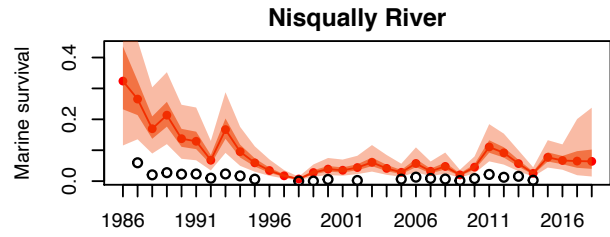
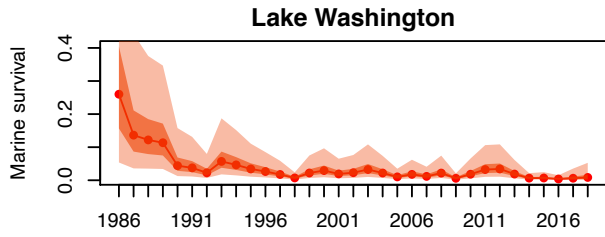


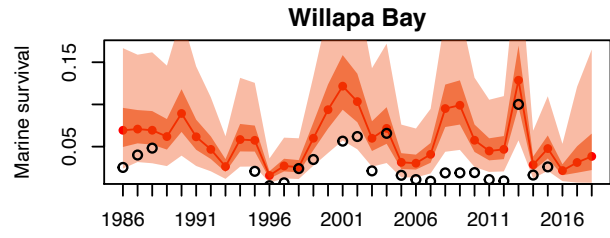
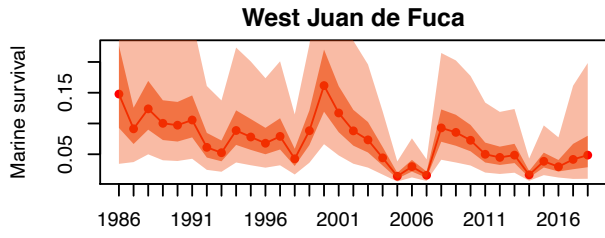
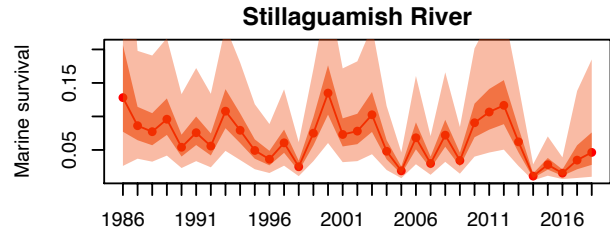
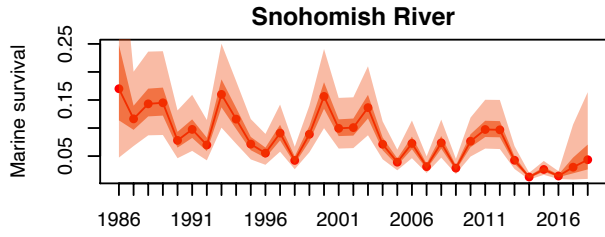
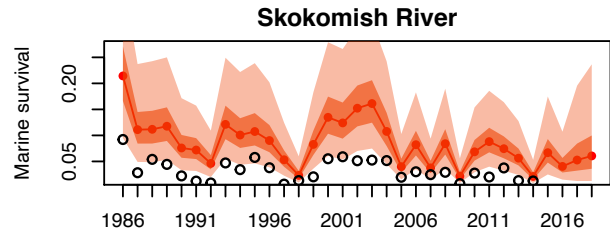
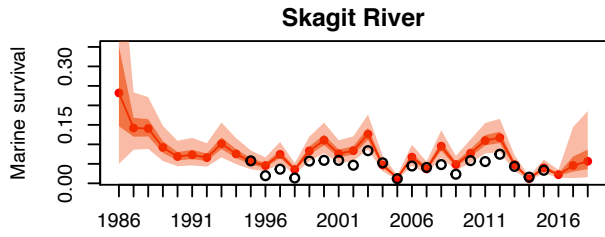


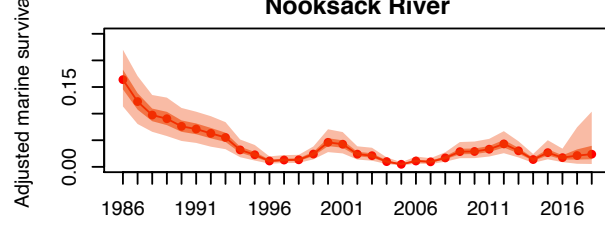
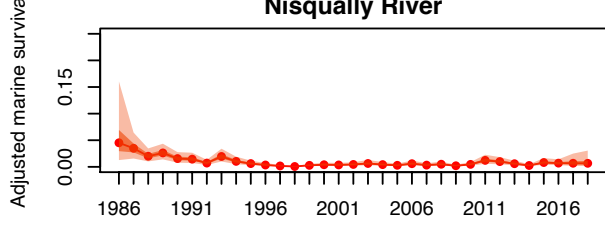
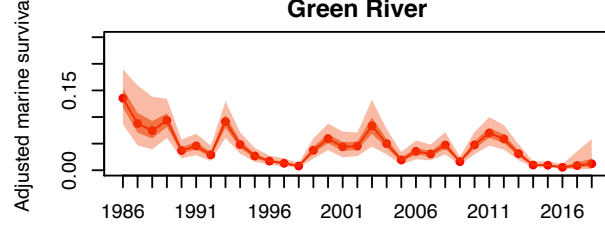
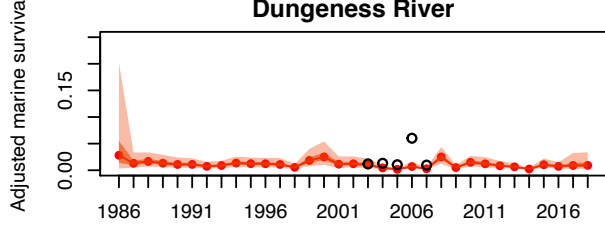
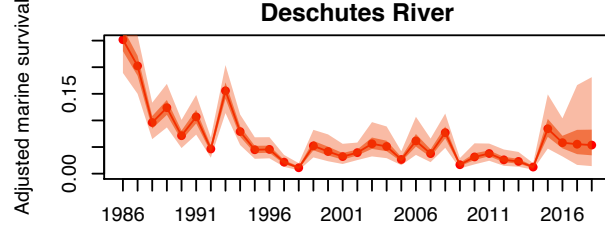
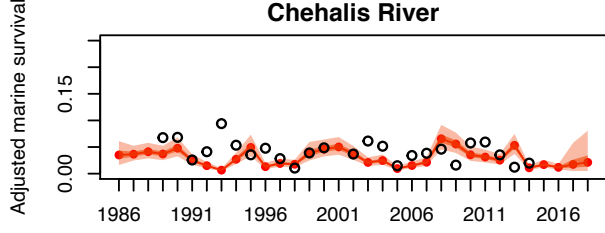
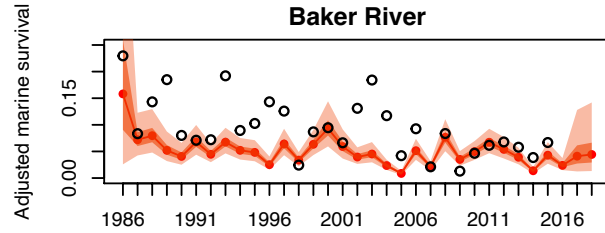
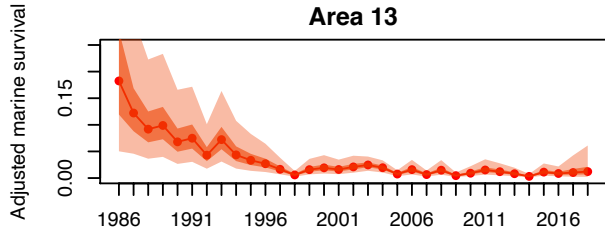
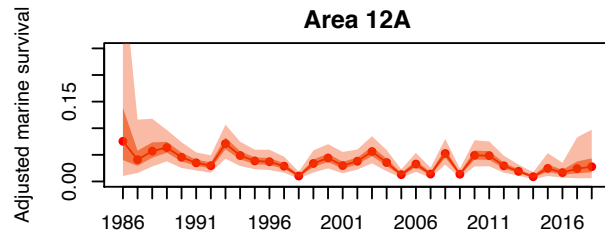
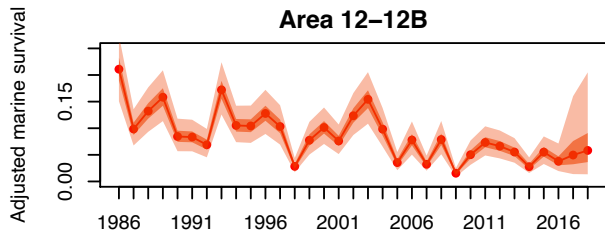












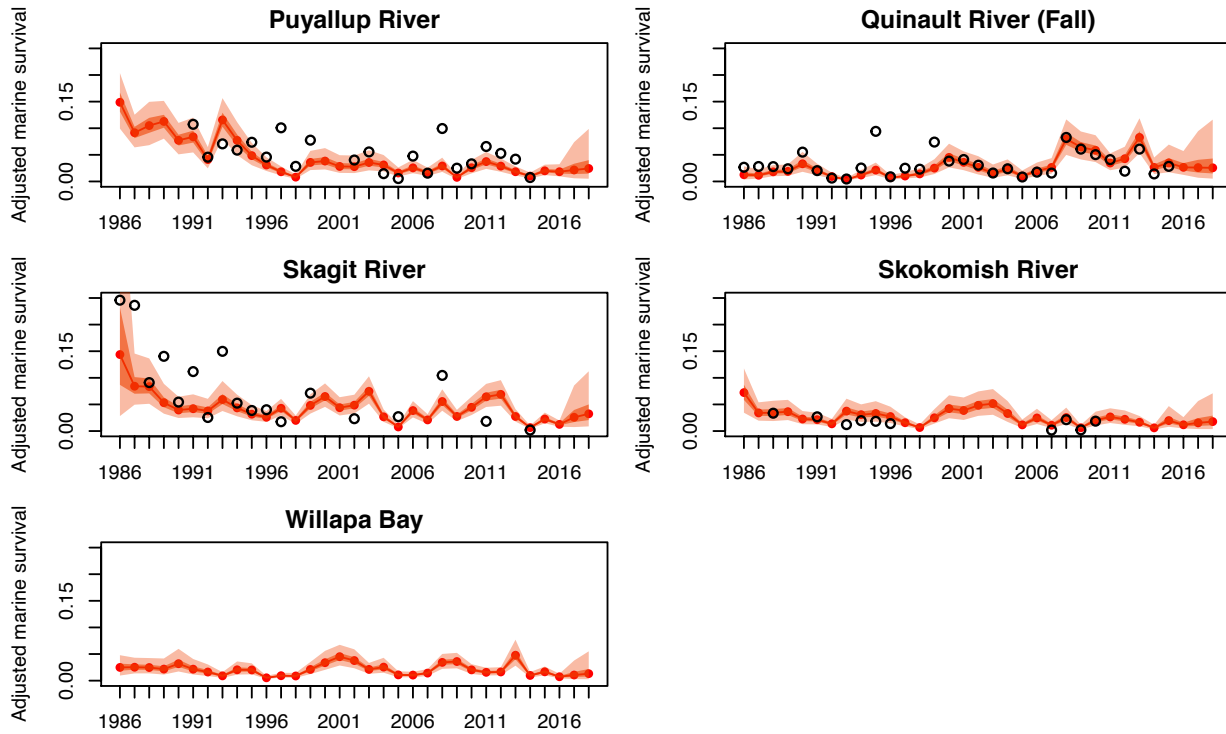
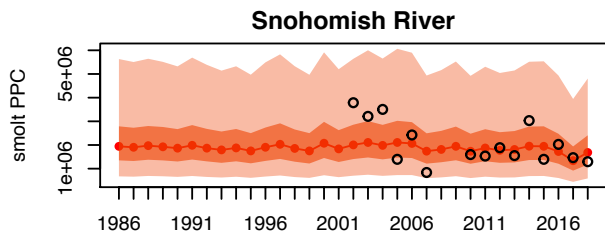
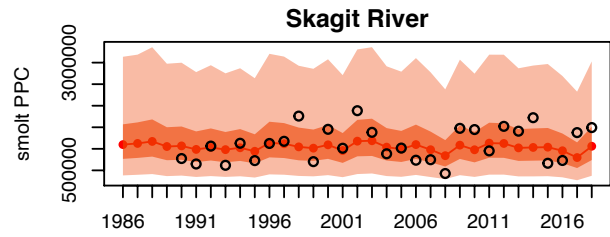
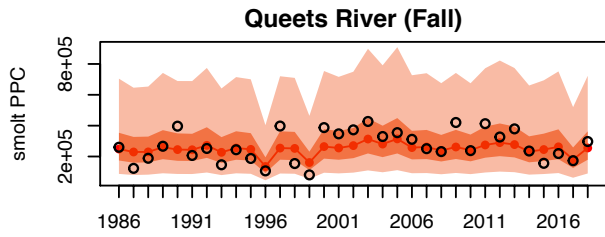
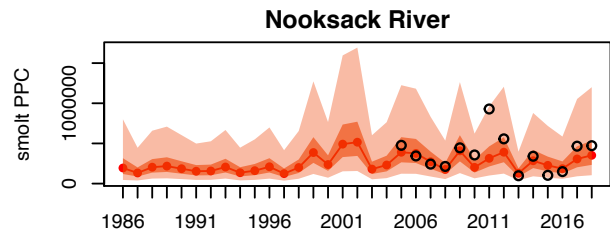
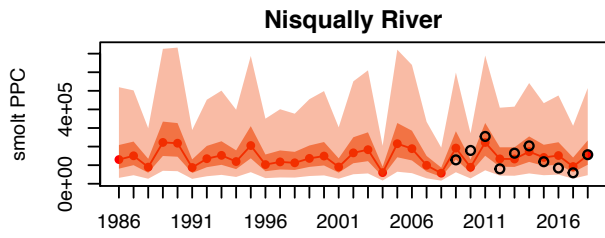
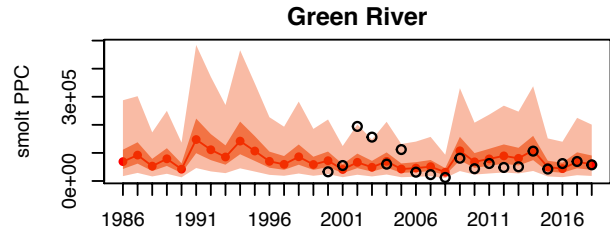
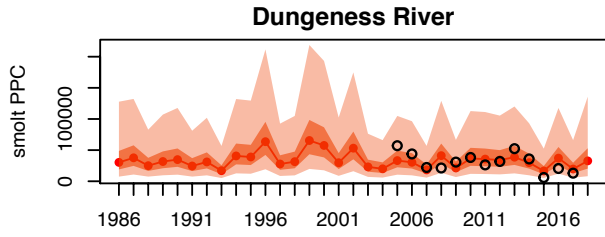
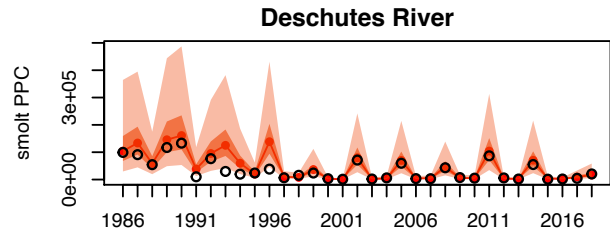
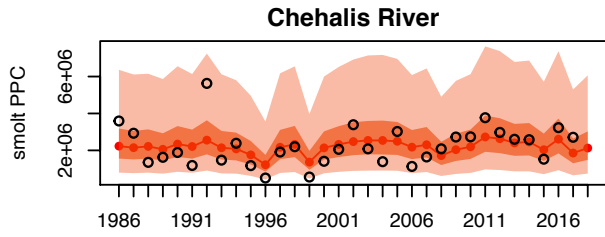
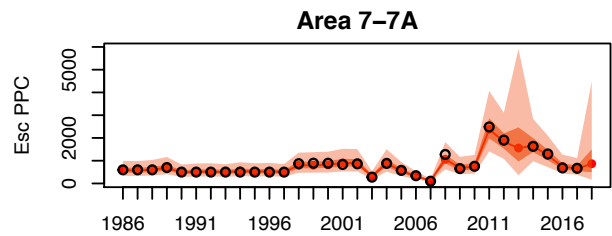
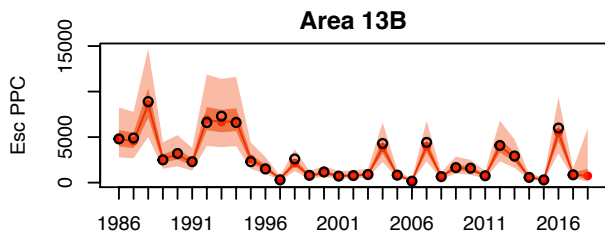
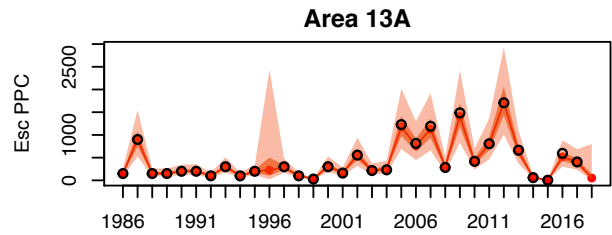
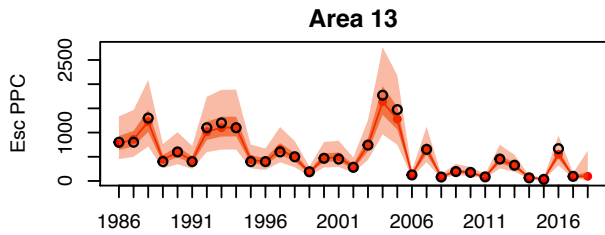
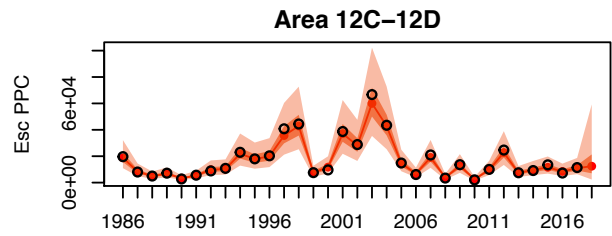
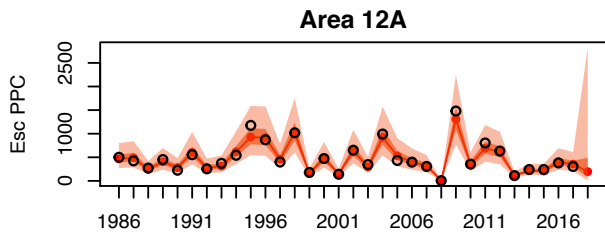
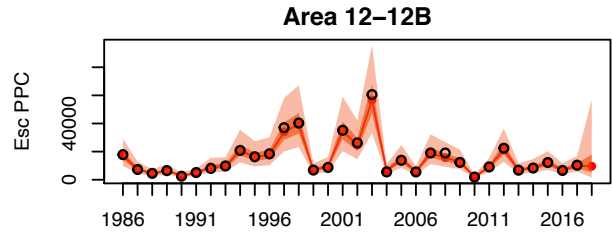
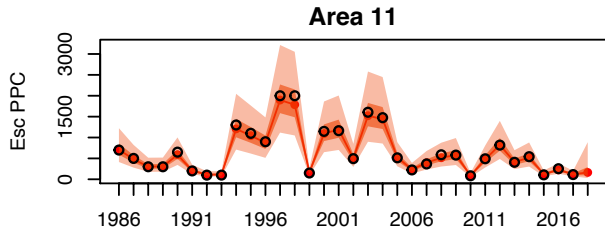
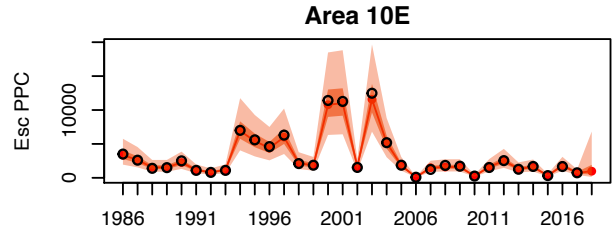
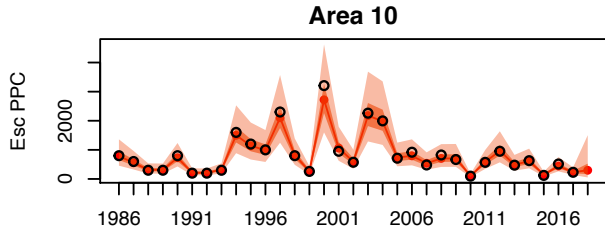
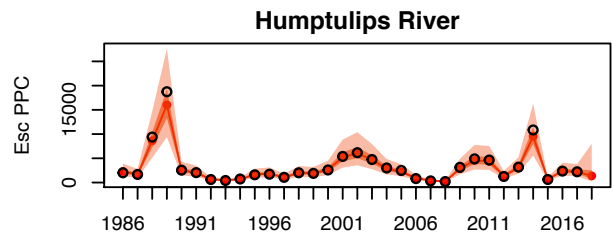
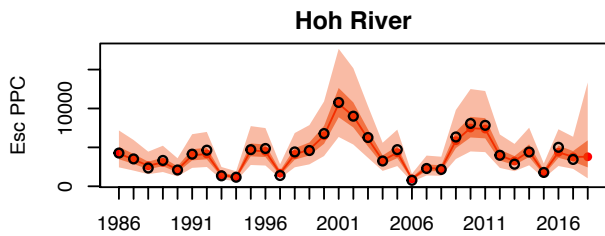
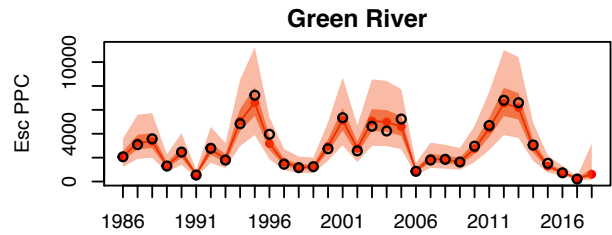
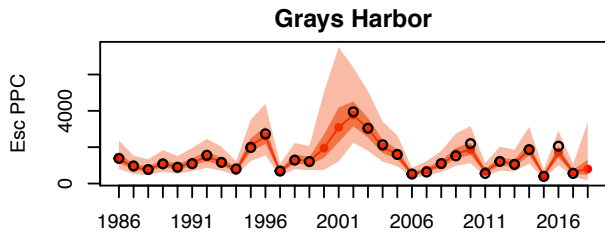
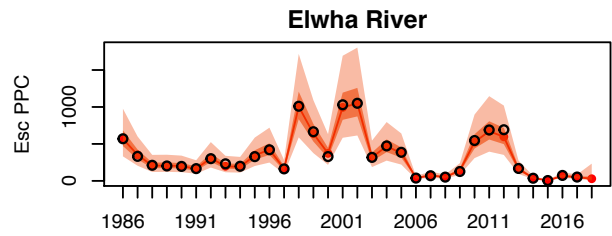
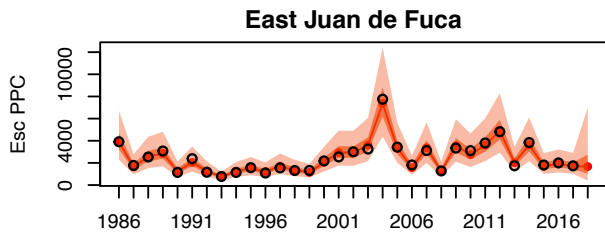
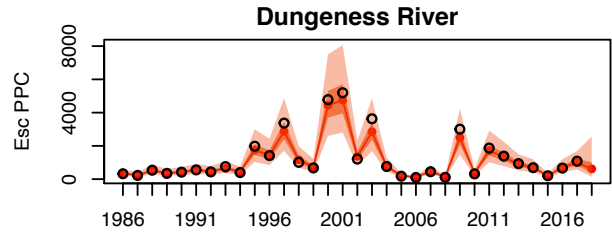
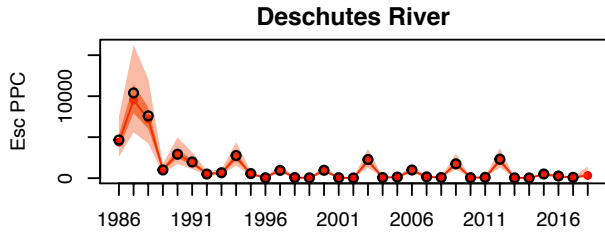
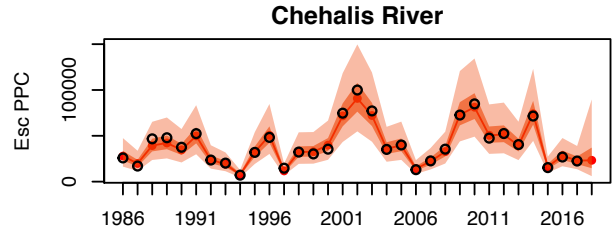
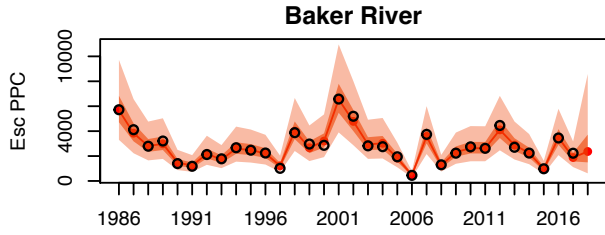
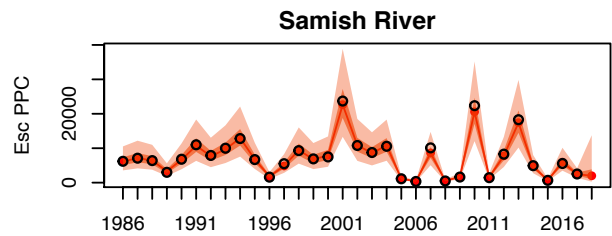
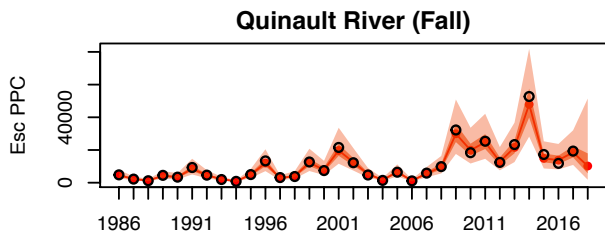
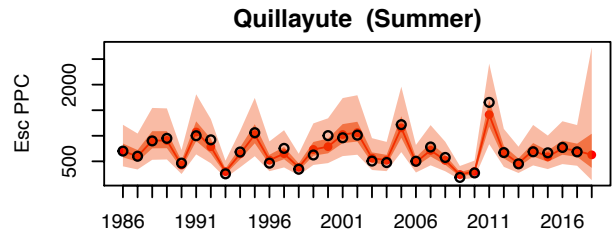
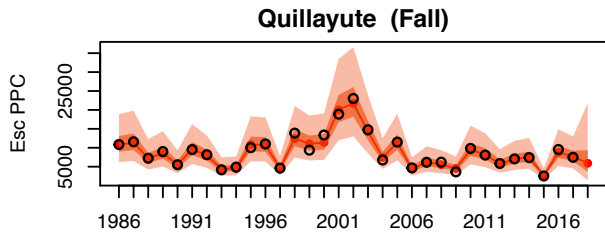
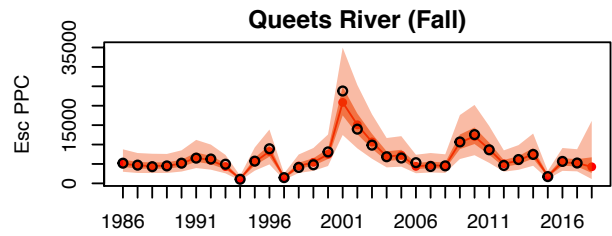
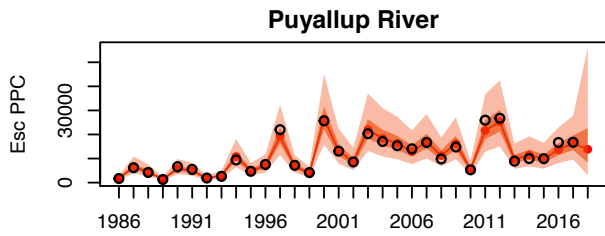
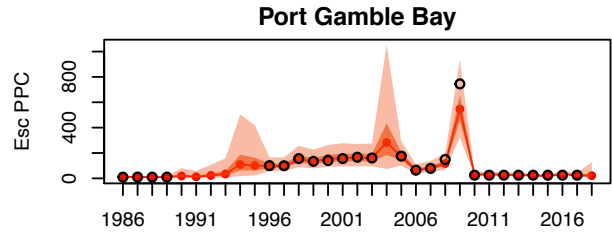
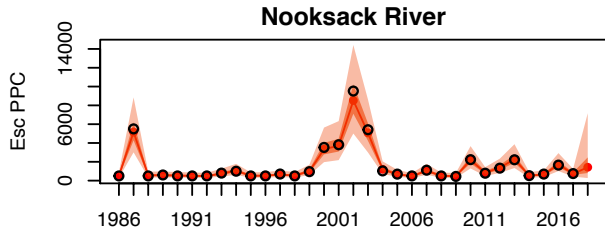
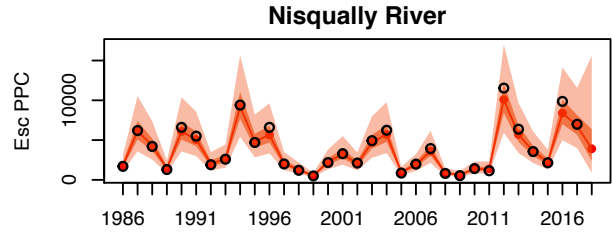
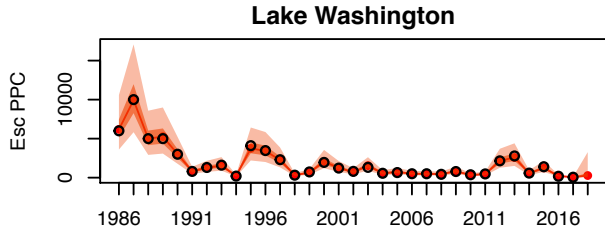


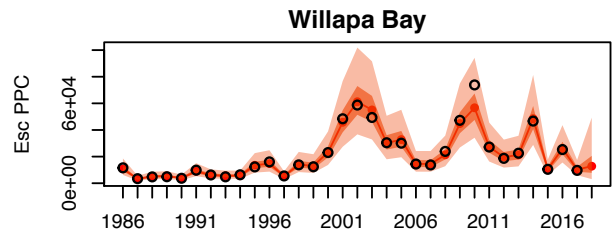
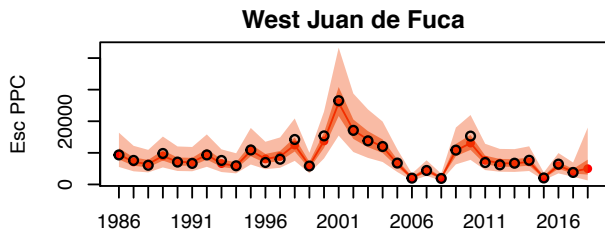
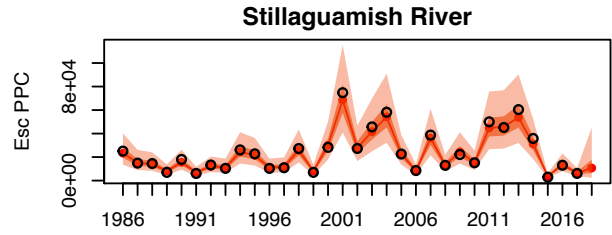
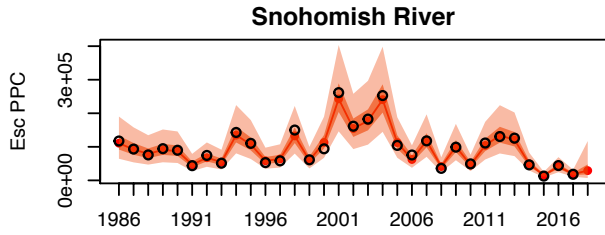
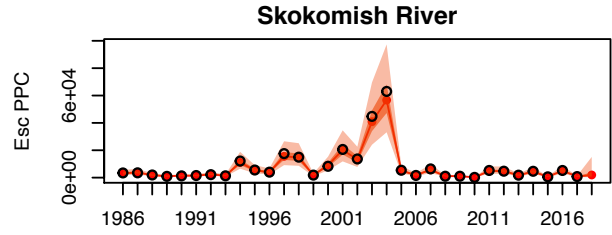
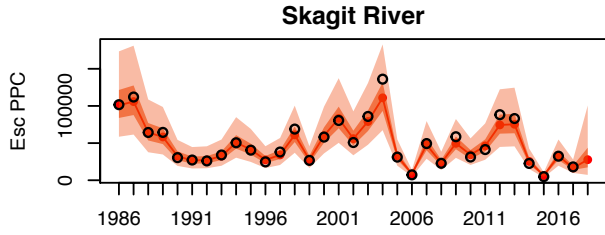
Figure S2. Model fits of the spatiotemporal integrated population model (ST-IPM) to observed smolt, escapement, harvest, and coded wire tag (CWT) data. In all panels, median state estimates are shown as red dots and lines, while 50% and 95% credible intervals are shown as dark and light shaded boundaries respectively. Where available, observed data points are shown as black open circles. Adjusted marine survival refers to the marine survival estimate including hatchery offset terms (eq. 24) where specified.

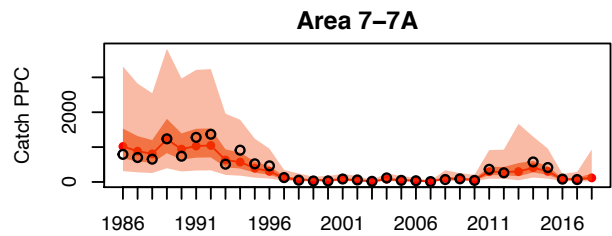
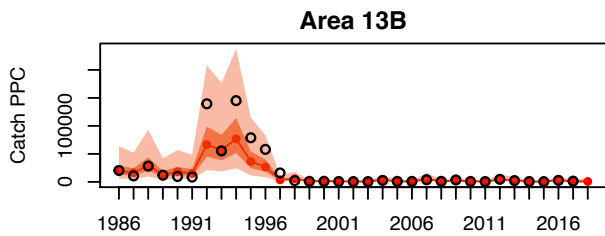
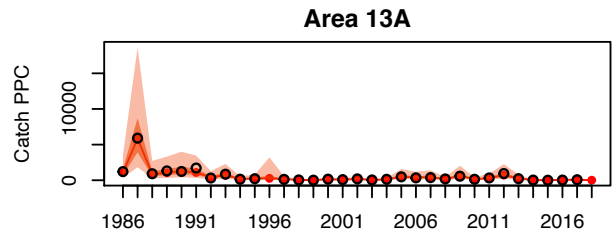
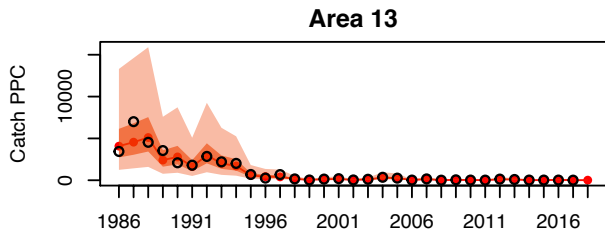
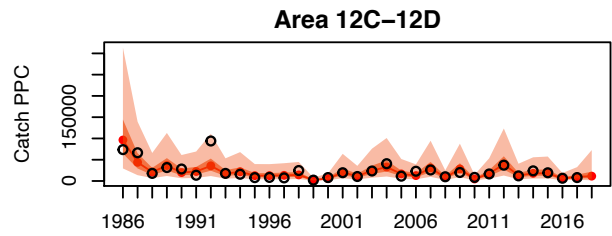
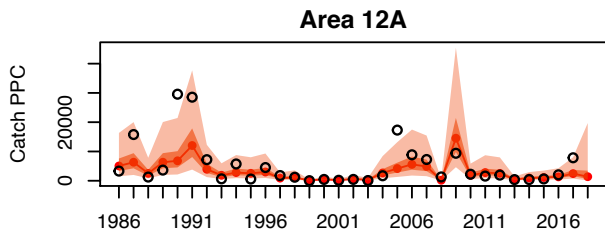
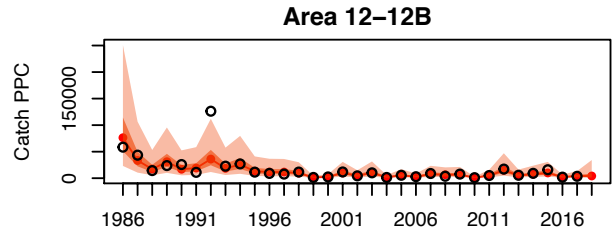
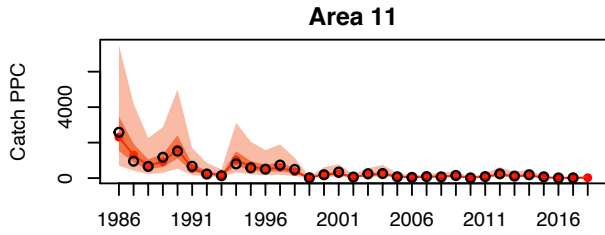
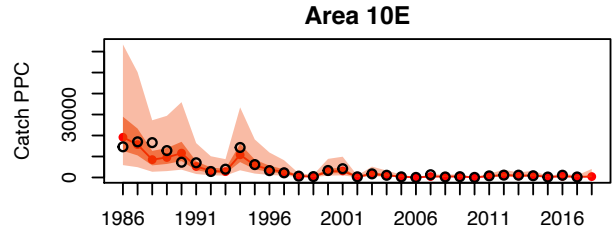
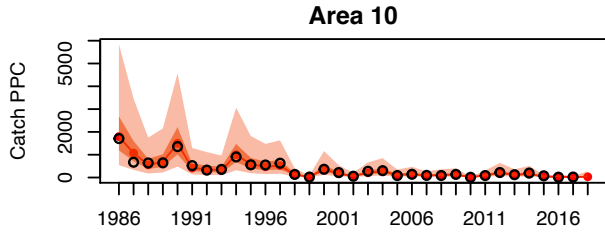


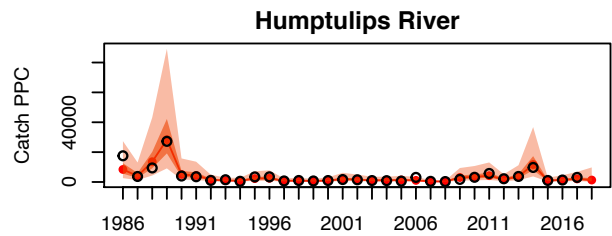
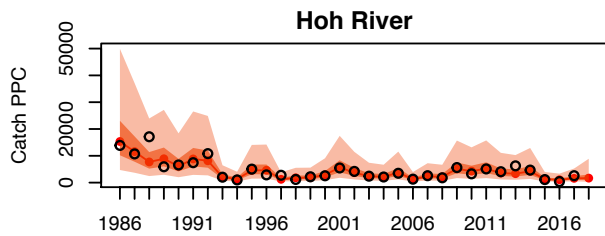
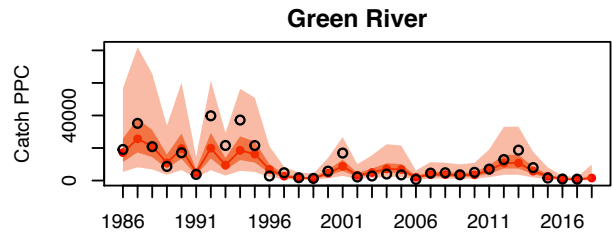
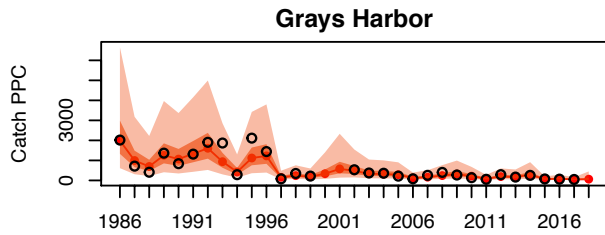
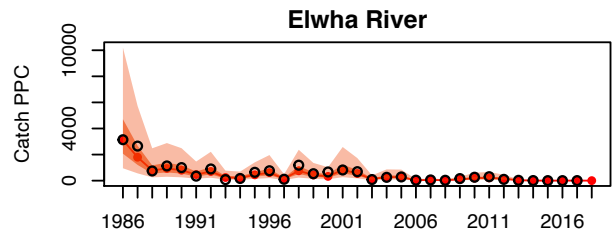
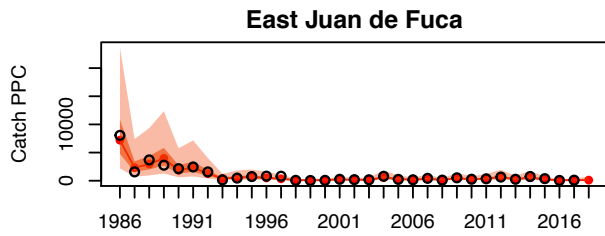
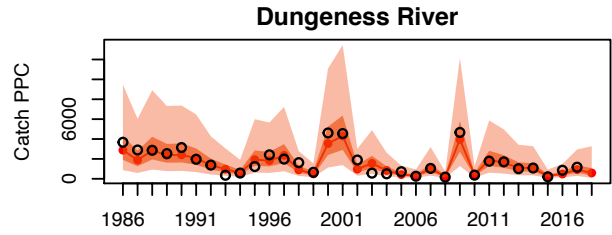
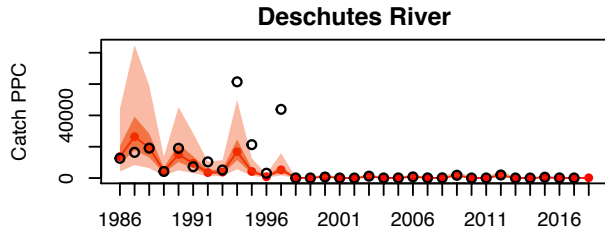
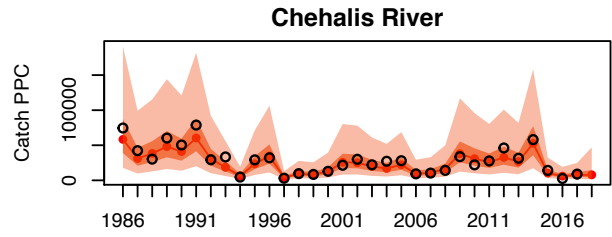
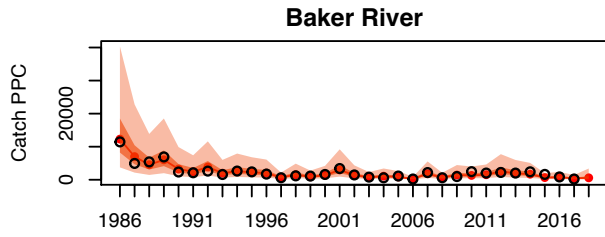


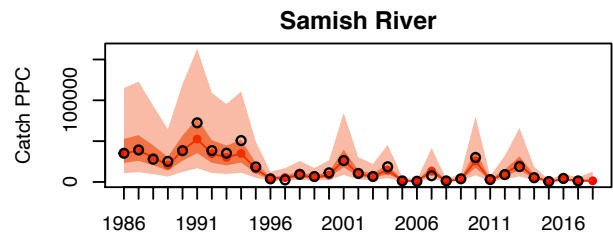
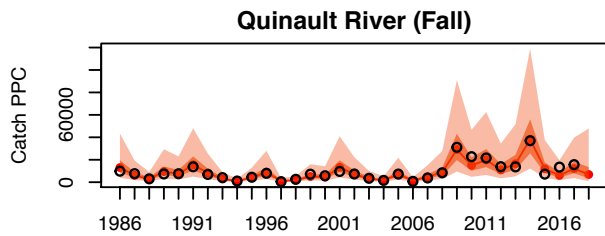
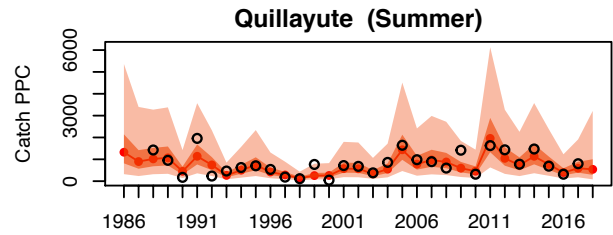
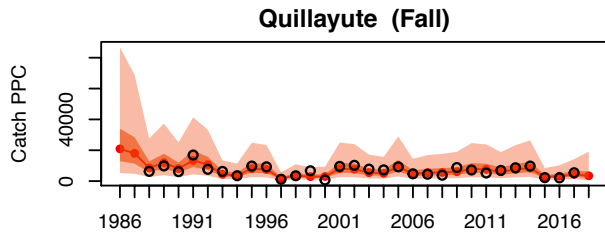
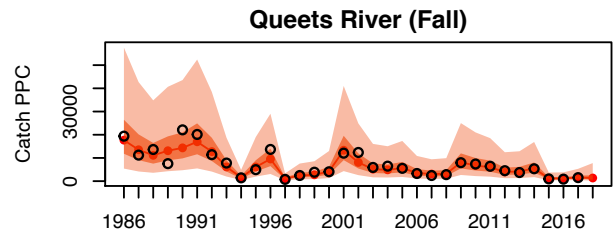
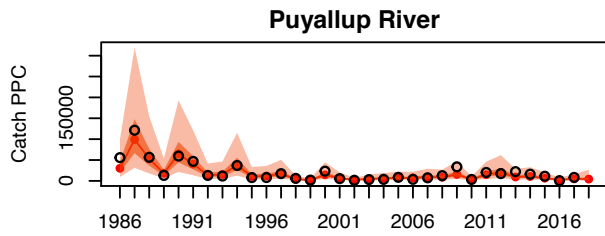
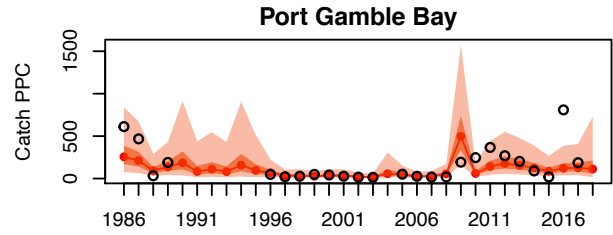
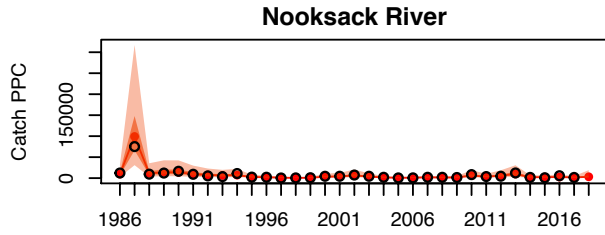
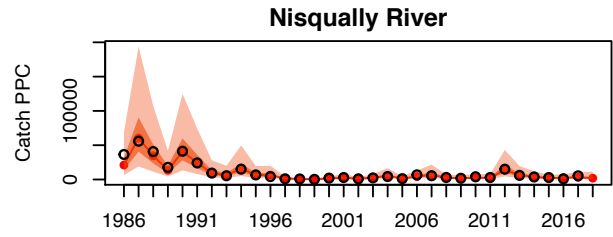
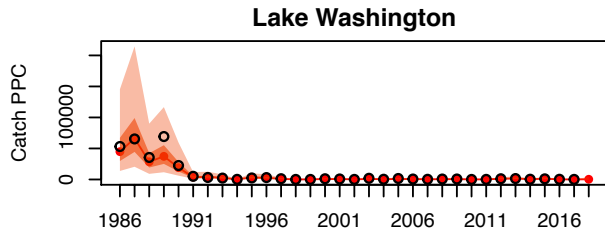


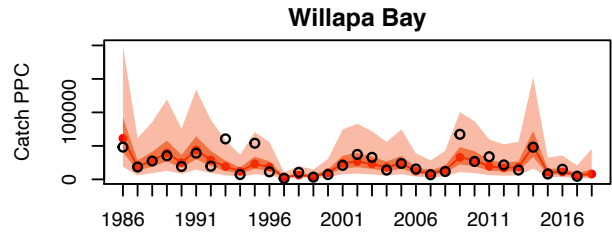
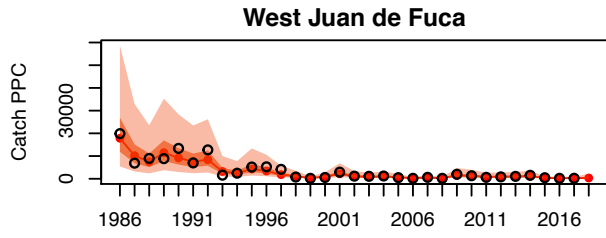
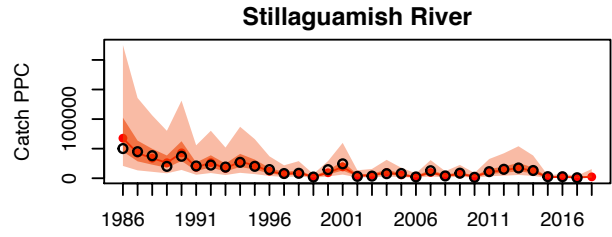
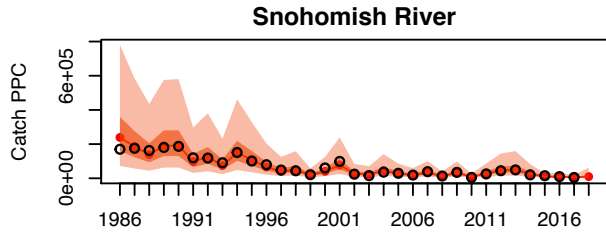
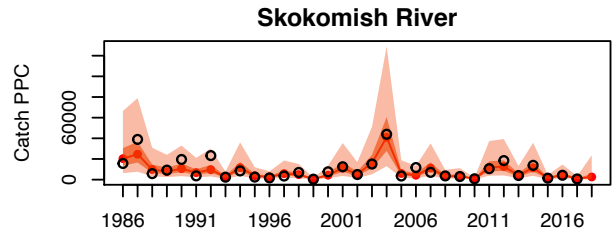
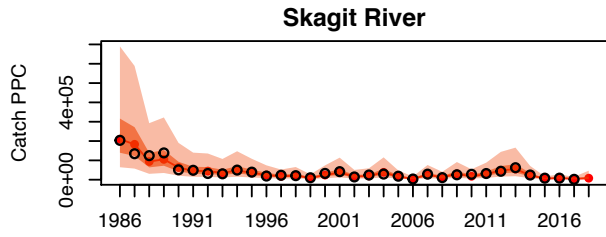


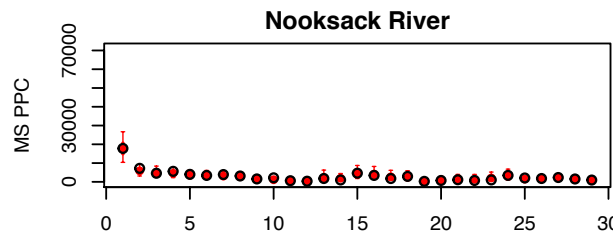
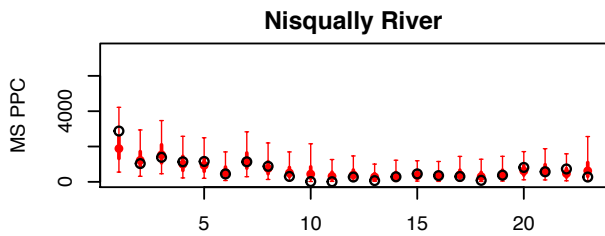
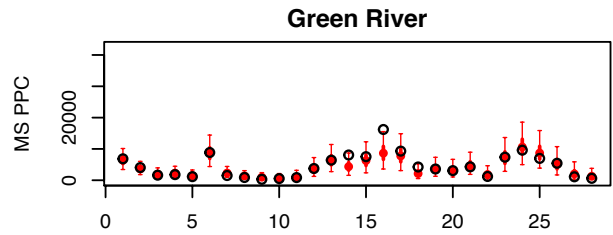
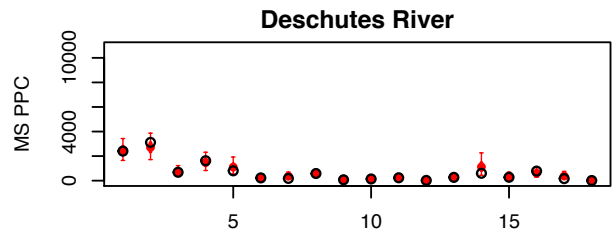
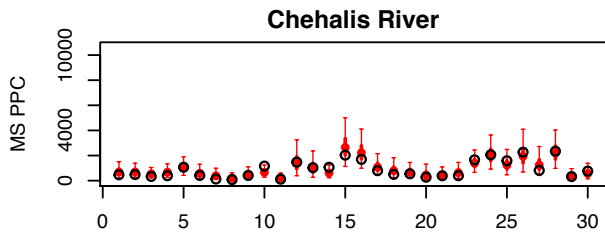
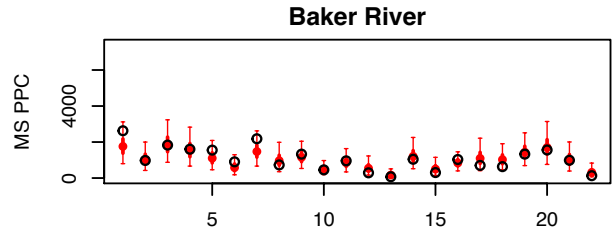
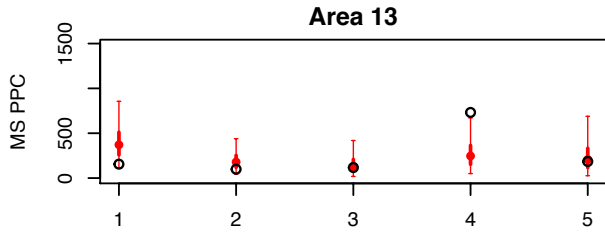
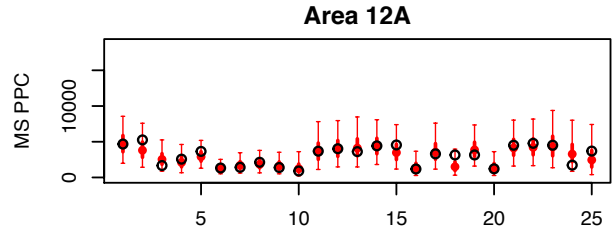
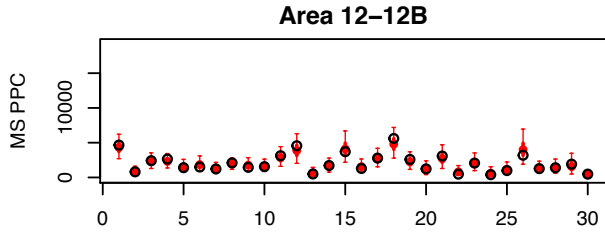












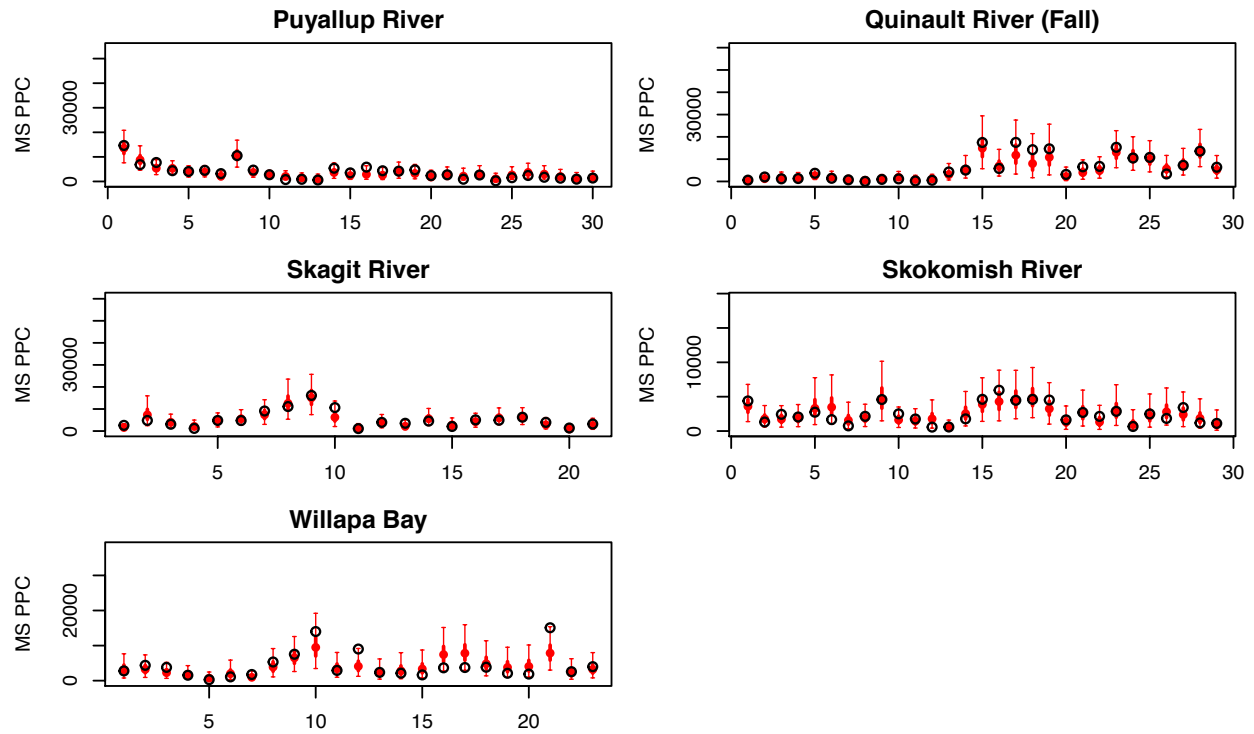


Figure S3. Posterior predictive checks for smolt, escapement, harvest and coded wire tag (CWT) data. For the smolt, escapement, and harvest abundance data, red dots and lines represent the median of the predictive distribution for each quantity, and dark and light shading represent the 50% and 95% predictive intervals respectively. For the CWT data, the median of the predictive distribution is shown as a red dot, and thick and thin lines represent the 50% and 95% predictive intervals respectively. Observed data are shown as open black circles

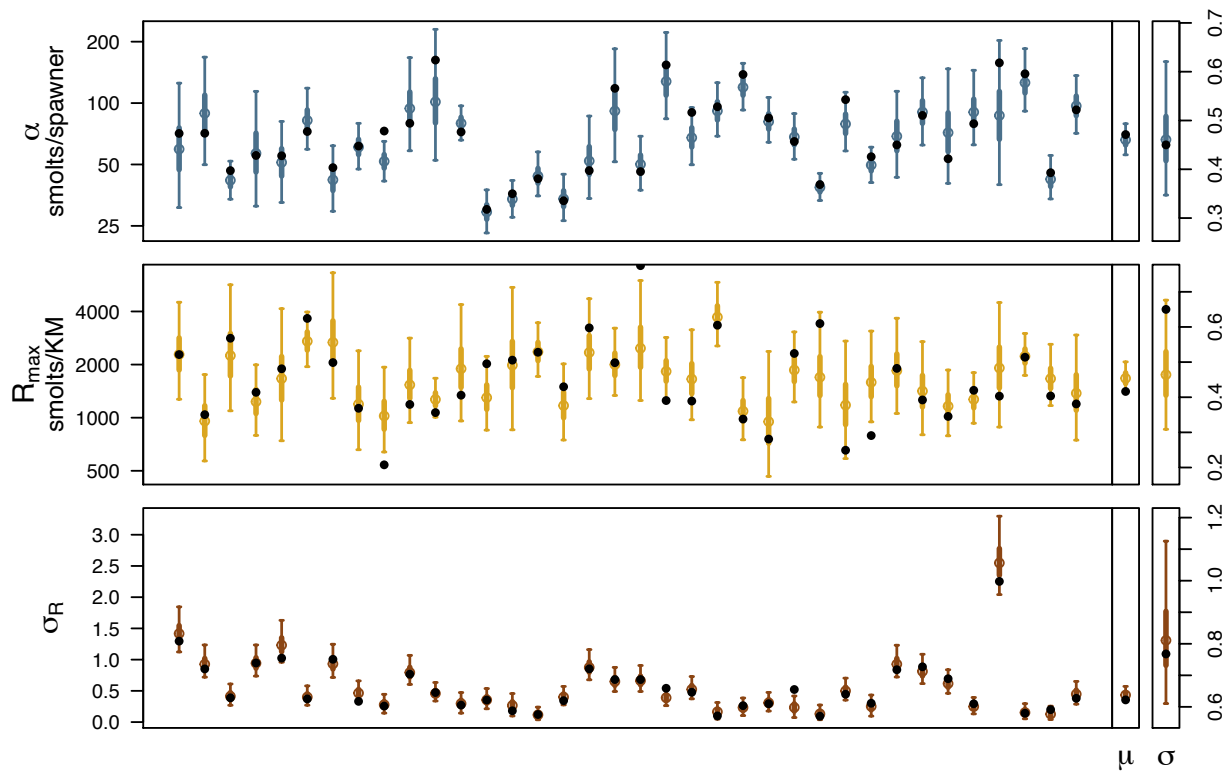


Figure S4. Model estimation of simulated adult-to-smolt Beverton-Holt parameters. Solid black dots represent the true underlying parameter values from which the simulated data were generated and the colored dots, colored thick lines, and colored thin lines represent the median estimate, 50% credible interval, and 95% credible interval of the model's estimate of each parameter respectively.

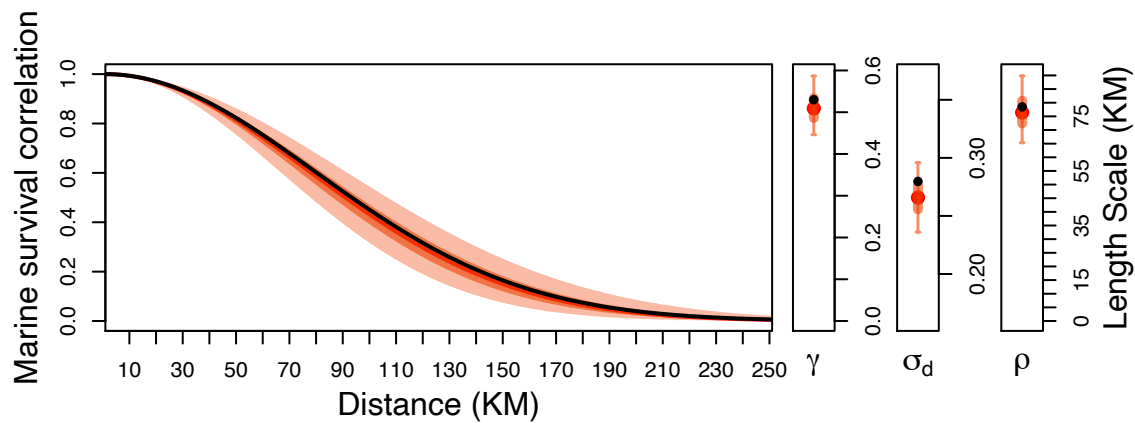
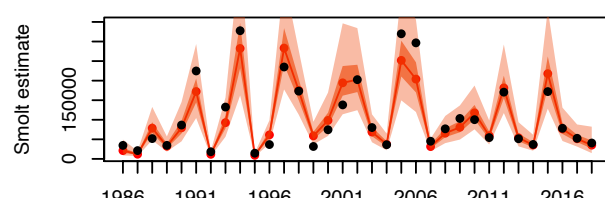
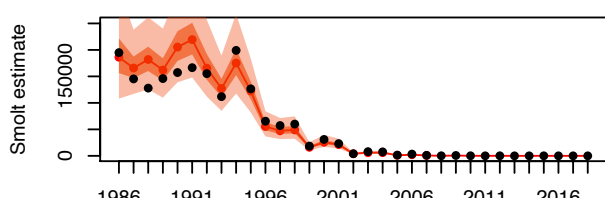
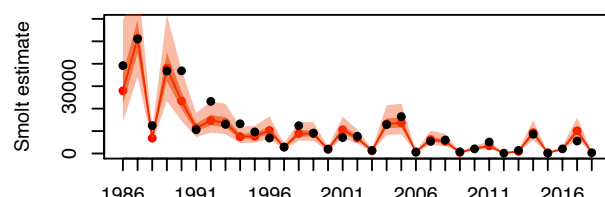
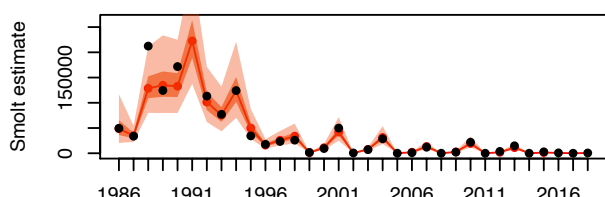
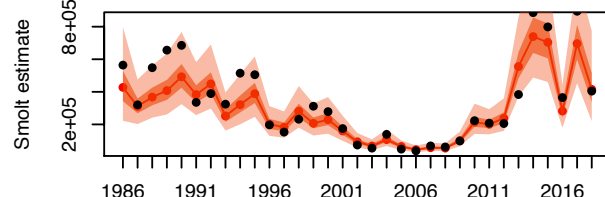
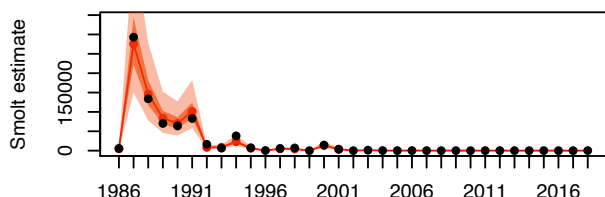
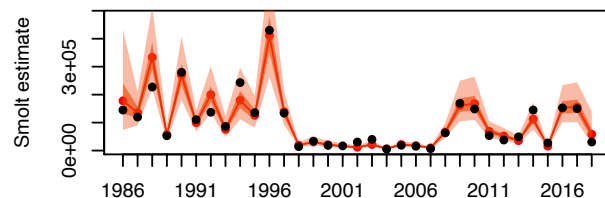
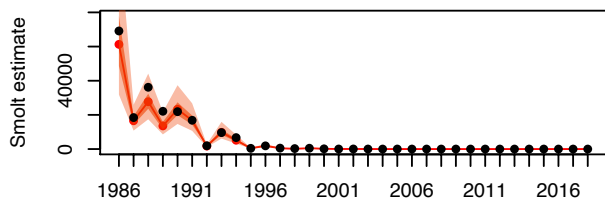
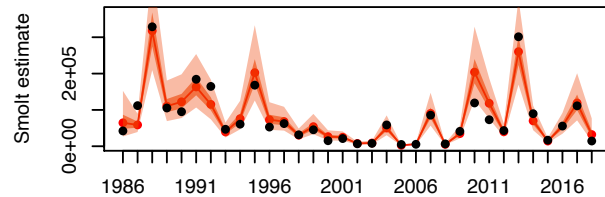
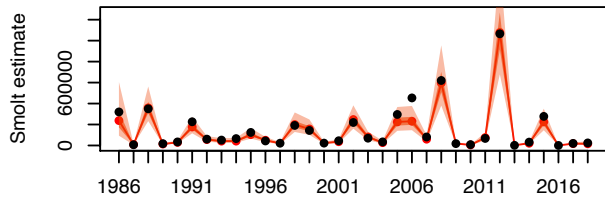
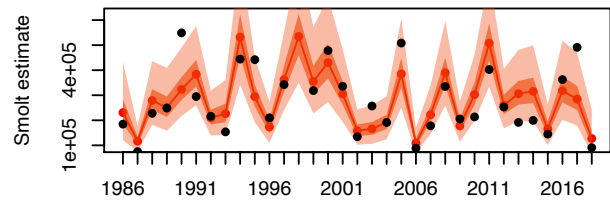
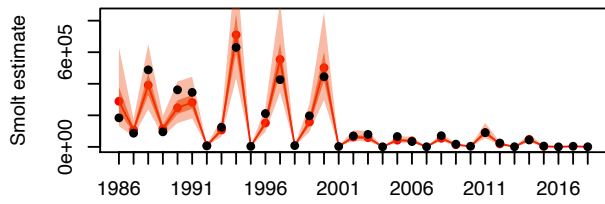
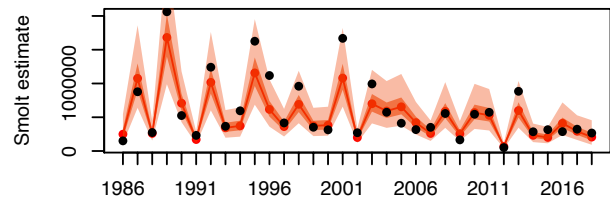
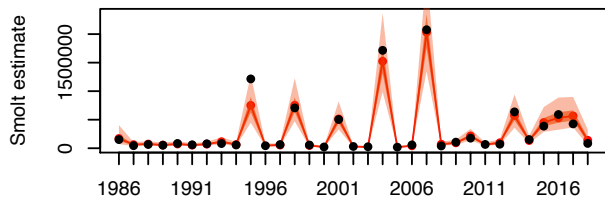
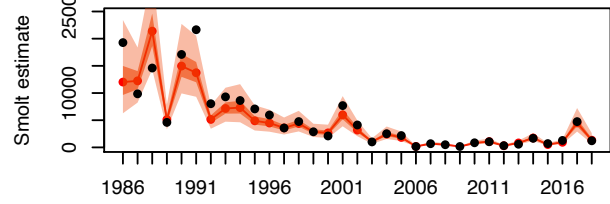
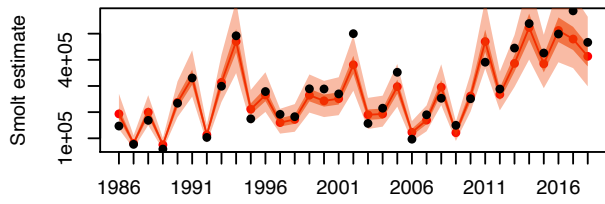
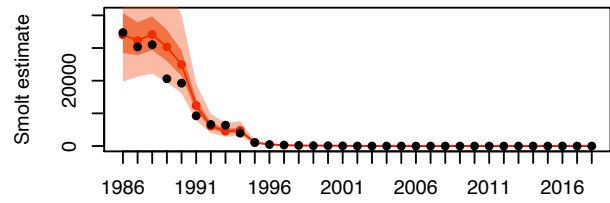
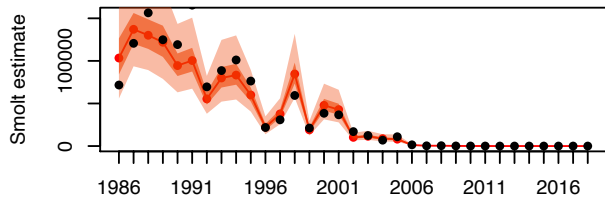
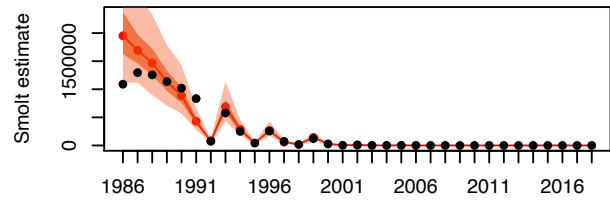
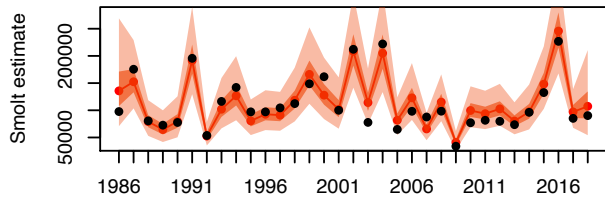
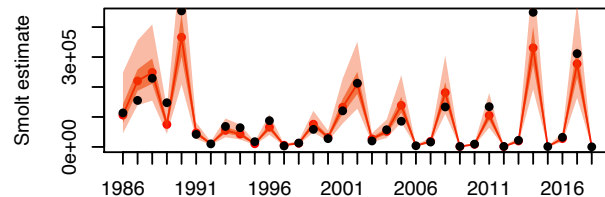
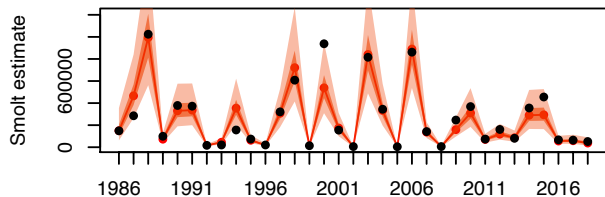
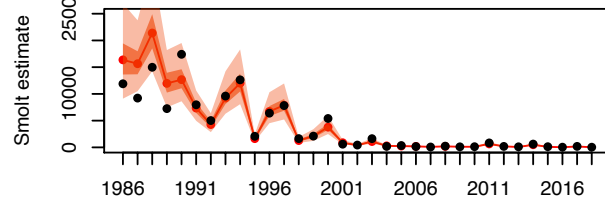
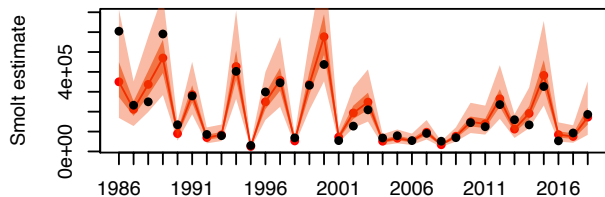
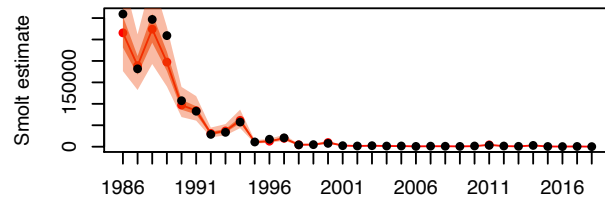
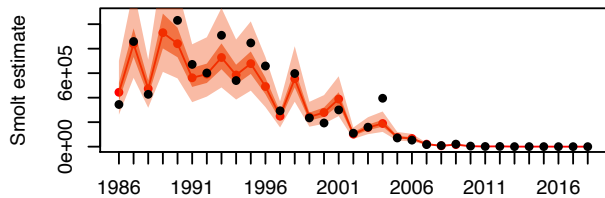
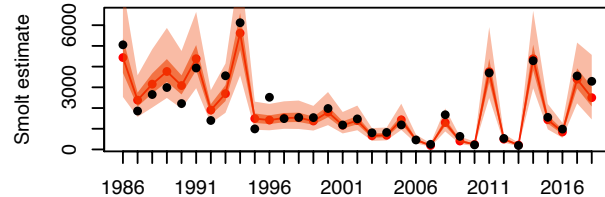
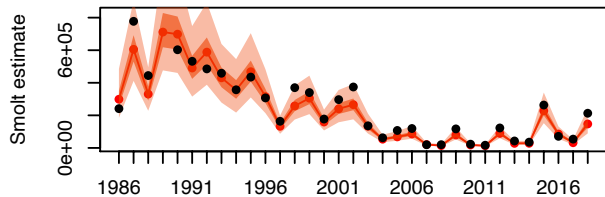
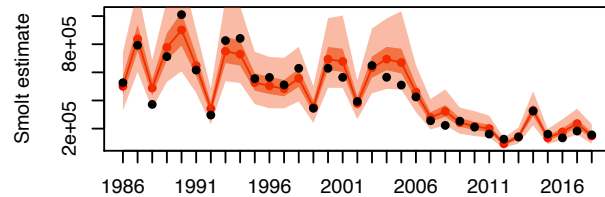
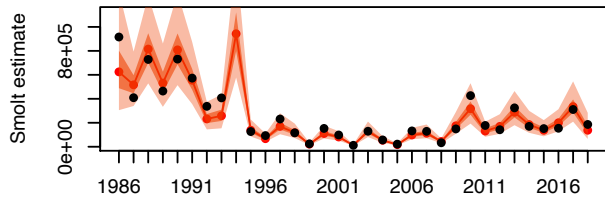
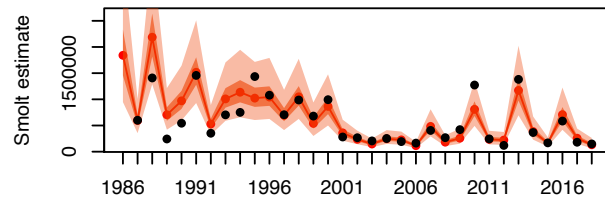
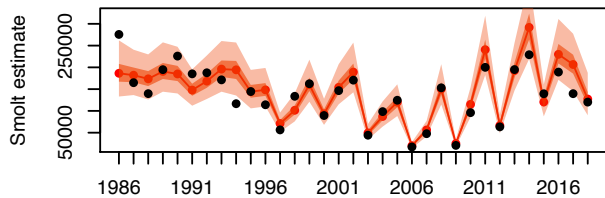
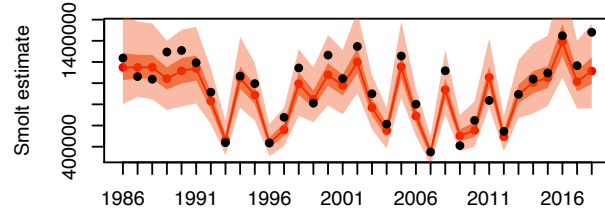
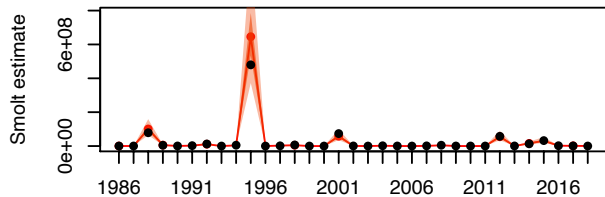
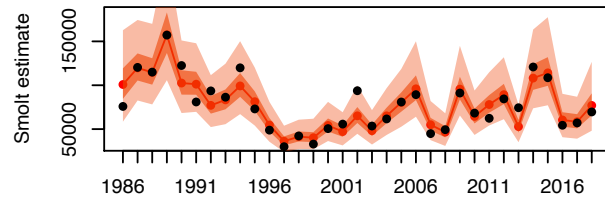
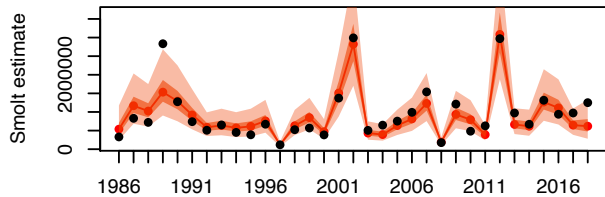


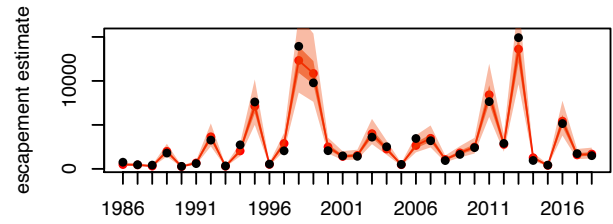
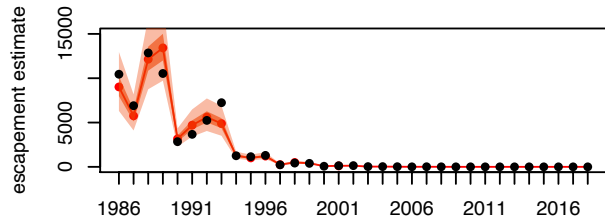
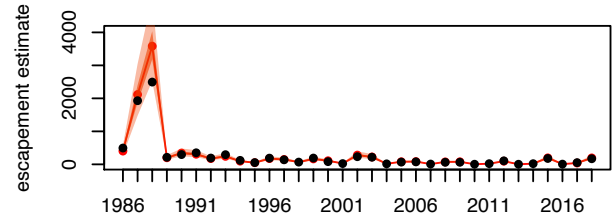
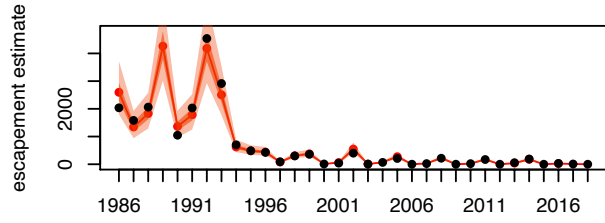
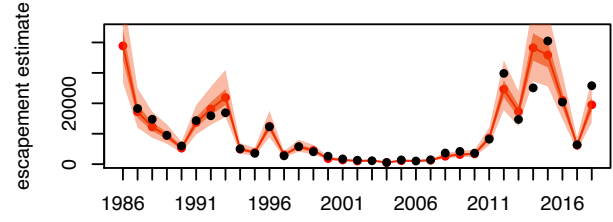
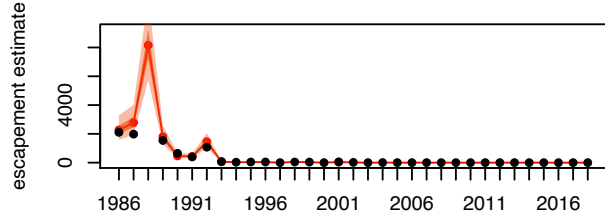
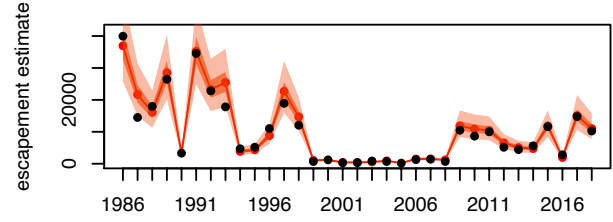
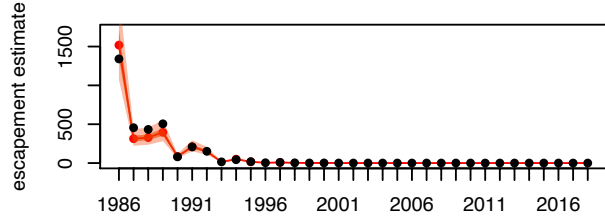
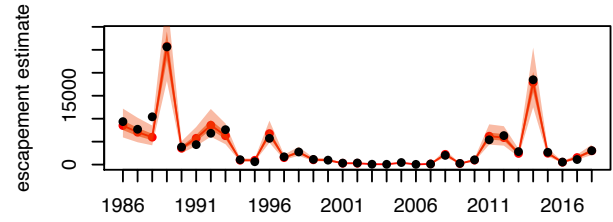
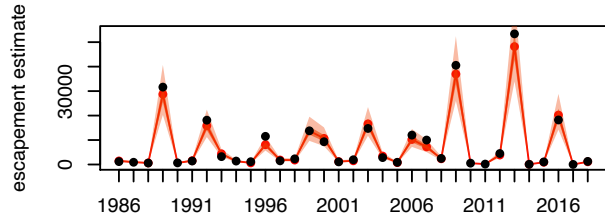
Figure S5. Model estimation of simulated marine survival Gaussian field. In the three right hand panels, the solid black dots represent the underlying true parameter values for the length scale, marginal standard deviation, and error standard deviation of the squared exponential kernel. Red dots, thick, and thin lines represent the median, 50% and 95% credible interval of the model's estimates when fitted to data generated using these parameters. In the left hand panel, the black line represents the true curve implied by the given length scale relative to the model fit in red.

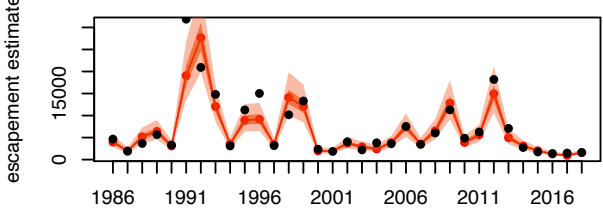
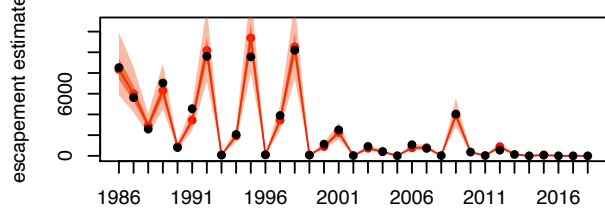
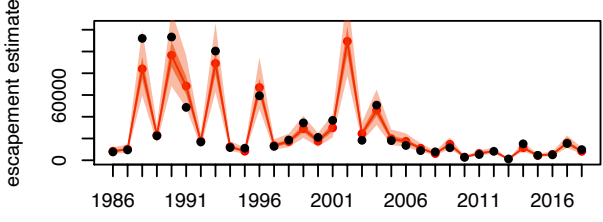
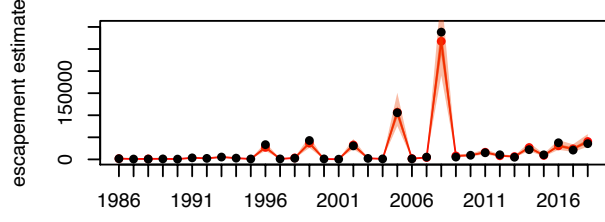
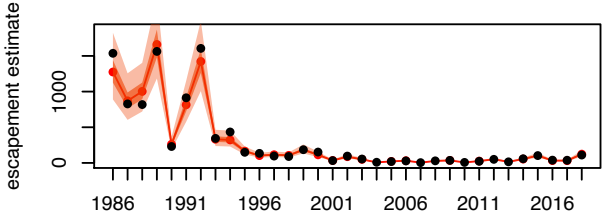
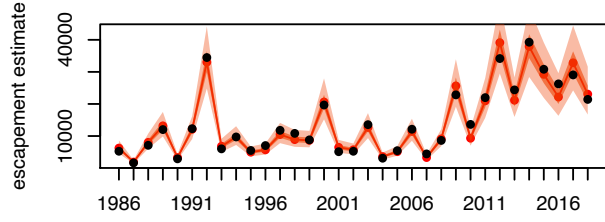
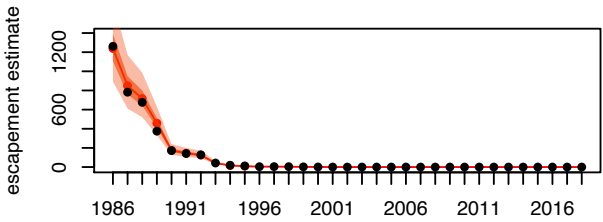
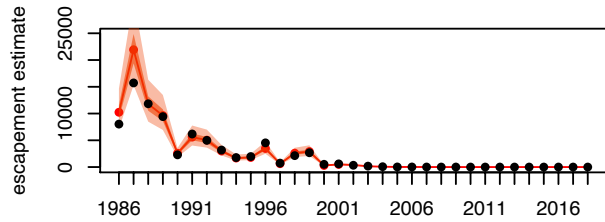
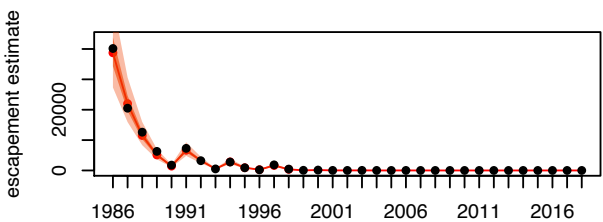
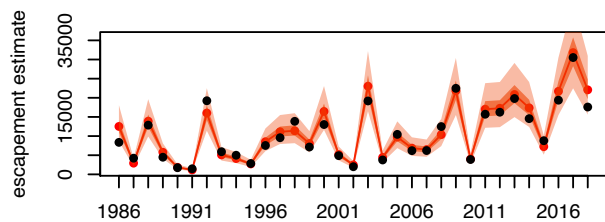


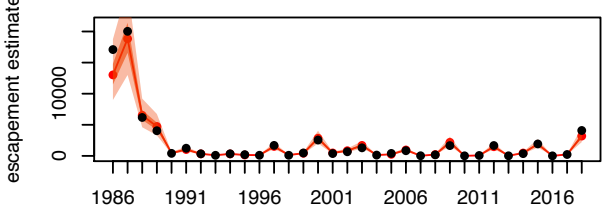
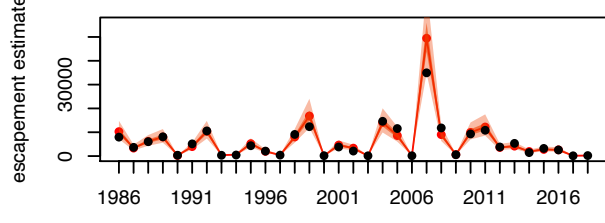
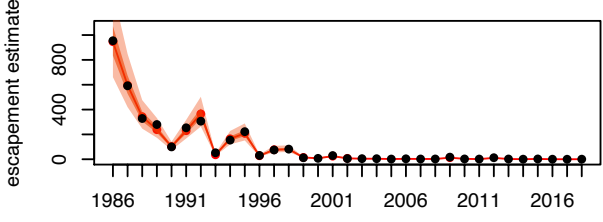
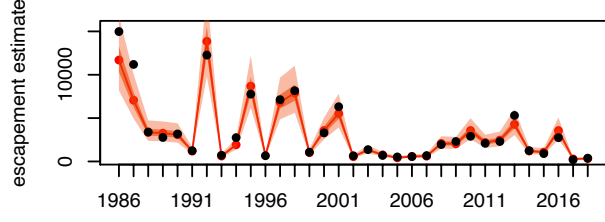
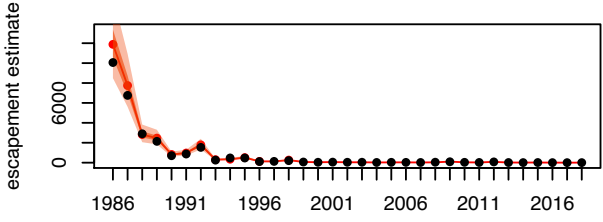
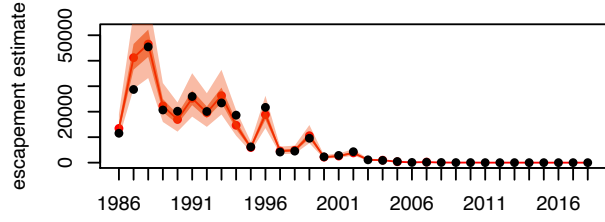
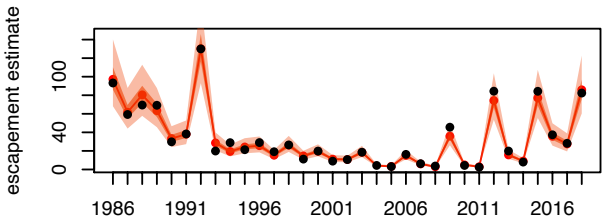
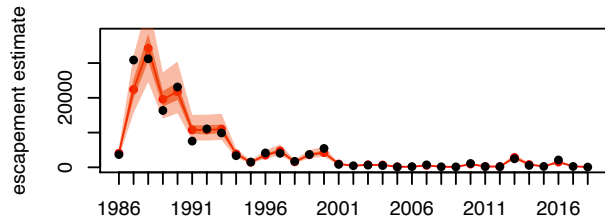
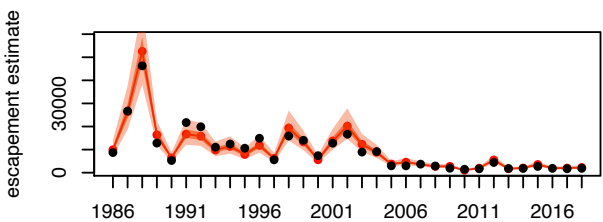
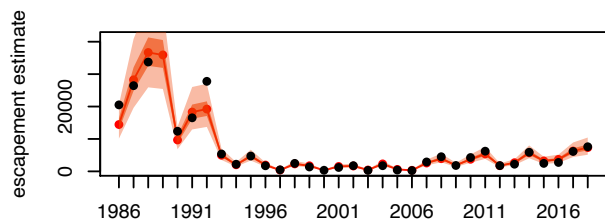


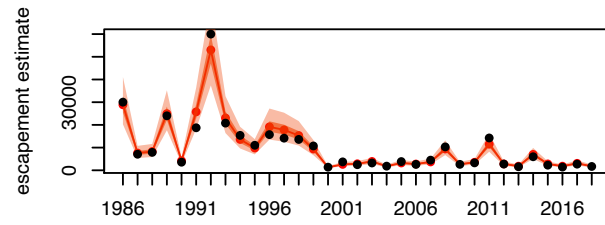
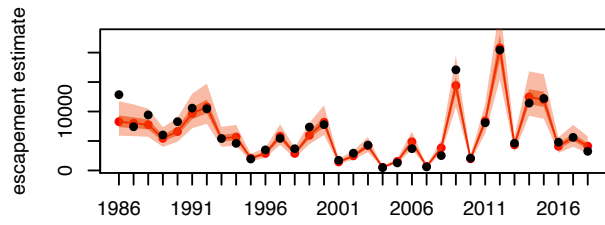
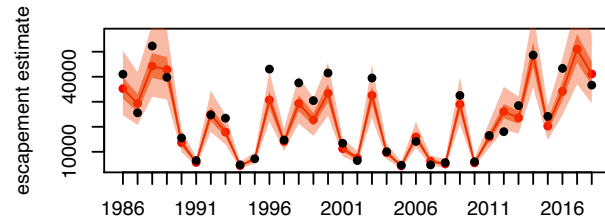
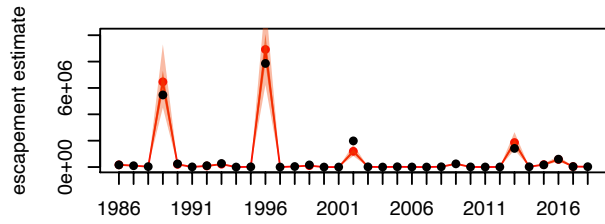
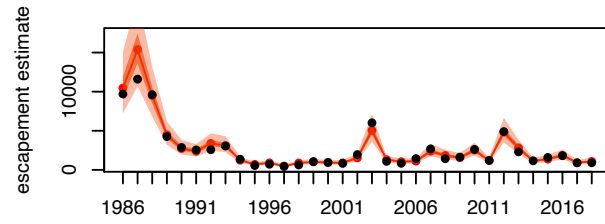
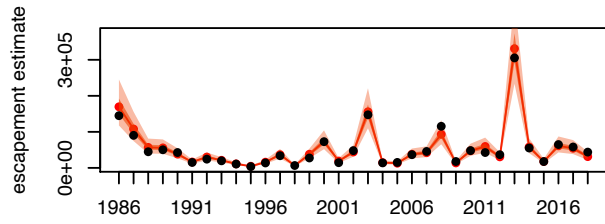


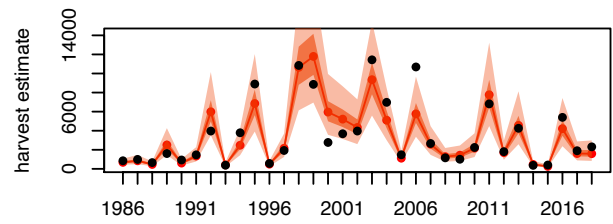
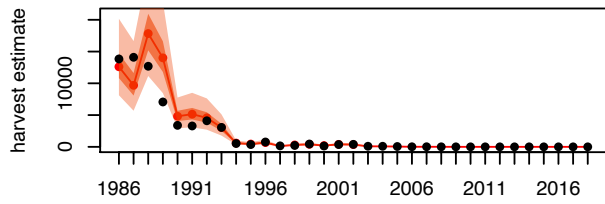
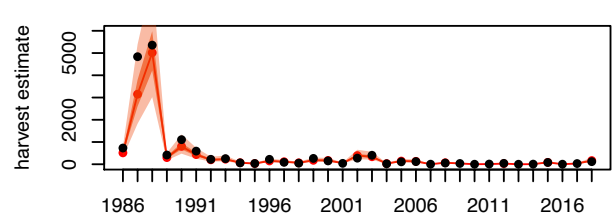
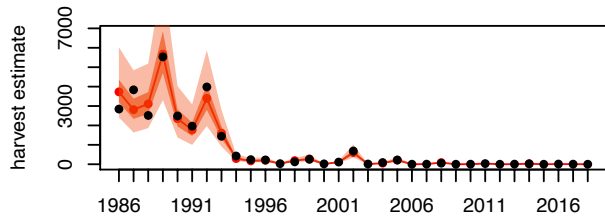
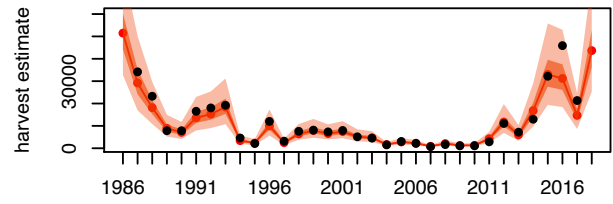
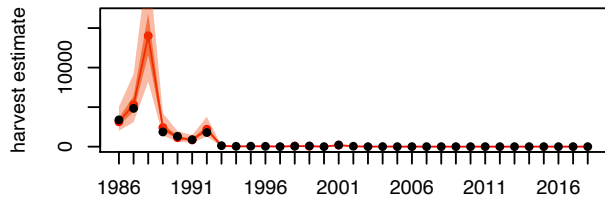
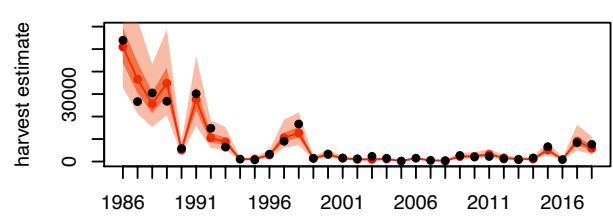
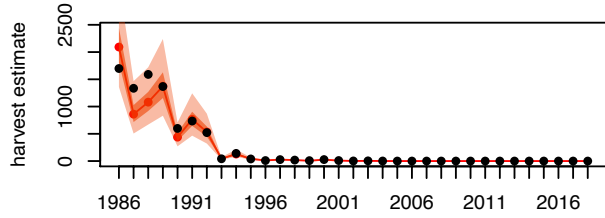
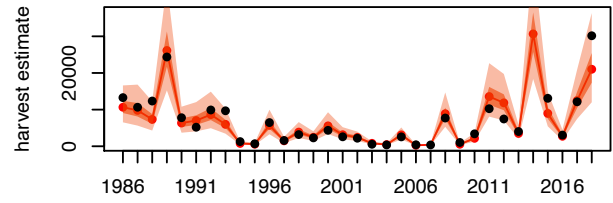
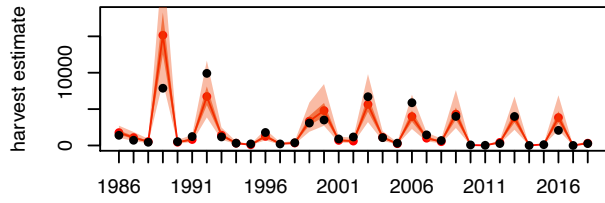


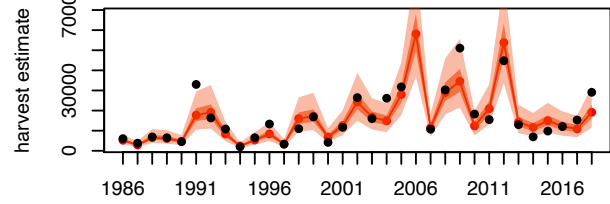
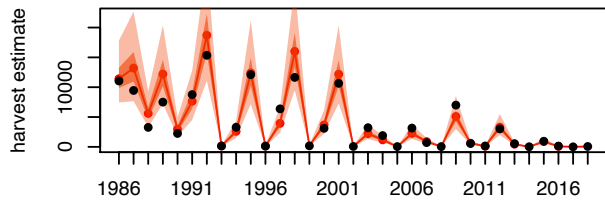
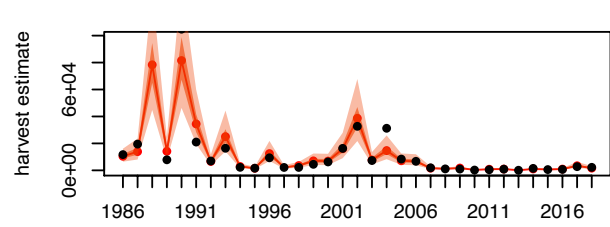
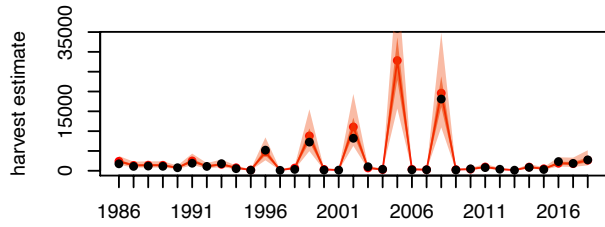
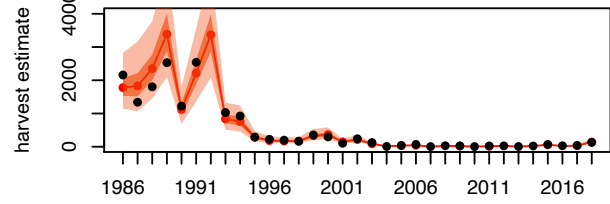
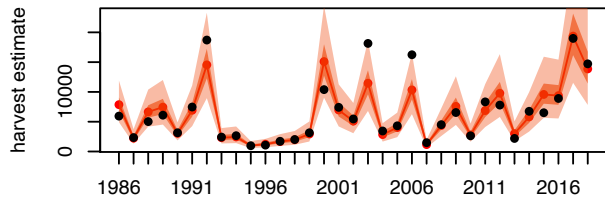
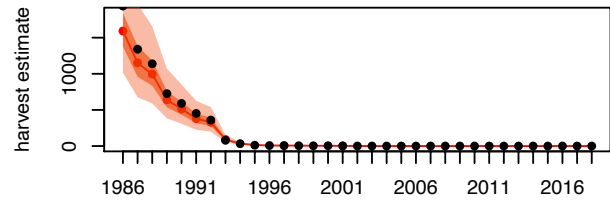
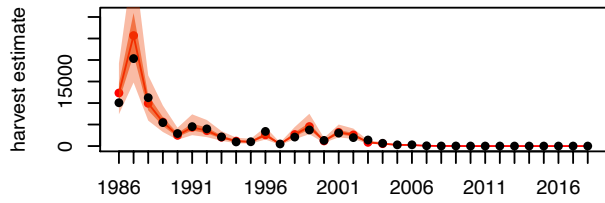
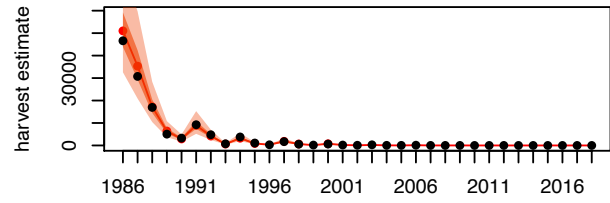
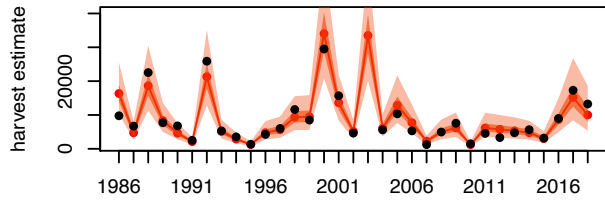


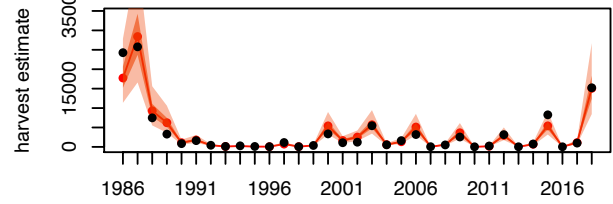
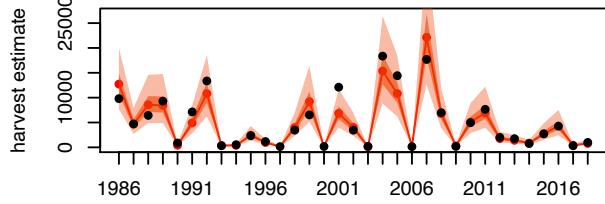
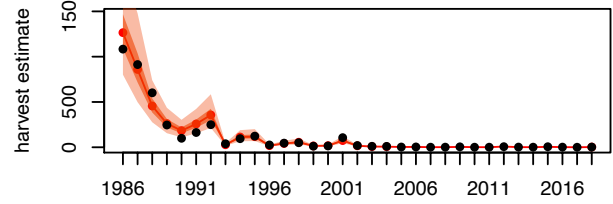
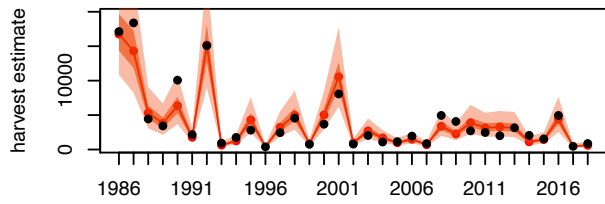
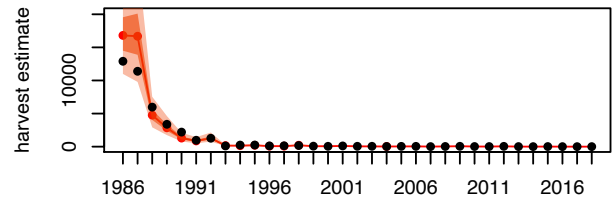
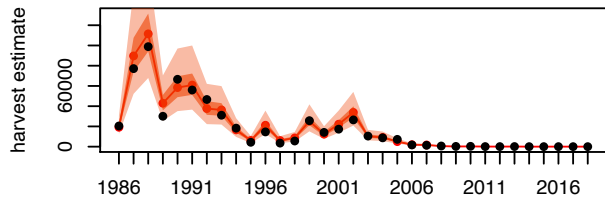
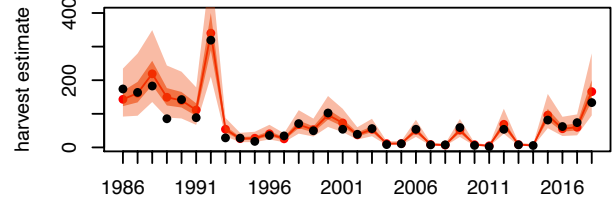
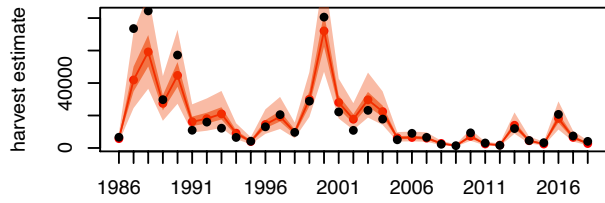
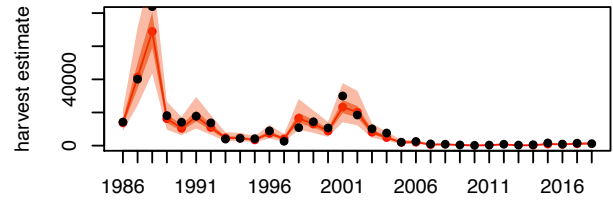
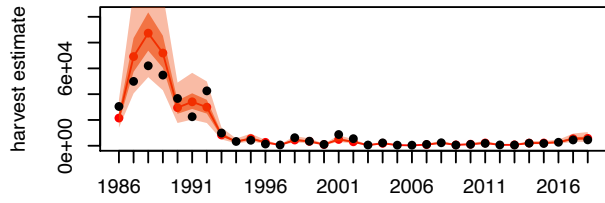


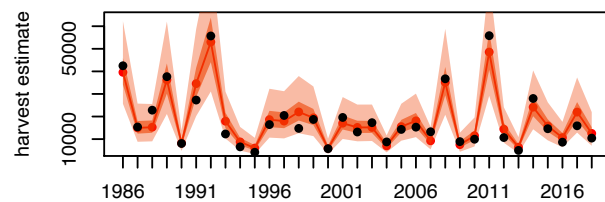
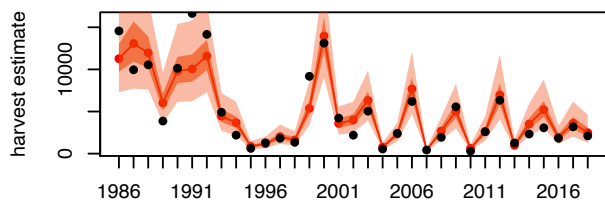
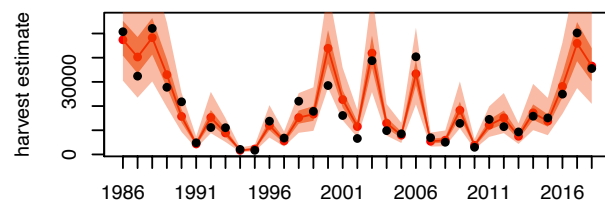
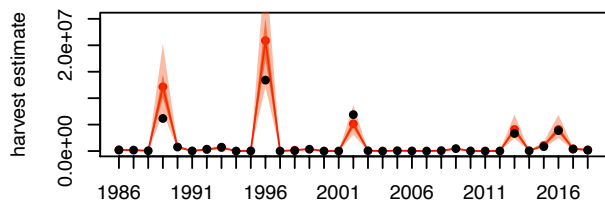
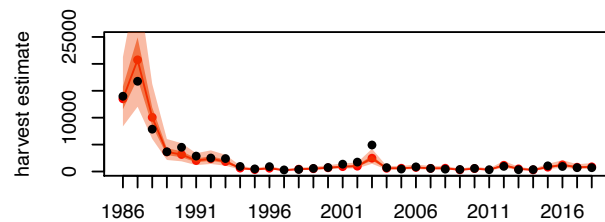
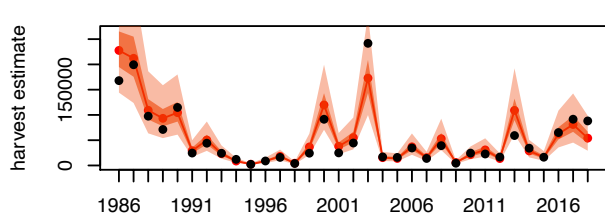


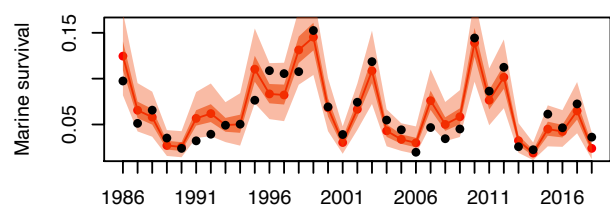
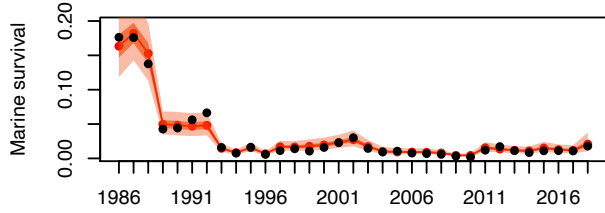
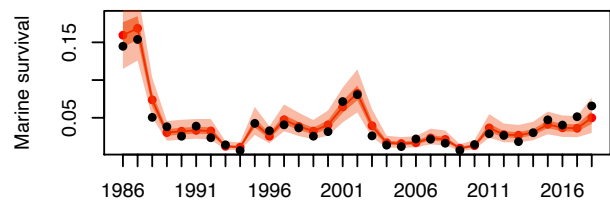
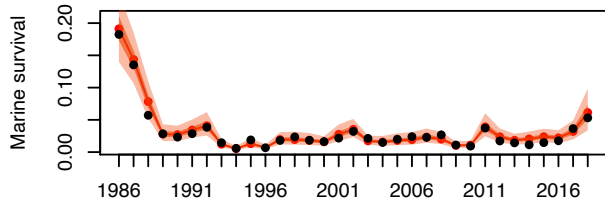
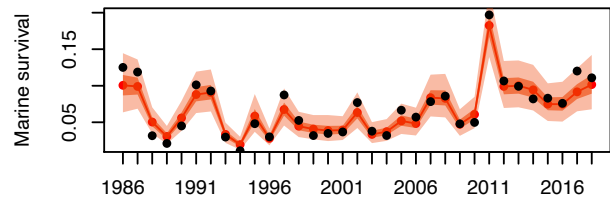
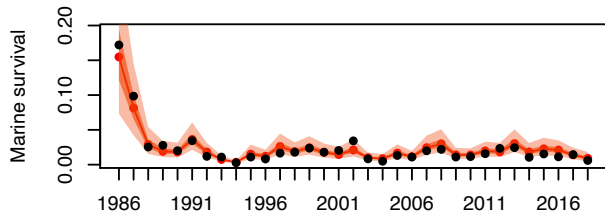
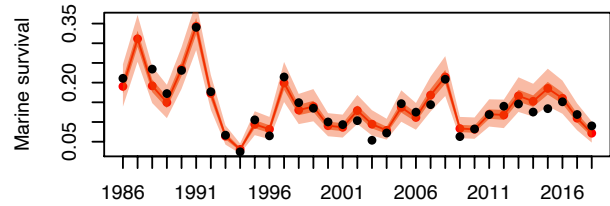
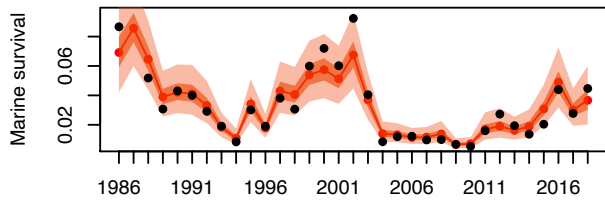
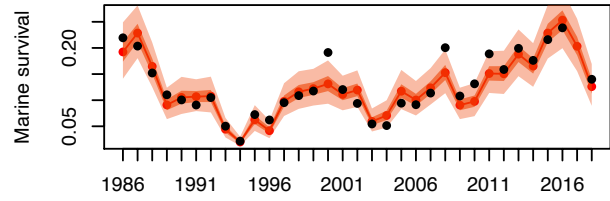
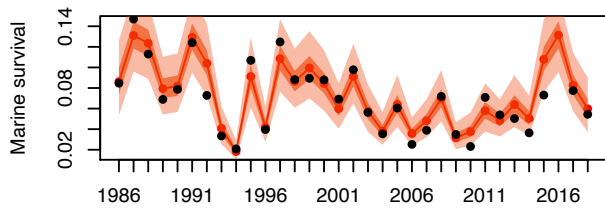


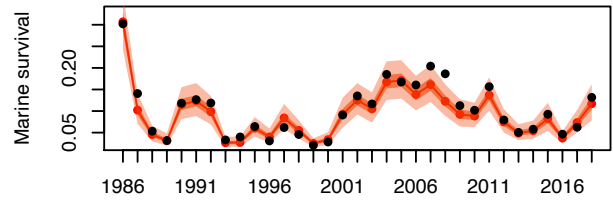
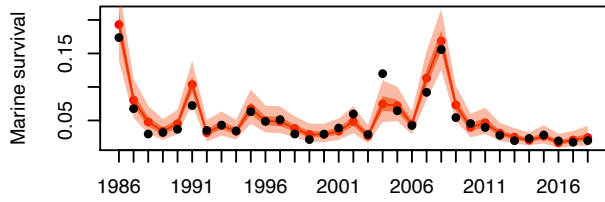
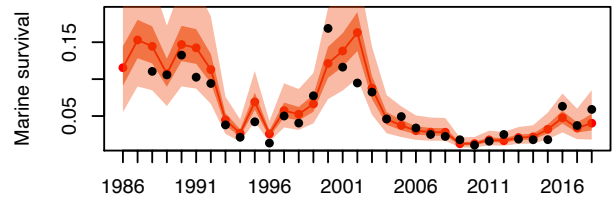
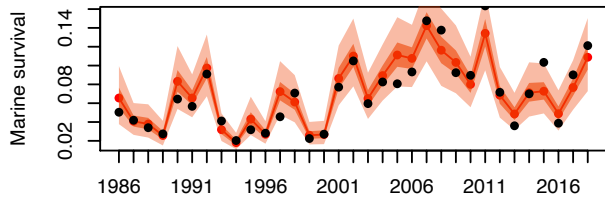
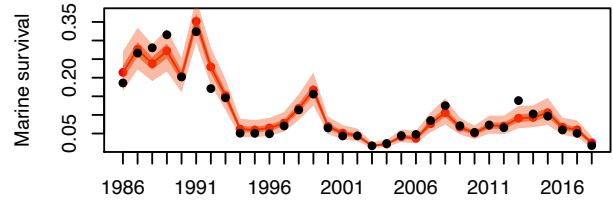
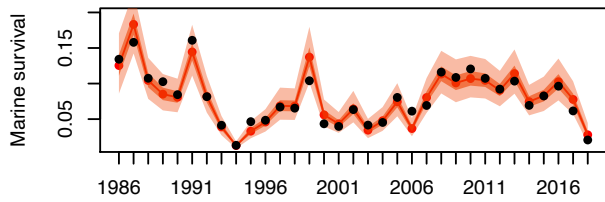
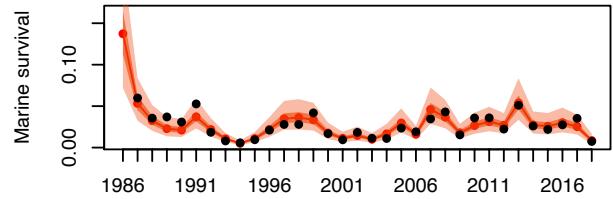
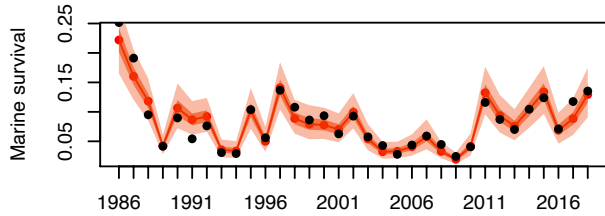
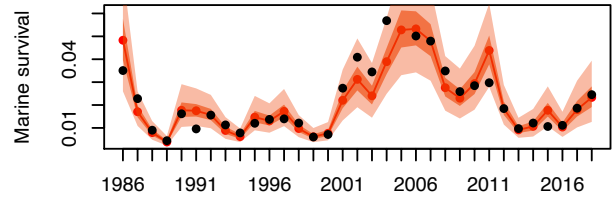
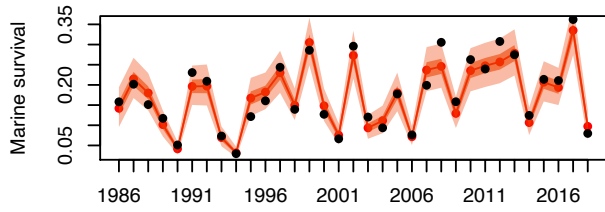


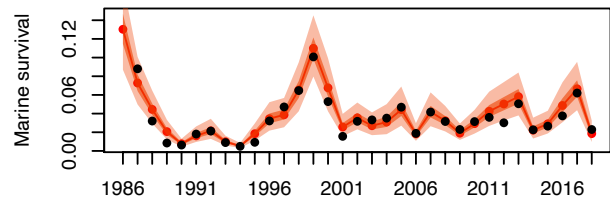
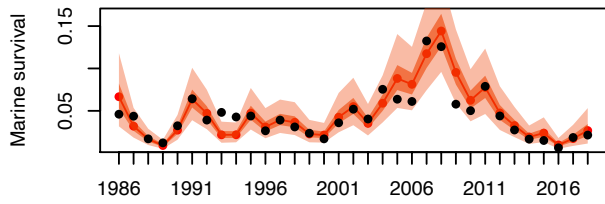
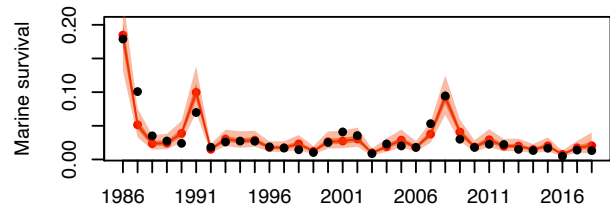
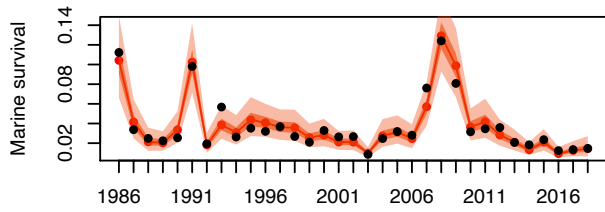
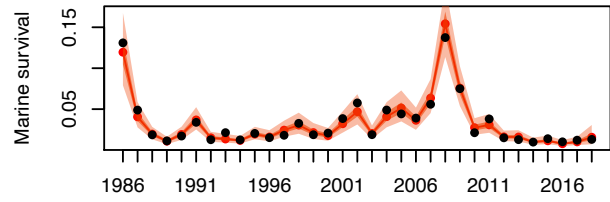
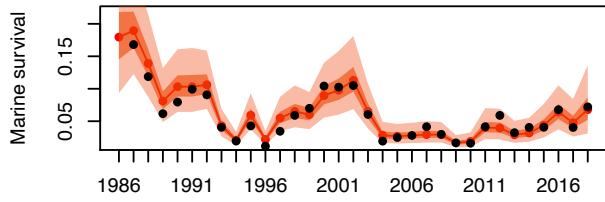
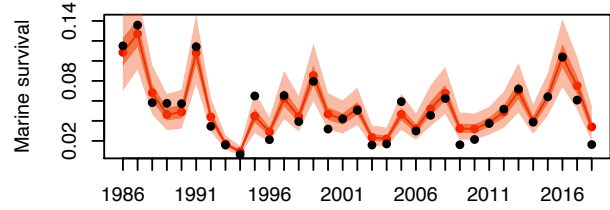
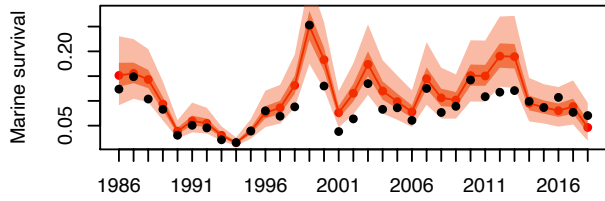
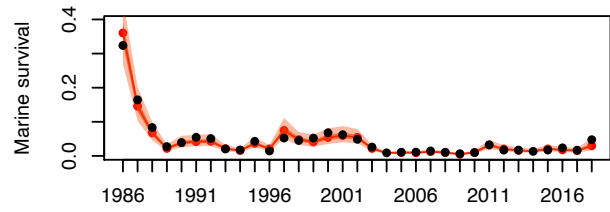
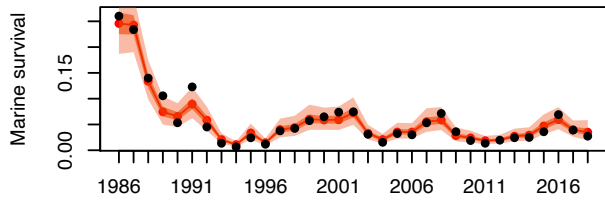












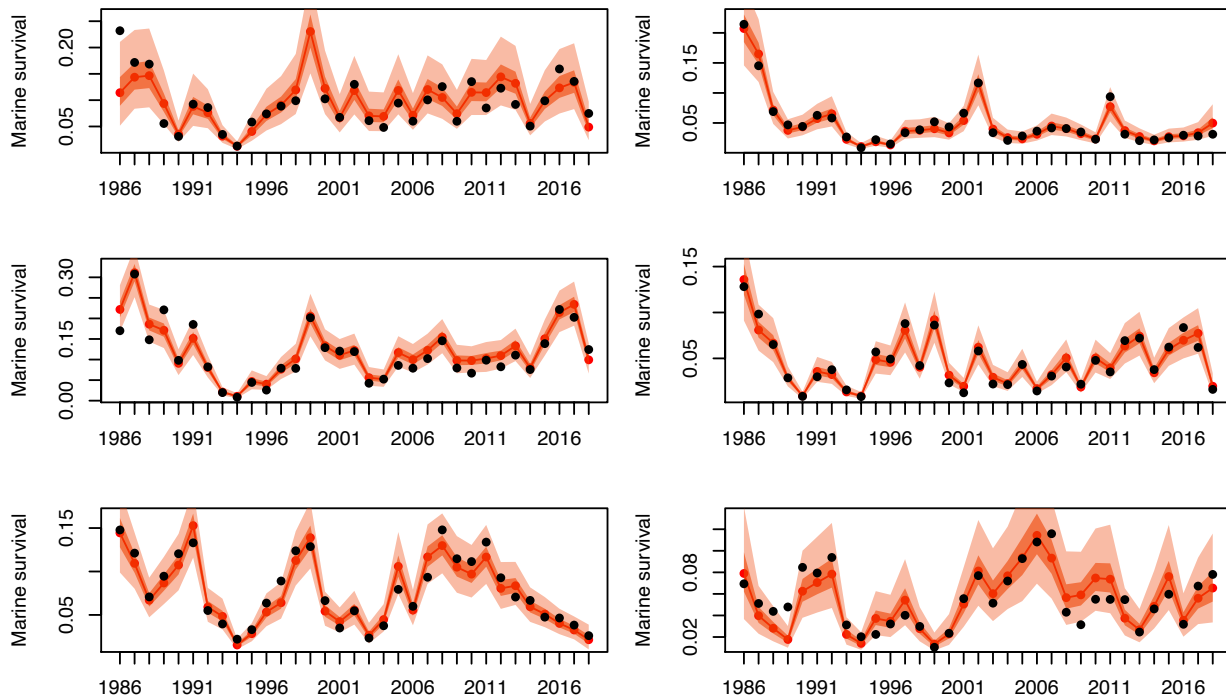
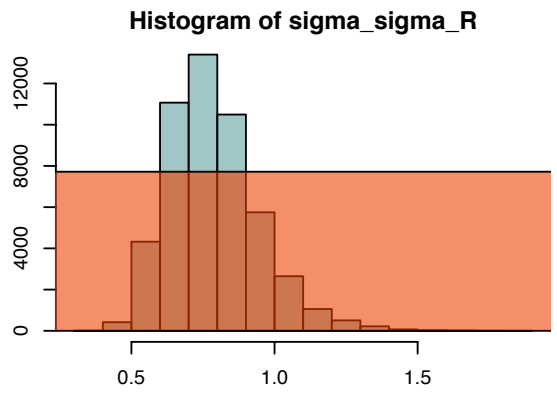
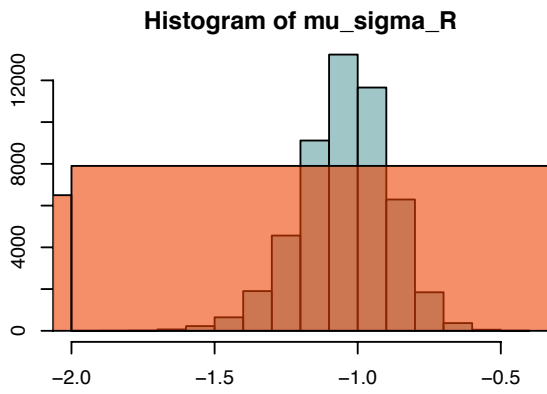
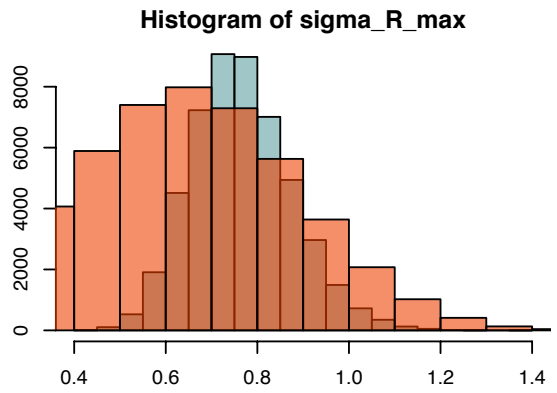
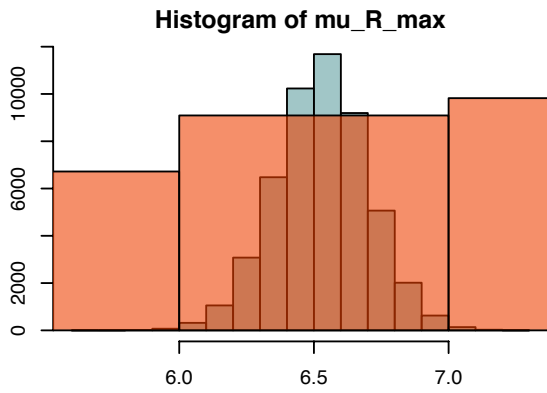
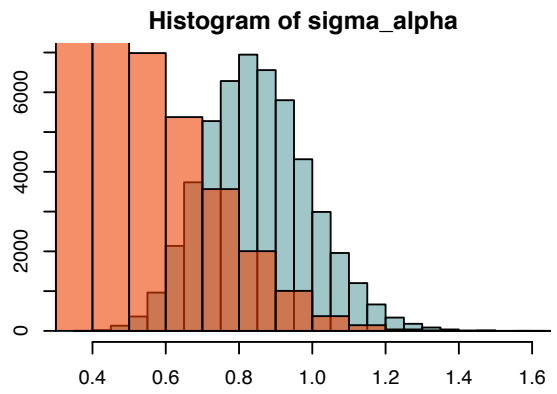
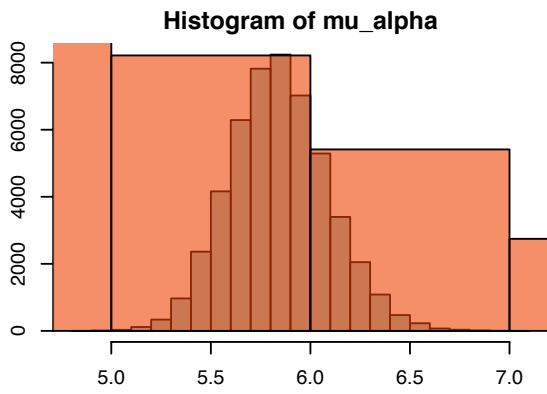
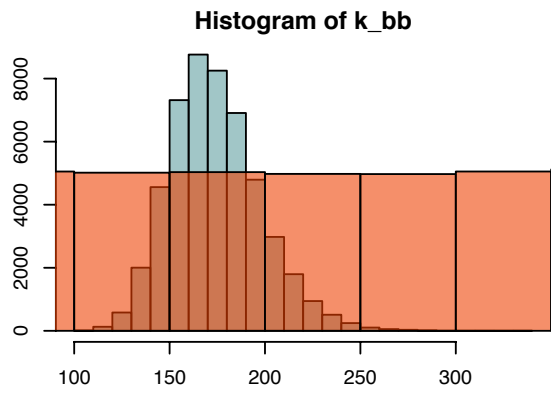
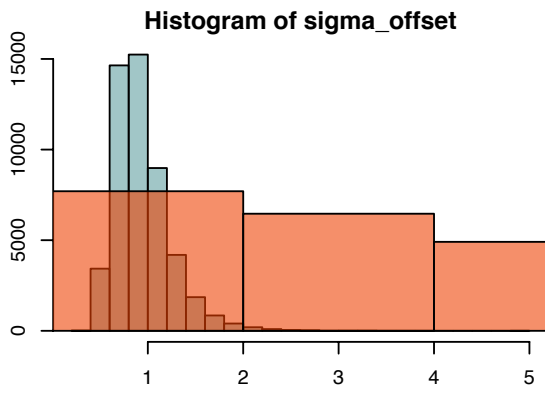
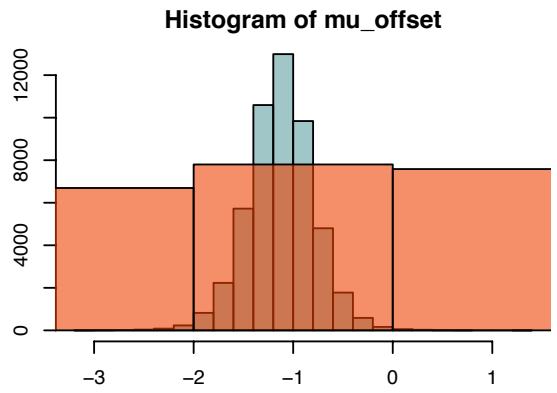
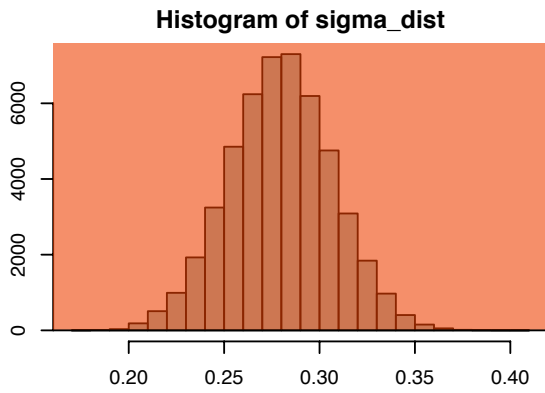
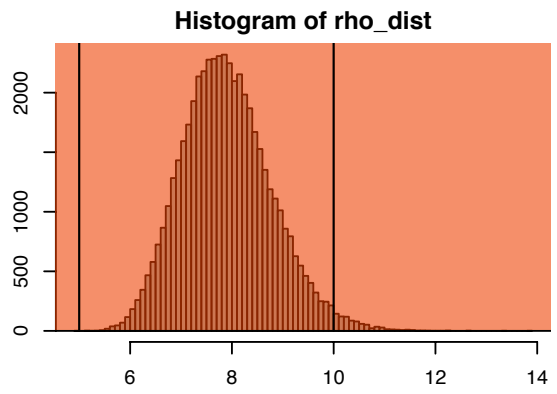
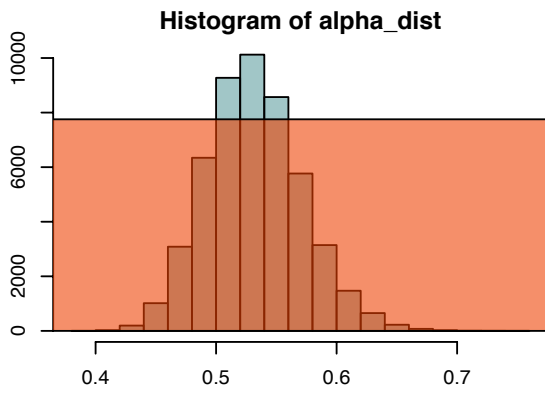
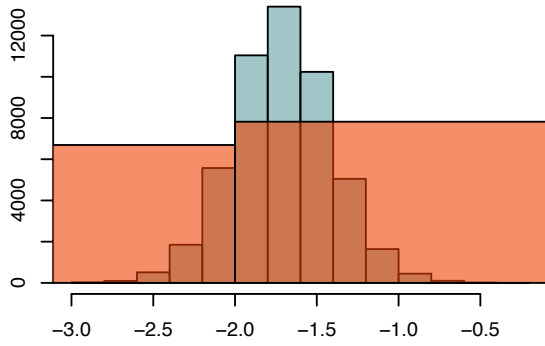


Figure S6. Model estimation of simulated ‘true’ smolt, escapement, harvest, and marine survival. In all panels, solid black dots represent the ‘true’ values of the smolt, escapement, and harvest abundance, and ‘true’ marine survival proportions from which the simulated data were generated. These represent the underlying quantities from which data were simulated (with errors) that the model was then fitted to. The model’s median state estimates of these quantities are shown as red dots and lines, while the 50% and 95% credible intervals are depicted as dark and light shaded boundaries respectively.

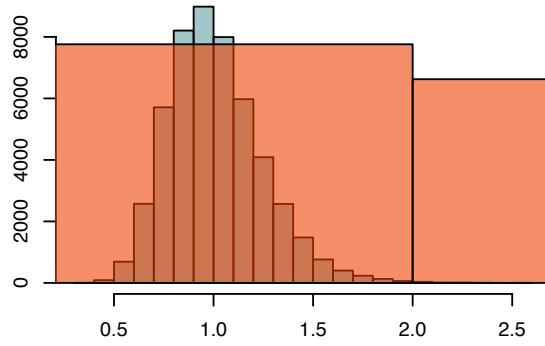




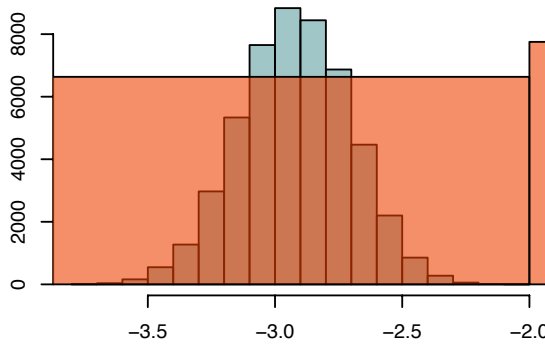
Histogram of mu_init_surv



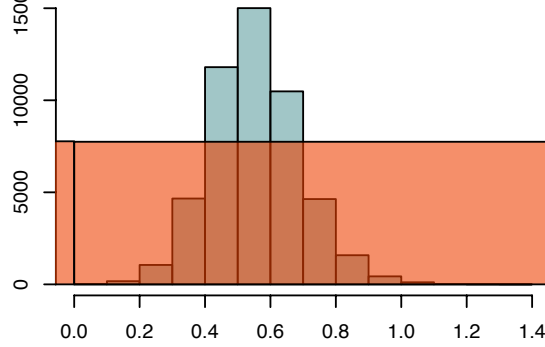
Histogram of sigma_init_surv



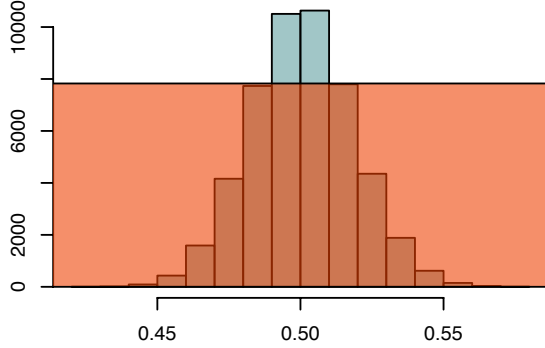
Histogram of mu_mu_surv



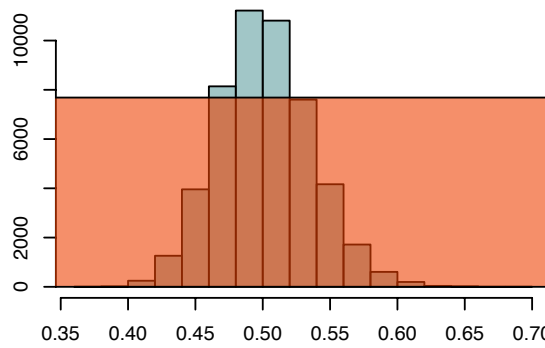
Histogram of sigma_mu_surv

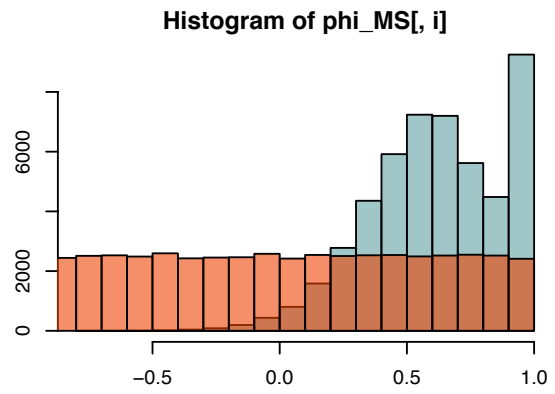
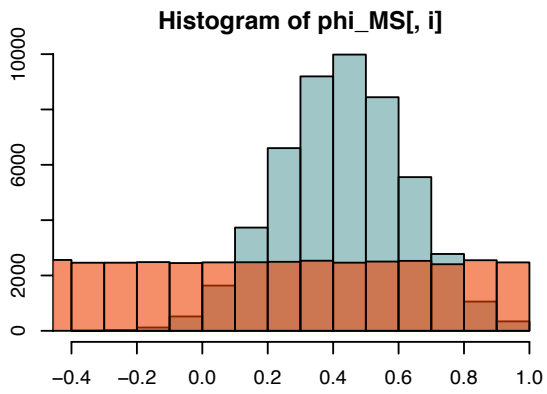
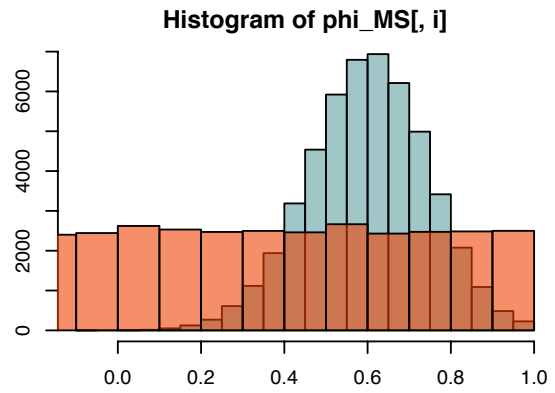
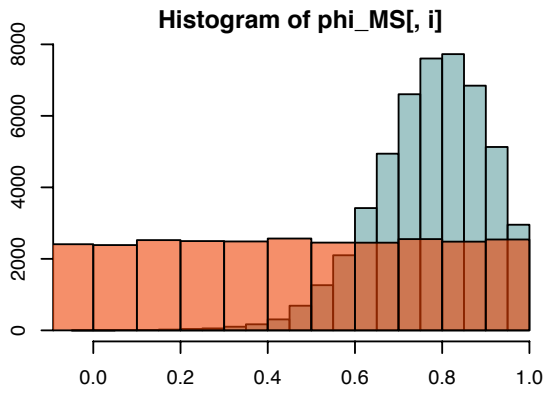
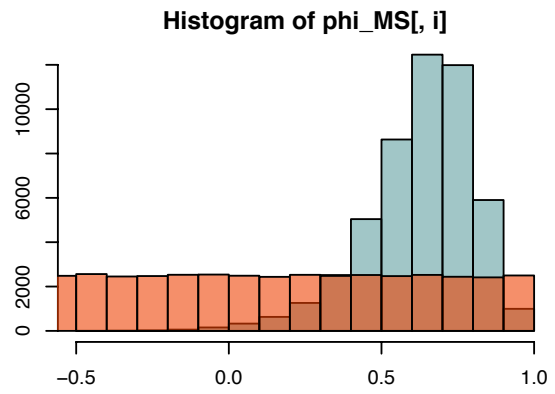
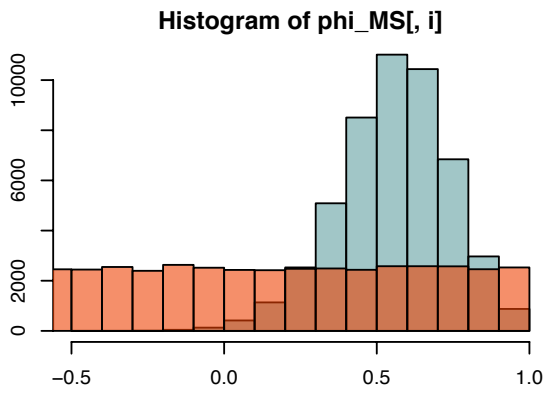


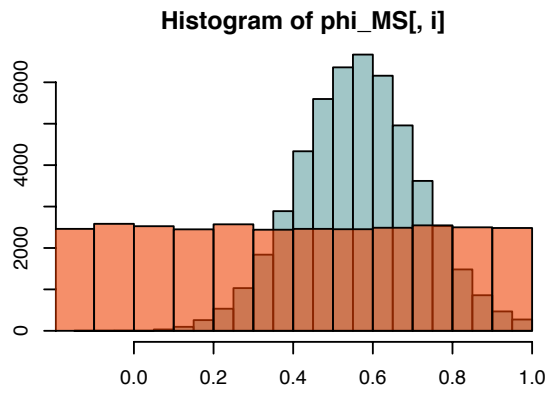
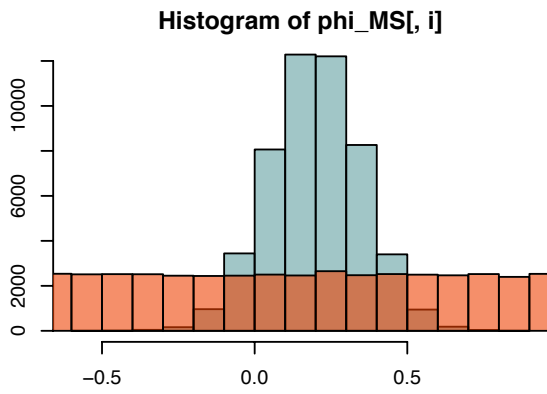
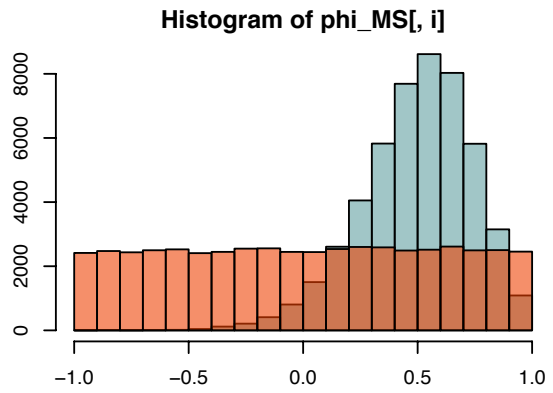
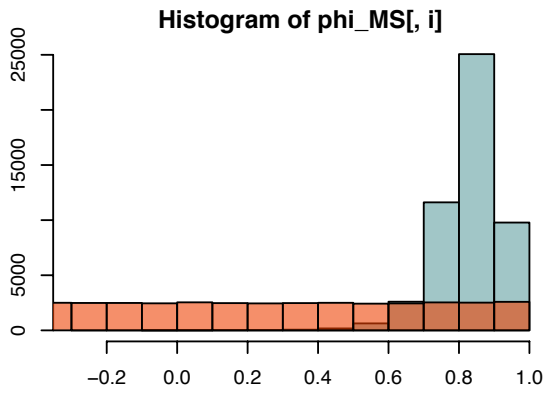
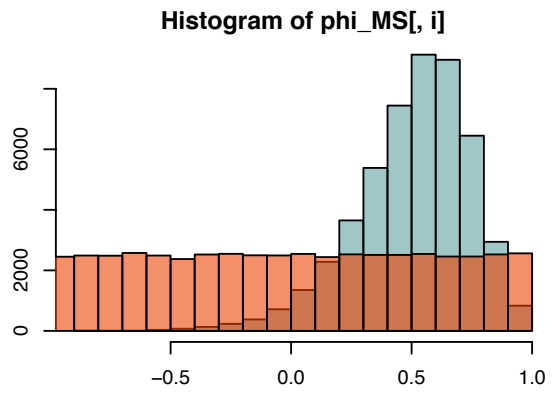
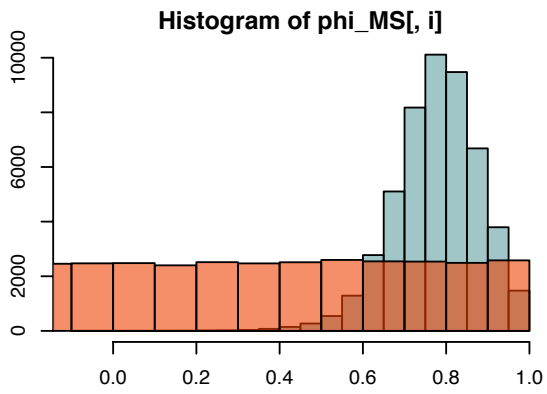
Histogram of sigma_catch

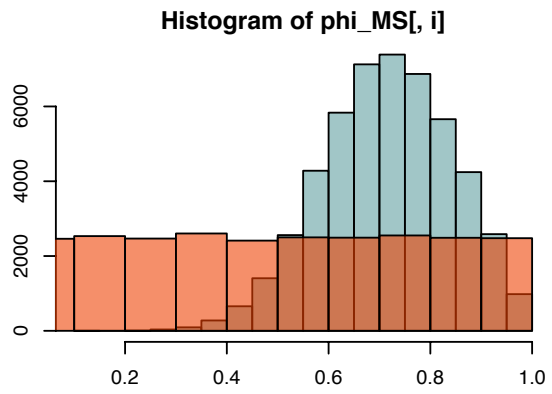
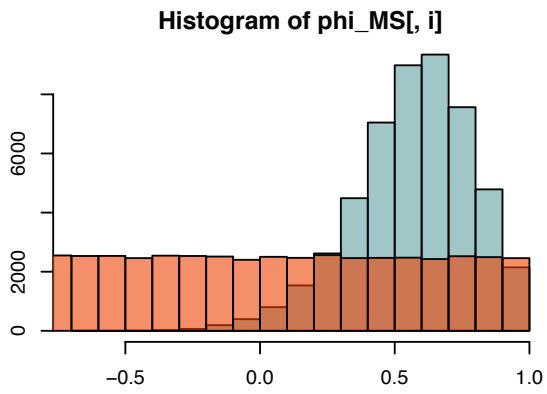
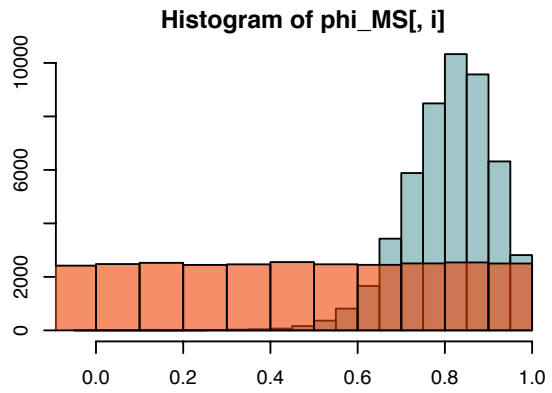
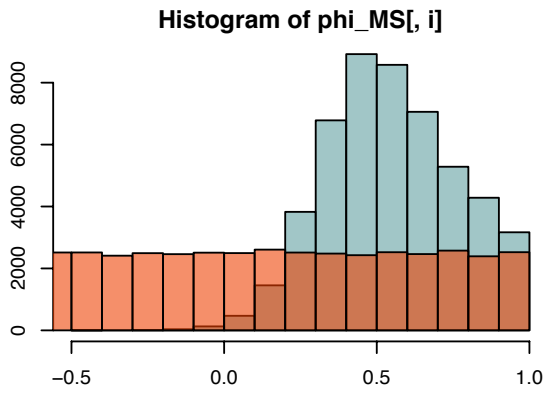
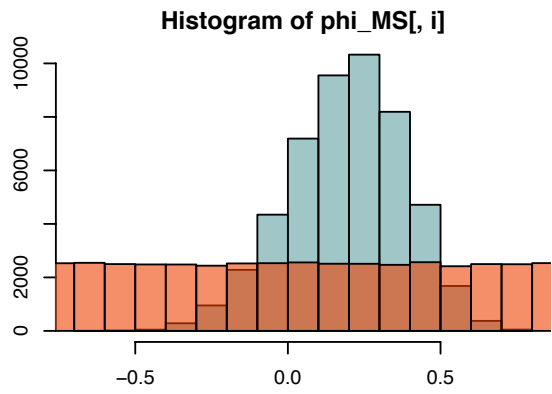
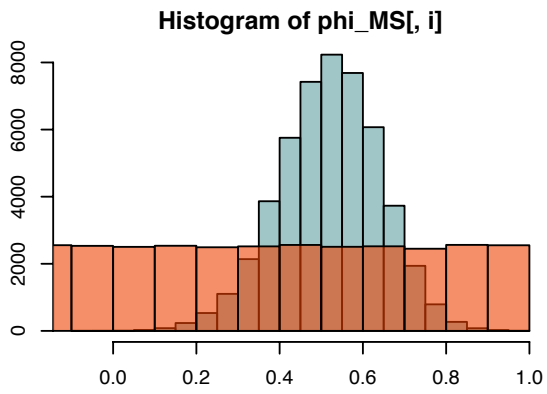


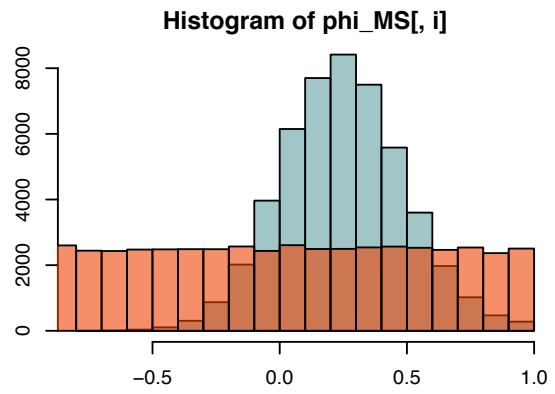
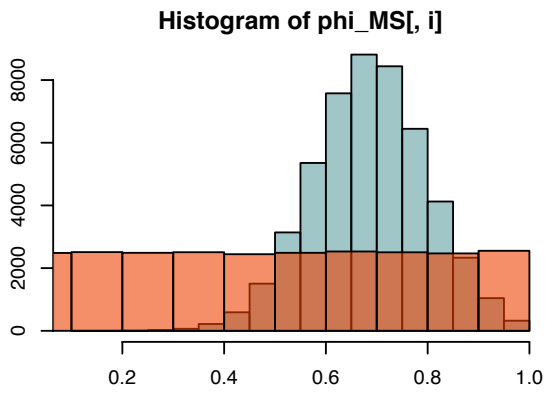
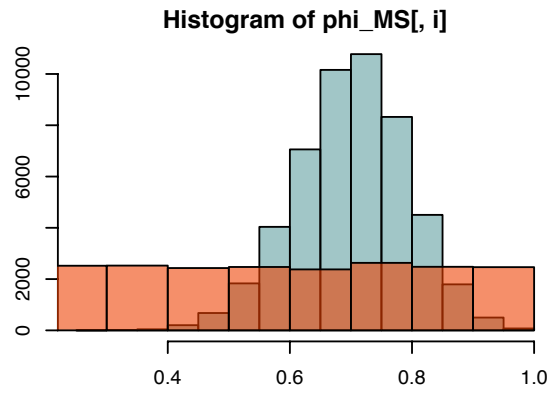
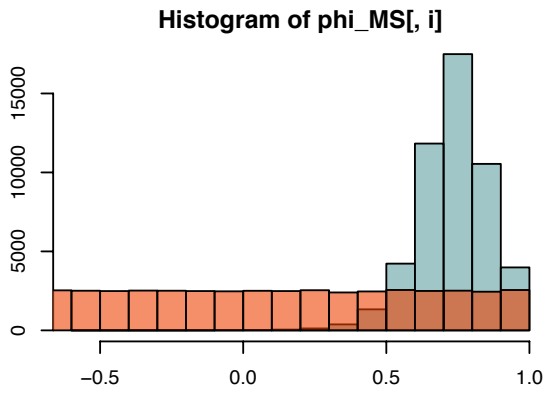
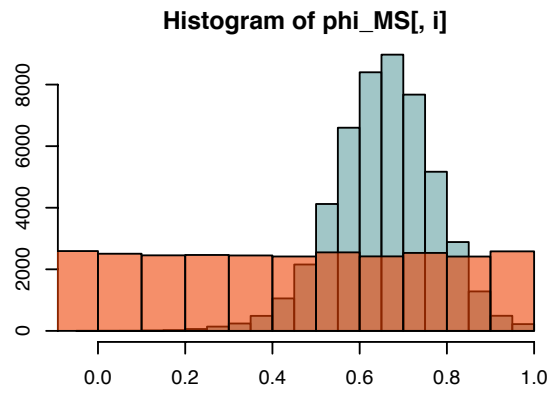
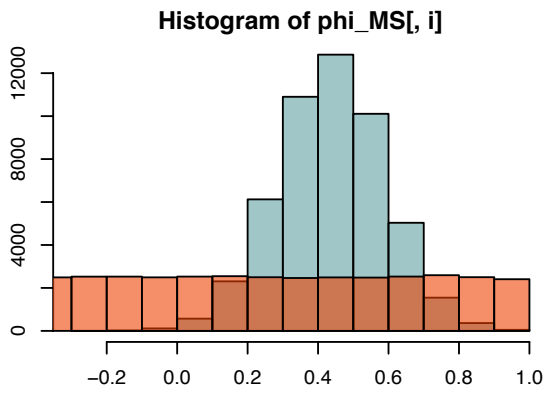
Histogram of sigma_smolt



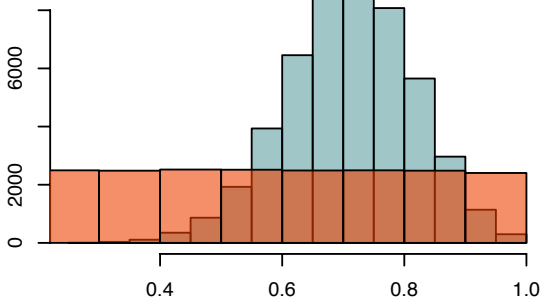




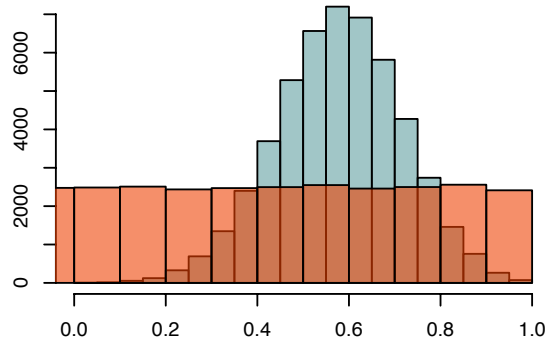




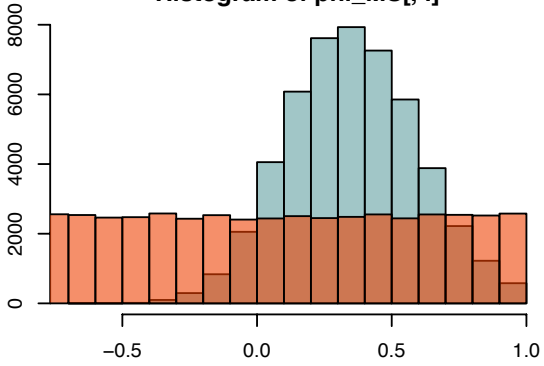
Histogram of phi_MS[, i]



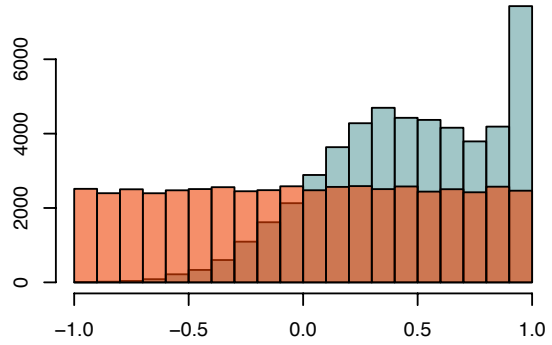
Histogram of phi_MS[, i]



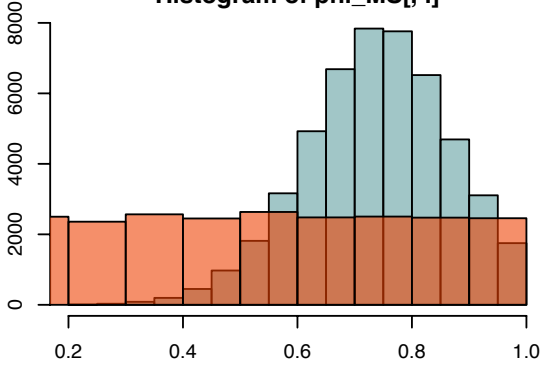
Histogram of phi_MS[, i]



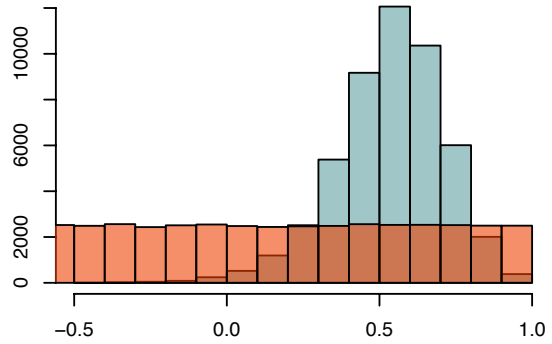
Histogram of phi_MS[, i]

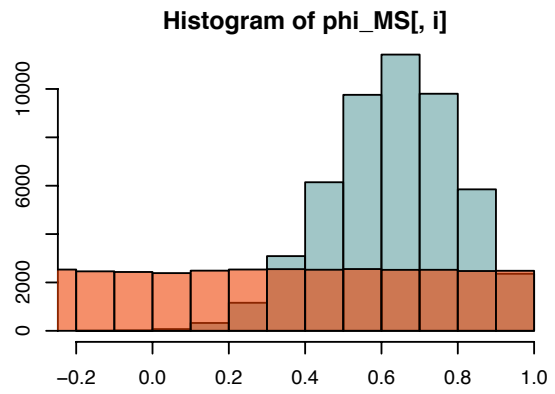
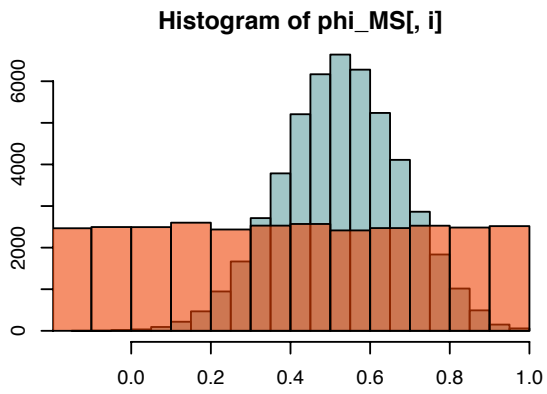
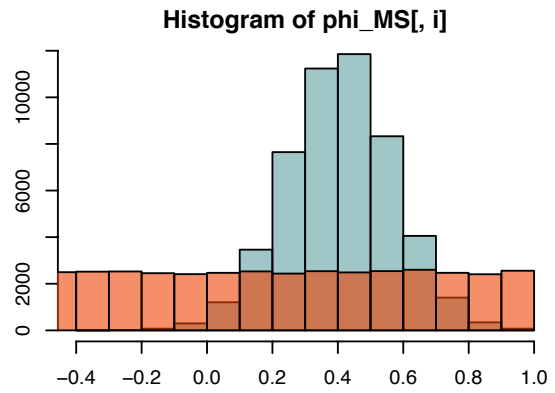
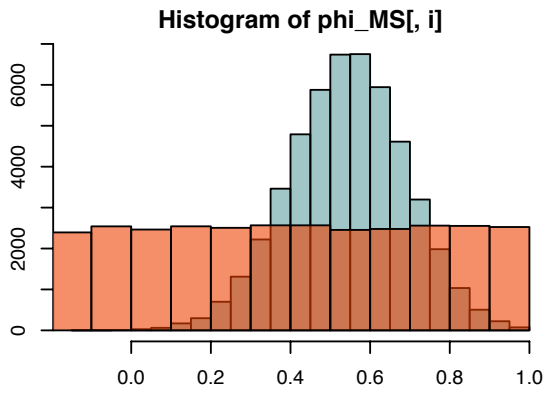
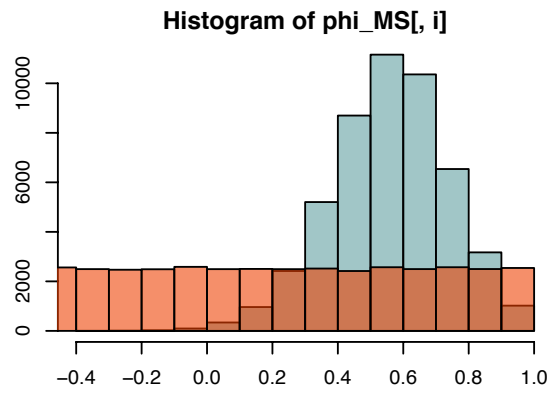
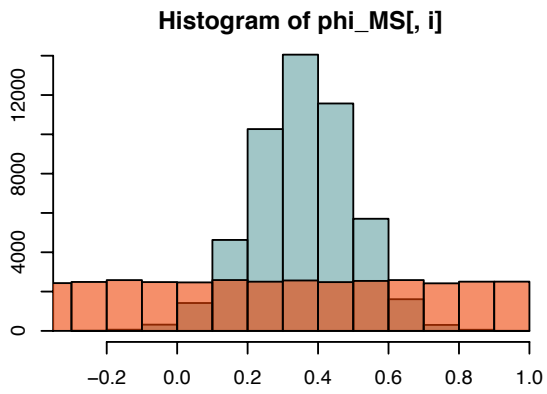


Histogram of phi_MS[, i]

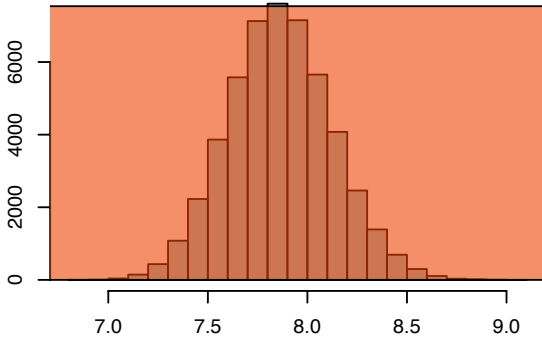


Histogram of phi_MS[, i]

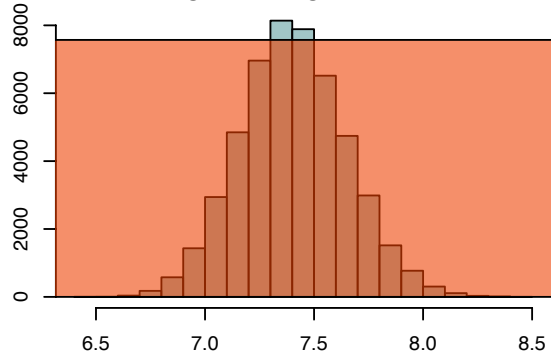




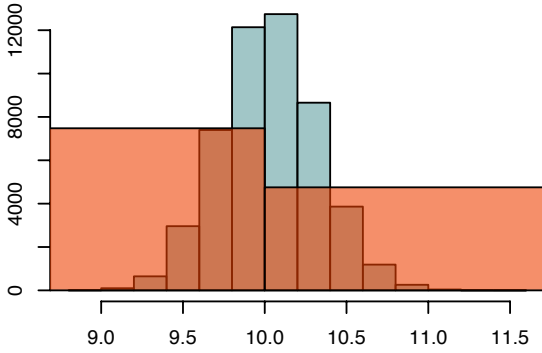
Histogram of log_adult_init[, i]



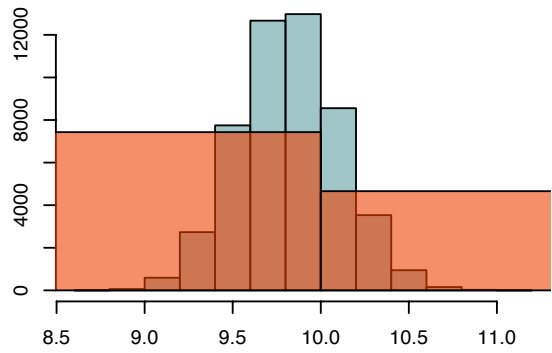
Histogram of log_adult_init[, i]



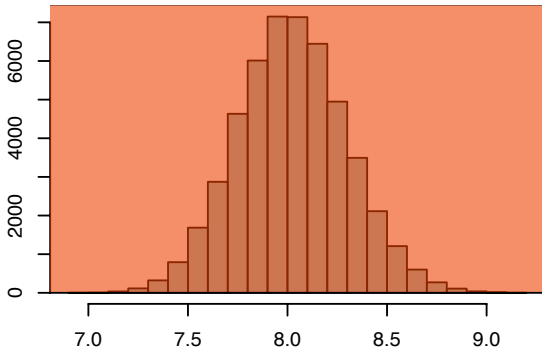
Histogram of log_adult_init[, i]



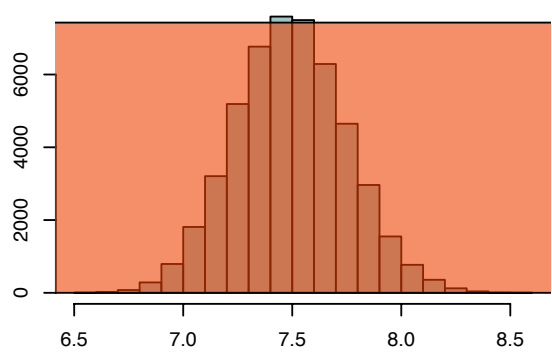
Histogram of log_adult_init[, i]



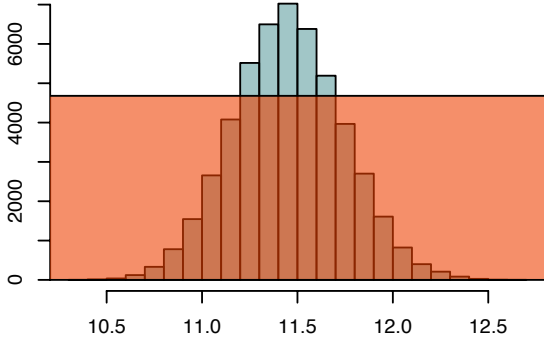
Histogram of log_adult_init[, i]



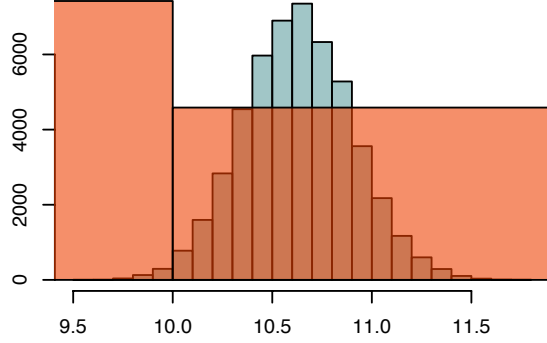
Histogram of log_adult_init[, i]



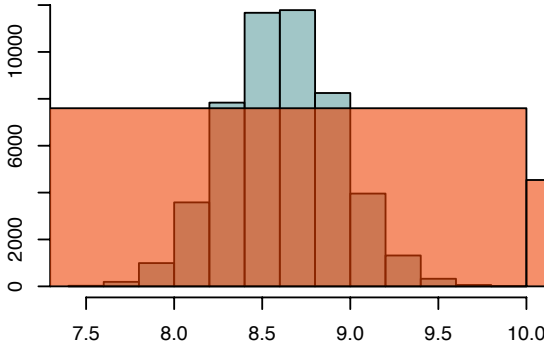
Histogram of log_adult_init[, i]



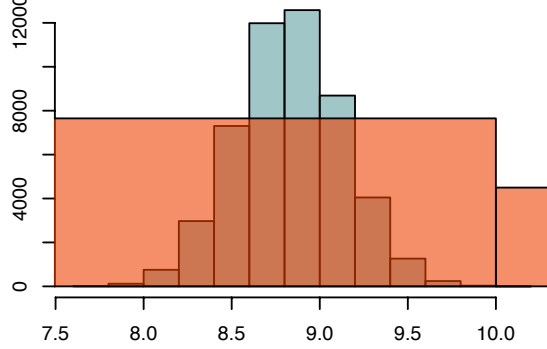
Histogram of log_adult_init[, i]



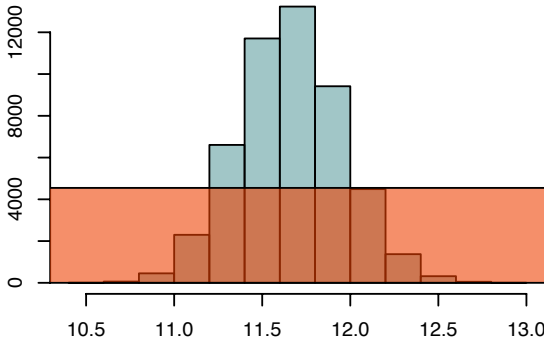
Histogram of log_adult_init[, i]



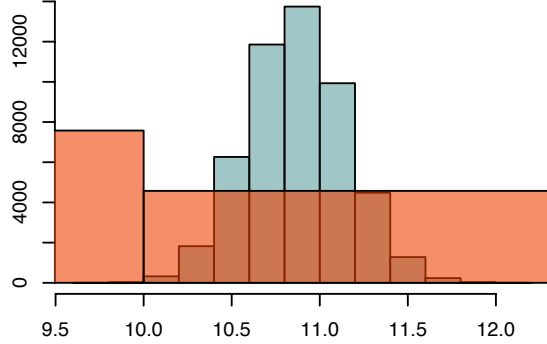
Histogram of log_adult_init[, i]

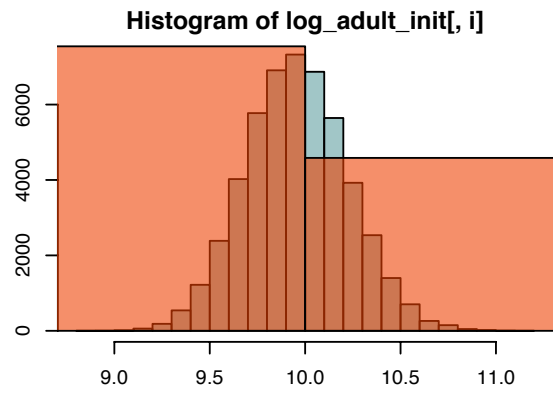
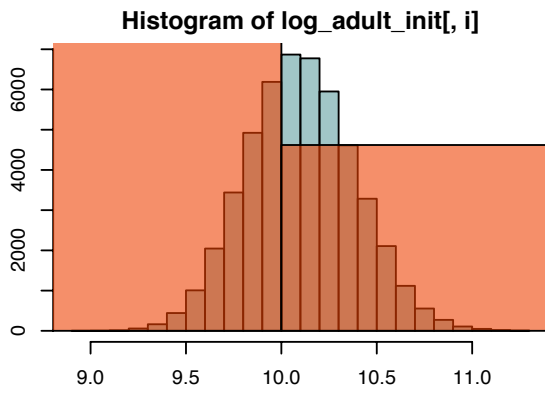
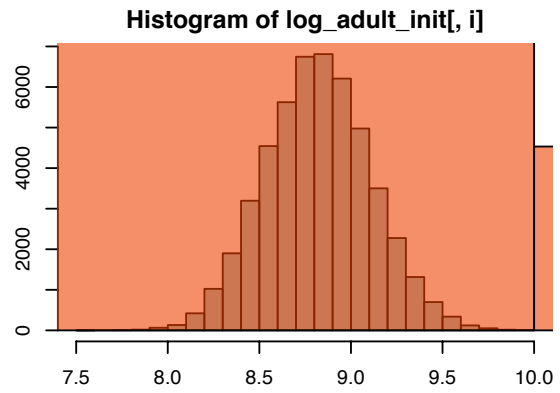
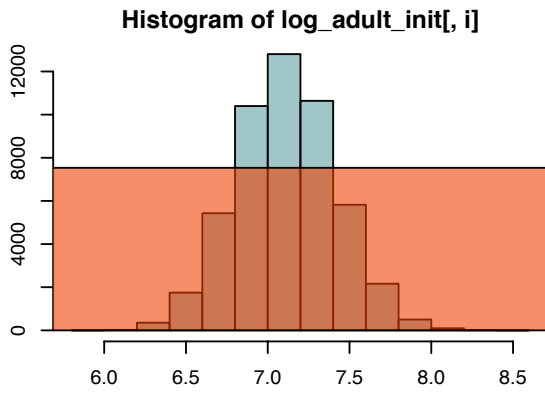
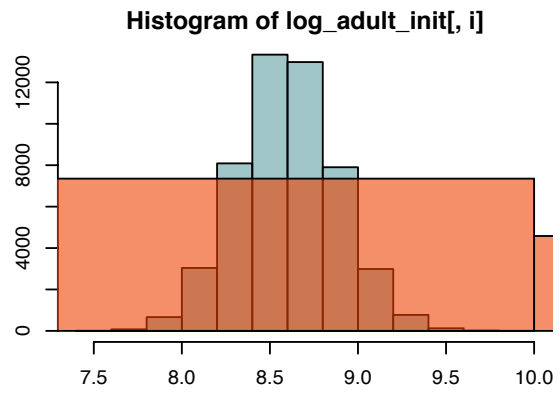
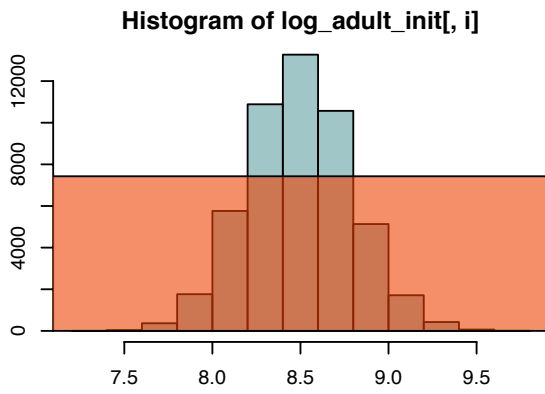


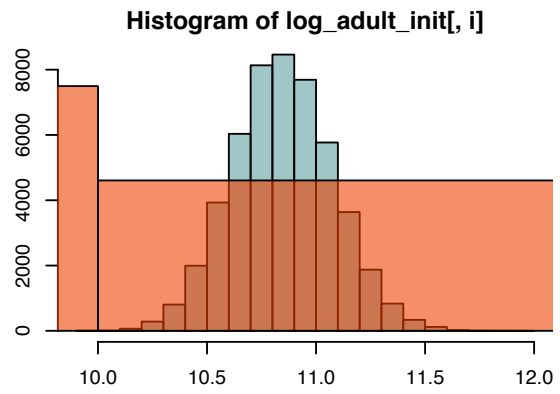
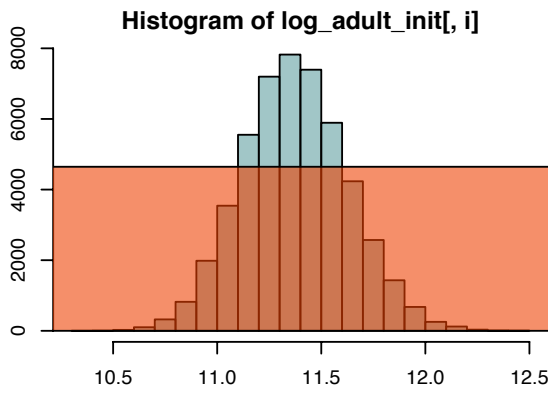
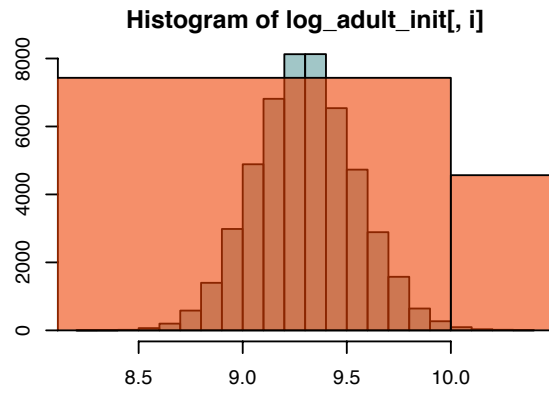
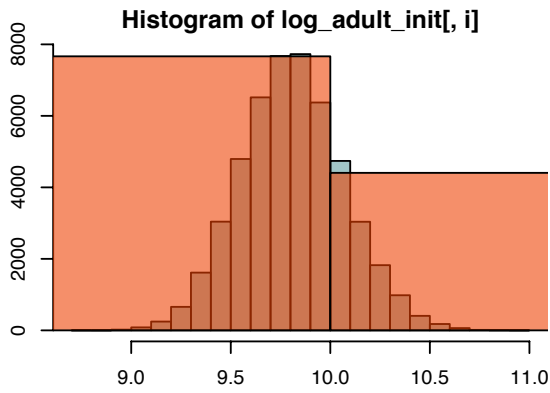
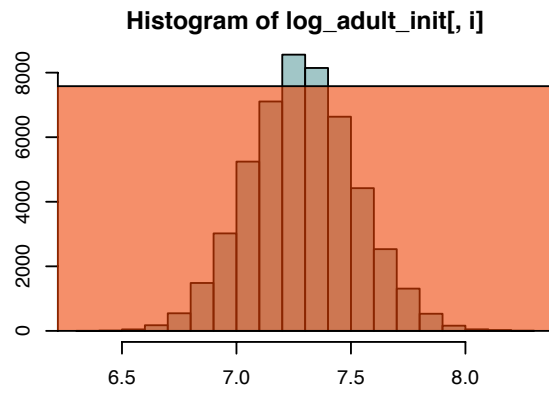
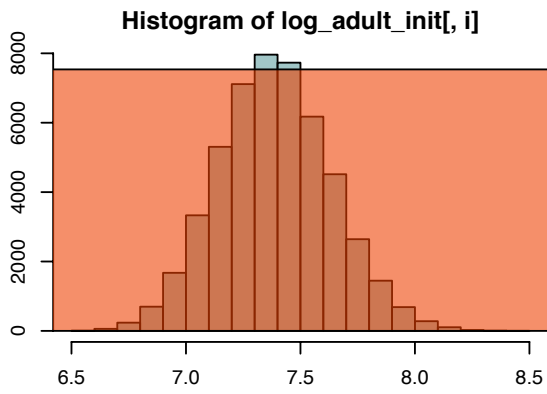
Histogram of log_adult_init[, i]

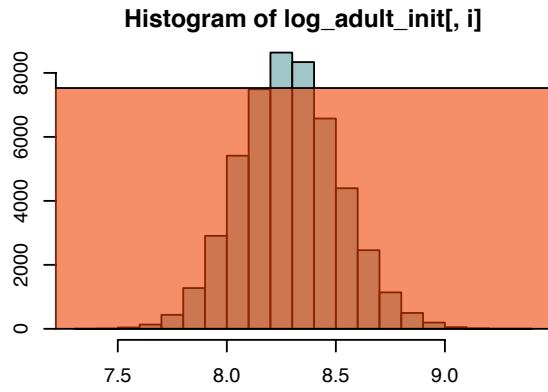
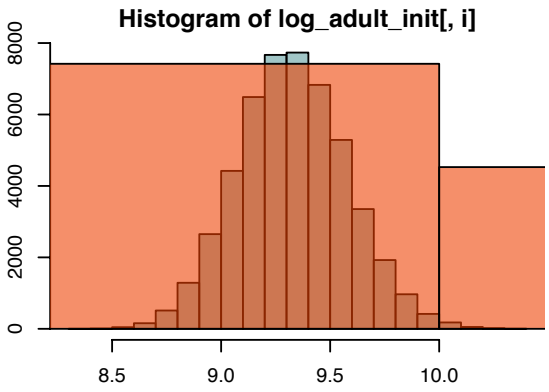
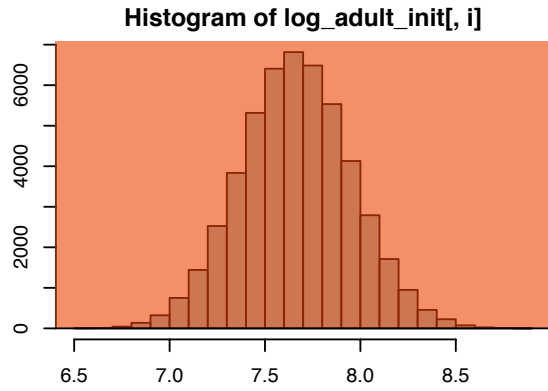
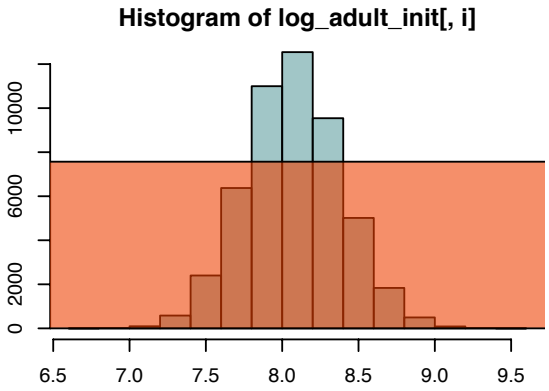
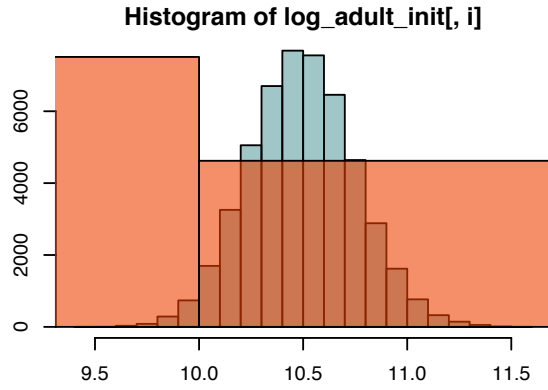
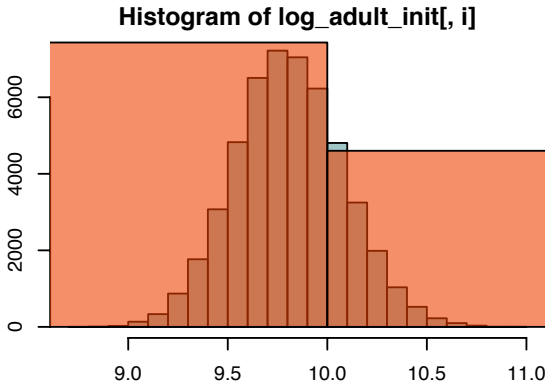


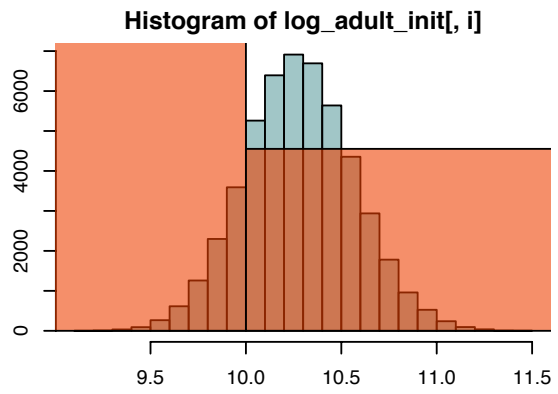
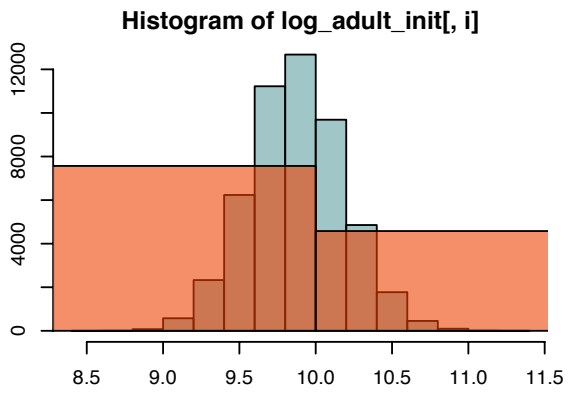
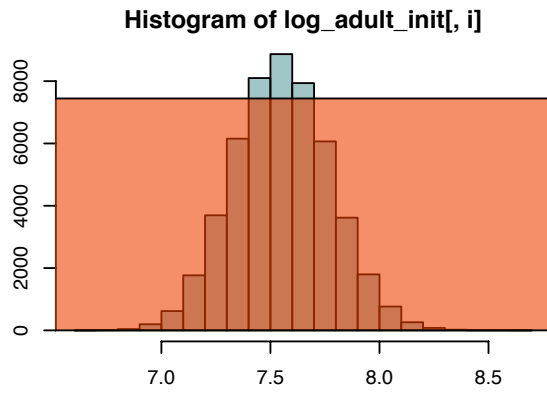
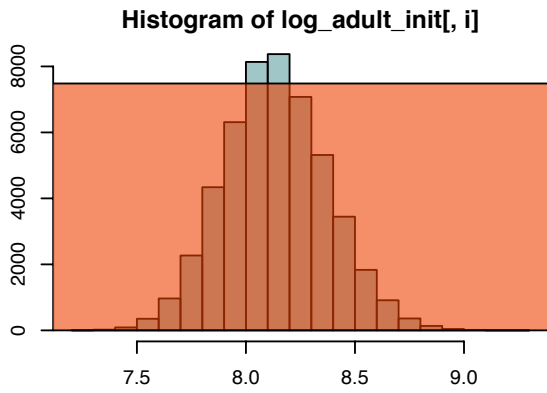
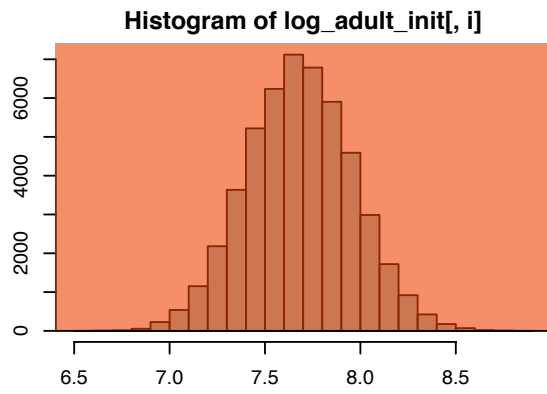
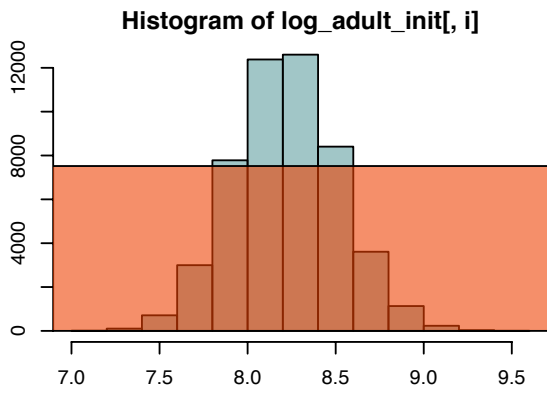
Histogram of log_adult_init[, i]

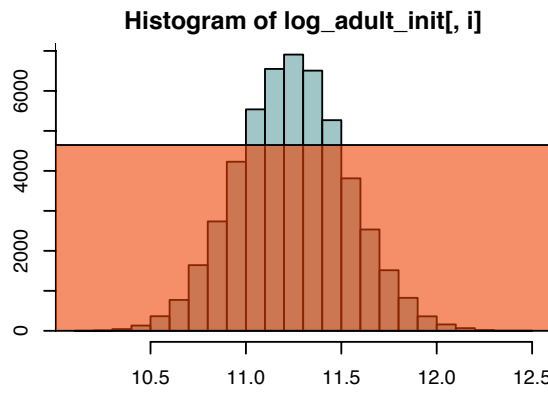
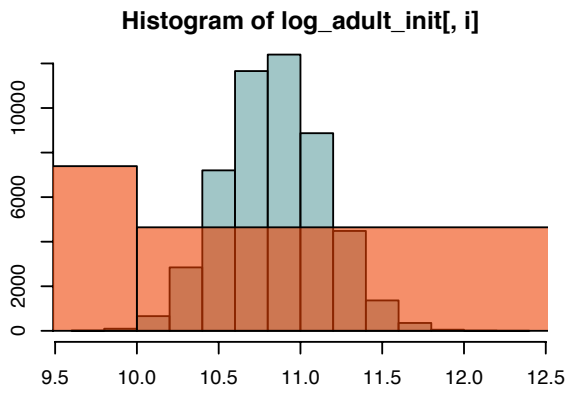
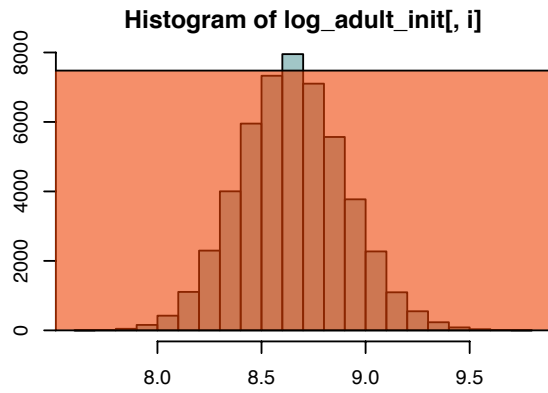
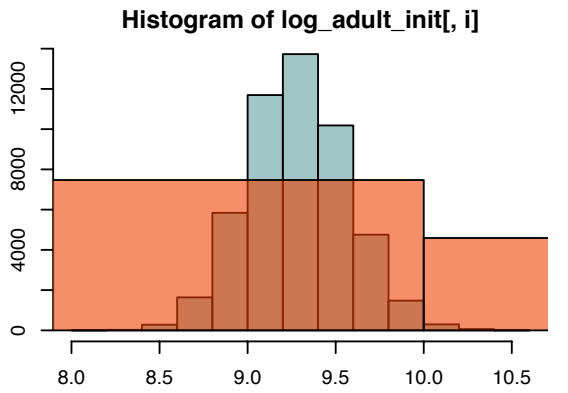
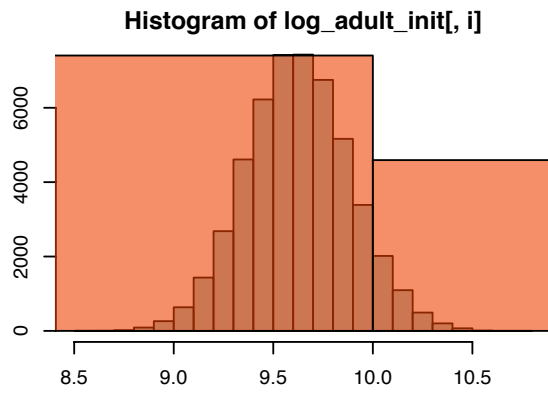
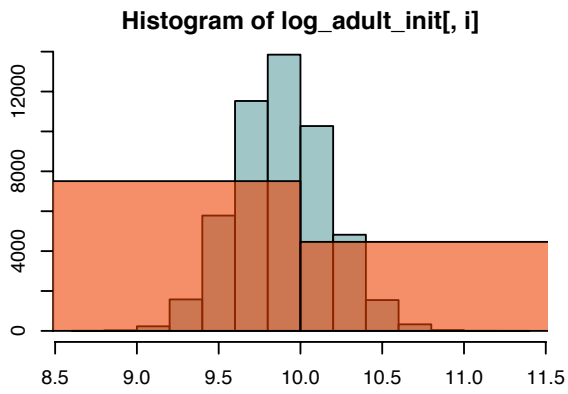


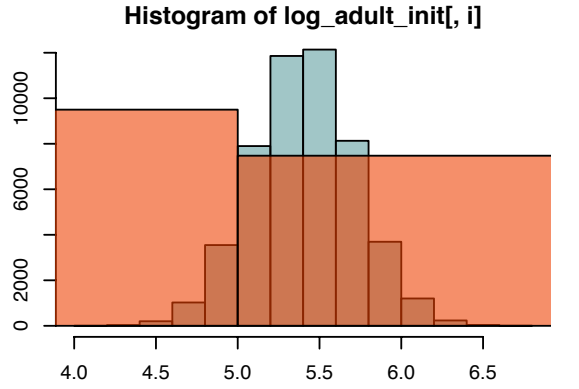
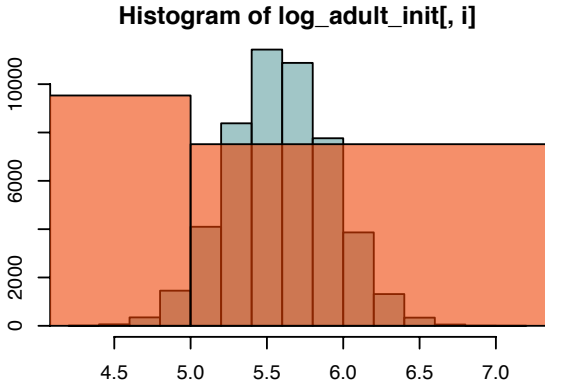
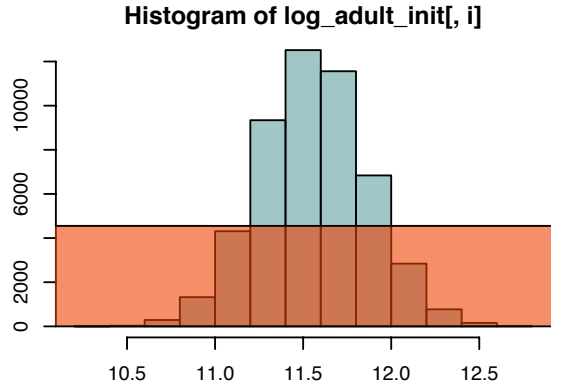
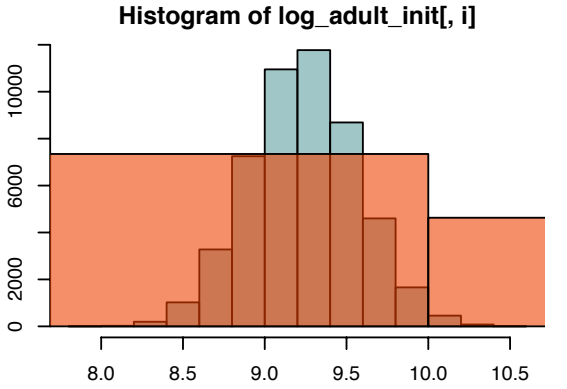
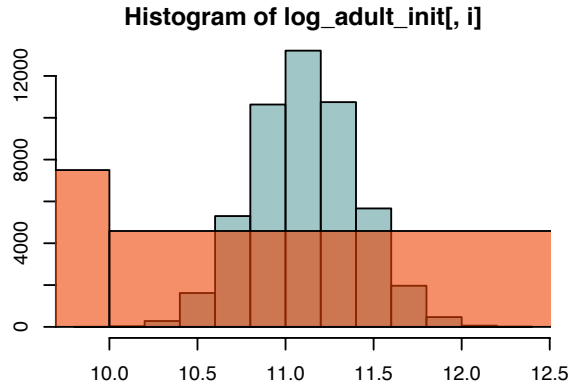
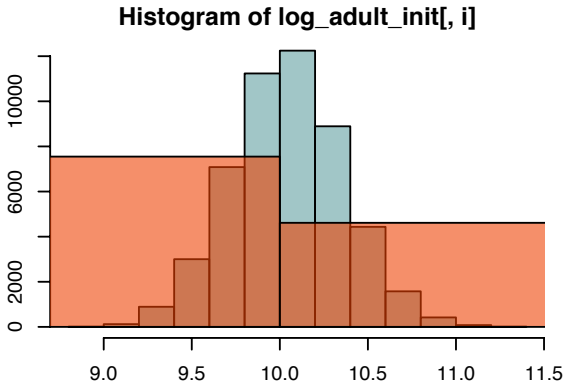


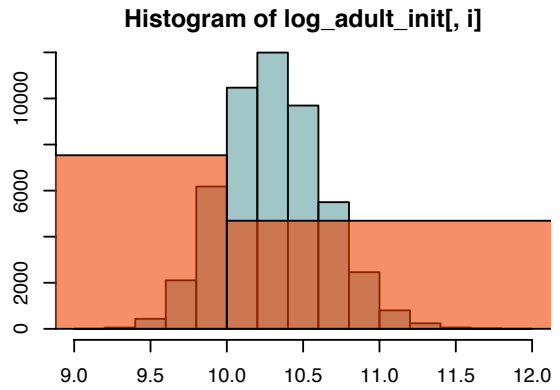
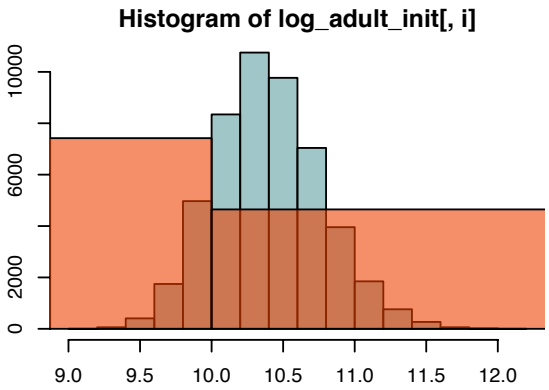
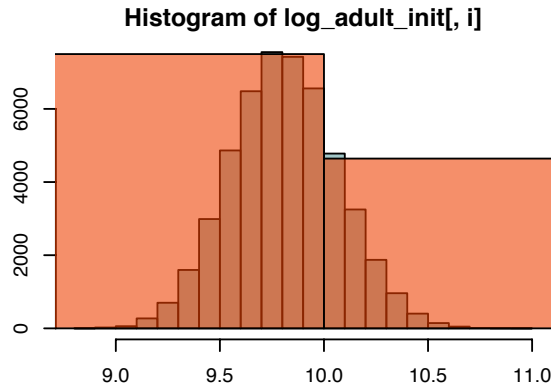
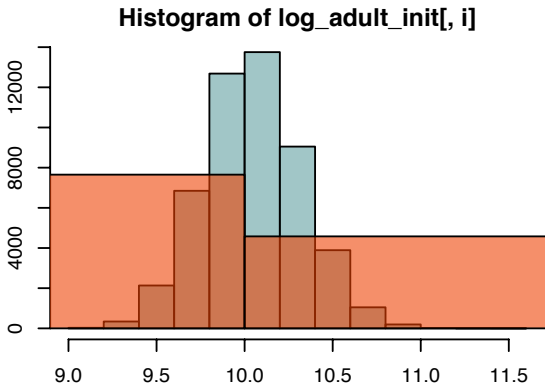
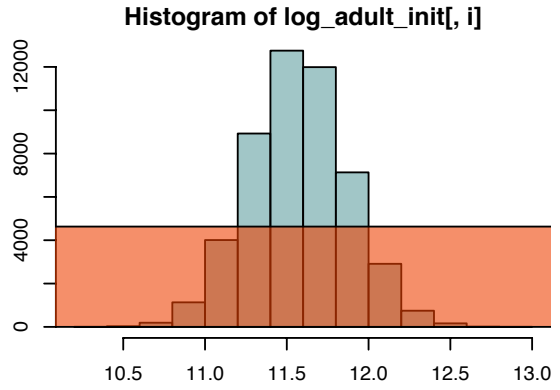
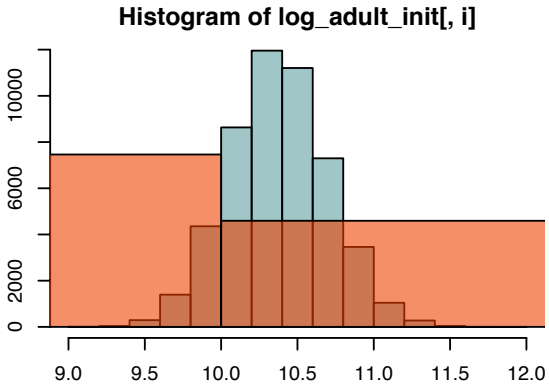


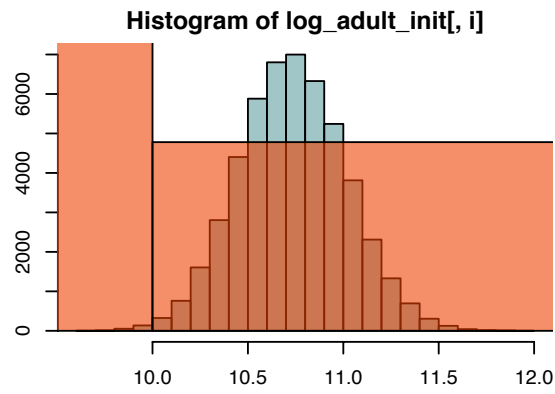
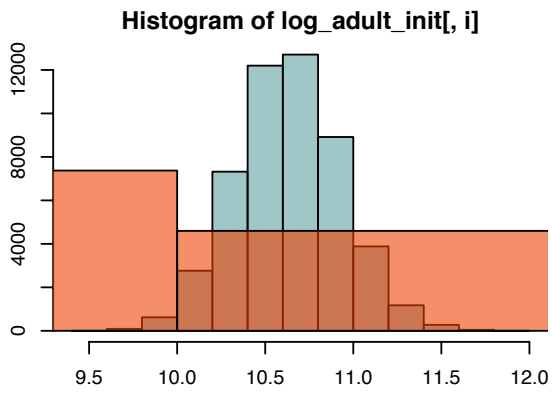
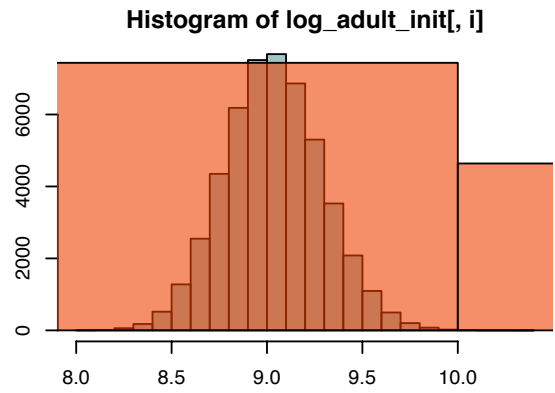
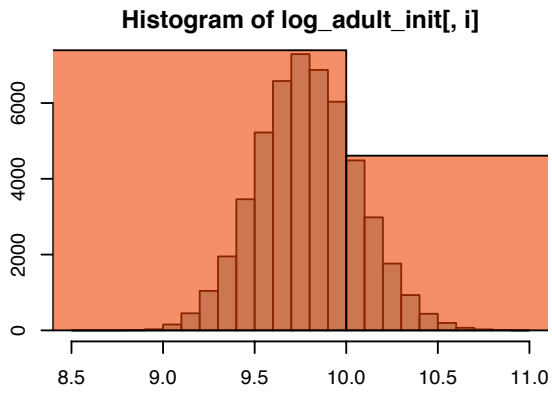
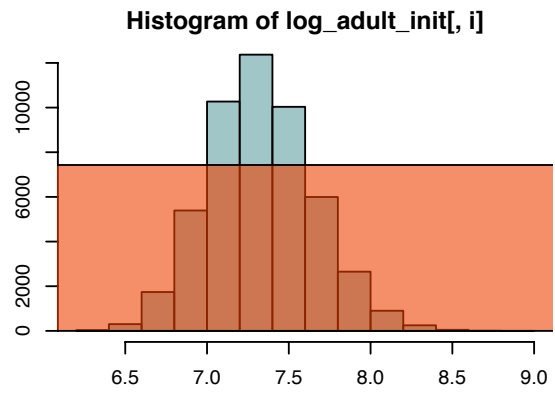
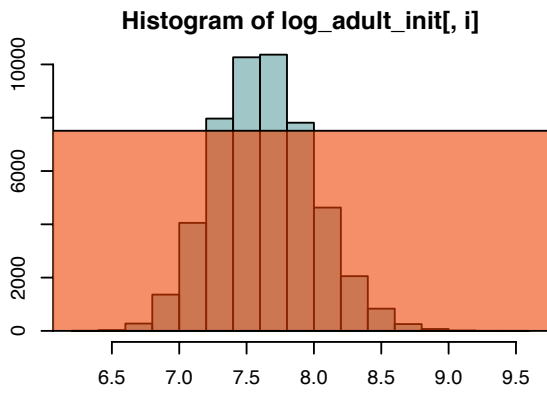




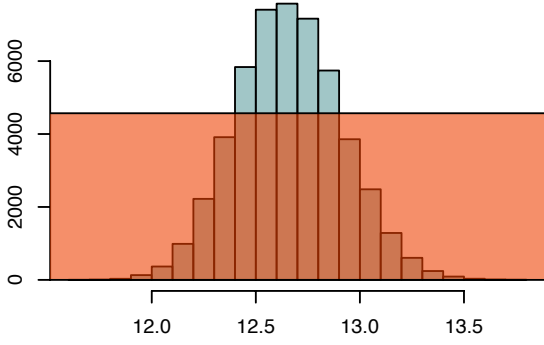




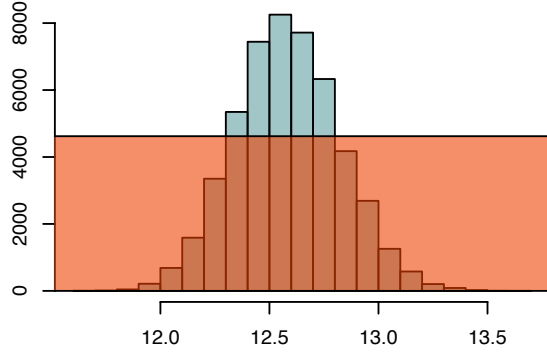




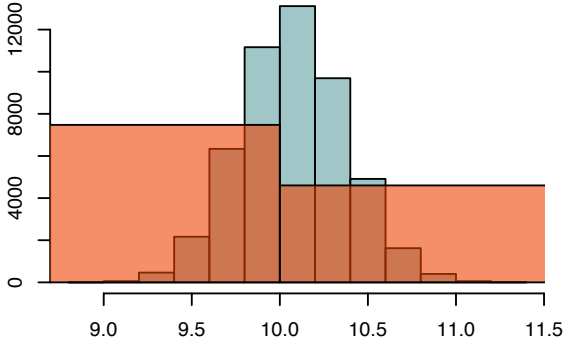
Histogram of log_adult_init[, i]



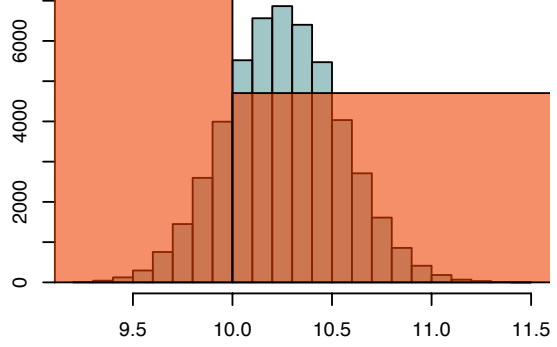
Histogram of log_adult_init[, i]



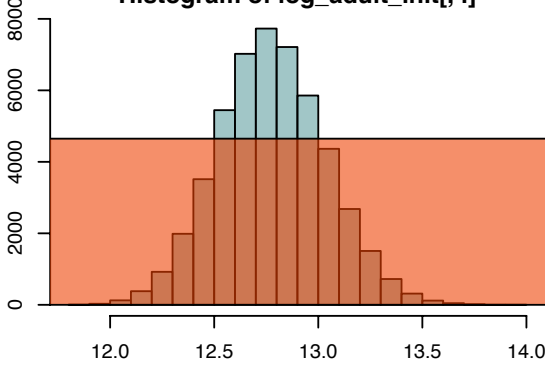
Histogram of log_adult_init[, i]



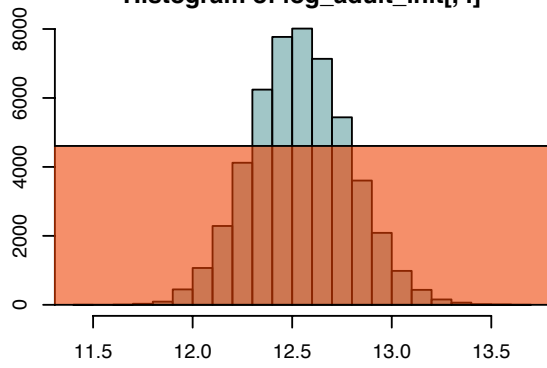
Histogram of log_adult_init[, i]



Histogram of log_adult_init[, i]



Histogram of log_adult_init[, i]



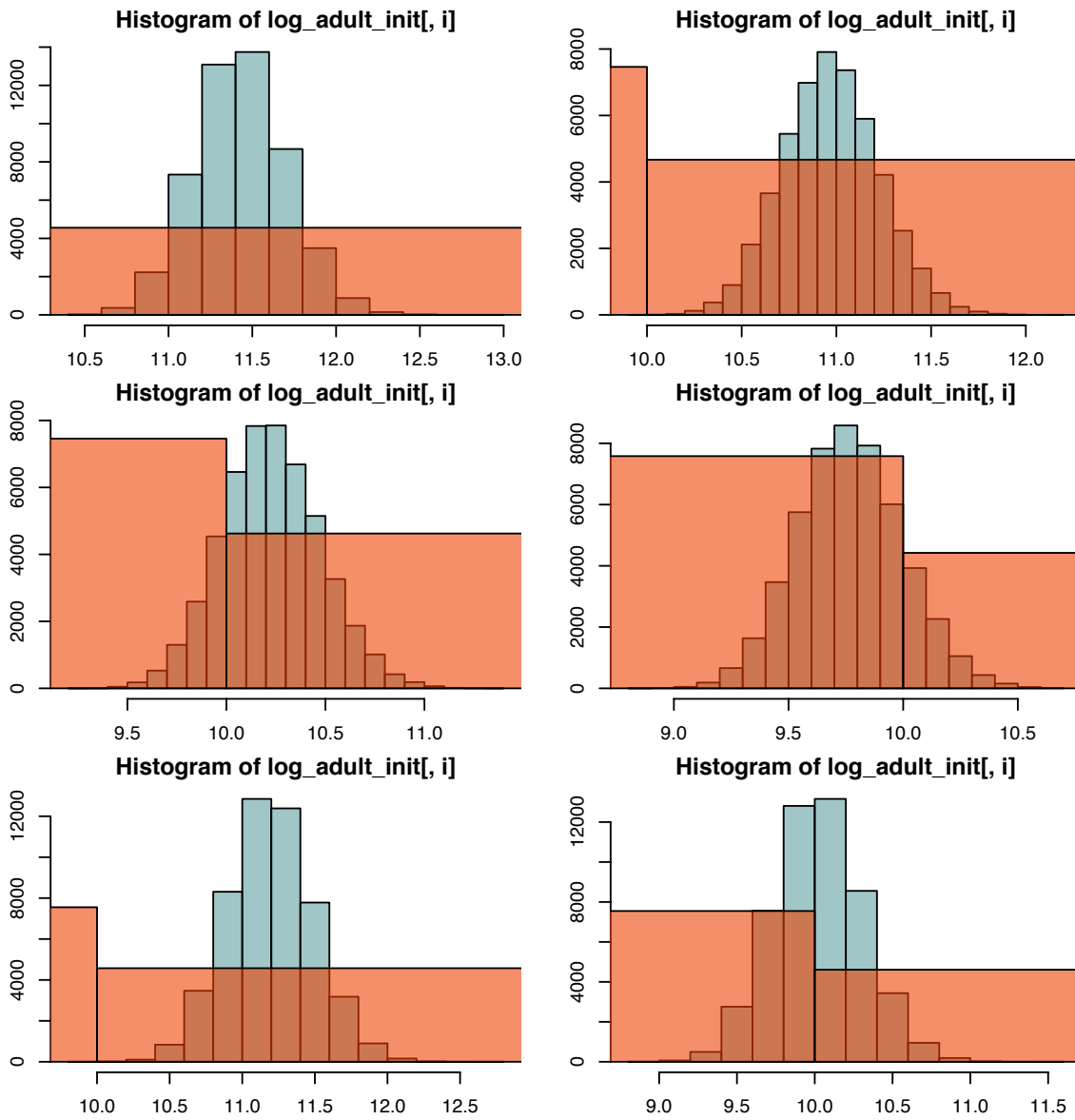


Figure S7. Prior and posterior comparison. In each panel, the prior distribution for the parameter is shown as a transparent red histogram, and the posterior is shown as a green histogram.

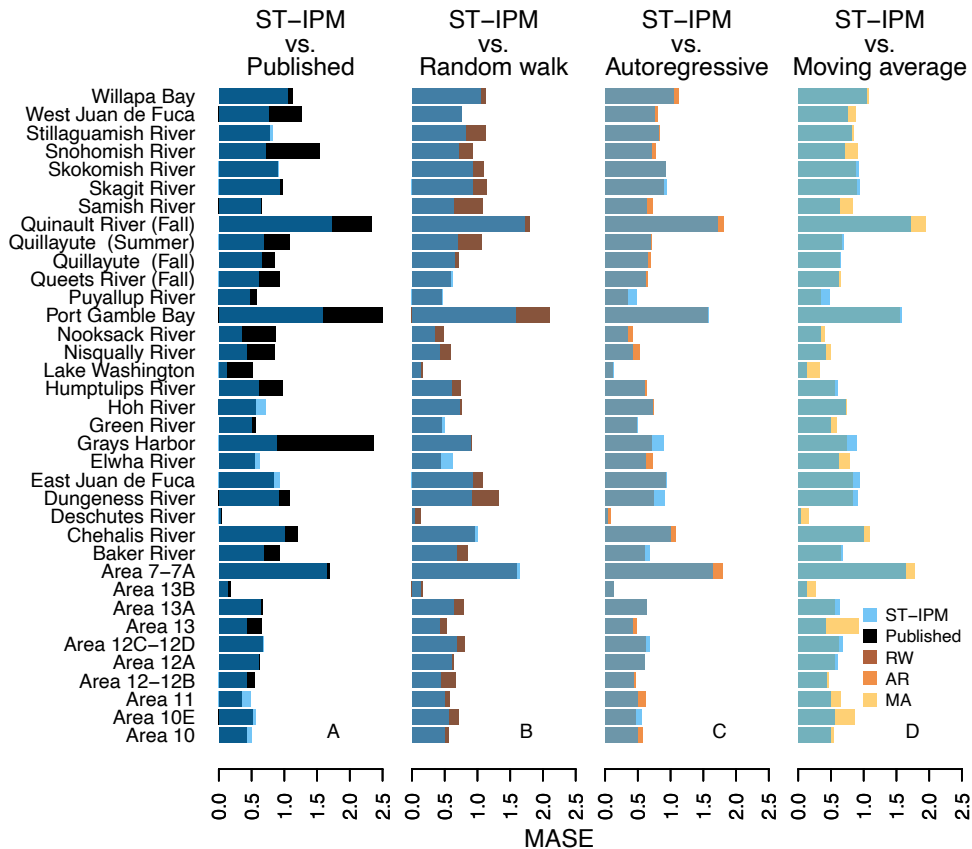


Figure S8. One-year ahead forecast skill of alternative forecast approaches from 2002-2017. Blue bars for each population show the mean absolute scaled error (MASE) for one-year-ahead forecasts under the spatiotemporal integrated population model (ST-IPM) (all panels). Panel A compares the MASE of the ST-IPM to that of the existing published forecast methods, while panels B-D compare the MASE of the ST-IPM to that of a state-space random walk (B), lag-1 autoregressive model (C), and lag-1 moving average model (D).

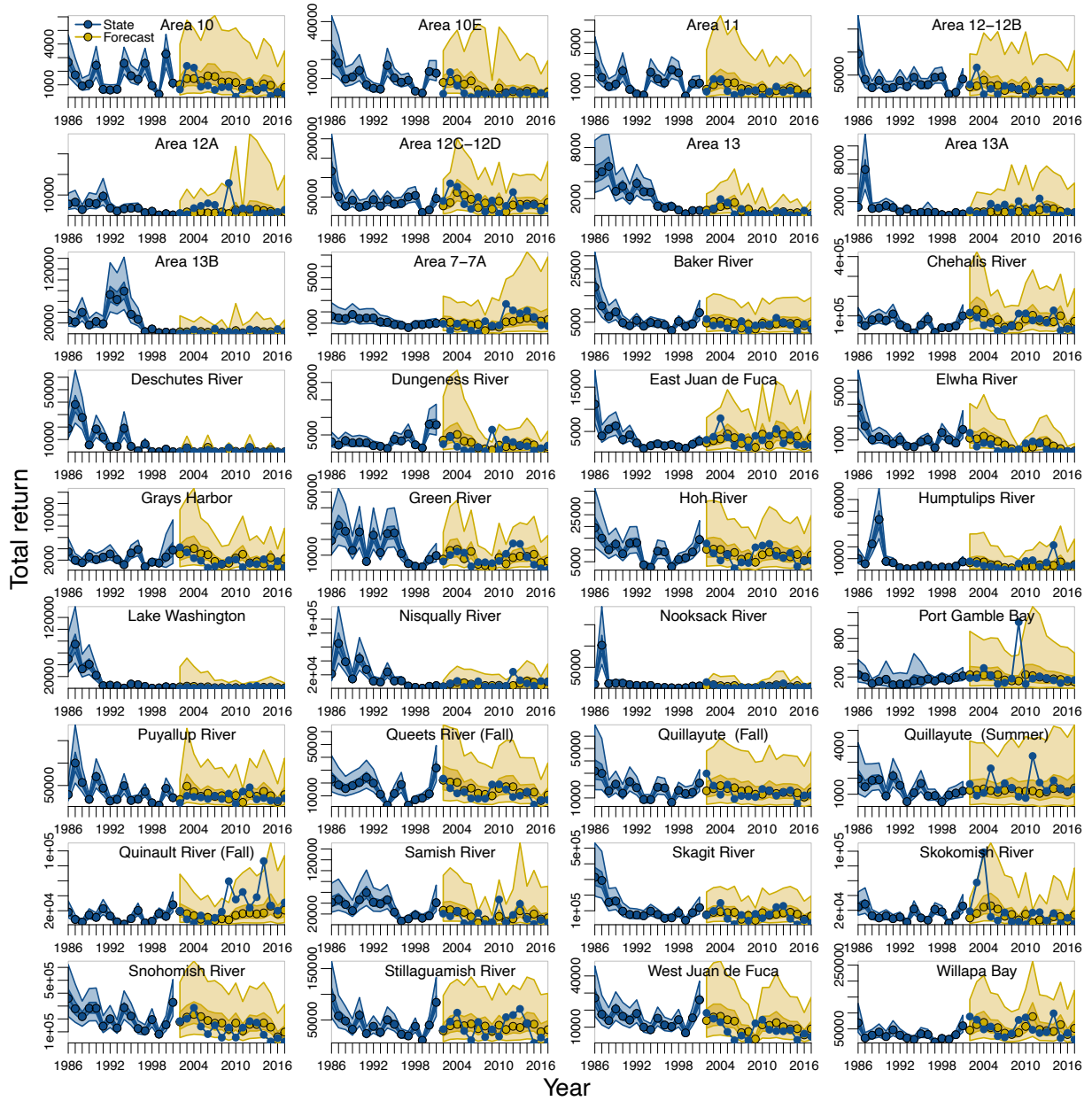


Figure S9. One-year-ahead forecasts of total adult returns from the spatiotemporal integrated population model (ST-IPM) with respect to state estimates of adult returns. The details of this figure are identical to figure 6 except that the forecasts are being compared to state estimates of adult abundance (blue) rather than observed data.

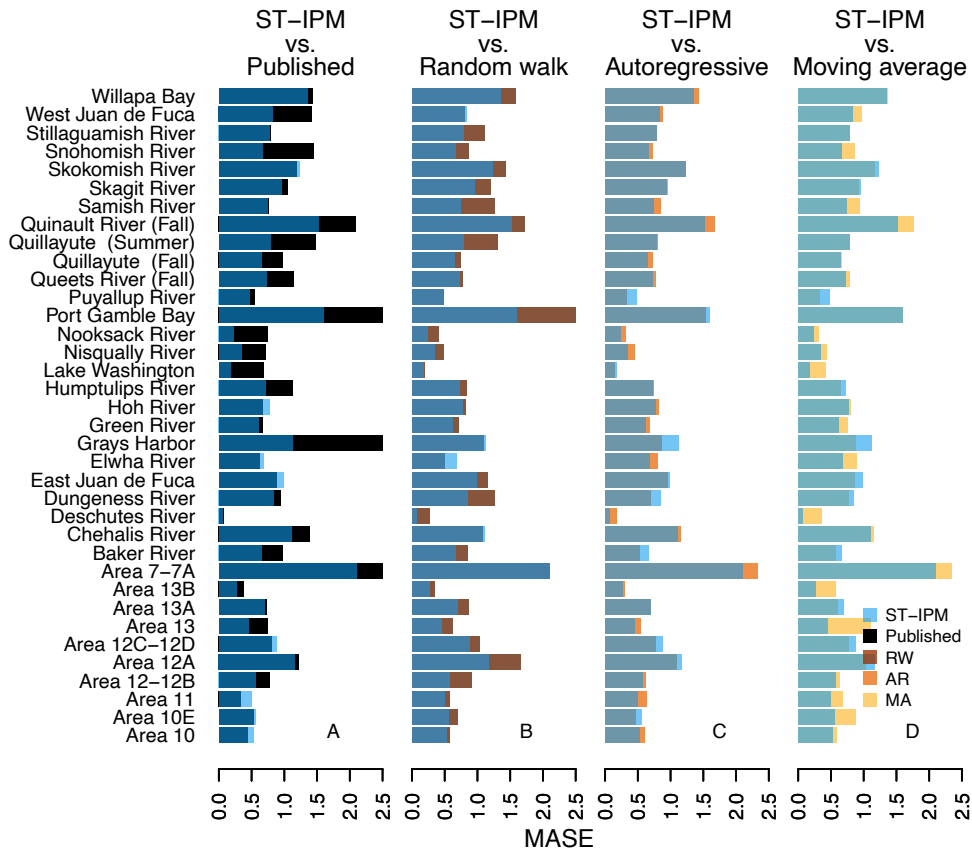


Figure S10. One-year ahead forecast skill of alternative forecast approaches from 2002-2017 with respect to state estimates of adult abundance. The details of this figure are identical to those of figure S8 except that MASE is calculated by comparing forecasts to state estimates of total adult returns from model fits of the ST-IPM to all years' data rather than the observed adult return data.